TABLE DES MATIÈRES :

LISTE DES FIGURES

INTRODUCTION

CHAPITRE 1

CHAPITRE 2

CHAPITRE 3

LISTE DES TABLEAUX

INTRODUCTION

CHAPITRE 1

CHAPITRE 2

CHAPITRE 3

LISTE DES ABBRÉVIATIONS

a : coefficient d'absorption

a_{ph} : coefficient d'absorption du phytoplancton

a^*_{ph}: coefficient d'absorption du phytoplancton spécifique à la chlorophylle *a*

b : coefficient de diffusion

b_{ph} : coefficient de diffusion du phytoplancton

b^* : coefficient de diffusion spécifique à la chlorophylle *a*

c : coefficient d'attenuation

CDOM : matière organique dissoute colorée

chl-*a* : chlorophylle *a*

FCM : cytomètre en flux

FL3 : fluorescence cellulaire associée à la chlorophylle

FSC : indice de diffusion par particule pour les petits angles (1-19°)

IOPs : propriétés optiques inhérentes

K_d : coefficient d'atténuation diffuse

PPC : pigments caroténoïdiens photoprotecteurs

PSC : pigments caroténoïdiens photosynthétiques

SPM : matière particulaire en suspension

SSC : indice de diffusion par particule pour les grands angles (73-109°)

T° : température

INTRODUCTION GÉNÉRALE

LA TÉLÉDETECTION

Dans les dernières décennies, un grand nombre de recherches ont été menées dans le but de décrire les variations spatio-temporelles de la biomasse phytoplanctonique (indicateur universel : concentration en chlorophylle *a*, chl-*a*) à grande échelle spatiale; ceci dans une optique de compréhension des cycles biogéochimiques et du rôle du phytoplancton sur l'atténuation de la lumière dans les océans (Denman et Powel 1984, Platt et Sathyendranath 1988, Platt et al. 1989), et de gestion et conservation des pêcheries. La télédétection de la couleur de l'océan a permis d'accroître les observations des variations spatio-temporelles des concentrations en chlorophylle de la couche de surface de l'océan, avec certains avantages : une fréquence élevée (quasiment journalière), une résolution spatiale élevée (quelques centaines de mètres à quelques kilomètres), une couverture spatiale étendue (environ 80% de la surface du globe) et sur de longues périodes (quelques années) (Dupouy et al. 1988, Platt et Sathyendranath 1988, Babin et al. 1996, Sathyendranath et al. 1995, Fuentes Yaco 1997).

La télédétection de la couleur de l'océan par satellite a débuté avec le lancement en 1978 du premier senseur satellite CZCS (Coastal Zone Colour Scanner). Initialement prévu pour fonctionner un an, ce senseur expérimental a fourni des données jusqu'en 1986. La répétitivité, le caractère synoptique et la qualité des observations faites par le CZCS, ont permis de conclure à la nécessité de poursuivre l'observation de la couleur de l'océan à partir de l'espace. Toutefois, il aura fallu attendre 10 ans (1996-1997) pour la mise en

fonction de satellites équipés de senseurs de couleur de l'océan plus sophistiqués tels que MOS (Modular Optoelectric Scanner), OCTS (Ocean Colour and Temperature Scanner), POLDER (Polarization and Directionality of the Earth's Reflectances) ou SeaWiFs (Sea-viewing Wide Field-of-view Sensor). Ces senseurs sont en mesure de générer des données susceptibles d'être utilisées pour paramétriser des modèles bio-optiques beaucoup plus précis, et pouvant être validés par des observations de terrain (Morel et Berthon 1989, Reynolds *et al.* 2001). Actuellement, les images satellitaires SeaWiFs sont couramment utilisées pour obtenir des bases de données sur la biomasse phytoplanctonique, du fait de leur grande résolution et de leur grande couverture spectrale (9 bandes spectrales) et spatiale. Les signaux captés par SeaWiFs proviennent de l'atmosphère, de la surface de la terre et des océans, mais également des éléments présents dans les premiers mètres sous la surface des océans (IOCCG 2000). Ce sont les signaux provenant de cette dernière source, appelés couleur des océans (Garver et Siegel 1997, IOCCG 2000), qui intéressent le plus les océanographes. La couleur des océans est une caractéristique optique facile à mesurer, qui apporte une quantité importante d'informations directement liées aux propriétés optiques de ceux-ci (Cullen et al. 1994). En effet, la variabilité des propriétés optiques des océans régule les variations de la couleur des océans (Prieur et Morel 1975, Gordon 1989, Morel et Gentili 1991, Kirk 1994). La couleur des océans est extrêmement variable : verte dans les eaux au large des côtes mauritaniennes, bleue limpide dans l'océan Pacifique, brune ou jaune dans les eaux côtières ou encore rouge lors de floraison de certaines algues toxiques (« marées rouges »). La gamme de couleurs dépend directement de la quantité et de la nature du matériel en suspension et dissous dans l'eau de mer. Ainsi, la couleur verte

des eaux est due à la teneur élevée en chlorophylle, alors que la couleur brune des eaux côtières est liée à la forte teneur en particules minérales et/ou en matières dissoutes d'origine continentale. Les constituants présents dans le milieu océanique sont donc à l'origine d'une perturbation significative de la propagation de la lumière. Cette modification du champ lumineux sous-marin est due à l'absorption et à la diffusion des photons par les constituants "optiquement significatifs" présents dans l'eau de mer (eau pure, phytoplancton, particules non chlorophylliennes, fraction colorée de la matière organique dissoute). La couleur perçue à la surface de l'océan est à la fois fonction de ces phénomènes (absorption et diffusion) et du champ lumineux incident à la surface de l'océan.

PROPRIÉTÉS OPTIQUES DES OCÉANS

Durant les années 90, l'intérêt porté aux propriétés optiques des océans s'est rapidement accru, suite aux efforts mis en œuvre pour estimer précisément, par des mesures satellitaires, la biomasse phytoplanctonique (Gordon et Morel 1983) et la production primaire (Platt et Sathyendranath 1988, Morel et André 1991, Sathyendranath et al. 1995) et pour décrire la variabilité spatio-temporelle du phytoplancton (Smith et Baker 1978a, b, Brown et al. 1985).

Considérations générales

Les propriétés optiques des océans sont de deux types: apparentes et inhérentes (Preisendorfer 1961). Les propriétés optiques apparentes (Apparent Optical Properties – AOPs) des océans sont celles qui sont affectées par la distribution angulaire de la lumière, ainsi que par la nature et la quantité des substances présentes dans le milieu. Les propriétés optiques inhérentes (Inherent Optical Properties – IOPs) des océans sont, quant à elles, indépendantes des variations de la distribution angulaire de la lumière. Elles sont uniquement associées aux caractéristiques (nature, abondance et propriétés optiques) des particules et aux caractéristiques de la matière organique dissoute (MOD), présentes dans l'eau (Sosik et al. 2001).

Les IOPs des océans sont très variables (Bricaud et al. 1995) et sont, depuis une dizaine d'années, couramment déterminées *in situ*, à l'aide d'instruments capables de discriminer les photons absorbés et diffusés (Tableau 1).

Tableau 1 : Les différentes propriétés optiques inhérentes (IOPs) des océans (sr : stéradian) (Mobley 1994).

IOPs	Unités S.I.	Symbole recommandé
Indice de réfraction Partie réelle Partie imaginaire	Sans dimension	m n n`
Coefficient d'absorption	m^{-1}	a
Coefficient angulaire de diffusion (VSF)	m^{-1} sr^{-1}	β
Coefficient de fonction de phase de diffusion	sr^{-1}	$\tilde{\beta}$
Coefficient de diffusion de rétrodiffusion	m^{-1} m^{-1}	b b_b
Coefficient d'atténuation	m^{-1}	c
Albédo de diffusion simple	Sans dimension	ϖ ou ω_0

De toutes les IOPs mesurées dans l'eau, la plus simple à mesurer est le coefficient d'atténuation c. L'atténuation traduit la perte d'énergie lumineuse (photons) par rapport à la direction initiale du flux lumineux incident; cette perte peut avoir deux origines. L'énergie des photons est utilisée, ce qui implique leur disparition ; c'est le phénomène d'absorption évalué par son coefficient $a(\lambda)$ (m^{-1}). Les photons peuvent aussi être renvoyés dans une autre direction par les constituants de ce milieu, tout en restant sous forme radiative et sans perte d'énergie. L'intensité de cet évènement est caractérisée par le coefficient de diffusion $b(\lambda)$ (m^{-1}). On a donc :

$$c(\lambda) = a(\lambda) + b(\lambda) \qquad (1)$$

Le coefficient de diffusion $b(\lambda)$ est le résultat de l'intégration du coefficient angulaire de diffusion $\beta(\lambda, \theta)$ ou "volume scattering function" (en m^{-1} sr^{-1}, θ : angle de diffusion) entre 0 et π:

$$b(\lambda) = 2\pi \int_0^{\pi} \beta(\lambda, \theta) \sin(\theta)\, d\theta \qquad (2)$$

La courbe de variation de $\beta(\theta)$ en fonction de l'angle de diffusion θ est essentielle pour caractériser la diffusion. Par intégration de $\beta(\theta)$ non plus sur l'intervalle [0-π] mais [π/2-π], nous avons aussi accès au coefficient de rétrodiffusion, $b_b(\lambda)$, correspondant à la partie arrière de la diffusion (i.e., la composante de la diffusion dont l'angle est supérieur à 90°, Kirk 1994):

$$b_b(\lambda) = 2\pi \int_{\frac{\pi}{2}}^{\pi} \beta(\lambda, \theta) \sin(\theta)\, d\theta \qquad (3)$$

Enfin, la couleur de l'océan dépend des IOPs (Garver et Siegel 1997). Ainsi, les changements des coefficients d'absorption a et de diffusion b dans les océans entraînent des modifications de la couleur de l'océan (Gordon et Morel 1983, Bricaud et al. 1983, Reynolds et al. 2001). Par conséquent, la détermination de ces IOPs est essentielle pour comprendre les variations de la couleur de l'océan (Gordon et al. 1988, Roesler et Perry 1995, Garver et Siegel 1997).

Les coefficients, servant à estimer les propriétés optiques inhérentes, dépendent directement des propriétés optiques individuelles de chaque constituant du milieu. Parmi ces constituants, les particules sont certainement ceux dont la variabilité en termes d'origine, de taille, ou de constitution est la plus grande. Des outils théoriques ont été développés afin de relier les coefficients optiques aux caractéristiques des particules responsables de leurs variations (Bricaud et al. 1983, Morel et Ahn 1990, Ahn et al. 1992). Les facteurs d'efficacité permettent de relier les coefficients de diffusion (ou d'absorption) à la somme des sections géométriques des particules diffusantes (ou absorbantes). Les facteurs d'efficacité de diffusion (Q_b) ou d'absorption (Q_a) sont définis, respectivement, par le rapport entre l'énergie radiative diffusée ou absorbée par une particule sur l'énergie incidente atteignant la surface géométrique (G) de cette particule (mesurée

perpendiculairement à la direction de propagation du flux lumineux considéré). Pour une population de particules monodispersées de densité numérique N/V (N : nombre de particules ; V : volume), les coefficients de diffusion et d'absorption sont exprimés par

$$a(\lambda) = Q_a(\lambda)\,\frac{N}{V} \times G \tag{4}$$

$$b(\lambda) = Q_b(\lambda)\,\frac{N}{V} \times G \tag{5}$$

Pour une population de particules polydispersées suivant une distribution de taille n(r) (n : nombre de particules ; r : rayon), les équations (4) et (5) deviennent :

$$a(\lambda) = \int_{r=0}^{\infty} Q_a(\lambda, r) \times n(r) \times \pi r^2\, dr \tag{6}$$

$$b(\lambda) = \int_{r=0}^{\infty} Q_b(\lambda, r) \times n(r) \times \pi r^2\, dr \tag{7}$$

Le facteur d'efficacité de l'atténuation est égal à la somme des facteurs d'efficacité de l'absorption et de la diffusion

$$Q_c(\lambda) = Q_a(\lambda) + Q_b(\lambda) \tag{8}$$

Ces facteurs d'efficacité sont sans dimension. Les produits $Q_b \times G$ et $Q_a \times G$ sont respectivement définis comme la section efficace de diffusion (σ_b) et la section efficace d'absorption (σ_a) d'une particule.

La propagation d'ondes électromagnétiques dans un milieu est caractérisée par son indice de réfraction relatif complexe m, défini par :

$$m = n - (i \times n') \tag{9}$$

où n est la partie réelle de cet indice et n' sa partie imaginaire. La partie réelle de l'indice de réfraction (n) est un des principaux facteurs contrôlant la diffusion par les particules et est fonction de leur nature. La partie réelle de l'indice de réfraction – par rapport à l'eau - des particules rencontrées en milieu océanique est comprise entre 1,05 (cellules phytoplanctoniques) et 1,2 (particules minérales) (Morel 1991). La partie imaginaire (n') décrit les propriétés absorbantes des particules.

En milieu marin, les particules sont orientées de façon aléatoire ; on peut alors les considérer dans leur ensemble comme une population de sphères dont le diamètre est plus grand que la longueur d'onde et d'indice de réfraction relatif m proche de celui de l'eau (i.e. proche de 1). Ces caractéristiques correspondent aux conditions nécessaires pour appliquer l'approximation de la diffraction anormale (Van de Hulst 1957). Les facteurs d'efficacité Q_c et Q_a sont alors prédictibles en fonction des paramètres ρ et ρ' (sans dimension), combinant à la fois la taille relative des particules α, et la partie réelle ou imaginaire de l'indice de réfraction relatif m. ρ et ρ' sont définis comme :

$$\rho = 2\alpha\,(n - 1) \tag{10}$$

$$\rho' = 4\alpha\, n' \tag{11}$$

où

$$\alpha = \frac{\pi d}{\lambda_w} \tag{12}$$

d est le diamètre de la particule et λ_w est la longueur d'onde dans le milieu environnant (en l'occurrence ici l'eau). L'approximation de Van de Hulst prédit donc d'une part l'évolution

de Q_a en fonction de ρ', et d'autre part l'évolution Q_c en fonction de ρ lorsque les particules sont non-absorbantes et en fonction de ρ et ρ' lorsque les particules sont absorbantes.

$$Q_a = 1 + \frac{e^{(-\rho')}}{\rho'} + 2\,\frac{e^{(-\rho')} - 1}{\rho'^2} \tag{13}$$

$$Q_c = 2 - 4e^{(-\rho\tan\xi)}\left[\frac{\cos\xi}{\rho}\sin(\rho-\xi) + \left(\frac{\cos\xi}{\rho}\right)^2\cos(\rho-2\xi)\right] + 4\left(\frac{\cos\xi}{\rho}\right)\cos(2\xi)$$

$$\text{où } \tan\xi = \frac{n'}{(n-1)} \tag{14}$$

Q_b est déterminé par différence entre Q_c et Q_a et atteint donc sa valeur maximale quand Q_a est minimum (et inversement). On obtient alors les variations des facteurs d'efficacité en fonction du paramètre de taille (ρ) (Fig. 1) ; cette figure met en évidence le comportement asymptotique (en accord avec la théorie) des facteurs d'efficacité lorsque la taille des particules augmente.

Pour des particules absorbantes, Q_a tend asymptotiquement vers 1 quand ρ tend vers l'infini, ce qui veut dire que la particule est capable d'absorber toute l'énergie incidente sur sa section géométrique et se comporte donc comme un corps noir. Étant donné que Q_a tend vers 1 dans le cas de grosses particules, Q_b tend vers 1 (Fig. 1). Pour des particules non absorbantes (ρ'= 0, Q_a=0), Q_c est égal à Q_b (Fig. 1). Cela signifie que toute l'énergie rencontrant la surface géométrique de la particule est diffusée par réflexion ou réfraction dans une direction différente du flux initial. L'amplitude des minima et maxima successifs se réduit progressivement pour atteindre une valeur limite de 2 (quand ρ tend vers l'infini).

Le double de la quantité d'énergie interceptée géométriquement par la particule est retiré du champ radiatif initial (on parle alors du paradoxe de l'extinction).

Dans le cas d'une population naturelle de particules pour lesquelles les tailles ne sont pas uniformes (population polydispersée), le facteur d'efficacité moyen $\bar{Q}_c$, valide pour une particule « moyenne » représentative de la population, est estimé pour une valeur de $\bar{\rho}$ correspondant au maximum de la distribution de taille (Morel et Bricaud 1986). La valeur de $\bar{Q}_c$ est alors dépendante de la largeur de la distribution (effet de la polydispersion sur la taille des particules) et cela induit un phénomène de lissage des oscillations de $\bar{Q}_c$ en fonction de $\bar{\rho}$ (Fig. 2). De plus, une population naturelle est constituée d'une multitude de particules ayant chacune une efficacité variable en terme d'absorption ou de diffusion en fonction de son origine. Il est donc nécessaire de discriminer l'influence des différents composants de la colonne d'eau sur ces propriétés optiques.

Figure 1 : Variations des facteurs d'efficacité pour l'atténuation (Q_c), pour l'absorption (Q_a) et pour la diffusion (Q_b) en fonction du paramètre de taille (ρ) ou du diamètre (d) pour différentes valeurs de n' traduisant l'augmentation de l'absorption. Courbes établies pour une population monodispersée avec une valeur de n de 1.05 représentative du phytoplancton (Stramski 1999) et à une longueur d'onde de 440 nm. Figure extraite de Merien 2003.

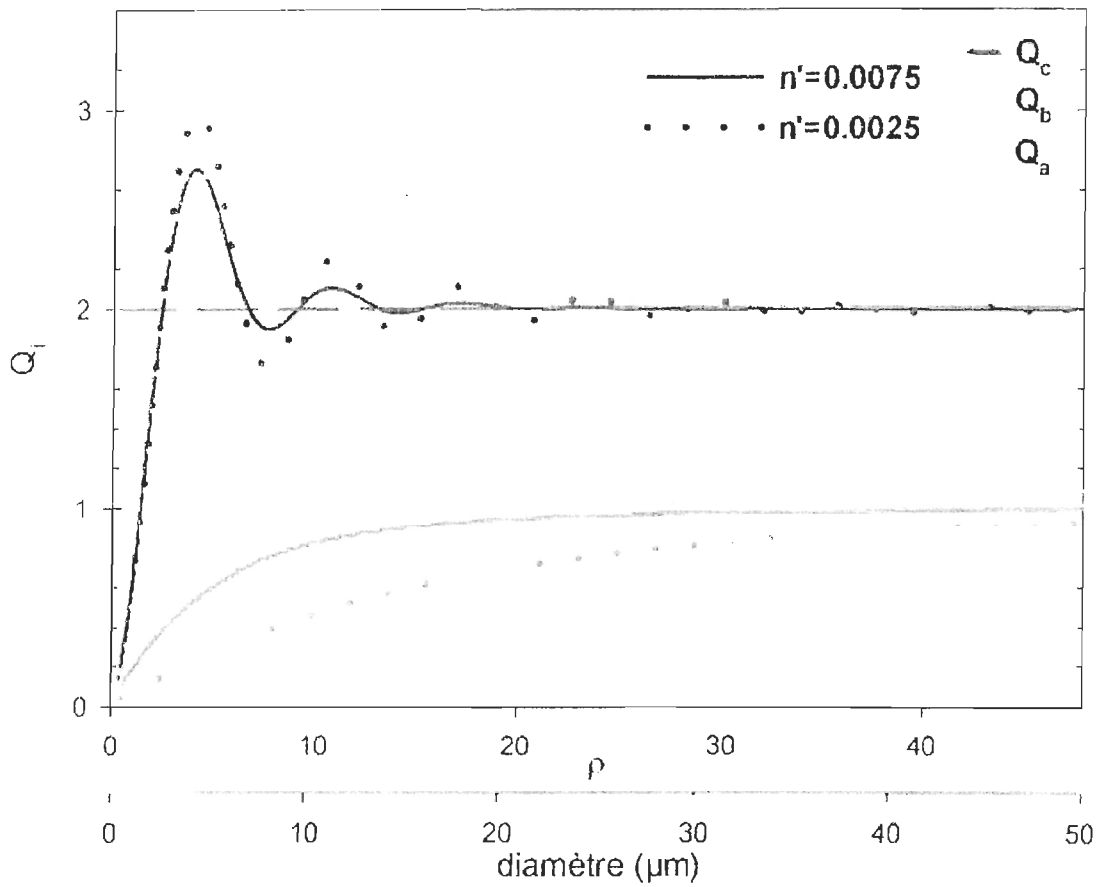
n'=0.0075
n'=0.0025
Q_c
Q_b
Q_a
Q_i
0
1
2
3
0
10
20
30
40
ρ
0
10
20
30
40
50
diamètre (µm)

Figure 2 : Valeur moyenne du facteur d'efficacité de l'atténuation $\overline{Q}_c$ d'une particule moyenne représentative d'une population polydispersée, tracée en fonction du paramètre de taille ($\overline{\rho}$) correspondant au maximum de la fonction de distribution de taille des particules F(ρ). Toutes les courbes ont été établies dans le cas d'une particule non-absorbante (n'=0), les courbes 1 à 3 traduisent une augmentation de la largeur de la distribution de taille (log-normale), et la courbe en pointillés représente le cas limite d'une population monodispersée. Figure extraite de Morel et Bricaud (1986).

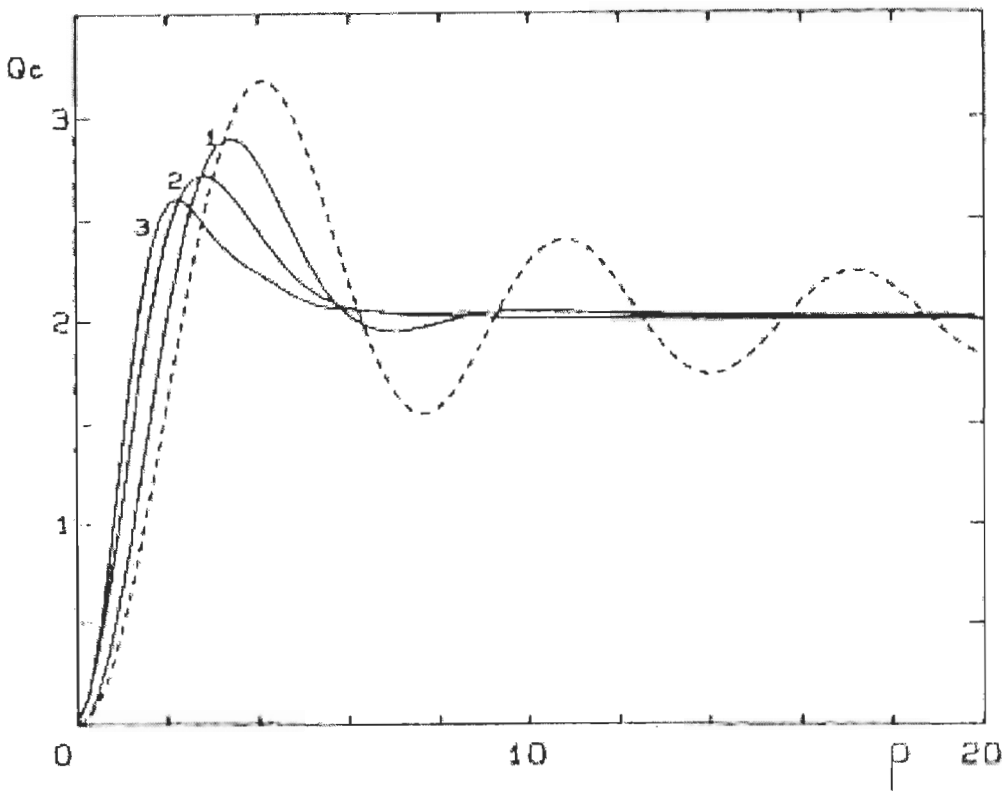
Qc
3
2
1
0
10
p
20
1
2
3

IOPs et constituants "optiquement significatifs"

Les IOPs des océans, telles que les coefficients d'absorption et de diffusion de l'eau de mer, varient principalement en fonction du contenu de la masse d'eau en matière particulaire, inorganique et organique (i.e., phytoplancton, bactéries et virus) ainsi qu'en matière organique dissoute colorée (CDOM). Dans l'océan ouvert, les coefficients d'absorption et de diffusion totaux [$a_{tot}(\lambda)$ et $b_{tot}(\lambda)$] sont le résultat des contributions additives de ces divers constituants, de telle façon que :

$$a_{tot}(\lambda) = a_w(\lambda) + a_{CDOM}(\lambda) + a_{ph}(\lambda) + a_{NAP}(\lambda) \quad (15)$$

$$b_{tot}(\lambda) = b_w(\lambda) + b_{ph}(\lambda) + b_{NAP}(\lambda) \quad (16)$$

Où les indices w, CDOM, ph et NAP désignent, respectivement, l'eau pure, la matière organique dissoute colorée, le phytoplancton et la matière particulaire non chlorophyllienne. Il est à noter que la matière organique dissoute colorée est supposée non diffusante. D'après les équations (15) et (16), le coefficient d'atténuation peut aussi être exprimé comme :

$$c_{tot}(\lambda) = c_w(\lambda) + c_{CDOM}(\lambda) + c_{ph}(\lambda) + c_{NAP}(\lambda) \quad (17)$$

Chacun de ces constituants (eau pure, matière organique dissoute colorée, phytoplancton et matière particulaire non chlorophyllienne) est caractérisé par une signature optique spécifique. La forme du spectre d'absorption (ou de diffusion) totale résulte de l'effet conjugué de la magnitude et de la dépendance spectrale de l'absorption (ou de la diffusion) par chacune de ces composantes.

Propriétés optiques des constituants "optiquement significatifs"

Absorption

De nombreuses études se sont attachées à définir les propriétés optiques de l'eau de mer pure (Morel et Prieur 1977, Smith et Baker 1981, Buiteveld et al. 1994, Pope et Fry 1997, Sogandares et Fry 1997). L'absorption par l'eau de mer pure (eau pure + minéraux dissous) est faible dans les domaines spectraux du bleu et du vert, et augmente à partir de 550 nm pour devenir nettement significative dans le rouge (Fig. 3).

Les diverses espèces phytoplanctoniques ont des propriétés d'absorption différentes. Ainsi leur spectre d'absorption normalisée par la concentration en chl-*a* (absorption spécifique à la chl-*a*, a^*_{ph}) présentent une grande variabilité spectrale, résultant principalement de l'effet conjugué de (1) la composition pigmentaire des cellules (Bricaud et al. 1988, Hoepffner et Sathyendranath 1991, Stuart et al. 1998) et (2) du « package effect » expliqué plus loin dans ce texte (Morel et Bricaud 1981) (Fig. 4).

Tous les organismes phytoplanctoniques captent l'énergie lumineuse à l'aide de pigments, dont les propriétés d'absorption diffèrent. Le spectre d'absorption du phytoplancton présente généralement deux maxima d'absorption dans le visible : un premier vers 440 nm et un second vers 676 nm principalement dus à l'absorption par la chl-*a*, pigment universel et majoritairement impliqué dans la photosynthèse. Les cellules phytoplanctoniques disposent de toute une gamme de pigments accessoires tels que la chlorophylle *b*, les chlorophylles *c* (c_1, c_2, c_3 et autres dérivés), les caroténoïdes et les biliprotéines qui présentent des bandes d'absorption principalement réparties dans le bleu, le vert et le rouge (Fig. 5). La majeure partie des pigments accessoires transmettent leur énergie à la chl-*a* et sont dits photosynthétiques, alors que certains caroténoïdes dits « non-photosynthétiques » ont une fonction photoprotectrice (essentiellement la zéaxanthine, la diadinoxanthine, la diatoxanthine et le β-carotène). Certains de ces pigments photoprotecteurs dissipent l'énergie absorbée sous forme de chaleur. La forme du spectre d'absorption est d'autant plus variable dans la région du bleu-vert où ces pigments accessoires présentent leurs maxima d'absorption (Jeffrey et al. 1997). Le contenu et la composition en pigments accessoires varient fortement entre les espèces. De plus, certains pigments sont spécifiques à des groupes phytoplanctoniques (Jeffrey et al. 1997) ; ainsi la fucoxanthine est surtout présente dans les diatomées et la 19'-hexanoyloxyfucoxanthine se retrouve principalement chez les prymnésiophycées. Ces quelques exemples, loin d'être exhaustifs, illustrent la possibilité de détecter la présence de groupes phytoplanctoniques par le biais de la composition pigmentaire (Roy et al. 1996, Vidussi et al. 1998). Par

conséquent, certaines caractéristiques sur le spectre d'absorption, initiées par la composition pigmentaire, peuvent donner des indices sur les groupes en présence.

D'autre part, pour une espèce donnée la concentration et la composition en pigment peuvent varier considérablement en fonction des conditions environnementales, telles que la disponibilité en sels nutritifs ou en lumière (Claustre et al. 1994, Johnsen et al. 1994, Babin et al. 1996) et ces variations se répercutent sur la forme du spectre d'absorption.

Le « package effect » correspond à un effet de discrétisation de la matière absorbante. Il a été mis en évidence expérimentalement (Duysens 1956) par l'observation suivante : l'absorption dans un milieu contenant une substance absorbante sous forme de particules en suspension est plus faible que l'absorption dans un milieu contenant la même quantité de la même substance sous forme dissoute. L'intensité de ce phénomène dépend simultanément du diamètre de la cellule phytoplanctonique et de son contenu interne en pigments (Morel et Bricaud 1981). Ainsi, le « package effect » est élevé dans le cas de cellules de grande taille et/ou à fort contenu interne en pigments et faible dans le cas de cellules de petite taille et/ou à faible contenu interne en pigments. Le « package effect » sera donc d'autant plus élevé dans une population dominée par du microphytoplancton (cellules phytoplanctoniques >20 µm), notamment par des diatomées, ou dans le cas de populations soumises à de faibles éclairements (Falkowski et LaRoche 1991, Berner et al. 1989). En milieu naturel, le « package effect » contribuerait pour 58 à 71% de la variabilité de

l'absorption spécifique du phytoplancton à 440 nm (Stuart et al. 1998), du fait de la grande diversité de taille et d'espèces phytoplanctoniques rencontrées.

Figure 3 : Contributions de l'eau de mer pure, de la matière organique dissoute colorée, du phytoplancton et de la matière particulaire non chlorophyllienne (notée « détritus » sur la figure) à l'absorption totale (trait épais), estimée pour des eaux productives (1 mg chl-*a*·m^{-3}). Figure extraite de Kirk (1994).

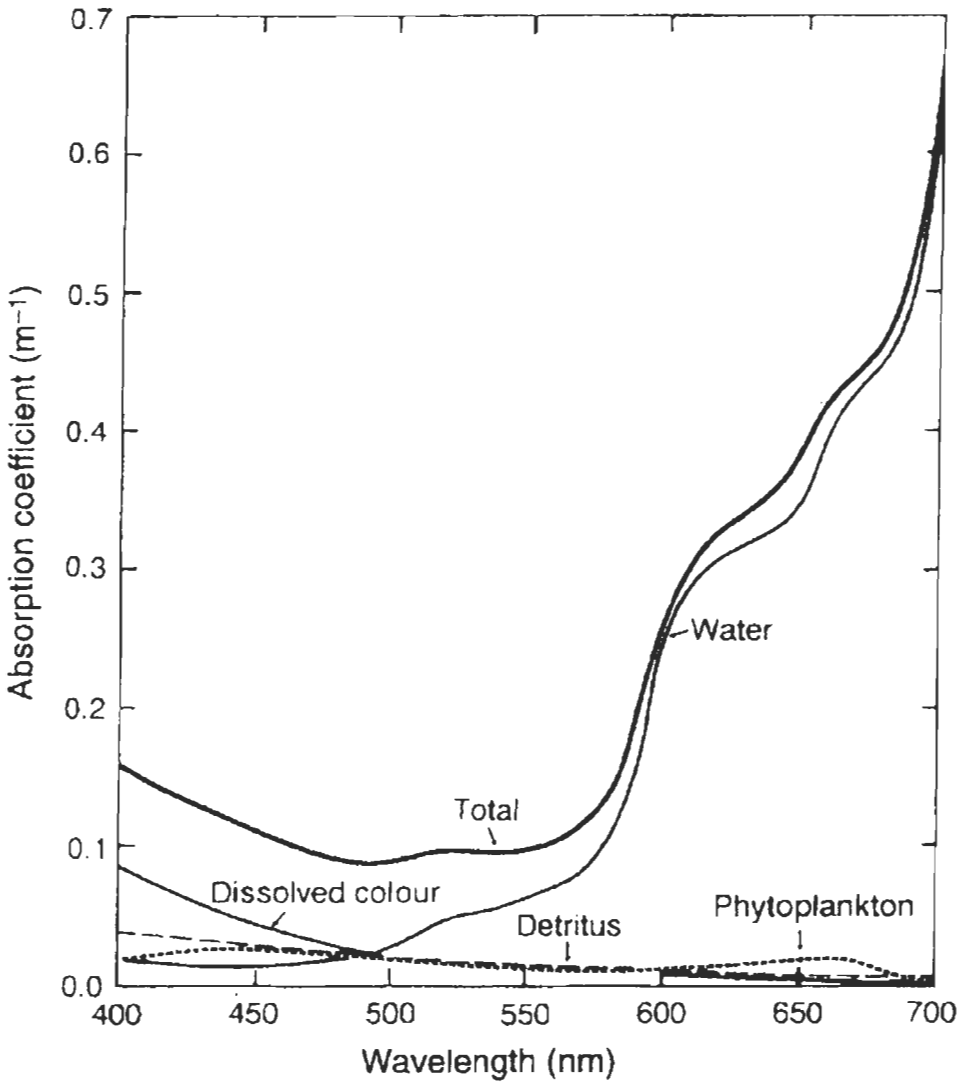
0.7
0.6
0.5
0.4
0.3
0.2
0.1
0.0
Absorption coefficient (m⁻¹)
400
450
500
550
600
650
700
Wavelength (nm)
Water
Total
Dissolved colour
Detritus
Phytoplankton

Figure 4 : Spectres d'absorption spécifique de quelques espèces phytoplanctoniques. Le spectre moyen est en trait épais. Figure extraite de Ahn (1990).

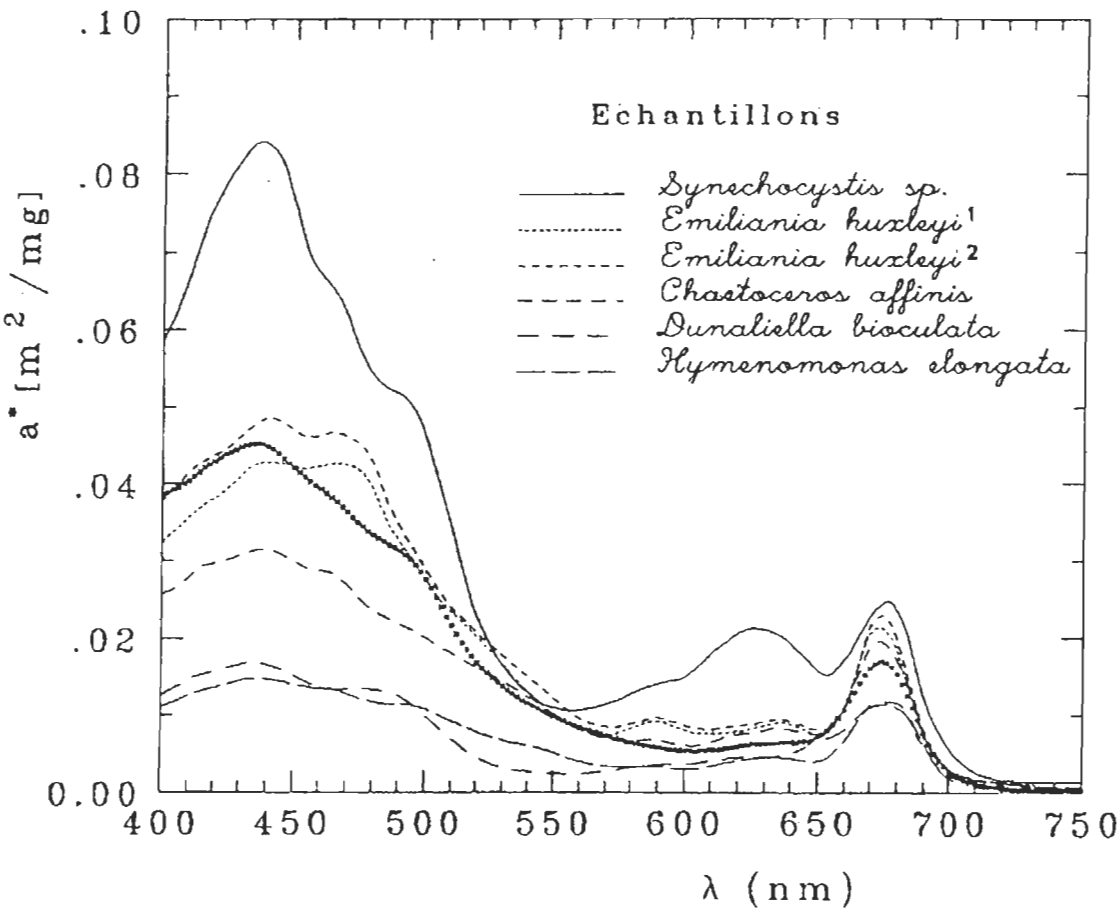
Echantillons
Synechocystis sp.
Emiliania huxleyi 1
Emiliania huxleyi 2
Chaetoceros affinis
Dunaliella bioculata
Hymenomonas elongata
a* [m2 / mg]
.10
.08
.06
.04
.02
0.00
400
450
500
550
600
650
700
750
λ (nm)

Figure 5 : Spectres d'absorption spécifique de certains pigments en solution. Figure extraite de Bricaud et al. (2004).

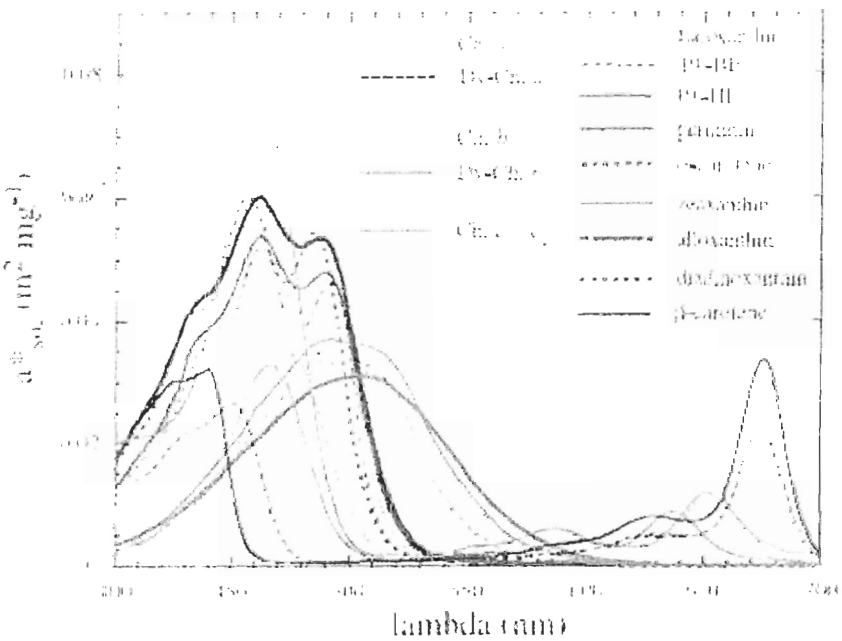
lambda (nm)

La matière particulaire non chlorophyllienne est constitué d'une grande diversité de matériels, tels que les organismes hétérotrophes (bactéries, flagellés, ciliés et virus), le matériel détritique "vrai" associé au phytoplancton et au zooplancton (fragments de micro-organismes, exsudats, pelotes fécales...) ainsi que les particules terrigènes minérales ou organiques (Duce et Tindale 1991, Romero et al. 1999, Claustre et al. 2002). La dépendance spectrale du coefficient d'absorption de cette matière particulaire non chlorophyllienne peut être approximée par une décroissance exponentielle depuis les courtes (ultraviolet) vers les grandes longueurs d'onde (infrarouge) (Bricaud et Stramski, 1990) ; celle-ci se traduit par la relation :

$$a_{NAP}(\lambda) = a_{NAP}(\lambda_0) \times e^{[-S_1(\lambda - \lambda_0)]} \qquad (18)$$

où a_{NAP} (λ_0) est le coefficient d'absorption (m^{-1}) à une longueur d'onde de référence (λ_0, généralement choisie à la limite du rayonnement visible, i.e. autour de 400 nm) et S_1 est la pente caractérisant le matériel rencontré. Les différentes pentes S_1 (de 0.006 à 0.014 nm^{-1}, Kishino et al. 1986, Maske et Haardt 1987, Bricaud et al. 1998) ainsi que les différentes valeurs de a_{NAP} (λ_0) obtenues (de 0.01 à 0.4 m^{-1} - Morrison et Sosik 2002, Chang et Dickey 1999) traduisent la variabilité de l'absorption par la matière particulaire non chlorophyllienne.

La majorité des études s'est attachée à décrire l'absorption de la matière particulaire non chlorophyllienne dans son ensemble. Certains auteurs se sont cependant intéressés de façon plus spécifique à certaines de ses composantes, tels que les organismes hétérotrophes. Le spectre d'absorption des bactéries, ciliés et flagellés hétérotrophes est caractérisé par

une décroissance exponentielle en fonction de la longueur d'onde et présente un maximum entre 410 et 415 nm (associé à la présence de pigments respiratoires, les cytochromes). L'importance de ces organismes en terme d'absorption est toutefois mineure (Morel et Ahn 1990, Ahn 1990). Cependant, certaines bactéries hétérotrophes sont capables de synthétiser des caroténoïdes, à l'origine d'une forte absorption dans le bleu (Stramski et Kiefer 1998). De plus, tout comme leurs hôtes potentiels (les bactéries), les virus sont faiblement absorbants (Stramski et Mobley 1997).

La matière organique dissoute colorée (CDOM) correspond à la fraction absorbante de la matière organique dissoute (Vodacek et al. 1995). Celle-ci est constituée majoritairement d'acides fulviques et humiques (Carder et al. 1989, Coble et al. 1990, Vodacek 1992), mais aussi de carbohydrates (majoritaires), de lipides et d'acétates dans des proportions qui dépendent de la source de production : marine (phytoplancton, zooplancton, bactéries...) ou terrigène (drainage de sols chargés en humus, érosion côtière...) (Aluwihare et al. 1997, Aluwihare et Repeta 1999, Vodacek et al. 1997, Hoge et al. 1998). La composante CDOM est définie expérimentalement comme l'ensemble de la matière absorbante passant au travers d'un filtre de 0,2 µm de porosité. Il englobe une mixture complexe d'espèces chimiques (Coble et al. 1990, Vodacek 1992), en l'occurrence de la matière organique dissoute colorée "vraie", mais aussi de petites particules, des colloïdes (Koike et al. 1990), ainsi que des virus (Balch 2000).

Le spectre d'absorption du CDOM est caractérisé par une décroissance exponentielle en fonction de la longueur d'onde, analogue à celle de l'absorption par la matière particulaire non chlorophyllienne (Jerlov 1968, Bricaud et al. 1981) :

$$a_{CDOM}(\lambda) = a_{CDOM}(\lambda_0) \times e^{[-S_2(\lambda - \lambda_0)]} \quad (19)$$

où $a_{CDOM}(\lambda_0)$ est le coefficient d'absorption de la matière organique dissoute (m^{-1}) à une longueur d'onde de référence λ_0, généralement égale à 400 nm, et S_2 est la pente caractérisant la forme du spectre (nm^{-1}).

La seule différence avec le matériel détritique réside dans la valeur de la pente S_2 généralement plus élevée que S_1 (de 0.011 à 0.035nm^{-1}, Bricaud et al. 1981, Carder et al. 1989, Green et Blough 1994). La pente S_2 varie, selon les sources et les sites étudiés, de 0.011 nm^{-1} dans les eaux côtières (Carder et al. 1989) à 0.014-0.015 nm^{-1} dans l'océan ouvert (Bricaud et al. 1981, Davies-Colley 1992). Des pentes de 0.025 nm^{-1} et 0.034 nm^{-1} ont également été mesurées dans certaines zones restreintes de l'océan ouvert (Green et Blough 1994, D'Sa et al. 1999). La forte absorption du CDOM aux courtes longueurs d'ondes (bleu et UV), est en fait due à l'utilisation de l'énergie lumineuse pour la transformation des molécules organiques en des formes optiquement inactives de carbone organique dissous (Vodacek et al. 1997, Moran et al. 2000, Whitehead et al. 2000), ou bien de façon moins importante en carbone inorganique dissous (Miller et Zepp 1995, Vodacek et al. 1997, Zafiriou et al. 2003) ou encore en peroxyde d'hydrogène (H_2O_2, Andrews et al. 2000).

Diffusion

Le coefficient de diffusion moléculaire de l'eau de mer pure est obtenu par la théorie d'Einstein-Schmoluchowski. Plusieurs études ont mis en évidence une dépendance spectrale de la diffusion de l'eau de mer pure en $\lambda^{-4.3}$ (Morel 1974, Buiteveld et al. 1994).

La valeur du coefficient de diffusion est principalement dépendante de la concentration en particules, de la distribution de taille de ces particules, ainsi que de leur indice de réfraction et de leur forme (Gordon et al. 1984, Kitchen et al. 1982, Spinrad et al. 1983, Baker et Lavelle 1984, Bricaud et Morel 1986, Gardner et al. 1993). La taille et l'indice de réfraction varient fortement entre les différents composants de l'assemblage particulaire (phytoplancton, détritus, hétérotrophes, ...). De ce fait, même s'il existe des informations sur les tailles et indices de réfractions de ces différents composants (Aas 1984) ainsi que sur les contributions relatives de ces derniers à la diffusion totale (Stramski et al. 2004), il est difficile de présenter l'influence de chacun de ces stocks sur le spectre de diffusion. Ainsi, contrairement à l'absorption, les particules diffusantes de la colonne d'eau sont généralement étudiées suivant leur taille ou leur indice de réfraction complexe (m) plutôt qu'en fonction de leur état dans le système (vivant ou détritique) (Morel et Ahn 1991, Voss et al. 1998, Balch 2000).

La valeur de l'indice de réfraction dépend de la composition chimique des particules et de leur densité. La présence dans le milieu d'un grand nombre de constituants avec un

indice de réfraction élevé, tels que le matériel inorganique, augmente le coefficient de diffusion. Dans le cas de particules absorbantes (phytoplancton), l'indice de réfraction est diminué par sa partie imaginaire (n'). L'influence de n' sur n est plus importante à proximité des pics d'absorption caractéristiques des pigments (Bricaud et al. 1983, Morel et Bricaud 1986, Ahn et al. 1992). Ceci se traduit par des dépressions du spectre du coefficient de diffusion à proximité de ces pics (400 à 500 nm et autour de 676 nm) en présence de phytoplancton (Bricaud et al. 1983, Morel et Bricaud 1986, Ahn et al. 1992). En 1991, Morel et Ahn, d'une part, et Stramski et Kiefer, d'autre part, ont établi un bilan de la contribution des micro-organismes au coefficient de diffusion mesuré dans les eaux oligotrophes. Selon ces deux études, plus de 92 % du coefficient de diffusion ou de rétrodiffusion à 550 nm sont dus à la présence des particules de diamètre inférieur à 20 µm. Dans ce compartiment, qui représente la majorité des micro-organismes, les très petites cellules (inférieures à 1 µm, notamment les bactéries hétérotrophes) sont responsables de 86% de la rétrodiffusion alors qu'elles n'interviennent que dans 14% de la diffusion. Les micro-organismes les plus efficaces vis-à-vis de la diffusion sont de taille comprise entre 1 et 10 µm.

En 1973, Morel a établi, pour une population répartie selon une loi de Junge, que la dépendance spectrale du coefficient d'efficacité de la diffusion (x) est liée à l'exposant de Junge (j) caractérisant la distribution de taille des particules.

$$x = \mathrm{j} - 3 \qquad (20)$$

Pour des valeurs suffisamment faibles du paramètre de taille ρ correspondant à la première partie ascendante de la figure 1, Q_b varie alors en λ^{-x} (Morel, 1973). Par exemple, dans le cas de cellules picophytoplanctoniques, la diffusion est fonction de la longueur d'onde et suit approximativement une loi en λ^{-2} (Ahn et al. 1992). Cette tendance s'inverse dans le cas de cellules de plus grande taille, le spectre de diffusion devient neutre.

Rappelons que la distribution de taille des particules dans l'océan est généralement décrite par la fonction puissance suivante, dite loi de Junge (Bader 1970, Jonasz 1983) :

$$\frac{dN}{dd} = K\, d^{-j} \qquad (21)$$

où dN/dd est le nombre de particules dans un intervalle de taille donné (dd), d est la taille moyenne de cet intervalle de taille, K une constante d'amplitude et j l'exposant de Junge. Les valeurs de la constante j dans une population naturelle sont comprises entre 2,5 et 5, la plupart appartenant à l'intervalle [3,5-4] (Bader 1970, Jonasz 1983). De telles valeurs traduisent la prédominance des particules de petite taille.

Tout comme pour l'absorption, le coefficient de diffusion spécifique à la chl-*a* (b^*) dépend de la concentration intracellulaire en pigments et de la taille des cellules (Morel 1987). Les faibles valeurs de b^* correspondent à de grosses cellules phytoplanctoniques ayant des contenus cellulaires en chlorophylle relativement élevés. Cependant, les coccolithophoridés (recouverts de plaques de carbonate de calcium diffusantes, les

coccolithes) diffusent plus par unité de chlorophylle, que les espèces de même taille appartenant à d'autres groupes phytoplanctoniques (Balch et al. 1991).

La composition du milieu marin influence donc fortement les propriétés absorbantes et diffusantes de celui-ci. Une connaissance détaillée des caractéristiques (abondance, taille, propriétés optiques...) des principaux éléments qui absorbent et diffusent la lumière dans la colonne d'eau ainsi que des différents paramètres physiques, chimiques et biologiques qui en contrôlent les variations est nécessaire pour caractériser les IOPs des océans (Iturriaga et Siegel 1989) (Tableau 2). Parmi les particules marines, les détritus organiques, le phytoplancton et les bactéries sont des sources majeures de variabilité des IOPs des océans (Stramski et Kiefer 1991) ceci en raison de leur concentration nettement supérieure à celle des grandes particules (Kiefer 1984). Par ailleurs, afin de déterminer l'impact du phytoplancton sur les variations de la couleur des océans, il est nécessaire de quantifier son influence sur les IOPs (Morel 1988, Bricaud et al. 1983).

D'autre part, l'utilisation des coefficients spécifiques d'absorption et de diffusion se rapportant à la chl-*a* permet de relier les propriétés optiques du milieu (absorption ou diffusion) au contenu en phytoplancton qui reste le principal acteur de la modification du champ radiatif notamment en océan ouvert (Bricaud et al. 1983, Morel 1987, Bricaud et al. 1995, 1998, Loisel et Morel 1998).

Tableau 2 : Les différents composants contribuant aux variations des IOPs des océans (- : contribution non-significative, + : contribution significative, + + : contribution très significative, + + + : contributeur majeur) (modifié d'après Mobley 1994 et Zhang et al. 2002).

Type	Taille (µm)	Concentration (particules /m^3)	Contribution		
			a	*b*	b_b
Virus	2×10^{-2} - 25×10^{-2}	10^{12} - 10^{15}	–	–	+ +
Colloïdes	≤ 0,1 - 1	10^{13} - 10^{15}	+		+ +
Bactéries	0,2 - 1	10^{11} - 10^{13}	+	+ +	+ + +
Bulles d'air	> 10	Très variable		–	+ + +
Phytoplancton	0,2 - 200	Très variable	+ +	+ +	+ ou ++ (selon la taille)
Détritus organiques	Très variable	Très variable	– ou ++ (selon la présence de pigment)		+++ (si < 1 µm et faible n)
Grandes particules (zooplancton et agrégat de petites particules : neige marine)	> 100 - 10^5	0-10^3		+ +	+ +
Particules inorganiques	< 1 - 10^4	Très variable	Une attention insuffisante a été portée aux effets optiques de ces particules dans les océans		

LE PHYTOPLANCTON

Les propriétés optiques des cellules phytoplanctoniques

Les cellules vivantes répondent rapidement (i.e., en l'espace de quelques minutes à quelques heures) aux changements environnementaux par des changements d'abondance, de taille, de forme et de composition interne. Les facteurs environnementaux régulent non seulement la concentration mais également les propriétés optiques des cellules phytoplanctoniques. Ces facteurs sont donc importants pour l'interprétation des variabilités des IOPs dans les océans (Reynolds et al. 1997, Sosik et al. 1998, 2001).

La variabilité des IOPs des océans (Kirk 1994, Stramski et al. 1995, Stramski et Mobley 1997, Green et al. 2000, Stramski et al. 2002) est due pour une part importante :

(1) aux changements de caractéristiques optiques de la communauté phytoplanctonique, caractéristiques qui dépendent de la composition en espèces de la communauté et de la concentration de chaque espèce phytoplanctonique, liées aux variations des conditions physico-chimiques du milieu.

(2) aux changements des caractéristiques optiques (absorption et diffusion) de la cellule phytoplanctonique, caractéristiques qui dépendent de l'espèce considérée et des

processus d'acclimatation morphologique et physiologique de cette espèce (Claustre et al. 1999). Ces processus peuvent être cycliques et prédictibles (diurne et saisonnier) et/ou épisodiques et imprédictibles (périodes de floraison, tempête, advection horizontale et/ou verticale) et peuvent varier dans l'espace.

L'interprétation de la variabilité des IOPs des océans passe donc par une prise en compte non seulement des concentrations cellulaires et de la structure des communautés phytoplanctoniques mais également des caractéristiques optiques cellulaires (Ackleson et Cullen 1991, Babin et al. 1993) (Tableau 3).

D'autre part, les petites cellules phytoplanctoniques (<20 µm) sont une des composantes principales, avec les bactéries, du réseau trophique microbien marin (Sherr et Sherr 2000). Elles jouent un rôle essentiel dans les écosystèmes marins (Johnson et Sieburth 1979, Li et al. 1983, Platt et al. 1983, Takahashi et Bienfang 1983, Glover et al. 1985, Mostajir et al. 2001). De plus, le plancton de taille <20 µm, incluant les bactéries hétérotrophes, les cyanobactéries et les eucaryotes autotrophes, forme la principale source de variations des IOPs des océans (Kiefer 1984, Stramski et Kiefer 1991, Morel 1991, Mobley et Stramski 1997, DuRand et Olson 1996). Il s'avère donc indispensable de connaître et de comprendre les processus régulant l'abondance et les caractéristiques optiques cellulaires du phytoplancton de petite taille (Reynolds et al. 1997, Sosik et al. 2001), ainsi que de déterminer leur contribution aux variations des IOPs des océans. Ceci

pourrait alors mener à une meilleure interprétation des mesures de la couleur des océans et à une meilleure estimation de la biomasse et de la production primaire à grande échelle (DuRand et Olson 1996).

Avant d'entreprendre les mesures sur le terrain, il est nécessaire de déterminer, en laboratoire, le comportement des propriétés optiques cellulaires du phytoplancton (<20 µm) face aux variations de facteurs environnementaux. Par exemple, des variations de l'intensité de la lumière incidente entraînent des changements de composition et de concentration en pigments des cellules phytoplanctoniques (Falkowski 1980, 1984a). Des variations de la composition pigmentaire affectent alors les propriétés d'absorption et de diffusion des cellules phytoplanctoniques (Zaneveld et Kitchen 1995). La principale difficulté réside toutefois dans la variabilité inter- et intraspécifique de ces propriétés optiques cellulaires. Afin d'évaluer et de comprendre cette variabilité inter et intra-spécifique des propriétés optiques cellulaires du phytoplancton, des expériences doivent être réalisées sur différentes espèces phytoplanctoniques (<20 µm) et à différentes échelles temporelles (quelques heures à quelques jours), en contrôlant les paramètres environnementaux.

Tableau 3 : Propriétés optiques cellulaires (N : nombre de cellules par m^3, d : diamètre cellulaire, PSD : distribution de taille, n : partie réelle de l'indice de réfraction, n' : partie imaginaire de l'indice de réfraction, *a* : coefficient d'absorption) (Mobley 1994).

Propriétés optiques cellulaires	Unités	Symbole	Données nécessaires	Autres Formules
Section efficace optique :				Exemple
d'atténuation	$m^2 \cdot cellule^{-1}$	σ_c		$\sigma_a = a / N$
d'absorption		σ_a		$\sigma_a = Q_a \times (\pi d^2/4)$
de diffusion		σ_b		
Facteur d'efficacité :				
d'atténuation	Sans	Q_c	PSD, n et n' $\rightarrow Q_c$	Exemple
d'absorption	dimension	Q_a	PSD et n' $\rightarrow Q_a$	$Q_a = \sigma_a / (\pi d^2/4)$
de diffusion		Q_b	Q_a et $Q_c \rightarrow Q_b$	

La cytométrie en flux offre la possibilité d'obtenir des mesures à l'échelle de la cellule (Yentsch et al. 1983, Olson et al. 1985, Cullen et al. 1988) et de fournir des informations quantitatives sur les caractéristiques cellulaires de la majorité des constituants du plancton de petite taille (0,2-20 µm) (Olson et al. 1990). L'utilité de la cytométrie en flux pour le dénombrement des plus petits composants des communautés phytoplanctoniques a été clairement démontrée ces dernières années dans diverses études sur le picophytoplancton (<2 µm) (Olson et al. 1985, 1990, Li et Wood 1988, Mostajir et al. 2001). La cytométrie en flux est, de plus, une technique de mesure rapide de la diffusion de la lumière et de la fluorescence des particules individuelles (Shapiro 1988). Elle a été appliquée, dans un premier temps, dans des études d'identification et de caractérisation du phytoplancton (Olson et al. 1985, Demers et al. 1989, Moreira-Turcq et Martin 1998, Collier 2000) puis dans la détermination des propriétés optiques cellulaires du phytoplancton (Spinrad et Brown 1986, Spinrad et Yentsch 1987, Ackleson et Spinrad 1988, Jacquet et al. 1998, 2002, Green et al. 2000). La cytométrie en flux offre donc la possibilité d'évaluer rapidement et de façon précise les propriétés optiques cellulaires du phytoplancton de taille comprise entre 0,2 et 20 µm (Spinrad 1984, Ackleson et Spinrad 1988, Perry et Porter 1989, DuRand et Olson 1996, Green et al. 2000). Cette technique permet (1) de mieux caractériser les IOPs des océans par la détermination des propriétés optiques cellulaires du phytoplancton (<20µm) et ainsi (2) d'évaluer le rôle de ces cellules phytoplanctoniques sur les variations des IOPs des océans.

Particularités des propriétés optiques cellulaires du phytoplancton

Une littérature considérable a été accumulée sur les propriétés optiques cellulaires de différentes espèces phytoplanctoniques (<20 µm) en culture mono-spécifique. Un certain nombre de travaux ont montré que les caractéristiques optiques (atténuation, diffusion, rétrodiffusion et absorption de la lumière) des cellules phytoplanctoniques étaient influencées par : 1) la taille (Morel et Bricaud 1986, Bricaud et al. 1988, Mitchell et Kiefer 1988, Morel et al. 1993, DuRand et Olson 1996, 1998), 2) la forme et l'indice de réfraction (Ackleson et al. 1990), 3) la structure interne (Król et al. 1992, Volten et al. 1998), 4) la concentration et la composition pigmentaire de ces cellules (Morel et al. 1993, Babin et al. 1993, Ohi et al. 2002), 5) la nature et l'état de développement de leurs structures internes (Stramski et Reynolds 1993, Stramski et al. 1995, DuRand et al. 2000). Par exemple, les structures internes cellulaires telles que les vacuoles altèrent considérablement la diffusion de la lumière des cellules phytoplanctoniques. De plus, des travaux ont souligné les variations temporelles des propriétés optiques cellulaires des micro-organismes et la grande variabilité inter- et intra-spécifique de ces propriétés (Kiefer et al. 1979, Bricaud et al. 1983, Mobley et Stramski 1997, Bricaud et al. 1998, Balch et al. 1999). En effet, l'absorption et la diffusion des cellules algales varient soit d'une espèce à l'autre, constituant dans certains cas une caractéristique optique exclusive d'une espèce donnée, soit pour une espèce donnée, selon les changements de taille, de forme, de composition en pigments, de physiologie et de stratégie adaptative des cellules phytoplanctoniques, en réponse aux conditions environnementales (Reynolds et al. 1997).

Facteurs de variabilité des propriétés optiques cellulaires du phytoplancton

Les propriétés optiques des cellules phytoplanctoniques (absorption et diffusion) varient en fonction des phénomènes qui modifient la taille, la forme, l'indice de réfraction, la structure interne, et la concentration et composition pigmentaire, tels que : (1) le cycle jour-nuit, (2) les variations physiologiques dues à la photoacclimatation et (3) les variations physiologiques dues à la phase de croissance (Kiefer et al. 1979).

• *Le cycle journalier*. Ces dernières années, une attention grandissante est prêtée aux variations journalières des IOPs des océans. En effet, la plus importante gamme de variations des caractéristiques cellulaires du phytoplancton est due au cycle jour-nuit (Owens et al. 1980, DuRand et Olson 1998, DuRand et al. 2000, 2002, Jacquet et al. 2001, Bruyant et al. 2005), coïncidant souvent avec le temps de génération d'une cellule phytoplanctonique. Cependant, ces variations ont généralement été ignorées dans l'interprétation des IOPs. Elles pourraient, pourtant, expliquer une partie significative de la variabilité observée dans ces IOPs (Stramski et Reynolds 1993). Pour mieux interpréter les mesures des IOPs des océans, les variations journalières des propriétés optiques des cellules phytoplanctoniques doivent donc être mieux comprises (DuRand et Olson 1998). Par conséquent, les variations nycthémérales des propriétés optiques cellulaires du phytoplancton de petite taille (<20µm) liées aux processus de photosynthèse, de division cellulaire (changement de taille et d'indice de réfraction), à la fluorescence et à l'activité biochimique ont été étudiées intensivement sur le terrain et en laboratoire (Ackleson et al.

1990, Stramski et Reynolds 1993, Van Bleijswijk et al. 1994, Stramski et al. 1995, Fisher et al. 1996, DuRand et Olson 1996, 1998, Stramski et Mobley 1997, DuRand et al. 2000, 2002, Claustre et al. 2002, Jacquet et al. 2002, Ohi et al. 2002). De nombreuses études ont ainsi montré que les variations journalières de ces propriétés optiques cellulaires s'effectuaient sur une échelle de temps allant de l'heure à la journée (Stramski et Reynolds 1993, Van Bleijswijk et al. 1994, Stramski et al. 1995, DuRand et Olson 1996, 1998, Stramski et Mobley 1997, DuRand et al. 2000, 2002, Claustre et al. 2002, Ohi et al. 2002). Ces travaux montrent ainsi que les sections efficaces d'absorption σ_a et de diffusion σ_b augmentent le jour au cours de la photosynthèse et diminuent la nuit lors de la division cellulaire. Cependant les différentes espèces étudiées ont montré des contributions très variables de la taille et de l'indice de réfraction des cellules phytoplanctoniques sur les variations journalières de leurs $\sigma_{a,b}$. Par exemple, chez *Synechococcus*, les variations journalières de l'indice de réfraction et de la taille cellulaire sont reliées significativement aux variations journalières des $\sigma_{a,b}$ (Stramski *et al.* 1995). Par contre, chez *Micromonas pusilla*, seule la variation journalière de la taille des cellules est associée significativement à celle de leur σ_b (DuRand et al. 2002).

• *La photoacclimatation.* Le phénomène d'ajustement de la physiologie cellulaire en réponse aux variations d'intensité lumineuse est appelé photoacclimatation (Geider et al. 1996). La photoacclimatation consiste en des modifications de caractéristiques cellulaires, c'est-à-dire des changements de taille, morphologiques et physiologiques des cellules

phytoplanctoniques (Falkowski 1980, 1992, Richardson et al. 1983, Claustre et Gostan 1987, Falkowski et LaRoche 1991, Geider et al. 1996, 1998). Par exemple, à de fortes intensités, le diamètre d'une cellule phytoplanctonique augmente alors que sa concentration en chlorophylle et son indice de réfraction diminuent (Green et al. 2000). La photoacclimatation des cellules phytoplanctoniques se fait également à différentes échelles temporelles (Falkowski 1984a et b, Stramski et al. 1993). Ainsi, les modifications de la composition pigmentaire des cellules se manifestent en l'espace de quelques heures à quelques jours (Falkowski 1980, Prézelin et Matlick 1980, Gallegos et al. 1983, Post et al. 1984). Par contre les changements de concentration de certains pigments photoprotecteurs (exemple : diatoxanthine et diadinoxanthine) opèrent en quelques minutes (Sakshaug et al. 1987, Demers et al. 1991). Enfin, la cinétique et l'amplitude des variations du contenu pigmentaire dépendent de l'espèce phytoplanctonique considérée (Falkowski 1980, Richardson et al. 1983). Falkowski (1980) a montré que les chlorophycées ont une plus grande capacité à changer leur contenu pigmentaire que les diatomées et les dinoflagellés. De plus, par modification des caractéristiques cellulaires du phytoplancton, la photoacclimatation contribue aux variations des propriétés optiques des cellules phytoplanctoniques (Neori et al. 1984, Ackleson et al. 1990, Stramski et Morel 1990, Ackleson et Cullen 1991, Babin et al. 1997, DuRand et Olson 1998, Bricaud et al. 1999, Moisan et Mitchell 1999, Sciandra et al. 2000, Fujiki et Taguchi 2001, Ohi et al. 2002). Parmi les études traitant de l'effet de la photoacclimatation sur les variations des propriétés optiques des cellules phytoplanctoniques (<20µm) (Ackleson et al. 1990, Morel et Bricaud 1986, Morel et al. 1987, DuRand et Olson 1998, DuRand et al. 2000, 2002, Sciandra et al.

2000, Green et al. 2002, Ohi et al. 2002), peu d'entre elles ont combiné l'étude des variations journalières de ces propriétés (Stramski et Reynolds 1993, Stramski et al. 1995, DuRand et Olson 1998, Ohi et al. 2002).

• *La phase de croissance*. Les propriétés optiques cellulaires du phytoplancton varient selon l'espèce, mais également selon la phase de croissance des cellules (i.e., lag, exponentielle, stationnaire ou déclin), via des changements de concentration et/ou de composition pigmentaire, de développement de chloroplastes et de morphologie cellulaire (Kiefer et al. 1979, Spinrad et Yentsch 1987, Voss et al. 1998, McLeroy-Etheridge et Roesler 1998). Il serait alors intéressant de déterminer les propriétés optiques cellulaires, aux différents stades de développement, pour plusieurs espèces phytoplanctoniques. Or, dans la majorité des cas, les études sur les propriétés optiques cellulaires du phytoplancton (<20 μm) sont restreintes à la phase exponentielle, et seules certaines ont porté sur ces propriétés optiques cellulaires durant plusieurs phases de croissance (Kiefer et al. 1979, Voss et al. 1998, McLeroy-Etheridge et Roesler 1998, Stramski et al. 2002). Par exemple, Stramski et al. (2002) montrent que la section efficace d'absorption σ_a et la partie imaginaire de l'indice de réfraction n' d'une cellule de *Thalassiosira pseudonana* sont plus élevées quand cette dernière est en phase exponentielle (non limitée en nitrates) que lorsqu'elle est en phase stationnaire (limitée en nitrates). Par contre, la section efficace de diffusion σ_b, la partie réelle de l'indice de réfraction n et la taille de cette cellule sont moins élevées en phase exponentielle qu'en phase stationnaire. Il est à noter, que ce type d'étude permet de simuler un bloom phytoplanctonique avec une diminution temporelle des sels

nutritifs disponibles. Les phases lag, exponentielle et déclin correspondent alors aux périodes de pré-bloom, de bloom et de post-bloom.

Malgré le nombre croissant d'études sur les particularités des différentes propriétés optiques cellulaires (absorption et diffusion) du phytoplancton, les informations sont encore manquantes pour une large gamme d'espèces phytoplanctoniques de petite taille (<20 µm), ce qui reste un obstacle à une meilleure compréhension du rôle joué par ce phytoplancton (<20 µm) sur la variabilité des IOPs des océans.

Le phytoplancton de petite taille (<20 µm), facteur de variations des IOPs des océans

Au début des années 1990, les premiers modèles d'IOPs des océans ne considéraient qu'un petit nombre de constituants, tels que le CDOM, le phytoplancton, les détritus, et l'eau (Mobley 1994). Plus récemment, Stramski et al. (2001) ont amélioré ces modèles en simulant les contributions aux IOPs des océans de 18 composants planctoniques allant de la taille d'un virus (<0,2 µm) à celle d'espèces microplanctoniques de 30 µm de diamètre, de détritus, de particules minérales, et de bulles d'air. Pour appliquer ce type de modèle au milieu naturel, il est nécessaire de caractériser les différents types de particules, qui contribuent de façon significative aux IOPs des océans, en terme de concentration et de

propriétés cellulaires (distribution de taille, indice de réfraction, caractéristiques physiologiques et optiques) (Stramski et al. 2001).

Les quelques études réalisées en milieu naturel sur la contribution du phytoplancton de petite taille aux IOPs des océans montrent une grande diversité de réponses (Chung et al. 1998, Green et al. 2003). Ainsi, dans le Pacifique équatorial, Chung et al. (1998) ont montré que les principales formes responsables de l'atténuation particulaire totale sont les particules détritiques non-vivantes (50%), les bactéries hétérotrophes (16%) ainsi que les grandes cellules nanophytoplanctoniques (10-20 µm), microphytoplanctoniques (>20 µm) et les protistes hétérotrophes (20%). Les petits eucaryotes autotrophes (<3 µm), quant à eux, représentent seulement 2% de l'atténuation particulaire totale. Par contre, Green et al. (2003) ont montré que dans les eaux de surface des côtes de la Nouvelle Angleterre, les cellules phytoplanctoniques (<20 µm) sont les principaux contributeurs de l'absorption particulaire totale (28% en été et 39% au printemps) et de la diffusion particulaire totale (44% en été et 61% au printemps).

Les différentes études démontrent que les variations spatio-temporelles de la contribution du phytoplancton de petite taille (<20 µm) aux IOPs des océans sont largement associées aux variabilités de leurs propriétés optiques cellulaires. Ces dernières, en milieu naturel, sont régulées par leur environnement (stratification, cycle jour-nuit, disponibilité en

lumière et en nutriments...), via des changements de forme, de taille, d'indice de réfraction et de physiologie de ces cellules phytoplanctoniques (Chung et al. 1998, Green et al. 2003).

CARACTERISTIQUES OPTIQUES DES EAUX DE L'ESTUAIRE ET DU GOLFE DU SAINT-LAURENT

Morel et Prieur (1977) ont défini des eaux marines du Cas 1 et du Cas 2. Par définition, les eaux du Cas 1 sont celles où le phytoplancton et le matériel vivant (bactéries, etc.) et non vivant (dû au broutage, à la lyse virale ou à la mort de la cellule) qui lui sont associés, sont les principaux agents responsables des variations des IOPs de l'eau (Morel et Prieur 1977, Loisel et Morel 1998). La situation est plus complexe pour les eaux du Cas 2 car elles présentent (1) une grande variété de processus physico-chimiques (bathymétrie, mélange vertical, turbidité, salinité, température, éléments nutritifs) et biologiques (structure du réseau trophiques) (Morel et Prieur 1977, Bukata et al. 1995, Ciotti et al. 1999) et (2) de grandes quantités de matériels absorbants et diffusants (particules terrigènes, CDOM ...) introduites dans l'eau de surface par remise en suspension des sédiments et par apports continentaux (Carder et al. 1989).

A l'heure actuelle, les algorithmes qui permettent de déduire la biomasse algale (chl-*a*) à partir des signaux satellitaires, ne sont pas applicables à tous les milieux. Ils ont été développés pour certaines eaux du Cas 1 et ne fonctionnent généralement pas pour les eaux du Cas 2, qui se caractérisent par une forte hétérogénéité optique (Gordon et al. 1988, Morel 1988, Morel et Maritorena 2001). Par exemple, dans les eaux du Cas 2, les concentrations de chl-*a,* dérivées des mesures satellitaires et calculées avec l'algorithme standard SeaWiFs, présentent souvent des valeurs plus grandes que celles mesurées *in situ* (Gons et al. 2000). Ceci souligne, par conséquent, la difficulté à prédire, dans les eaux du Cas 2, la concentration en chlorophylle phytoplanctonique à partir des propriétés optiques des océans (Smith et Baker 1978a et b, Gordon 1989).

Contrairement à d'autres régions caractérisées par des eaux du Cas 1 et du Cas 2, l'Estuaire et le Golfe du Saint-Laurent (Canada) ont été peu étudiés du point de vue des IOPs et des facteurs qui en contrôlent la variabilité (Babin et al. 1993 et 1995, Nieke et al. 1997). Le système du Saint-Laurent est une mer intérieure partiellement fermée, avec des ouvertures vers l'océan Atlantique par les détroits de Cabot et de Belle-Isle (Fig. 4). Ses masses d'eau sont fortement stratifiées (El-Sabh 1979). Il peut être divisé en trois régions distinctes : l'Estuaire fluvial, l'Estuaire maritime, et le Golfe (Brunel 1970, El-Sabh 1979). L'Estuaire fluvial est caractérisé en surface par la présence d'un fort gradient horizontal de salinité avec des eaux douces près de la ville de Québec et des eaux plus salées (20 psu) près de l'embouchure du fjord du Saguenay (El-Sabh 1979). L'Estuaire maritime, qui s'étend du fjord du Saguenay à Pointe des Monts, est caractérisé par des salinités de surface

variant entre 20 et 30 psu. La distribution spatiale des eaux de surface démontre une forte influence des caractéristiques physiques telles qu'une zone d'upwelling près de l'embouchure du fjord du Saguenay (Forrester 1974, Therriault et Lacroix 1976), un grand panache d'eau douce provenant des rivières Manicouagan et Aux-Outardes (Therriault et Levasseur 1985, 1986, Therriault et al. 1985), et le courant de Gaspé le long de la péninsule de la Gaspésie (Tang 1980, El-Sabh 1979). Les eaux de surface du Golfe sont la plupart du temps caractérisées par des eaux du Cas 1, reflétant leur connexion avec l'Atlantique. La région sud-ouest du golfe est fortement influencée par la sortie du Courant de Gaspé. La circulation de surface dans le système du Saint-Laurent est principalement régie par les entrées d'eau douce provenant de l'estuaire fluvial et des nombreuses rivières affluentes et par les eaux salées entrant dans le Golfe par les détroits de Belle-Isle et de Cabot (Neu 1970). Le Saint-Laurent marin est donc une région complexe où des eaux du Cas 1 côtoient des eaux du Cas 2 (Babin et al. 1993). Cette complexité est liée à une importante variabilité spatio-temporelle des caractéristiques physiques et chimiques (Ingram 1975, Levasseur et al. 1984, Ingram et El-Sabh 1990), entraînant des variations rapides et répétées de la salinité, de la température, de la turbidité, de l'intensité du mélange vertical, des concentrations en sels nutritifs et en substances humiques,... (El Sabh 1979). Comme mentionné plus haut, les variations des facteurs abiotiques entraînent des variations de la biomasse phytoplanctonique, des taux de production primaire, de la structure, de la distribution spatiale et temporelle des communautés phytoplanctoniques (Prakask 1975, Olson et al. 1985, Therriault et Levasseur 1985, 1986, Therriault et al. 1990, de Lafontaine et al. 1991, Agawin et al. 2000, Doyon et al. 2000) ainsi que des changements des

caractéristiques cellulaires et des propriétés optiques (encore mal connues) des cellules phytoplanctoniques, contribuant aux erreurs d'estimation de la biomasse phytoplanctonique par les algorithmes.

Figure 6 : Le système du Saint-Laurent. Figure extraite d'El-Sabh (1979).

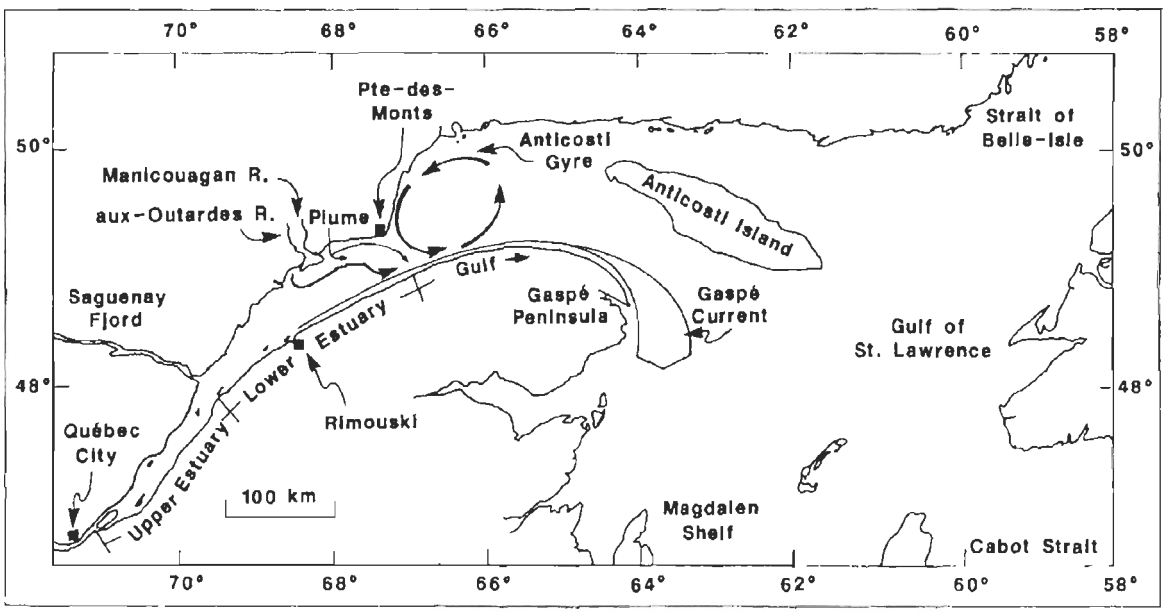
70°
68°
66°
64°
62°
60°
58°
50°
48°
Pte-des-Monts
Anticosti Gyre
Strait of Belle-Isle
Manicouagan R.
aux-Outardes R.
Plume
Anticosti Island
Gulf
Saguenay Fjord
Gaspé Peninsula
Gaspé Current
Gulf of St. Lawrence
Lower Estuary
Upper Estuary
Rimouski
Québec City
100 km
Magdalen Shelf
Cabot Strait

Le système de l'Estuaire et du Golfe du Saint-Laurent, combinant des eaux du Cas 1 et du Cas 2, est donc un excellent laboratoire naturel pour valider les données de télédétection. De plus, la taille de ce système permet un échantillonnage relativement aisé sur le terrain (minimum de déploiement de navires) facilitant la validation de nouveaux modèles de télédétection pour le Saint-Laurent.

Les premiers travaux appliquant la télédétection à l'estimation de chlorophylle dans le Saint-Laurent suggèrent de fortes variations spatio-temporelles de concentration en chlorophylle dans le Golfe du Saint-Laurent (Fuentes-Yaco 1995, 1998). Ces concentrations semblent varier selon un cycle bi-modal, en accord avec les données *in-situ*, avec de fortes valeurs au début du printemps et à la fin de l'été.

Certaines études ont montré la forte présence de phytoplancton de petite taille (<20 µm) dans l'écosystème du Saint-Laurent (Sévigny et al. 1979, de Lafontaine et al. 1991, Lovejoy et al. 1993, Rivkin et al. 1996, Martin-Olivier 1997). Par exemple, Lovejoy et al. (1993) notent que durant le printemps, les cellules picophytoplanctoniques sont les organismes autotrophes les plus abondants des eaux de l'Estuaire fluvial du Saint-Laurent. Les travaux de Rivkin et al. (1996) ont par ailleurs montré que sous des conditions ne favorisant pas une floraison printanière, les eaux du golfe du Saint-Laurent sont largement dominées par le picophytoplancton et les processus de régénération. Sévigny et al. (1979) ont, quant à eux, montré que dans la partie Nord-Ouest des eaux du golfe du Saint-Laurent

(gyre cyclonique permanente), la croissance phytoplanctonique était limitée par les concentrations en sels nutritifs en été. Par conséquent, les diatomées de grande taille étaient remplacées par des flagellés de petite taille. Les eaux du golfe ont une structure de communauté phytoplanctonique mal connue, mais, les petites cellules devraient également prédominer (Sévigny et al. 1979). Enfin, en période estivale dans les eaux de la région de l'île d'Anticosti, 80% des cellules phytoplanctoniques ont une taille inférieure à 15 µm (de Lafontaine et al. 1991).

En raison de l'importance du phytoplancton de petite taille (<20 µm) dans l'écosystème du Saint-Laurent (Estuaire et Golfe) il nous parait donc essentiel de connaître et de comprendre comment la variabilité spatio-temporelle des caractéristiques physiques et chimiques de cet écosystème influence les propriétés optiques et cellulaires des communautés phytoplanctoniques de petite taille (<20 µm) ainsi que leur abondance. Ceci permettra de déterminer le rôle de ces communautés sur les IOPs des eaux du Saint-Laurent et par la suite d'améliorer les algorithmes appropriés pour cet écosystème.

OBJECTIFS

En 1998, le groupe CARTEL de l'université de Sherbrooke, en collaboration avec des chercheurs de l'Institut des sciences de la mer à Rimouski (ISMER) et du Ministère de Pêches et Océans (MPO), Institut Maurice Lamontagne (IML), a mis en place un programme de recherche ayant pour but d'élaborer des algorithmes semi-analytiques qui permettront d'estimer les concentrations de chl-*a* dans les eaux de l'estuaire et du golfe du Saint-Laurent à partir d'images satellitaires. Afin de valider ces algorithmes ou modèles, il est nécessaire de les paramétrer. De ce fait, chaque projet de ce programme de recherche correspond à l'étude d'une composante des signaux reçus par SeaWiFs, tels que la composante venant de l'atmosphère, celle venant de l'ensemble des constituants des eaux de surface ou celle venant d'un de ces constituants (CDOM, phytoplancton total, phytoplancton de petite taille (<20 µm) ...). Ce projet de doctorat, qui porte sur « Le rôle des cellules phytoplanctoniques de petite taille (<20 µm) sur les variations des propriétés optiques des eaux du Saint-Laurent» s'inscrit dans le cadre de ce programme de recherche multidisciplinaire.

Afin de définir l'impact du phytoplancton de petite taille (<20 µm) sur les variations des propriétés optiques du Saint-Laurent, il est nécessaire (1) de déterminer en milieu contrôlé les particularités et les facteurs de variabilité des propriétés optiques cellulaires du phytoplancton de petite taille (<20 µm) des eaux du Saint-Laurent, et (2) d'évaluer la

contribution des cellules phytoplanctoniques de petite taille (<20 µm) sur les propriétés optiques globales des masses d'eau du Saint-Laurent marin.

Le premier objectif spécifique de cette thèse est d'évaluer l'influence des variations liées au cycle journalier, ainsi qu'aux processus de photoacclimatation à court terme, sur les propriétés optiques cellulaires et les IOPs d'espèces phytoplanctoniques (<20 µm) en milieu contrôlé. Le deuxième objectif est d'estimer l'effet des conditions physiologiques liées à la succession des phases de croissance à long terme sur les propriétés optiques cellulaires et les IOPs d'espèces phytoplanctoniques, ainsi que l'interférence de la présence des bactéries et du matériel détritique sur la mesure des IOPs. Et enfin, le troisième objectif est de déterminer la contribution des cellules phytoplanctoniques (<20 µm) aux IOPs des eaux de l'estuaire et du golfe du Saint-Laurent, après avoir déterminé la distribution spatio-temporelle de l'abondance et des propriétés cellulaires (taille, physiologie et caractéristiques optiques) des cellules phytoplanctoniques (<20 µm).

Les deux premiers objectifs ont été réalisés au moyen de cultures de plusieurs espèces phytoplanctoniques présentes dans les eaux de l'estuaire et du golfe du Saint-Laurent : *Thalassiosira pseudonana* et *Imantonia rotunda* lors des expériences à court et à long terme, et *Nannochloropsis* sp. et *Alexandrium tamarense* lors des expériences à long terme. Le troisième objectif a été complété suite à deux campagnes de validation SeaWiFs en 2000 et en 2001 dans l'estuaire et le golfe du Saint-Laurent.

CHAPITRE 1:

DIEL VARIATIONS IN OPTICAL PROPERTIES OF *IMANTONIA ROTUNDA* (HAPTOPHYCAE) AND *THALASSIOSIRA PSEUDONANA* (BACILLARIOPHYCAE) EXPOSED TO DIFFERENT IRRADIANCE LEVELS.

RÉSUMÉ

Les variations journalières des propriétés optiques cellulaires ont été étudiées pour deux espèces, l'haptophyte *Imantonia rotunda* Reynolds et la diatomée *Thalassiossira pseudonana* (Hustedt) Hasle, cultivées sous un cycle jour-nuit de 14 :10-h et transférées de 100 µmol photon·m^{-2}·s^{-1} à de plus forte intensités lumineuse de 250 et 500 µmol photon·m^{-2}·s^{-1}. Le volume cellulaire, l'abondance, les coefficients d'absorption du phytoplancton, la diffusion de la lumière et la fluorescence cellulaire estimées par cytométrie en flux, ainsi que la composition pigmentaire ont été mesurés toutes les 2-h sur une période de 24-h. Les résultats montrent que la division cellulaire était plus synchrone pour *I. rotunda* que pour *T. pseudonana*. Plusieurs variables présentaient des variations journalières d'une amplitude >100%, notamment le volume cellulaire moyen pour l'haptophyte, et les caroténoïdes photoprotecteurs pour les deux espèces ; alors que l'amplitude des variations journalières des propriétés optiques, telles que la diffusion estimée par cytométrie en flux et l'absorption du phytoplancton spécifique à la chl-*a*, était généralement <50%. L'augmentation d'intensité lumineuse provoquait des changements pigmentaires (pour les deux espèces) et de volume cellulaire moyen (pour la diatomée), et amplifiait les variations journalières pour la plupart des variables. Cette augmentation des amplitudes des variations journalières était plus forte pour les pigments (facteur 2 ou plus, notamment pour le contenu cellulaire en caroténoïdes photoprotecteurs pour *I. rotunda*, et pour les pigments photosynthétiques pour *T. pseudonana*) que pour les propriétés optiques (facteur 1,5 pour l'absorption spécifique à la chl-*a* à 440 nm pour *I. rotunda* et facteur 2 pour la section efficace d'absorption et la

diffusion spécifique à la chl-*a* pour *T. pseudonana*). Par conséquent, les variations journalières des propriétés optiques et de la pigmentation associées au cycle jour-nuit, et amplifiées par des changements concomitants d'intensité lumineuse, contribueraient significativement à la variabilité des propriétés optiques observée dans les études bio-optiques en milieu naturel.

ABSTRACT

Diel variations of cellular optical properties were examined for cultures of the haptophyte *Imantonia rotunda* N. Reynolds and the diatom *Thalassiosira pseudonana* (Hust.) Hasle and Heimdal grown under a 14:10 light:dark (L:D) cycle and transferred from 100 μmol photon·m^{-2}·s^{-1} to higher irradiances of 250 and 500 μmol photon·m^{-2}·s^{-1}. Cell volume and abundance, phytoplankton absorption coefficients, flow-cytometric light scattering and chlorophyll fluorescence, and pigment composition were measured every 2-h over a 24-h period. Results showed that cell division was more synchronous for *I. rotunda* than for *T. pseudonana*. Several variables exhibited diel variability with an amplitude >100%, notably mean cell volume for the haptophyte, and photoprotective carotenoids for both species, while optical properties such as flow-cytometric scattering and chl-*a* specific phytoplankton absorption generally showed <50% diel variability. Increased irradiance induced changes in pigments (both species) and mean cell volume (for the diatom), and amplified diel variability for most variables. This increase in amplitude is larger for pigments (factor of 2 or more notably for cellular photoprotective carotenoids content in *I. rotunda* and for photosynthetic pigments in *T. pseudonana*) than for optical properties (a factor of 1.5 for chl-*a* specific absorption, at 440 nm, in *I. rotunda* and factor of 2 for the absorption cross-section and the chl-*a* specific scattering in *T. pseudonana*). Consequently, diel changes in optical properties and pigmentation associated with the L:D cycle and amplified by concurrent changes in irradiance, likely contribute significantly to the variability in optical properties observed in bio-optical field studies.

INTRODUCTION

Estimating oceanographic variables (phytoplankton pigment concentrations and primary production rates) from ocean color is based on the knowledge of the inherent optical properties (IOPs) of surface waters such as the absorption (a) and backscattering (b_b) coefficients (Gordon and Morel 1983, Mobley 1994). Variations of these coefficients are linked to changes in the composition, cell abundance, and optical characteristics of phytoplankton assemblages (Stramski and Reynolds 1993, Mobley 1994, Stramski and Mobley 1997). These variations in optical properties are induced by changes in cell characteristics, such as size, refractive index, chemical composition, and pigment composition and concentration, which are strongly influenced by the physical and chemical environment of the phytoplankton (Reynolds et al. 1997, Bricaud et al. 1999, Stramski et al. 2002). Therefore, variations in optical properties of phytoplankton assemblages can have a significant impact on the retrieval of chl-a measurements from remotely-sensed data, and it is important to improve our understanding of this variability (Stramski and Reynolds 1993, DuRand and Olson 1998).

Diel variations in IOPs have frequently been ignored in previous studies. These diel variations have received increased attention recently, associated with the processes of photosynthesis and the cycle of cellular division (Stramska and Dickey 1992, Stramski and Reynolds 1993, DuRand and Olson 1996, Claustre et al. 2002). However, few studies on diel variations of absorption and scattering properties have combined them with changes in

irradiance, as often occurs in the natural environment, associated with water movement, time of day, or climatic conditions (e.g., cloudy skies) (but see Stramski and Reynolds 1993, Stramski et al. 1995, DuRand and Olson 1998). The few studies that have looked at diel variations in relation to irradiance have examined diel changes after several days of acclimation to experimental irradiances such that a new steady state is reached (e.g., DuRand and Olson 1998). A few studies have examined the rapid changes in optical properties (forward light scattering and beam attenuation) in response to irradiance changes, but they have not considered diel variations over a 24-h period (Ackleson et al. 1990, 1993, Ackleson and Cullen 1991). In this study, we focus instead on the short-term (24-h) and rapid (2-h) phytoplankton responses of two phytoplankton cultures that were maintained in a 14:10 L:D cycle, when transferred from a control growth irradiance of 100 μmol photons·m^{-2}·s^{-1} to higher irradiances of 250 and 500 μmol photons·m^{-2}·s^{-1}. These short-term responses should be representative of variations in cloud cover (transition from cloudy skies to clear skies, Jacquet et al. 1998) or of rapid vertical displacements of phytoplankton cells from low irradiance at depth to higher irradiance near the surface due to various mixing processes (e.g. turbulence, upwelling, internal tides) such as occurs in dynamic marine and estuarine systems, for example the Estuary and Gulf of St. Lawrence (Demers and Legendre 1981, Levasseur et al. 1992, Zakardjian et al. 2000).

The two phytoplankton species studied here, the marine diatom *T. pseudonana* and the haptophyte *I. rotunda*, are of similar size (3-5 μm). Both nanoplanktonic species are commonly present in St. Lawrence waters (Bérard-Therriault et al. 1999) and they show a

widespread distribution in marine waters (Armbrust et al. 2004, Fuller et al. 2006, LeRoi and Hallegraeff 2006). The inclusion of a diatom species is of additional interest because it possesses a vacuole that will probably affect its optical properties (Vaillancourt et al. 2004).

MATERIALS AND METHODS

The list of mathematical symbols and acronyms used in this paper is provided in Table 1.

Phytoplankton cultures - Cultures of the marine centric diatom *T. pseudonana* (CCMP1335) and the haptophyte *I. rotunda* (CCMP457) were obtained from the Provasoli-Guillard National Center for Culture of Marine Phytoplankton (CCMP; West Boothbay Harbor, ME, USA). These cultures were grown at 15°C (± 2°C) in 6 L Kimax flasks. The culture medium was prepared with 0.2 µm-filtered natural seawater (salinity of 31), autoclaved and enriched with f/2 nutrients (Guillard and Ryther 1962). Before the experiment, the cultures were pre-acclimated for 5 d at an irradiance of 100 µmol photons·m^{-2}·s^{-1} (cool-white fluorescent lights) with a 14:10 L:D photoperiod cycle. Irradiance was measured using a PAR sensor (QSL-100; Biospherical Instruments Inc., San Diego, CA, USA). When the cultures reached the exponential growth phase, six 1 L subsamples were removed and put in 1 L Kimax flasks, stirred, and exposed in duplicate for 24-h to the three irradiance levels: control (100 µmol photons·m^{-2}·s^{-1}), an intermediate (250 µmol photons·m^{-2}·s^{-1}) and a high (500 µmol photons·m^{-2}·s^{-1}) light regime, maintaining a 14:10 photoperiod. Then, over the next 24-h period, these cultures were stirred every 2-h, and 50 mL subsamples were collected from each one of the incubated 1 L flasks for the various analyses described below.

Table 1: Mathematical symbols and acronyms used in this study with associated units.

Symbol	Definition	Units
$\overline{V}$	Mean cell volume	μm^3
FSC	Forward-angle light scatter: proxy of scattering cross-section at 488 nm	bead unit (bu)
*FSC**	Chl-*a* specific scattering coefficient proxy at 488 nm	$bu \cdot (pg\ chl\text{-}a)^{-1}$
$Chla_c$	Cellular chl-*a* content	$pg \cdot cell^{-1}$
$Chla_i$	Intracellular concentration of chl-*a*	$kg \cdot m^{-3}$
$Chlc_c$	Cellular chl-*c* content	$pg \cdot cell^{-1}$
$Chlc_i$	Intracellular concentration of chl-*c*	$kg \cdot m^{-3}$
FL3	Cell chlorophyll fluorescence	bu
PPC_c	Cellular concentration of PPC	$pg \cdot cell^{-1}$
PPC_i	Intracellular concentration of PPC	$kg \cdot m^{-3}$
PSC_c	Cellular concentration of PSC	$pg \cdot cell^{-1}$
PSC_i	Intracellular concentration of PSC	$kg \cdot m^{-3}$
SSC	Side-angle light scatter: cell complexity index	bu
λ	Wavelength	nm
OD_{fp}	Optical density of particulate matter	—
OD_{fd}	Optical density of detritus	—
s	Clearance area of the filter	m^2
V_f	Volume of filtered sample	m^3
β	Path length amplification factor	—
a_p, a_d, a_{ph}	Absorption coefficient of particulate matter, detritus, and phytoplankton	m^{-1}
a^*_{ph}	Chl-*a* specific absorption coefficient	$m^2 \cdot (mg\ chl\text{-}a)^{-1}$
σ_a	Absorption cross-section	$\mu m^2 \cdot cell^{-1}$

Flow cytometry – Immediately upon collection, fresh duplicate subsamples of 2 mL were analyzed with a FACSort Analyser flow cytometer (FCM; Becton Dickinson, San Jose, CA, USA, equipped with a 488 nm laser beam of 15 mW) following the addition of 2, 6 and 10 μm beads as internal standards (YG, Fluoresbrites, Polyscience Inc., Warrington, PA, USA). This analysis produced the following data: cell abundance determined from the pump flow rate (60 $\mu L \cdot min^{-1}$) and sample run time, forward-angle light scatter (FSC; $\theta = 1$-10°), side-angle light scatter (SSC; $\theta = 90°$) and cell chlorophyll fluorescence (FL3; >650 nm). Statistical analyses of these data were performed using the Cell Quest and Attractors softwares of Becton-Dickinson. For each sample, mean values of FSC, SSC and FL3 were normalized with reference to the fluorescent beads of 2 μm.

As it is reasonable to expect that FSC (i.e., light scatter at low angles relative to the excitation light) contributes strongly (>90%) to total scattering, changes in FSC at 488 nm can be treated as proxies of changes in scattering cross-section, σ_b, at the same wavelength (DuRand and Olson 1996, DuRand et al. 2002). By comparison, the SSC is a cell complexity index (i.e., a measure of cell structure and cell morphology) (Dubelaar et al. 1987, Shapiro 1988). Finally, *FSC**, where FSC is divided by the cellular content of chl-*a*, gives an idea of the changes in the chl-*a* specific scattering coefficient at 488 nm, *b**(488).

Size estimates by microscopy – Other subsamples (10 mL) from the incubation flasks were preserved with formaldehyde (0.2% in final concentration) and stored in the dark at 4°C. The size of 50-100 cells was measured within 1 week using an inverted phase-contrast microscope (Axiovert 100; Carl Zeiss Canada Ltd., Toronto, Canada) with a micrometer ocular at ×1000 magnification. The mean cell volume ($\overline{V}$) was calculated from standard geometric shapes (Hillebrand et al. 1999). We have previously determined for these species that the formaldehyde preservation treatment over 1 week only induced minor and constant changes of cell volume (<5%), so a correction has been applied.

Determination of pigments- For each 2-h subsample from the culture flasks, 5 to 10 mL subsamples were filtered through a 25 mm GF/F filter (Whatman International Ltd.,Maidstone, UK), frozen in liquid nitrogen, and stored at -80°C. Pigments were analyzed following the method of Zapata et al. (2000). The frozen filter was sonicated in 3 mL of 95% methanol to extract pigments and then centrifuged at 7,100 rpm (i.e. 3,900 g) for 5 min. The extract was then clarified by filtration through a Gelman Acrodisc 0.22 µm PTFE (13 mm) membrane syringe filter (Gelman Sciences, Ann Arbor, MI, USA) and injected in the HPLC system composed of a P4000 quaternary pump, AS3000 autosampler, SCM1000 solvent degasser, SN4000 interface controller (Finnigan SpectraSYSTEM; Thermo Separation Products Inc., Riviera Beach,FL, USA; now Thermo Fisher Scientific Inc., Waltham, MA, USA), SpectraFocus absorbance detector (400-700 nm) and a Spectroflow 980 fluorometer (set at 412 nm). The whole system was computer-controlled using TSP's PC1000 software. Peak separation was done on a reversed phase C8 Symmetry

column (150 × 4.6 mm, 3.5 µm; Waters Corporation, Milford, MA, USA) maintained at 25°C using a water jacket. The mobile phase was composed of (A) a mixture of methanol:acetonitrile:aqueous pyridine solution (0.25 M pyridine) (50:25:25 v:v:v) and (B) methanol:acetonitrile:acetone (20:60:20 v:v:v). The chromatogram values were transformed into volumetric concentrations of chl-*a* (chlorophyll *a*, and chlorophyll *a* allomers and epimers), chl-*c*, photosynthetic carotenoids (PSC; including fucoxanthin, 19'-butanoyloxyfucoxanthin, 19'-hexanoyloxyfucoxanthin, and 4-keto-19'-hexanoyloxyfucoxanthin) and photoprotective carotenoids (PPC; including β, β-carotene, diadinoxanthin, and diatoxanthin). These values were standardized by their corresponding cell abundance in order to obtain the corresponding cellular pigment content. Finally, intracellular concentrations, respectively $Chla_i$, $Chlc_i$, PSC_i, and PPC_i were calculated by dividing the corresponding cellular pigment content by the mean cell volume, based on microscopic measurements.

Absorption measurements – To determine the chl-*a* specific absorption coefficient, $a^*_{ph}(\lambda)$, where λ is the wavelength, 5 to 10 mL subsamples of the cultures were filtered through Whatman GF/F glass-fiber filters and stored at -80°C in Fisher HistoPrep tissue capsules (Fisher Scientific, Ottawa, Canada). The optical density of the particulate matter, $OD_{fp}(\lambda)$, was measured directly on filters wet with 100 µL of filtered seawater, using a double-beam spectrophotometer (Lambda 2; Perkin-Elmer, Waltham, MA, USA) with an integrating sphere (RSA-PE-20; scan speed: 240 $nm \cdot min^{-1}$). The filters were then submitted

to two successive extraction procedures using 3 mL of absolute methanol (15 min total extraction time). Following the extraction, 10 mL of filtered seawater were passed through the bleached filter and a new scan was done for detritus, $OD_{fd}(\lambda)$. The same treatment was applied to blank reference filters. Spectral absorption coefficients of particulate matter, $a_p(\lambda)$, and of detritus, $a_d(\lambda)$, were determined following the method described in Mitchell and Kiefer (1984, 1988):

$$a_x(\lambda) = (2.3\ OD_x\ (\lambda)\ s) / [V_f\ \beta(\lambda)],$$

where x corresponds to particles or detritus, OD_x is OD_{fp} or OD_{fd} corrected for blank measurement, s is the clearance area of the filter, V_f is the volume of filtered seawater and $\beta(\lambda)$ is the path length amplification factor. The path length amplification factor used was $\beta(\lambda) = [0.344 + 0.300\ OD(\lambda)]^{-1}$ for *T. pseudonana* and $\beta(\lambda) = [0.361 + 0.167\ OD(\lambda)]^{-1}$ for *I. rotunda* (locally determined from algal cultures, Laurion et al. 2003). The phytoplankton absorption coefficients, $a_{ph}(\lambda)$, were obtained by subtracting $a_d(\lambda)$ from $a_p(\lambda)$. These coefficients were converted to chl-*a* specific coefficients, $a^*_{ph}(\lambda)$ and average absorption cross-sections (σ_a), by dividing $a_{ph}(\lambda)$ by the chl-*a* concentration and by the cell number, respectively. Diel variations of a^*_{ph} are shown in this study at two wavelengths (440 and 488 nm) selected to correspond to two channels of the SeaWiFs color sensor and the laser wavelength of the FCM, and at a third wavelength (675 nm) corresponding to the red absorption band of chl-*a*.

Mathematical and statistical analysis – After verifying normality and homoscedasticity, a repeated measure analysis of variance (ANOVA) was used to evaluate the effect of time and time × light level interactions on the different parameters. For each sampling point, the effect of the light levels on the various parameters was further tested using a one-way ANOVA. Finally, when the ANOVA showed a statistically significant effect ($P \leq 0.05$), a post hoc Tukey's test was used to evaluate whether the effects of three light treatments on the various parameters showed significant differences. A confidence level of 95% was used throughout these analyses, and the differences between the regression parameters, obtained for the three irradiances tested for each species, were assessed using an analysis of covariance (ANCOVA) (Zar 1999). All statistical analyses were carried out using the SPSS for Windows 13.0 package (SPSS Inc., Chicago,IL, USA).

The amplitude of the diel variation for each variable was calculated in terms of percentage variation, as follows:

$$\text{Amplitude of diel variation (\%)} = ((|\text{Max} - \text{Min}|) / \text{Min}) \times 100.$$

RESULTS

Cell growth and size – Diel variations of the cell abundance, mean cell volume ($\bar{V}$), and complexity index (SSC) for *I. rotunda* and *T. pseudonana* are shown in Fig. 1 and Table 2 for the different light-level incubations. For the same irradiance level, *I. rotunda* showed a slower growth than *T. pseudonana* (i.e., 0.46 and 0.63 d^{-1} under control irradiance, respectively), but both species showed the usual daytime increase in mean cell volume $\bar{V}$ (Fig. 1, a and c), followed by a nighttime decrease as the cell division took place, resulting in an increased cell number (Fig. 1a). The pattern of changes in mean cell volume $\bar{V}$ for *T. pseudonana*, characterized by a more gradual increase in cell number throughout the 24 h period, suggests that cell division in the diatom was less tightly related to the L:D cycle.

The two species responded differently to the increased irradiance since no significant difference in mean cell volume $\bar{V}$ was observed for the haptophyte species ($P>0.05$), while the diatom showed significantly higher mean cell volume $\bar{V}$ and cell abundance compared with the control, after 4-h and 8-h, respectively, following the beginning of incubation at higher light levels. For the diatom species, there was no significant difference in mean cell volume $\bar{V}$ between the 250 and 500 µmol photons·m^{-2}·s^{-1} irradiances ($P>0.05$), but cell abundance was the highest at 250 µmol photons·m^{-2}·s^{-1}.

Figure 1: Diel variations of cell abundance (cells·mL^{-1}) and mean cell volume ($\bar{V}$, µm^3) (a, c), cell complexity index (SSC; bead unit) and chlorophyll fluorescence (FL3; bead unit) (b, d), for cultures of *Imantonia rotunda* and *Thalassiosira pseudonana* exposed to the following irradiances: 100 (●), 250 (▼ and 500 ( ) µmol photons·m^{-2}·s^{-1}. The black bars on the x-axis indicate the dark (lights-off) period. The average value and standard deviation are shown for each sampling point.

Imantonia rotunda *Thalassiosira pseudonana*

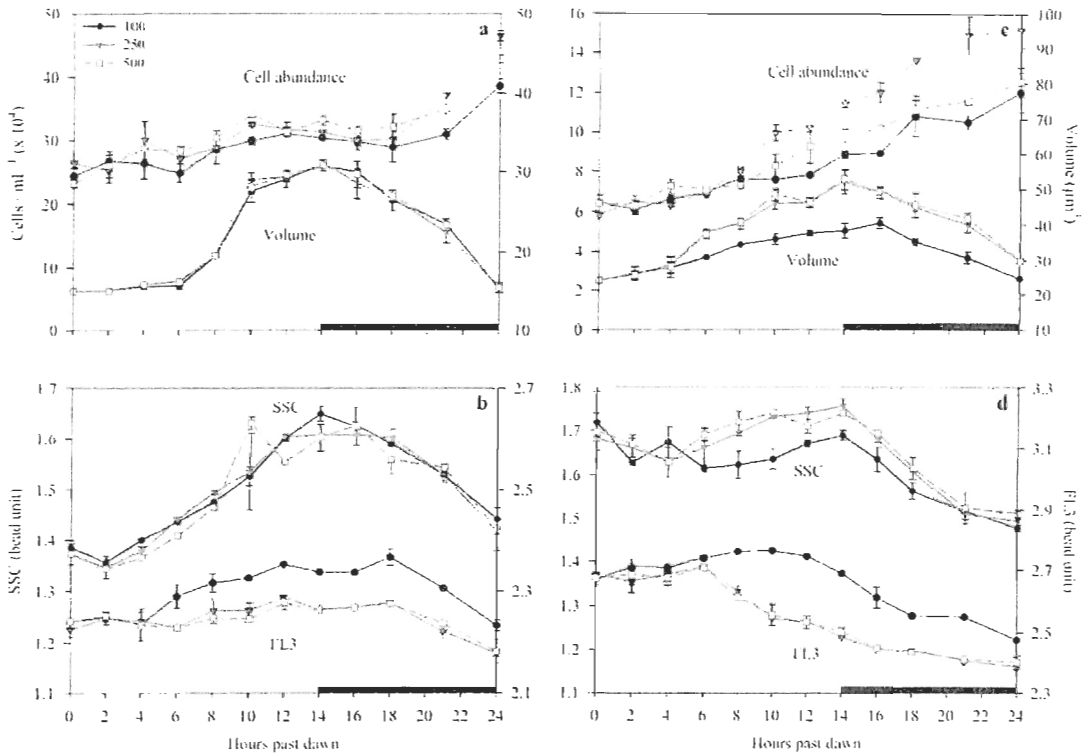

The diel variations of the cell complexity index (SSC) differed between the two species (Fig. 1, b and d, and Table 2). For *I. rotunda*, the diel variation of SSC had the same temporal evolution as $\overline{V}$ (Fig. 1a), with an increase during the light period and a decrease during the night period for all irradiances. For *T. pseudonana*, the SSC remained roughly constant during the light phase and decreased rapidly during the dark phase in all cases. Similar to the irradiance-related changes in $\overline{V}$, no significant differences in SSC were detected for *I. rotunda* among the different light levels ($P>0.05$). In contrast, *T. pseudonana* SSC showed higher values under the two higher irradiances after the first 6-h of exposure, and no significant difference was observed between the two higher irradiances ($P>0.05$).

Cell physiological properties – Figure 1 (b and d) shows the diel variations of mean normalized chlorophyll fluorescence per cell (FL3) (Table 2), and Figure 2 and Table 2 represent the diel variations of cell-specific and intracellular chl-*a* (Chla_c and Chla_i), photoprotective carotenoid pigments (PPC_c and PPC_i), and pigment ratios (PPC/chl-*a* and PSC/chl-*a*).

Figure 2: Diel variations of cellular content ($pg \cdot cell^{-1}$) and intracellular concentration ($kg \cdot m^{-3}$) of chl-*a* (Chla_c and Chla_i) (a, d), photoprotective carotenoid pigments (PPC_c and PPC_i) (b, e) and pigment ratios (PSC/chl-*a* and PPC/chl-*a*) (c, f) for cultures of *Imantonia rotunda* and *Thalassiosira pseudonana* exposed to the following irradiances: 100 (●), 250 (▼) and 500 ( ) μmol photons$\cdot m^{-2} \cdot s^{-1}$. The black bars on the x-axis indicate the dark (lights-off) period. The average value and standard deviation are shown for each sampling point.

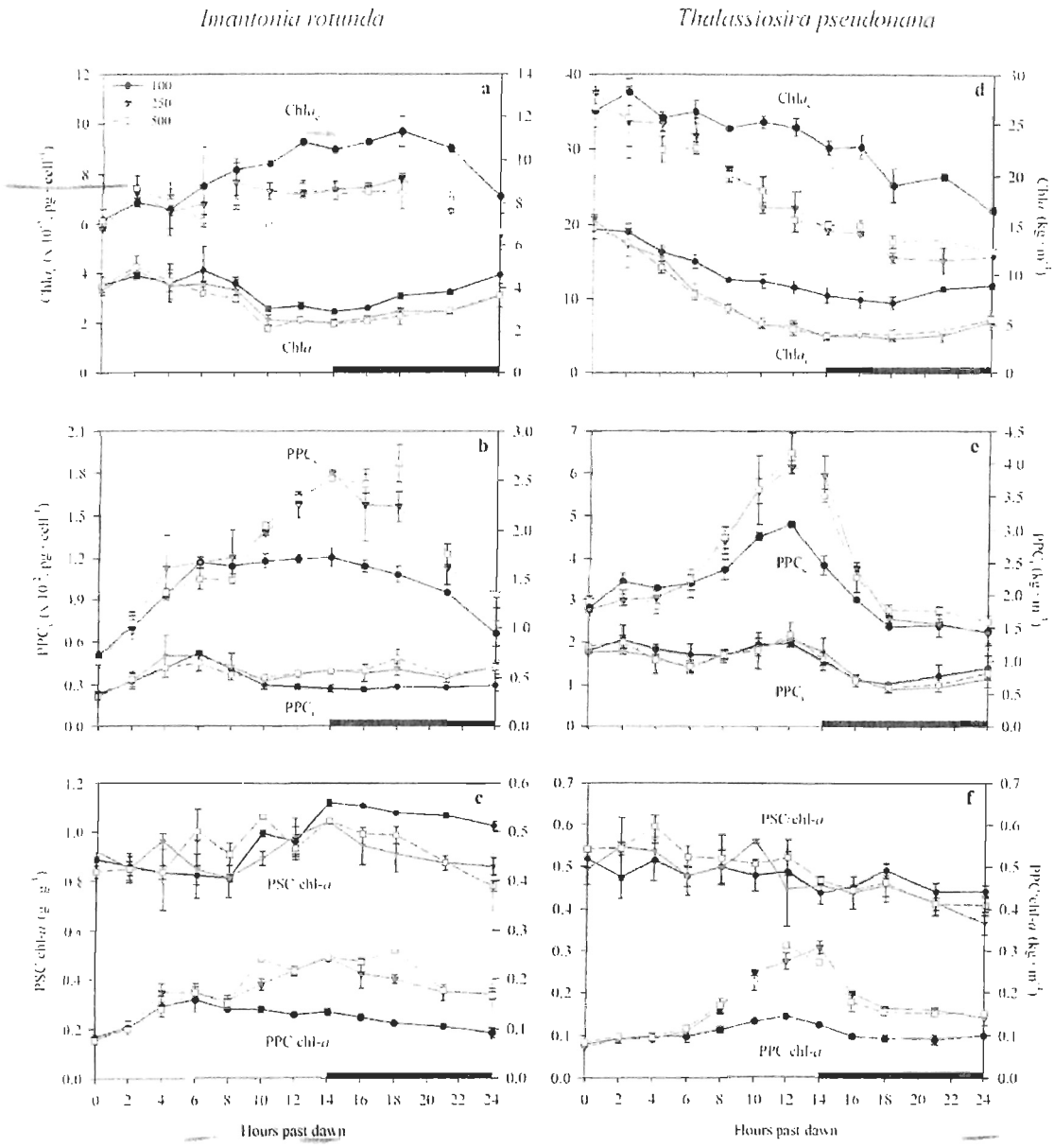
Imantonia rotunda
Thalassiosira pseudonana
100
250
500
a
b
c
d
e
f
Chla$_c$
Chla
PPC$_c$
PPC$_t$
PSC chl-a
PPC chl-a
Hours past dawn
Hours past dawn

For the three light regimes, cell-specific chl-*a*, photoprotective carotenoid pigments, and cell chlorophyll fluorescence (Chla_c, PPC_c and FL3) increased significantly for *I. rotunda* during the light period, before decreasing after 18-h of incubation, while cell-volume-related values of the same variables (Chla_i and PPC_i) showed a general decrease during the light period and an increase during the dark period (Fig. 2, a and b). The cell-related variables are affected by the changes in mean cell volume (Table 2), since an increase in pigments content per cell accompanied by a decrease in pigments per cell volume was observed as cells grew during the light phase. The diel pattern observed for *T. pseudonana* showed a similar daytime decrease for chl-*a* per cell volume (Fig. 2e) but fluorescence and chl-*a* per cell had a different pattern since they remained more constant or even decreased during the light period, suggesting less daytime pigment synthesis compared with the haptophyte species.

Initial pigment contents per cell, however, were much higher for *T. pseudonana* (~36 $\times 10^{-2}$ pg chl-*a*·cell^{-1}) than for *I. rotunda* (6×10^{-2} pg chl-*a*·cell^{-1}). It is apparent here that the response to the various light levels was influenced by whether or not the mean cell volume changed during the incubation period. In *I. rotunda*, where no mean cell volume changes were observed between the different incubation irradiances (Fig. 1a), changes in pigments (per cell or cell volume) and cell fluorescence took place since FL3, PSC and chl-*a* decreased while photoprotective carotenoid pigments increased with increasing irradiance (Fig. 2, a and b). In the diatom, mean cell volume increased with higher irradiance and consequently, Chla_i decreased (Fig. 2d).

Table 2: Maximal and minimal values and amplitude of diel variations [%, calculated as (| Max-Min | / Min) × 100] in cell and optical properties for *Imantonia rotunda* and *Thalassiosira pseudonana* cultures exposed to the different irradiances (control irrad.: 100 µmol photons·m^{-2}·s^{-1}, high irrad: 250 and 500 µmol photons·m^{-2}·s^{-1}). Symbols and acronyms are given in Table 1.

	Imantonia rotunda						*Thalassiosira pseudonana*					
	Control irrad.			High irrad.			Control irrad.			High irrad.		
	Max	Min	%	Max	Min	%	Max	Min	%	Max	Min	%
Volume (μm^3)	31	15	**109**	31	15	**109**	41	24	**69**	55	24	**125**
SSC (bu)	1.66	1.35	**23**	1.63	1.34	**22**	1.77	1.47	**20**	1.75	1.50	**16**
FL3 (bu)	2.38	2.21	**8**	2.29	2.17	**6**	2.77	2.48	**12**	2.71	2.38	**14**
Chla_c (x 10^{-2}, pg·cell^{-1})	10.3	5.5	**86**	8.2	5.1	**59**	38	22	**70**	37	16	**130**
Chla_i (kg·m^{-3})	5.6	2.9	**97**	5.3	2.0	**161**	15	7	**120**	16	3	**355**
Chlc_c (x 10^{-2}, pg·cell^{-1})	3.8	2.0	**96**	2.9	1.4	**114**	12.0	7.8	**54**	11.9	4.1	**188**
Chlc_i (kg·m^{-3})	1.7	1.0	**68**	1.7	0.7	**126**	4.8	2.1	**131**	4.7	1.0	**382**
PPC_c (x 10^{-3}, pg·cell^{-1})	13	5	**167**	19	4	**346**	48	22	**114**	63	24	**168**
PPC_i (kg·m^{-3})	0.75	0.32	**138**	0.81	0.29	**181**	1.47	0.65	**151**	1.37	0.54	**151**
PSC_c (x 10^{-2}, pg·cell^{-1})	11.1	5.2	**115**	7.9	4.4	**81**	18	10	**86**	19	6	**202**
PSC_i (kg·m^{-3})	4.8	3.0	**63**	4.8	2.0	**136**	7.8	3.2	**148**	8.2	1.4	**486**
chl-*c* /chl-*a*	0.42	0.30	**38**	0.38	0.24	**59**	0.36	0.30	**22**	0.38	0.28	**37**
PPC/chl-*a*	0.18	0.08	**125**	0.25	0.07	**248**	0.15	0.08	**84**	0.31	0.08	**296**
PSC/chl-*a*	1.14	0.68	**66**	1.07	0.74	**44**	0.56	0.41	**37**	0.58	0.39	**49**
σ_a(488, μm^2·cell^{-1})	2.4	1.4	**78**	2.2	1.2	**88**	6.3	4.1	**55**	5.8	2.9	**100**
FSC (bu)	2.77	2.39	**16**	2.75	2.41	**14**	2.91	2.70	**8**	2.99	2.67	**12**
a^*_{ph}(440) (x 10^{-2}, m^2·(mg chl-*a*)$^{-1}$)	5.7	4.2	**35**	5.7	3.7	**53**	3.8	2.6	**47**	3.7	2.5	**46**
a^*_{ph}(488) (x 10^{-2}, m^2·(mg chl-*a*)$^{-1}$)	2.75	2.17	**27**	2.82	2.19	**29**	2.00	1.60	**25**	2.00	1.57	**27**
a^*_{ph}(675) (x 10^{-2}, m^2·(mg chl-*a*)$^{-1}$)	2.51	1.92	**31**	2.58	1.96	**31**	1.91	1.44	**32**	1.90	1.44	**32**
*FSC** (488, bu·(pg chl-*a*)$^{-1}$)	45	27	**71**	50	31	**60**	13	7	**81**	20	7	**176**
a_{ph}(440)/a_{ph}(488)	2.44	1.57	**56**	2.44	1.40	**74**	2.08	1.36	**53**	2.05	1.33	**53**
a_{ph}(488)/a_{ph}(555)	2.03	1.71	**19**	2.09	1.76	**19**	2.31	1.70	**36**	2.27	1.67	**36**

Larger cells had less fluorescence and chl-*a* per cell, as well as more photoprotective carotenoid pigments per cell, but the intracellular concentration of these variables did not increase (PPC_i), indicating that the PPC_c increase was only due to the increased mean cell volume (Fig. 2e). The diel patterns of PSC_c and $Chlc_c$, and PSC_i and $Chlc_i$ (data not shown) are similar to those of $Chla_c$ and $Chla_i$ for the two species. Furthemore the range of PPC/chl-*a* and chl-*c*/chl-*a* ratios were the same (0.15 ± 0.061 and 0.33 ± 0.038, respectively) for both species (Fig. 2, c and f, and Table 2) while *I. rotunda* cells had a PSC/chl-*a* ratio (0.94 ± 0.107) 2-fold higher than for *T. pseudonana* cells (0.48 ± 0.059) (Fig. 2, c and f, and Table 2).

The differences in $Chla_c$ (*T. pseudonana*) and PPC_c (*I. rotunda*) between the initial values and those after 24-h in the control cultures can probably be explained by a weak increase in irradiance due to the transfer from 6 L to 1 L flasks at the start of the experiment.

Bulk and cell optical properties – Figure 3 shows the diel variations of cell and chl-*a* specific absorption (σ_a and a^*_{ph}), and cell and chl-*a* specific scattering proxies (FSC and *FSC**), for both species (Table 2).

FSC followed the changes in mean cell volume, increasing during the light period and decreasing during the dark period (Fig. 3, a and d). The different incubation irradiances had

no effect on FSC for *I. rotunda* (Fig. 3a), while for *T. pseudonana,* FSC increased at the higher irradiances (Fig. 3d). The chl-*a* specific scattering coefficient proxy at 488 nm, *FSC**, was affected by both the change in cell scattering and pigment content, resulting in a slight decrease during the light period and an increase at the end of the night period (for control irradiance) or no clear change over the 24-h period (for the two higher irradiance treatments) for *I. rotunda* (Fig. 3b), due to the changes in Chla_c, which compensated for the changes in FSC. For the diatom species, a decrease in Chla_c combined with an increase in cell scattering resulted in an overall increase in *FSC**, both through time and with higher irradiances (Fig. 3e). For both species, cells exposed to 100 µmol photons·m^{-2}·s^{-1} had lower *FSC** than cells exposed to 250 and 500 µmol photons·m^{-2}·s^{-1} and these differences were evident after the first 8-h for *I. rotunda* and the first 10-h for *T. pseudonana*.

The absorption cross-section at 488 nm exhibited even larger variations than FSC. The changes in σ_a(488) followed the changes in Chla_c, with an increase during the light period and a decrease during the dark period for the haptophyte species (Fig. 3a). However, σ_a(488) showed a general decline mostly after the first 6 h for the diatom species (as did Chla_c) (Fig. 3d). Differences of σ_a(488) between the incubation irradiances showed up after the 4th hour for both species. The strong influence of chl-*a* on absorption was reflected in a strongly attenuated variability for all chl-*a* specific absorption values (a^*_{ph}), except for a^*_{ph}(440), because of the influence of photoprotective carotenoid pigments at this wavelength (Fig. 3, b, c, e and f). Increases in PPC_i (Fig. 2, b and e), either during the diel cycle or caused by change in incubation irradiance, matched the decreases in a^*_{ph}(440) for

both species (Fig. 3, c and f). The different incubation irradiances had a significant influence only for *I. rotunda* during the dark phase, associated with a clear increase in PPC_i which started a few hours before the lights were turned off (Fig. 2, b and c). However, no significant differences between the 250 and 500 μmol photons$\cdot m^{-2}\cdot s^{-1}$ incubation irradiances were observed (P>0.05). Finally, the diatom species displayed significantly lower ratios of absorption at 440/488 and 488/555 nm, compared with the haptophyte species (Table 2). Similar trends have been observed in field studies (Arrigo et al. 1998, Stuart et al. 2000, Cota et al. 2003).

Figure 3: Diel variations of absorption cross-section (σ_a, $\mu m^2 \cdot cell^{-1}$) and scattering cross-section proxy (FSC, bead unit), both at 488 nm (a, d); chl-*a* specific absorption coefficient [a^*_{ph}; $m^2 \cdot (mg\ chl\text{-}a)^{-1}$] and chl-*a* specific scattering coefficient proxy [*FSC**; bead unit·(pg chl-*a*)$^{-1}$], both at 488 nm (b, e); and chl-*a* specific absorption coefficients at 440 and 675 nm (c, f) for cultures of *Imantonia rotunda* and *Thalassiosira pseudonana* exposed to the following irradiances: 100 (●), 250 (▼) and 500 ( ) μmol photons·m^{-2}·s^{-1}. The black bars on the x-axis indicate the dark (lights-off) period. The average value and standard deviation are shown for each sampling point.

Imantonia rotunda *Thalassiosira pseudonana*

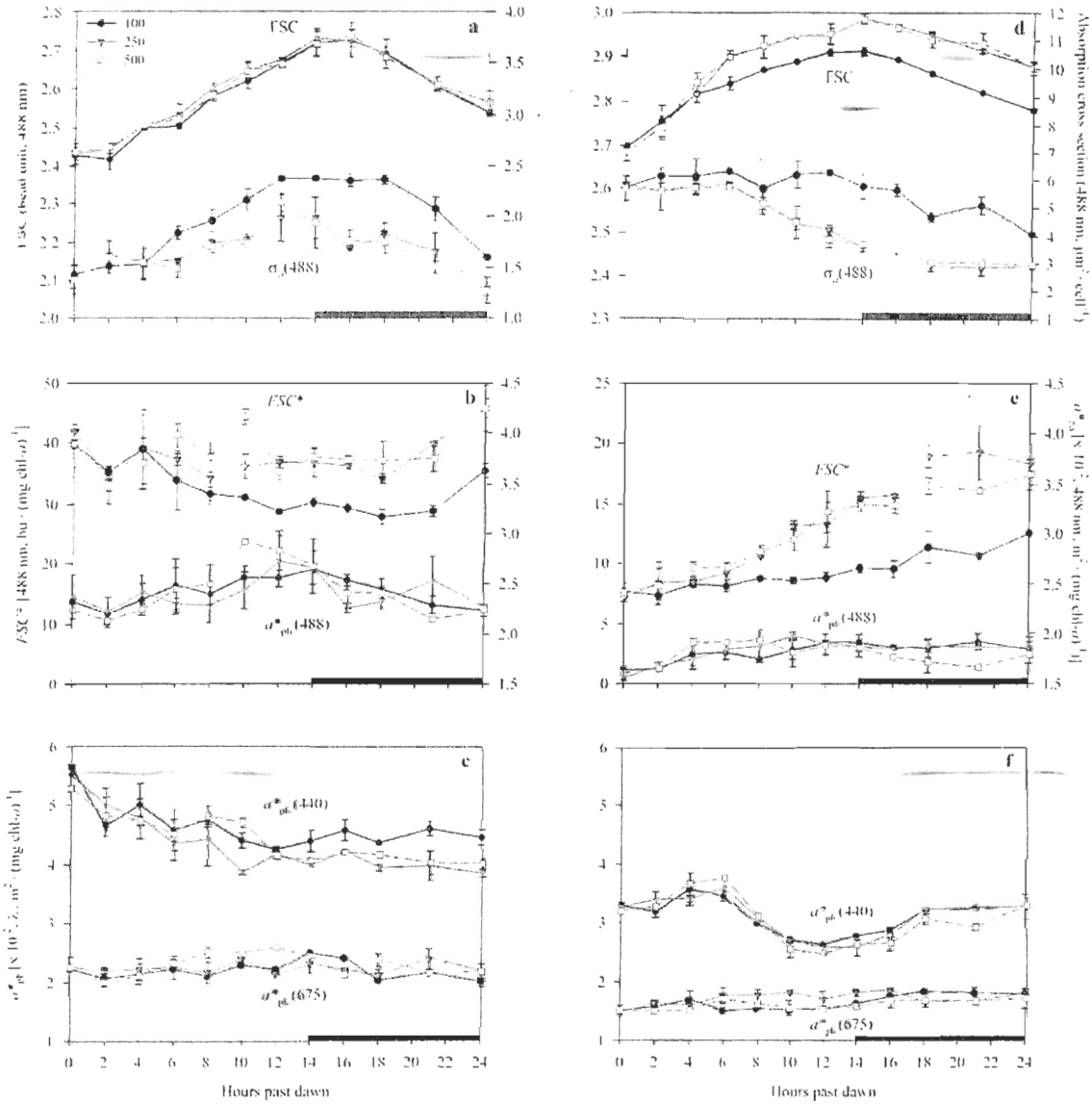

DISCUSSION

Diel patterns – Diel patterns of optical properties differed between the two phytoplankton species, with cell division occurring mostly during the night for *I. rotunda* and distributed throughout the day and night for *T. pseudonana*. This finding is in agreement with the pattern reported for diatoms (Chisholm and Costello 1980), while small flagellates divide mostly at night, in a more synchronous fashion (DuRand and Olson 1998, DuRand et al. 2002). Synchronous division can be achieved in diatom cultures, but after a longer time (4 d; Stramski and Reynolds 1993).

Several studies, both in the field (Blanchot et al. 1997, Vaulot and Marie 1999) and in cultures (Jacquet et al. 2001), have reported a diel pattern in the cell complexity index (SSC), which seems to be related to cell division. This pattern is characterized by an increase during the day and a decrease at night, following cell division (Stramski et al. 1995, DuRand and Olson 1998). This diel pattern was observed here only for the haptophyte, consistent with its synchronous cell division (Fig. 1b). The more synchronous pattern in the haptophyte resulted in a larger amplitude of diel variations for several variables in this species, including the mean cell volume, the scattering-related FSC, and cellular photosynthetic pigment content ($Chla_c$, $Chlc_c$, PSC_c; Table 2).

The observed diel pattern in optical cross-sections differed between the two species. The increase throughout the light period seen in the haptophyte is in agreement with previous culture observations for eukaryotes (Stramski and Reynolds 1993, DuRand and Olson 1998, DuRand et al. 2002) and nanophytoplankton field populations (DuRand et al. 1994, DuRand and Olson 1996). This pattern may be a general characteristic of night-dividing marine phytoplankton (DuRand et al. 2002). In the diatom, only the scattering cross-section proxy (FSC) exhibited this diel pattern (Fig. 3d), because FSC seemed to be mostly influenced by mean cell volume variations, while σ_a (488) was affected mostly by Chla_c and it showed a decrease during the light period (Fig. 2d).

Diel changes in a^*_{ph} were relatively small (<32%, Table 2) in the two species, particularly at 675 nm. The small haptophyte showed little packaging (mean value of $a^*_{ph}(675)$ close to the value for pure chl-*a* dissolved in acetone: 0.0207 $m^2 \cdot mg$ chl-a^{-1} at 663 nm; Morel and Bricaud 1986), while the diatom showed a larger packaging effect ($a^*_{ph}[675]$ between 0.0144 and 0.0191 $m^2 \cdot mg$ chl-a^{-1}; Table 2) consistent with its larger mean cell volume and higher chl-*a* per cell. The lack of a clear diel pattern in $a^*_{ph}(675)$ for both species (Fig. 3, c and f), indicates that packaging remained relatively constant, as for picophytoplankton (Claustre et al. 2002, DuRand et al. 2002). This contrasts with the results of Ohi et al. (2002) where packaging showed a clear diel variation for another haptophyte species, *Isochrysis galbana*. Smaller packaging in our results probably reflects compensation between an increase in cell size and a decrease in Chla_i during the light period (with inverse effects on $a^*_{ph}[675]$). The $a^*_{ph}(488)$ also showed little variation, with a

slight increase during the light period in *I. rotunda* (Fig. 3b), likely caused by an increase in photosynthetic carotenoids (PSC/chl-*a*; Fig. 2c), since fucoxanthin and its derivatives contribute significantly to the absorption in that spectral region (Bidigare et al. 1988, 1990, Johnsen and Sakshaug 1993). A slightly larger diel variability was observed for $a^*_{ph}(440)$ (Fig. 3, c and f), which is affected by packaging and/or accessory pigments (Claustre et al. 2002, Bricaud et al. 2004). As packaging showed little variation, most of the diel variation in a^*_{ph} (440) was attributed to changes in photoprotective carotenoids (Fig. 2, b and e). An inverse relationship between a^*_{ph} (440) and PPC_i (notably xanthophyll cycle pigments: Demers et al. 1991) was observed only for *T. pseudonana*. For *I. rotunda*, the PSC/chl-*a* ratio was 2-fold higher than for the diatom, and the contributions of the photoprotective and photosynthetic accessory pigments to absorption followed inverse trends and partially compensated each other, so that the actual impact of PPC on the diel variation in a^*_{ph} (440) was reduced.

In contrast to absorption, normalization of FSC to $Chla_c$ led to a strong increase in the amplitude of the diel variation under the control irradiance treatment. The amplitude of diel variations in *FSC** (Table 2) was higher (>70%) than in FSC (8%-16%) or in a^*_{ph} (<50%). Therefore, compared to absorption, the chl-*a* specific scattering coefficient varied more over the 24-h period, corroborating the previous reports on *Prochlorococcus* (Claustre et al. 2002) and the diatom *T. pseudonana* (Stramski and Reynolds 1993). The pattern was the clearest for the diatom, where *FSC** clearly increased throughout the 24-h period. In other culture studies, the diel pattern in chl-*a* specific scattering coefficient (*b**) showed rather

constant values during most of the light period, a maximum near the beginning of the dark period and a decline during the dark period (for *M. pusilla*, DuRand et al. 2002) or a regular increase during the light period and a decline during the dark (for *Prochlorococcus*, Claustre et al. 2002). These various patterns likely reflect the changes in cell composition and size during the L:D period as influenced by the pattern of growth of the culture. DuRand et al. (2002) suggested that as the diel variations in b^* were much smaller (21%) in small-sized species, compared to the 8- to 10-fold variations of b^* observed among phytoplankton (Bricaud et al. 1983, Morel 1987), models of scattering based on chl-*a* (Morel 1987) should be relatively insensitive to the time of day of sampling, even for phytoplankton that exhibit synchronous division patterns. Although our measurements of FSC^* are not the same as b^*, it seems that the amplitude of these diel variations may be larger than assumed by DuRand et al. (2002), with potential effects on optical data sets when the time of day is not considered (Stramski and Reynolds 1993, Claustre et al. 2002). However, the range of diel intraspecific variations in FSC^* observed here (>70%; Table 2) is still much smaller than the variation among species (up to ~ 6-fold or 550%) even if we consider only the two species studied here. Hence changes in FSC^* or b^* in the field are probably dominated by changes in community composition. Diel intra-specific variations as observed here will become significant mostly during single-species blooms.

Increased irradiance effects - As expected, cells exposed to higher irradiances grew faster. For both species, the weak or no difference observed between the two higher irradiances suggests that light saturation was reached. This finding is consistent with the

highest cell abundance observed for growth at the intermediate irradiance of 250 µmol photons·m^{-2}·s^{-1} (Fig. 1, a and c). However, the response to increased irradiance differed between the two species. The diatom showed an increased mean cell size accompanied by changes in cellular pigments contents (increase in PPC_c, and decrease in Chla_c, PSC_c and Chlc_c), whereas the mean cell size for the haptophyte was not affected. This observation is consistent with a higher ability to photoacclimate or a faster acclimation rate for diatoms than for some nanoflagellates (Ackleson et al. 1990, 1993, Ackleson and Cullen 1991), and with the lack of change in mean cell size with irradiance for some nanoflagellates (Claustre and Gostan 1987, Thompson et al. 1991). The time taken to reach maximum cell size after a transition from low to high light was about the same (~5-h) as found for *T. pseudonana* by Thompson et al. (1991). With exposure to increased irradiance, the photoacclimation strategy of the haptophyte centered on a large increase in photoprotective carotenoids (PPC_c and PPC_i) associated with a small decrease in chl-*a* content (Chla_c and Chla_i), leading to a large increase in PPC/chl-*a* ratio (Fig. 2c). The photoacclimation strategy of the diatom involved a large decrease in Chla_c and Chla_i (Fig. 2d) that reflects changes in number and/or size of photosynthetic units (Perry et al. 1981). The rapid decline in the PPC/chl-*a* ratio at night for the higher irradiances (Fig. 2f) suggests a quick response of diatoms to irradiance fluctuations as often observed in phytoplankton with large photosynthetic units (Perry et al. 1981). This finding could explain the greater and faster response of *T. pseudonana* to the increased growth irradiance compared to *I. rotunda*. Moreover, the increased irradiance generally led to an increased amplitude of the diel variability, up to >300% for photoprotective carotenoids in the haptophyte and for

photosynthetic pigments (chl-*a*, chl-*c* and PSC) in the diatom (Table 2). These changes in pigments affected the flow-cytometric FL3 response, which is inversely related to photoprotective pigments (favoring nonphotochemical quenching) but positively related to photosynthetic pigments (Vaulot and Marie 1999).

The observed patterns of σ_a and a^*_{ph} resulted primarily from the different photoacclimation strategies of *T. pseudonana* and *I. rotunda* (Fig. 3). At 488 nm, for both species, the high irradiance-related decrease of Chla_c (Fig. 2, a and d), coupled to a constant a^*_{ph} (Fig. 3, b and e), caused a decrease of σ_a (Agustí 1991). Relative constancy of $a^*_{ph}(\lambda)$ over a wide range of growth conditions has been observed for some species (Geider et al. 1985, Nielsen and Sakshaug 1993), especially *T. pseudonana* (Ackleson et al. 1990, Ackleson and Cullen 1991). However, in most published studies, an irradiance increase is accompanied by an increase of a^*_{ph} (e.g., Ohi et al. 2002, Stramski et al. 2002). Our short-term responses thus differ from these observations. The most conspicuous change in absorption with increased irradiance was a decrease in $a^*_{ph}(440)$ for *I. rotunda* only during the dark period, due to increased PPC_i accompanied by decreased Chlc_i and PSC_i (Fig. 3c). There was no short-term increase in PPC_i with increased irradiance in the diatom (Fig. 2e and Table 2), which could explain the lack of short-term response of $a^*_{ph}(440)$. The short-term strategy for the diatom species was to decrease Chla_i (which caused a slight decrease in packaging effect and hence the slight increase in $a^*_{ph}(675)$ at 250 μmol photons·m^{-2}·s^{-1}; Fig. 3f), and to increase mean cell volume.

Changes in the scattering cross-section proxy (FSC) and the cell complexity index (SSC) can be explained mostly by variations in both cell size and refractive index (Spinrad and Brown 1986, Spinrad and Yentsch 1987, Ackleson and Spinrad 1988). For *I. rotunda* at the three irradiances, the FSC versus SSC relationships were linear, and their slopes (related to refractive index, Spinrad and Brown 1986) were similar (Fig. 4a). We did not measure specifically the refractive index, but it should follow the same diel pattern as FSC, SSC, and cell size (Stramski and Reynolds 1993, Stramski et al. 1995, DuRand et al. 2002) and remain unaffected by increased irradiance. The diatom showed a small increase in FSC and SSC with increased irradiance (as in Ackleson et al. 1990, DuRand and Olson 1996, 1998, Stramski et al. 2002) caused by the contrasting influence of increased cell size and a probable decrease in refractive index due to cell swelling. Scattering changes in diatoms have been attributed mainly to cell swelling (i.e., cell water content increase) in response to increased irradiance (Ackleson et al. 1990, 1993, Ackleson and Cullen 1991). Diatoms possess water-containing vacuoles that can account for up to 55% of total cell volume (Stoermer and Sicko-Goad 1985) and changes in the cellular water content will strongly affect cell size and refractive index (Bricaud et al. 1988, Aas 1996). Cell swelling can be detected by increased cell size along with a constant a^*_{ph} coupled to a decrease in refractive index (Ackleson et al. 1990, 1993, Ackleson and Cullen 1991) and associated with a FSC increase (Shapiro 1988, Brussaard et al. 1999). These variations in cell size, a^*_{ph}, and FSC were observed here for *T. pseudonana* (Fig. 1, c and d), and although the refraction index was not specifically measured, it probably decreased. Break-down of the FSC versus SSC relationship (Fig. 4b) is a further indication of cell swelling. Other diel variability studies

showed an increase in refractive index during the day and a decrease at night for cultures of *T. pseudonana* (Stramski and Reynolds 1993), *Synechococcus* (Stramski et al. 1995), and *Nannochloris* sp. (DuRand and Olson 1998), as well as an increase in refractive index with increased irradiance (DuRand and Olson 1998, Stramski et al. 2002). Ongoing acclimative changes in cell properties in our experiments may explain diverging results with these previous studies that used fully acclimated cultures. The *FSC** response to increased irradiance reflected both the changes in FSC and Chla_c, and this response was amplified for the diatom since the decrease in Chla_c added its contribution to the increased cell size. Consequently, the increased irradiance doubled the diel variation in *FSC** (from 81 to 176%; Table 2) for the diatom species. The diel variations of *FSC** under high irradiances (up to 176%) thus reached 30% of the maximum *FSC** variation observed between our two species, which was up to ~600% or ~7-fold (from 7 to 50; Table 2).

Figure 4: Relationships between SSC and FSC for cultures of *Imantonia rotunda* (a) and *Thalassiosira pseudonana* (b) exposed to the following irradiances: 100 (●), 250 (▼), and 500 ( ) µmol photons·m^{-2}·s^{-1}. The solid line in panel (a) represents a linear regression between SSC and FSC for *I. rotunda*, regardless of the irradiance.

Imantonia rotunda

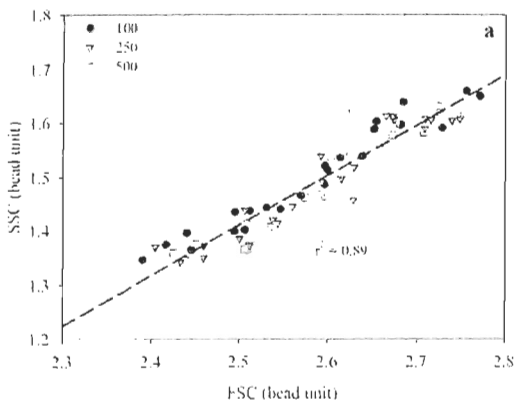

Thalassiosira pseudonana

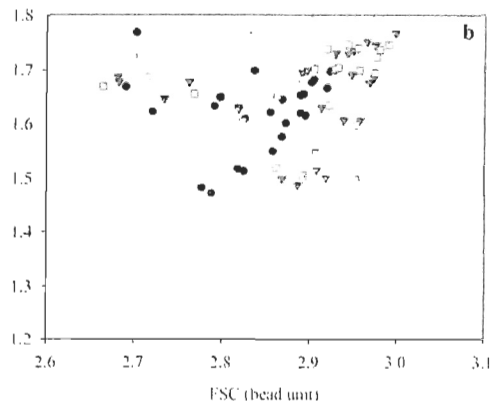

Estimates of chl-*a* and pigment composition from absorption characteristics – We next examined if diel and irradiance-induced variations affected the relationship between $a_{ph}(440)$ and chl-*a*, since there is a strong interest in extracting information on phytoplankton biomass from optical properties (DuRand et al. 2002). In the present study, for a given chlorophyll-*a* concentration, the haptophyte absorption was substantially higher than that for the diatom (Fig. 5), consistent with a greater pigment-packaging effect for the diatom. For both species, the diel and irradiance-induced variations did not significantly affect the $a_{ph}(440)$ versus. chl-*a* relationships, reflecting the small changes in packaging.

Changes in the phytoplankton absorption coefficient (a_{ph}) spectra can also affect the absorption ratios between wavebands (such as 440, 488, and 555 nm) typically used in standard ocean color algorithms to estimate chl-*a* concentrations (Arrigo et al. 1998, O'Reilly et al. 1998, Dierssen and Smith 2000). Such a_{ph} spectral variations are known to be influenced by the relative proportion of photosynthetic and photoprotective carotenoids (Bricaud et al. 1995, Culver and Perry 1999). The overall relationship between the ratio of photoprotective carotenoids to chl-*a* and $a_{ph}(440)/a_{ph}(488)$ when all the data were considered together was PPC/chl-*a* = 0.425 – 0.152 $a_{ph}(440)/a_{ph}(488)$ (r^2 = 0.45, n = 144, Fig. 6). This was fairly similar to the results of Stuart et al. (2000). There was no evidence for a significant influence of diel variation on this relationship. However, the relationship was clearly affected by the short-term response to increased irradiance, particularly for the diatom (Fig. 6 and Table 2).

Figure 5: Relationships between the phytoplankton absorption coefficient at 440 nm [$a_{ph}(440)$; m^{-1}] and chl-*a* concentration ($mg \cdot m^{-3}$) for cultures of *Imantonia rotunda* (Ir; closed symbols) and *Thalassiosira pseudonana* (Tp; open symbols) exposed to the following irradiances: 100 (circles), 250 (inverted triangles) and 500 (squares) µmol photons$\cdot m^{-2} \cdot s^{-1}$. The dark gray dashed line refers to a power regression between these variables for *I. rotunda* (all irradiances considered), and the black dotted line refers to a similar regression for *T. pseudonana*.

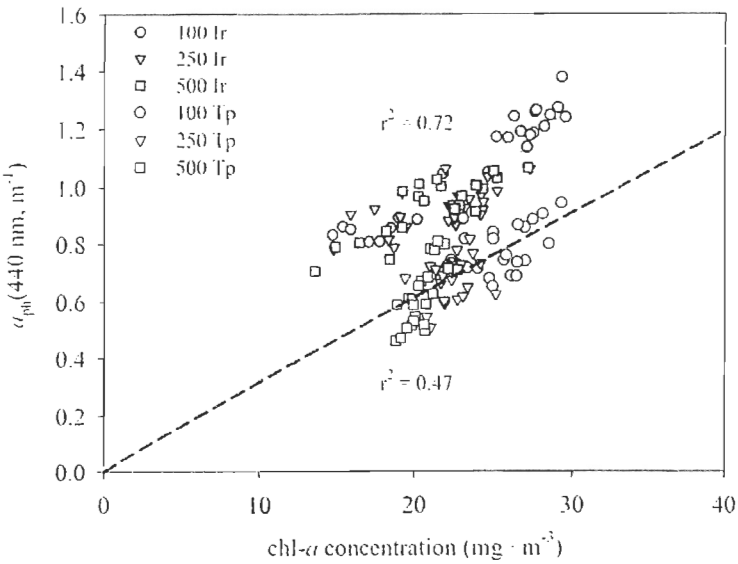
100 Ir
250 Ir
500 Ir
100 Tp
250 Tp
500 Tp
r² = 0.72
r² = 0.47
1.6
1.4
1.2
1.0
0.8
0.6
0.4
0.2
0.0
0
10
20
30
40
a_{ph}(440 nm, m^{-1})
chl-a concentration (mg · m^{-3})

Figure 6: Relationships between PPC/chl-*a* ratios and $a_{ph}(440)/a_{ph}(488)$ for cultures of *Imantonia rotunda* (Ir; circles) and *Thalassiosira pseudonana* (Tp; inverted triangles) exposed to the following irradiances: 100 (control irrad.; filled symbols), 250 and 500 µmol photons·m^{-2}·s^{-1} (high irrad.; open symbols). The red lines indicate linear regressions between these variables for *I. rotunda* under control [solid line; PPC/chl-*a* = 0.228 - 0.059 $a_{ph}(440)/a_{ph}(488)$, n = 24, r^2 = 0.36] and high irradiances [dashed line; PPC/chl-*a* = 0.473 - 0.166 $a_{ph}(440)/a_{ph}(488)$, n = 48, r^2 = 0.84]. The blue lines designate exponential regressions for *T. pseudonana* under control (solid line; PPC/chl-*a* = 0.09 + 24.62 exp {-4.55 [$a_{ph}(440)/a_{ph}(488)$]}, n = 24, r^2 = 0.58) and high irradiances (dashed line, PPC/chl-*a* = 0.04 + 3.39 exp {-1.98 [$a_{ph}(440)/a_{ph}(488)$]}, n = 48, r^2 = 0.85).

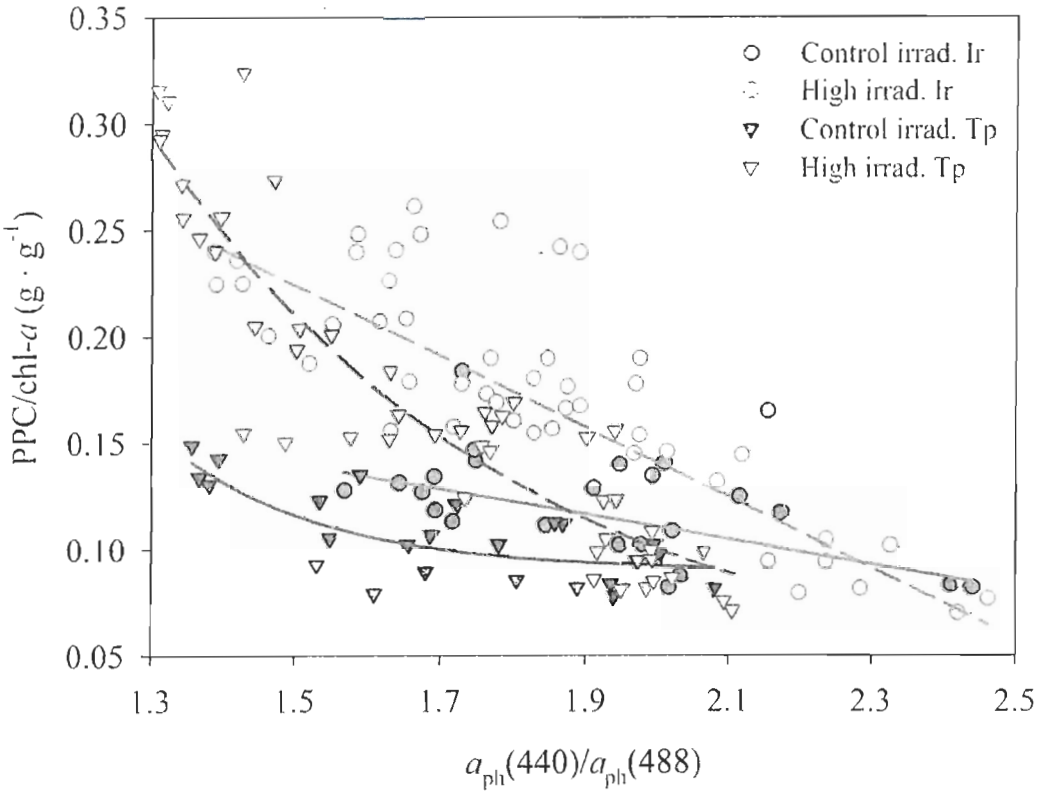
0.35
0.30
0.25
0.20
0.15
0.10
0.05
PPC/chl-a (g · g-1)
1.3
1.5
1.7
1.9
2.1
2.3
2.5
aph(440)/aph(488)
Control irrad. Ir
High irrad. Ir
Control irrad. Tp
High irrad. Tp

These short-term irradiance-induced changes can thus contribute to the variability in phytoplankton absorption spectra in natural environments (Bricaud et al. 1995) and in related chl-*a* retrieval.

Implications for field observations – We believe the diel changes reported in this work can be relevant for field observations, particularly in the context of remote-sensing. The amplitude of diel variations was >100% over 24 h for photoprotective carotenoids (both species), mean cell volume (*I. rotunda*), and intracellular photosynthetic pigment concentration (*T. pseudonana*) (Table 2). If these diel changes are combined with increased irradiance, then the amplitude of diel variations increases. This increase in amplitude was larger for pigments (up to 2-fold or more notably for PPC_c in *I. rotunda* and for photosynthetic pigments in *T. pseudonana*) than for optical properties (1.5-fold for $a^*_{ph}[440]$ in *I. rotunda* and 2-fold for $\sigma_a(488)$ and *FSC** in *T. pseudonana).*

The variations in optical characteristics due to taxonomy, diel pattern, and photoacclimation processes can thus have important implications for the interpretation of optical properties measured at sea and, consequently, can have a significant impact on the retrieval of chl-*a* from remotely-sensed data. In field studies, the diel and irradiance-induced variability in optical properties has been primarily attributed to particle abundance (Siegel et al. 1989). The contribution of particle morphology (refractive index and size) may have been overlooked since the plankton community structure was rarely studied. This

study states the importance of cell morphological and physiological variations and indicates the need to study the plankton community structure in field bio-optical studies. Our results also highlight the need to choose and report sampling times for optical measurements made at sea, as well as to have information on vertical mixing and photoacclimation of phytoplankton, in addition to taxonomic composition, to interpret the natural variability of *in situ* absorption and scattering coefficients.

CHAPITRE 2:

INHERENT OPTICAL PROPERTIES OF PHYTOPLANKTON CULTURES USING CELL-BASED FLOW CYTOMETRY AND TOTAL ABSORPTION AND ATTENUATION AC-9 MEASUREMENTS.

RÉSUMÉ

L'influence de l'état physiologique, associé aux phases de croissance, sur les propriétés optiques du phytoplancton a été étudiée sur quatre espèces phytoplanctoniques (*Thalassiossira pseudonana* (Hust.) Hasle and Heimdal, *Alexandrium tamarense* (Lebour) Balech, *Imantonia rotunda* Reynolds et *Nannochloropsis* sp.) en cultures à grand volume. Les coefficients d'absorption et de diffusion totaux (obtenus avec la sonde ac-9), la composition pigmentaire (HPLC), ainsi que les indices de diffusion, la fluorescence rouge et la concentration des cellules phytoplanctoniques (obtenus par cytométrie en flux, sauf pour *A. tamarense*), ont été mesurés à une fréquence journalière. Pour chaque espèce, au moins deux phases de croissance ont été étudiées (phase de latence, exponentielle, stationnaire et/ou de déclin). Les propriétés optiques totales et cellulaires étaient généralement affectées par la phase de croissance et différaient en fonction de l'espèce phytoplanctonique. Le spectre d'absorption spécifique à la chl-*a* était altéré par les phases de croissance. Les relations entre les ratios d'absorption du phytoplancton ($a_{ph}(440)/a_{ph}(488)$ et $a_{ph}(440)/a_{ph}(555)$) et les ratios pigmentaires (caroténoïdes photoprotecteurs (PPC)/chl-*a* et caroténoïdes photosynthétiques (PSC)/chl-*a*) n'étaient significatives que pour les phases exponentielles et stationnaires. Les propriétés de diffusion étaient également influencées par la phase de croissance, notamment aux courtes longueurs d'onde où le coefficient de diffusion normalisé ($b_p(\lambda)/b_p(555)$) était plus fort pour des cellules phytoplanctoniques en phase de latence ou de déclin. De plus, la présence de bactéries et de détritus, due au vieillissement des cultures, déformait le spectre de diffusion normalisé et modifiait la relation entre le

coefficient de diffusion du phytoplancton (b_{ph}) et la concentration en chl-*a*. Les détritus de petite taille (<20 µm), ainsi que les bactéries, augmentaient la diffusion aux courtes longueurs d'onde, alors que les détritus de grande taille, formés par agrégation au cours du temps, augmentaient la diffusion aux grandes longueurs d'onde. Les bactéries et les particules détritiques affectent la variabilité des IOPs totales, particulièrement la diffusion, en modifiant la distribution de taille des particules. Par conséquent, les variations des propriétés optiques dues aux phases de croissance et aux changements d'assemblages planctoniques peuvent contribuer à altérer la couleur des océans, particulièrement pendant les périodes de floraison, et devraient être prises en compte dans les études bio-optiques en milieu naturel.

ABSTRACT

The influence on phytoplankton optical properties of the physiological state associated with the growth phases was studied in four phytoplankton species (*Thalassiossira pseudonana* (Hust.) Hasle and Heimdal, *Alexandrium tamarense* (Lebour) Balech, *Imantonia rotunda* Reynolds and *Nannochloropsis* sp.) cultured in large volume (180 L). Total absorption and scattering coefficients (obtained with the ac-9 sensor), pigment composition (HPLC) and phytoplankton scattering indices, red fluorescence and cell concentration (obtained by flow cytometry, except for *A. tamarense*) were measured daily. For each species, at least two different growth states were examined (lag, exponential, stationary and/or decline). Total and cellular optical properties were generally affected by the growth phase and the species. The chl-*a*-specific absorption spectra changed according to the growth phase. The relationships between phytoplankton absorption ratios ($a_{ph}(440)/a_{ph}(488)$ and $a_{ph}(440)/a_{ph}(555)$) and pigment composition (photoprotective carotenoids (PPC)/chl-*a* and photosynthetic carotenoids (PSC)/chl-*a* ratio) were significant only under exponential and stationary phases. Scattering properties were also influenced by the growth phase, particularly at short wavelengths where the normalized scattering coefficient ($b_p(\lambda)/b_p(555)$) was higher for cells in lag or decline phase. Moreover, the presence of bacteria and detritus, as the culture aged, distorted the normalized scattering spectra, and disturbed the relationship between phytoplankton scattering coefficient (b_{ph}) and chl-*a* concentration. Small detritus (<20 µm), as well as bacteria, increased the scattering at short wavelengths, whereas large detritus formed through aggregation with time increased the scattering at longer

wavelengths. Bacteria and detrital particles affected the bulk IOPs variability, mostly scattering, by changing the particle size distribution. Optical properties variations due to growth phase and to changes in plankton assemblages can clearly contribute to the changes in ocean color particularly during bloom events and should be considered in bio-optical field studies.

INTRODUCTION

Understanding the component of the radiation field that emerges from the ocean's surface is essential for the interpretation of ocean color. Changes in the biogenic particulate matter present in surface waters affect ocean color in a large extent through the bulk inherent optical properties (IOPs; Gordon et al. 1975, Morel and Prieur 1977, Bricaud et al. 1998). Determining the concentration of chlorophyll or particulate carbon using reflectance spectra requires an accurate and comprehensive database of IOPs, such as absorption (a), scattering (b) and backscattering coefficients (b_b) (Kirk 1994, Bricaud et al. 1995, Stramski et al. 2001). Variations of these IOPs are linked to changes in the composition, cell abundance and optical characteristics of phytoplankton assemblages (Stramski and Reynolds 1993, Mobley 1994, Stramski and Mobley 1997). These variations are induced by changes in cell characteristics such as size, refractive index, chemical composition, intracellular pigment composition and phytoplankton concentration (Reynolds et al. 1997, Bricaud et al. 1999, Stramski et al. 2002). They can have a significant impact on the retrieval of chlorophyll a (chl-a) measurements from remotely-sensed data. It is thus important to improve our understanding of this variability (Stramski and Reynolds 1993, DuRand and Olson 1998).

Changes in growth phase may take place in the ocean during the development and decline of phytoplankton blooms, contributing to the variability of IOPs (McLeroy-Etheridge and Roesler 1998). Most bio-optical studies have been conducted on exponentially growing phytoplankton cultures; only a few considered several growth

phases (Kiefer et al. 1979, Voss et al. 1998, McLeroy-Etheridge and Roesler 1998). Few studies have examined the long-term response of cells during population decline following nutrient limitation (Reynolds et al. 1997, Stramski et al. 2002, Cleveland and Perry 1987).

Heterotrophic bacteria can also affect *in situ* measurements of IOPs (Spinrad et al. 1989, Mitchell and Kiefer 1984). During the development and decline of phytoplankton blooms, changes in the bacterial proportion relative to phytoplankton cells can contribute significantly to IOPs variations (Stramski and Kiefer 1991). Detritus frequently increase at the end of a bloom and they can also affect IOPs (Iturriaga and Siegel 1989, Kitchen and Zaneveld 1990, Babin et al. 2003). All these elements (phytoplankton, bacteria, detritus) are present during phytoplankton blooms and they contribute to the natural variability of IOPs.

We took advantage of a series of large-volume phytoplankton cultures, which had been set-up for calibration purposes, to examine the changes in IOPs taking place during the growth and decline of four algal species. Our objective was to determine the influence of the growth phases of these cultures on *in vivo* and *in situ*-determined IOPs, and to examine the interference by bacteria and detritus, particularly during the decline of the algal populations. Our experimental conditions simulate phytoplankton blooms, with the lag, exponential and stationary/decline phases corresponding to pre-bloom, bloom and post-bloom periods respectively.

MATERIALS AND METHODS

The list of mathematical symbols and acronyms used in this paper is provided in Table 1.

Experimental design - Mono-specific cultures of the toxic dinoflagellate *Alexandrium tamarense* (*At*, CCMP1771, 35-45 µm), the centric diatom *Thalassiosira pseudonana* (*Tp*, CCMP1335, 4-6 µm), the haptophyte *Imantonia rotunda* (*Ir*, CCMP457, 3-5 µm) and the eustigmatophyte *Nannochloropsis* sp. (*Na*, CCMP528, 2-3 µm) were obtained from the Provasoli-Guillard National Center for Culture of Marine Phytoplankton, Maine, USA. These cultures were grown at 22°C (± 2°C) in 20L glass bottles. The culture medium was prepared with 0.2 µm-filtered natural seawater (FSW, salinity of 29), autoclaved and enriched with f/2 -Si nutrients for *A. tamarense* and with f/2 nutrients for the other cultures (Guillard and Ryther 1962). Prior to the experiment, the cultures were pre-acclimated for 7 days at 400 µmol photons·m^{-2}·s^{-1} PAR with a 14:10-h light:dark photoperiod using cool-white fluorescent lights. Irradiance was measured daily with a PAR sensor (QSL-100 Biospherical Instruments Inc.). When the cultures reached the exponential growth phase, they were transferred to 180 L clear plastic containers filled with FSW enriched with f/8 medium. These large-volume cultures were bubbled with filtered air.

Table 1: Mathematical symbols and acronyms used in this study with associated units.

Symbol	Definition	Units
λ	Wavelength	nm
FSC	Forward-angle light scatter: proxy of scattering cross section at 488 nm	bead unit (bu)
FL3	Cell chlorophyll fluorescence	bu
SSC	Side-angle light scatter: cell complexity index	bu
$b_{ph\text{-}FCM}$	Phytoplankton scattering coefficient index measured by flow cytometry	bu·(cells·m^{-3})
$b_{bact\text{-}FCM}$	Bacteria scattering coefficient index measured by flow cytometry	bu·(cells·m^{-3})
$b_{ph+bact\text{-}FCM}$	Sum of $b_{ph\text{-}FCM}$ and $b_{bact\text{-}FCM}$	bu·(cells·m^{-3})
b_{ph}	Phytoplankton scattering coefficient estimated from ac-9/FCM relationship	m^{-1}
b_{bact}	Bacteria scattering coefficient estimated from ac-9/FCM relationship	m^{-1}
$b_{ph+bact}$	Sum of b_{ph} and b_{bact}	m^{-1}
b_p	Particulate matter scattering coefficient measured with the ac-9 sensor	m^{-1}
a_{tot}	Total absorption coefficient measured with the ac-9 sensor	m^{-1}
a_p, a_d, a_{ph}	Absorption coefficient of particulate matter, detritus and phytoplankton	m^{-1}
a^*_{ph}	Chl-*a* specific absorption coefficient	m^2·(mg chl-*a*)$^{-1}$
PPC/chl-*a*	Photoprotective carotenoid pigment to chl-*a* ratio	g·g^{-1}
PSC/chl-*a*	Photosynthetic carotenoid pigment to chl-*a* ratio	g·g^{-1}
σ_b	Scattering cross section	μm^2·cell^{-1}
σ_a	Absorption cross section	μm^2·cell^{-1}

For each culture, samples were taken daily for the *in vivo* parameters (flow cytometry, HPLC-determined pigments, phytoplankton absorption using a spectrophotometer) and for *in situ* measurements directly in the culture containers using an ac-9 profiler (absorption and scattering). Details of these measurements are given below.

Microscopic observations – Samples from the cultures were fixed in acid iodine Lugol solution at 2% v/v final concentration. The presence of non-living particulate matter (cell detritus and aggregates) or of contaminating cells in the different cultures was checked with an inverted phase-contrast microscope (Zeiss Axiovert 100).

Attenuation, absorption and scattering measurements - *In situ* total attenuation and absorption coefficients (c and a) were determined at nine wavelengths (412, 440, 488, 510, 532, 555, 650, 676 and 715 nm) with a flow-through absorption and attenuation meter (ac-9, WETLabs) equipped with a 25-cm long cell (Pegau et al. 1997, Zaneveld et al. 1994, Twardowski et al. 1999). Before inoculation of phytoplankton in the containers, measurements were taken to subtract the noise from the ac-9 data. The particulate scattering coefficient (b_p) was obtained from the difference between the ac-9 coefficients of total attenuation (c_{tot}) and total absorption (a_{tot}).

In vivo absorption spectra (280 to 850 nm by 1 nm) of particulate matter ($a_p(\lambda)$) and phytoplankton $a_{ph}(\lambda)$ suspensions were measured using the wet filter technique (Yentsch 1962, Mitchell and Kiefer 1984), with a double-beam spectrophotometer (Perkin-Elmer Lambda 2) equipped with an integrating sphere (RSA-PE-20) and using air as a reference. Samples were filtered through Whatman GF/F glass-fiber filters and stored flat at -80°C in Fisherbrand Histoprep tissue capsules. Sample and blank filters were wetted in filtered sea water and placed in the spectrophotometer immediately. The optical density of the particulate matter was measured directly and corrected for scattering by subtracting the optical density measured between 750 and 850 nm (Bricaud and Stramski 1990). The corrected optical density of the particulate matter was transformed into particulate/detrital matter absorption coefficient ($a_{p/d}(\lambda)$) using a quadratic equation (Hoepffner and Sathyendranath 1992, Cleveland and Weidemann 1993):

$$a_{p/d}(\lambda) = [2.3 \times (A \times OD(\lambda) + B \times OD(\lambda)^2)]/X \qquad (1)$$

where OD is the corrected optical density of the particulate material measured on a filter, λ is the wavelength, X is the volume filtered divided by the clearance area of the filter, and the coefficients A and B were determined locally and individually for each species (for *A. tamarense*: A=0.245 and B=0.511, for *Nannochloropsis sp.*: A=0.351 and B=0.15, for *I. rotunda*: A=0.361 and B=0.167, for *T. pseudonana* A=0.344 and B=0.300, for mixed cultures A=0.347 and B=0.522, Laurion et al. 2003).

The detrital absorption coefficient ($a_d(\lambda)$) was calculated using eq. (1) from the corrected optical density of non-pigmented particles by extracting the filter with methanol, rinsing with filtered sea water and scanning as above. Phytoplankton absorption coefficients, $a_{ph}(\lambda)$, were obtained by subtracting $a_d(\lambda)$ from $a_p(\lambda)$. The $a_{ph}(\lambda)$ values were then normalized by the cell concentration (determined by flow cytometry) to obtain the average absorption cross-section (σ_a), or by the chl-*a* concentration, to obtain the chlorophyll-specific absorption coefficient (a^*_{ph}).

Flow Cytometry - A FACSort flow cytometer analyzer (FCM, Becton Dickinson, San Jose, CA), equipped with a 488 nm laser beam of 15 mW, was used to measure the following characteristics of phytoplankton cells: forward-angle light scatter (FSC_{phy}, θ =1-10°), side-angle light scatter (SSC_{phy}, θ = 90°) and chlorophyll fluorescence (FL3, >650 nm), as well as to calculate the abundance of cells determined from the pump flow rate (60 $\mu L \cdot min^{-1}$) and sample run time. Fresh triplicate 2 mL samples were immediately analyzed with FCM, following the addition of 2.14 µm monodisperse standard latex-polystyrene beads (YG, Fluoresbrites, Polyscience, Inc., Warrington, PA, U.S.A.) as internal standards. Cells of *A. tamarense* were too large (35-45 µm) for analysis by the FCM instrument used in this study which could not detect particles >20 µm. The growth phases of *A. tamarense* cells were thus followed based on the chl-*a* concentrations measured by HPLC.

Data were analyzed using the Cell Quest and Attractors softwares (Becton-Dickinson). All values of FSC, SSC and FL3 were normalized with reference to the standard beads of 2.14 µm.

For determination of the abundance of heterotrophic bacteria present in the cultures, 5 mL samples were fixed with glutaraldehyde (0.1% final concentration), frozen in liquid nitrogen, and stored at -80°C. Within 6 months, 2 mL duplicate sub-samples were stained with a nucleic acid stain (SYBR Green II, Molecular Probes, according to the protocol of Marie et al. 1997). Monodisperse standard latex-polystyrene beads of 0.5, 1 and 2.14 µm (YG, Fluoresbrites) were systematically added as internal standards to each bacterial sample analyzed. Samples were analyzed with the FCM at a flow rate of 12 $\mu L \cdot min^{-1}$. Bacterial cells were discriminated and enumerated according to their signature in a plot of green fluorescence (FL1, Y-axis, green fluorescence form SYBR Green II) against side scatter (SSC, X-axis) (Lebaron et al. 1998), FSC_{bact} and SSC_{bact} were then obtained from these plots.

The SSC signal of phytoplankton and bacteria can give information about the intracellular distribution of cell material.

Since the light scatter at low angles relative to the excitation light (FSC), should contribute strongly (more than 90%) to total scattering from all angles (DuRand and

Olson 1996, DuRand et al. 2002), FSC at 488 nm constitutes a good proxy for the scattering cross section (σ_b), both for phytoplankton (FSC_{ph}) and bacteria (FSC_{bact}).

The approximations of the scattering coefficient at 488 nm for phytoplankton ($b_{ph\text{-}FCM}(488)$) and bacteria ($b_{bact\text{-}FCM}(488)$) were obtained by the product of FSC by cell concentration: FSC_{ph} × [phytoplankton] = $b_{ph\text{-}FCM}$ (488) for phytoplankton and FSC_{bact} × [bacteria] = $b_{bact\text{-}FCM}$ (488) for bacteria. The sum of $b_{ph\text{-}FCM}(488)$ and $b_{bact\text{-}FCM}(488)$ gives a proxy of the scattering coefficient of the (phytoplankton + bacteria) compartment, $b_{ph+bact\text{-}FCM}(488)$.

For all the cultures without microscopically detectable detrital particles, we assumed that phytoplankton and bacteria were the exclusive contributors to scattering. In this case, there was a strong relationship between $b_{ph+bact\text{-}FCM}(488)$ estimated by FCM and $b_p(488)$ measured by ac-9 ($b_{ph+bact\text{-}FCM}(488) = (0.25 \cdot 10^{12})\ b_p(488)$, $r^2 = 0.98$, n = 23). This relationship can thus be used to determine the real scattering coefficients of phytoplankton [b_{ph} (488)] and bacteria [$b_{bact}(488)$] from the approximation of the scattering coefficient at 488 nm for phytoplankton [$b_{ph\text{-}FCM}(488)$] and bacteria [$b_{bact\text{-}FCM}(488)$] in all the cultures, including those with detritus. The sum of b_{ph} (488) and b_{bact} (488) gives a real scattering coefficient of the (phytoplankton + bacteria) compartment, $b_{ph+bact}(488)$. Finally, the total detritus contribution to scattering can be obtained by subtraction of $b_{ph+bact}(488)$ from $b_p(488)$ measured by the ac-9.

The total <20 µm particles were enumerated using the FSC signal. The concentration of detritus (non-phytoplanktonic and non-bacterial <20 µm particles) was determined by subtraction of the concentrations of phytoplankton and bacteria from those of total <20 µm particles. The scattering coefficient at 488 nm of <20 µm detrital particles ($b_{d\ <20\mu m}$) can be approximated using an average scattering cross-section of <20 µm detrital particles ($\sigma_{b\ d\ <20\mu m}$, $19 \cdot 10^{-2} \pm 25 \cdot 10^{-2}$ μm^2) from Green et al. (2003). The product of $\sigma_{b\ d\ <20\mu m}$ by detrital particles concentration gives an approximation of $b_{d\ <20\mu m}$. However, ($b_{d\ <20\mu m}$) values are only approximations since detrital particles are diverse in size, refractive index and shape, and hence in their optical properties.

Pigments determination - For each culture, 5 to 50 mL samples were filtered through a 25 mm Whatman GF/F filter, frozen in liquid nitrogen, and stored at -80°C. Pigments were analyzed following the method of Zapata et al. (2000) with an HPLC system composed of a Thermo Separation (TSP) P4000 Quaternary Pump, AS3000 Autosampler, SCM1000 Solvent Degasser, SN4000 Interface Controller (SpectraSYSTEM), Spectrafocus Absorbance Detector (400-700 nm) and a Spectroflow 980 Fluorometer (set at 412 nm). The whole system was computer-controlled using TSP's PC1000 software. Peak separation was done on a reverse phase Waters Symmetry column (C_8, 3.5µ, 4.6x150 mm) thermostated at 25°C using a water jacket. The chromatogram values were transformed into volumetric concentrations of the pigments present in the samples using external pigment standards from DHI (Hørsholm, Denmark). The chl-*a* included chlorophyll *a*, and chlorophyll *a* allomers and epimers. For the present study, we grouped pigments into two categories: photosynthetic (PSC:

fucoxanthin, 19'-butanoyloxyfucoxanthin, 19'-hexanoyloxyfucoxanthin, 4-keto-19'-hexanoyloxyfucoxanthin, peridinin and vaucheriaxanthin-ester) and photoprotective carotenoid pigments (PPC: β,β-carotene, diadinoxanthin, diatoxanthin, violaxanthin and zeaxanthin).

Mathematical and statistical analysis – After testing for normality and homoscedasticity, a one-way ANOVA was used to evaluate the effect of time on the different parameters. A confidence level of 95% was used throughout these analyses and the differences between the regression parameters, for each species, were assessed using an analysis of covariance (ANCOVA) (Zar 1999). All statistical analyses were performed using SPSS 9.0 (SPSS Inc.).

RESULTS

The overall experiment lasted approximately 2 weeks, but actual duration varied according to the species. The experiment was stopped after 19 days for *Nannochloropsis* sp., after 5 days for *I. rotunda* (see below), after 12 days for *T. pseudonana* because of its rapid growth rate followed by a strong decline, and after 12 days for *A. tamarense* because it formed a brown patch at the surface of the container which prevented coherent sampling. Contamination by *T. pseudonana* was observed in the culture of *I. rotunda* from day 5 likely due to an incomplete cleaning of the ac-9 profiler, which was immersed in each culture in turn. This gave us the opportunity to study the optical properties of a mixed culture (*I. rotunda* and *T. pseudonana*) and we will refer hereafter to the next 14 days in this culture as the "Mixed culture". The sampling of this Mixed culture was stopped on day 19 of the experiment.

Phytoplankton and bacterial abundances - The presence and duration of each growth phase varied with species. For each species, at least two different growth states were examined (lag, exponential, stationary and/or decline, Fig. 1). *Nannochloropsis* sp. had the longest exponential phase, lasting 9 days (Fig. 1a). *T. pseudonana* and *I. rotunda* quickly reached the stationary or decline phase after 2-3 days (Fig. 1b and 1c). The total cell abundance in the Mixed culture increased from day 8 to 13 and then remained constant (not shown). The FCM data showed that the two species, present in the Mixed culture, grew differently. *T. pseudonana* grew exponentially from day 5 to 13, followed by a decline, whereas *I. rotunda* increased slowly between day 9 and 19 (Fig. 1c). *A.*

tamarense was the only species with a lag phase preceding the exponential phase, and it showed no stationary or decline phase during the 12-day experiment (Fig. 1d).

Bacteria concentrations at the beginning of the experiment, before phytoplankton inoculation, were between 9.7 and $11 \cdot 10^4$ mL^{-1}. For *T. pseudonana*, *I. rotunda*, *A. tamarense* and the Mixed culture, the abundance of bacteria increased during the experiment, with variable growth rates (Fig. 1b, c and d, Table 2). For *Nannochloropsis* sp., the bacterial abundance increased until day 9 and then remained rather constant, in a pattern similar to that of phytoplankton abundance (Fig. 1a).

Figure 1: Bacterial abundance (cells·mL^{-1}, red squares) and phytoplankton (cells·mL^{-1}, black circles) or chlorophyll *a* concentration (mg·m^{-3}) for (a) *Nannochloropsis* sp., (b) *I. rotunda*, (c) *T. pseudonana* and (d) *A. tamarense* cultures. In (b), the Mixed culture is shown from day 5 to day 19 with *I. rotunda* (black circles), *T. pseudonana* (gray inverted triangles) and bacterial abundance (red squares). Average values and standard deviations are shown for abundance.

Nannochloropsis sp.

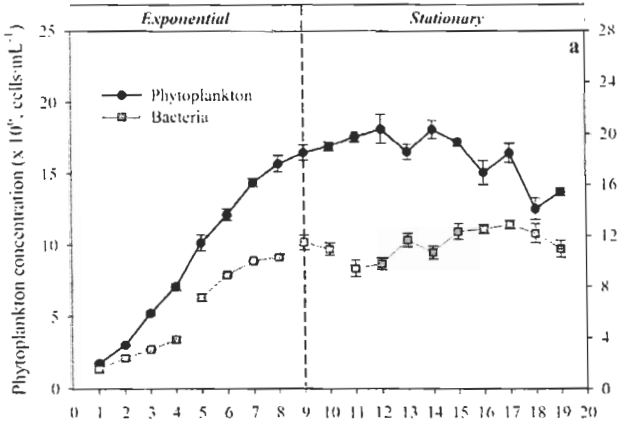

Thalassiosira pseudonana

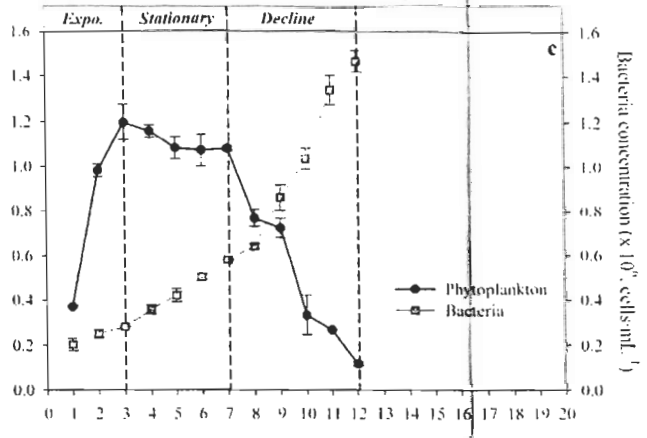

Imantonia rotunda

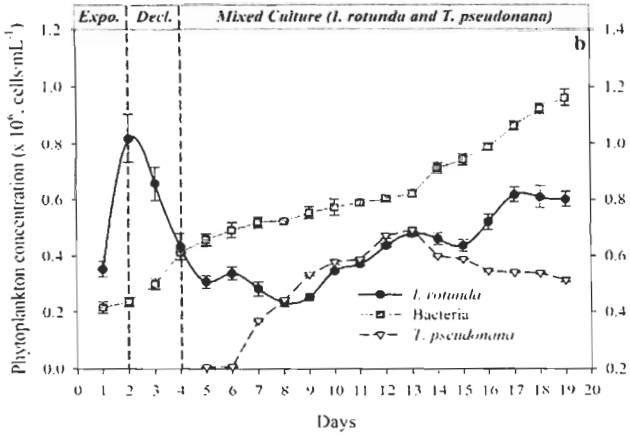

Alexandrium tamarense

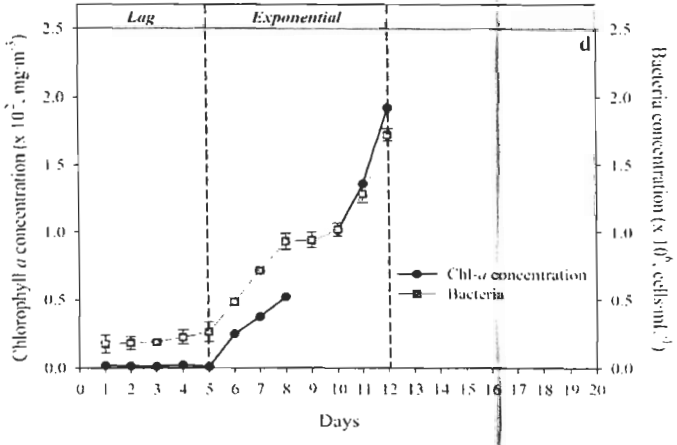

Table 2: Bacterial growth rates during the different phytoplankton growth phases in the cultures.

	Bacterial growth rates (d^{-1}) during the different phytoplankton growth phases			
	Lag	*Exponential*	*Stationary*	*Decline*
Nannochloropsis sp.	—	0.47	-0.005	—
Imantonia rotunda	—	0.07	—	0.17
Mixed culture *	—	0.03 (d_5 to d_{13})	—	0.06 (d_{13} to d_{19})
Thalassiosira pseudonana	—	0.16	0.18	0.23
Alexandrium tamarense	0.10	0.27	—	—

*The growth phases considered for the Mixed culture were those of *T. pseudonana*

Optical cross-sections from FCM - From previous experiments on diel variations of *T. pseudonana* and *I. rotunda* (Mas et al. 2008) and from this experiment, a strong relationship was observed between FL3 from FCM and spectrophotometric $\sigma_a(488)$ estimates ($\sigma_a(488) = 0.0092 \times (FL3)^{6.5}$, $r^2 = 0.95$, n = 194, Fig. 2), consistent with other studies (Iturriaga and Siegel 1988, Perry and Porter 1989, Green et al. 2003). This suggests that $\sigma_a(488)$ for phytoplankton cells can be estimated with reasonable accuracy from FL3 measurements. When this relationship is applied to the FL3 of the two species from the Mixed culture, the values of $\sigma_a(488)$ for *T. pseudonana* and *I. rotunda* obtained encompass the values reported for the corresponding mono-specific cultures.. Furthermore, the sum of the absorption coefficient of the two species, obtained by the product of FL3-based $\sigma_a(488)$ and cell abundance, was close to the phytoplankton spectrophotometric absorption coefficient for the Mixed culture. The error percentage between estimated and measured phytoplankton absorption coefficient was lower than 5% (Fig. 2b). This suggests that the FCM can be used to determine $a_{ph}(488)$ of the natural assemblages in the ocean for all individual species <20 μm.

Figure 2: (a) Relationship between FCM chlorophyll fluorescence (FL3, bead unit) and absorption cross-section ($\mu m^2 \cdot cell^{-1}$) at 488 nm, measured by spectrophotometry from data of the diel experiment of Mas et al. (2008) (open circles) and monospecific cultures from the present study (*Nannochloropsis* sp.: black circles; *I. rotunda*: red inverted triangles; *T. pseudonana*: blue squares). (b) Comparison between estimated a_{ph} (m^{-1}, 488 nm) from FCM (bars) and measured a_{ph} (m^{-1}, 488 nm) from spectrophotometer (open circles) for the Mixed culture, showing the contribution of *I. rotunda* (dark gray portion of the bars) and *T. pseudonana* (light gray portion of the bars). The standard deviation is shown for a_{ph} estimated from FCM.

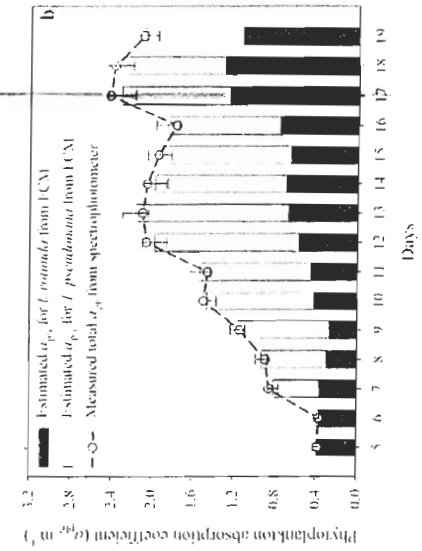
b
Estimated a_{ph} for *I. rotunda* from UCM
Estimated a_{ph} for *I. pseudonana* from UCM
Measured total a_{ph} from spectrophotometer
Phytoplankton absorption coefficient (a_{ph}, m^{-1})
Days

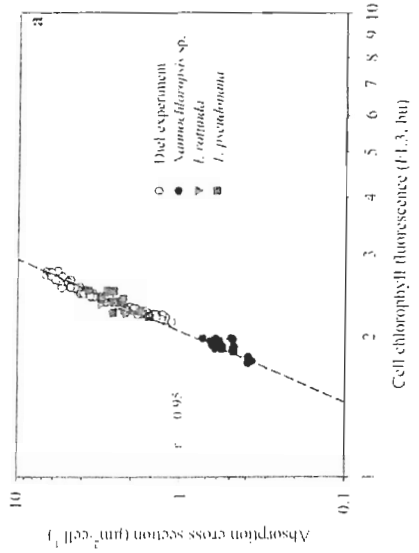
a
Del experiment
Nannochloropsis sp.
I. rotunda
I. pseudonana
Absorption cross section (μm^2·cell^{-1})
Cell chlorophyll fluorescence (FL3, bu)

The cellular optical properties followed closely but not totally the growth phase succession, a lag was sometimes observed. For *Nannochloropsis* sp., FL3 increased during the exponential phase and reached a plateau 4 days before the stationary phase started (Fig. 3a). For *T. pseudonana* and *I. rotunda*, FL3 increased over the first few days after cell abundance had started decreasing (in stationary or decline phase). For the Mixed culture, the patterns of FL3 variations for *I. rotunda* and *T. pseudonana* were similar to that of the corresponding mono-specific cultures with a lag of 1 or 2 days. Variations in phytoplankton FSC (FSC_{ph}) suggested a decrease in phytoplanton $\sigma_b(488)$ during the exponential phase and an increase during the stationary and decline phases (Fig. 3). Changes in bacteria FSC (FSC_{bact}) suggested an increase in bacterial $\sigma_b(488)$ following bacterial abundance, for *T. pseudonana*, *I. rotunda*, *A. tamarense* and the Mixed culture (Fig. 3b, c and d). For *Nannochloropsis* sp., the bacterial $\sigma_b(488)$ increased until day 9 and then decreased until the end of the experiment (Fig. 3a). The temporal variations of SSC showed a pattern similar to that of FSC for all species tested (data not shown).

Figure 3: Variations of chlorophyll fluorescence (FL3, open circles), forward-angle light scatter for phytoplankton (FSC_{phy}, black circles) and bacteria (FSC_{bact}, red squares), measured by FCM, for (a) *Nannochloropsis* sp., (b) *I. rotunda*, (c) *T. pseudonana* and (d) *A. tamarense* during the experiment. In (b), the Mixed culture is shown from day 5 to day 19 with FL3 for *I. rotunda* (open circles) and *T. pseudonana* (open squares) and FSC of *I. rotunda* (black circles), *T. pseudonana* (gray inverted triangles) and bacteria (red squares). Average values and standard deviations are shown for FL3, FSC_{phy} and FSC_{bact}.

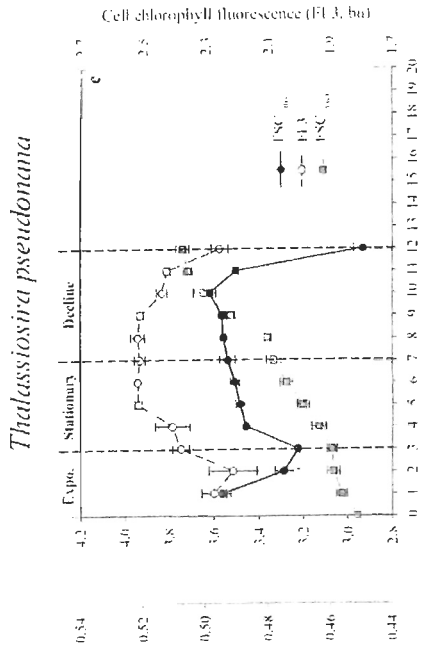
Thalassiosira pseudonana
Cell chlorophyll fluorescence (FL3, bu)
Expo.
Stationary
Decline
e
FL3
Bacteria forward-angle light scatter (FSC, bu)

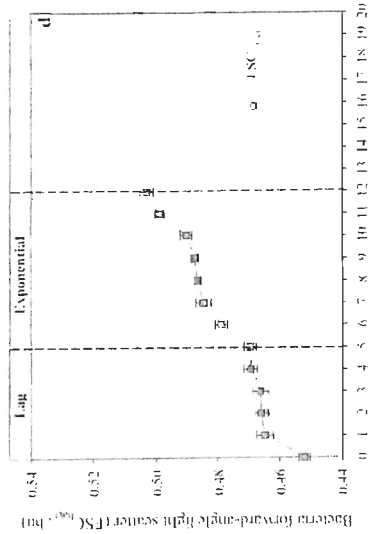
Alexandrium tamarense
Lag
Exponential
d
Days
Bacteria forward-angle light scatter (FSC, bu)

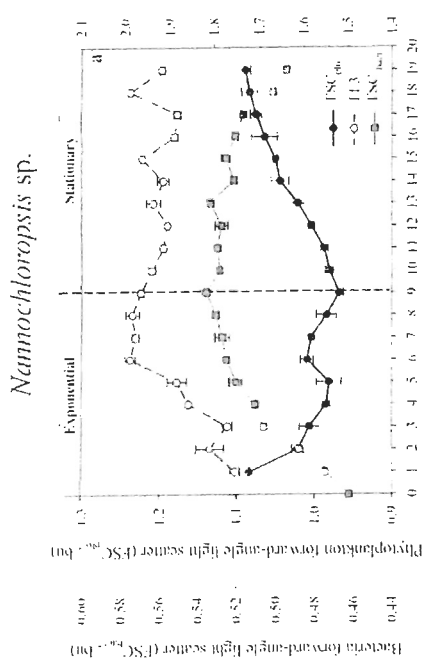
Nannochloropsis sp.
Exponential
Stationary
a
FL3
Phytoplankton forward-angle light scatter (FSC, bu)
Bacteria forward-angle light scatter (FSC, bu)

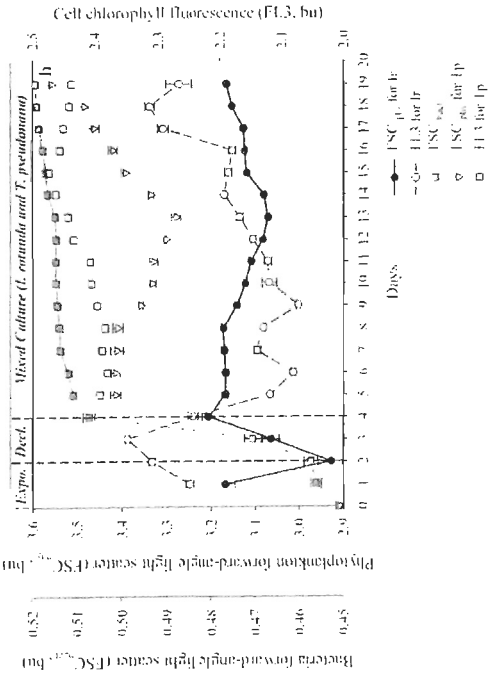
Imantonia rotunda
Cell chlorophyll fluorescence (FL3, bu)
Expo.
Decl.
Mixed Culture (I. rotunda and T. pseudonana)
b
Days
FL3 for Ir
FL3 for Ip
Phytoplankton forward-angle light scatter (FSC, bu)
Bacteria forward-angle light scatter (FSC, bu)

Pigments – The main accessory pigments were chlorophyll c_2 and peridinin for *A. tamarense*, chlorophylls c_1, c_2 and fucoxanthin for *T. pseudonana*, chlorophyll c_3, 19'-butanoyloxyfucoxanthin, fucoxanthin and 19'-hexanoyloxyfucoxanthin for *I. rotunda*, and vaucheriaxanthin and violaxanthin for *Nannochloropsis* sp.

The variations and ranges of pigment ratios differed between the four species (Fig. 4). However, in general, photoprotective pigments (PPC/chl-*a*) were relatively low during the exponential phase; they increased in stationary phase and decreased when cell abundance declined at the end of experiment. Photosynthetic carotenoids (PSC/chl-*a*) were also at their lowest concentrations during the exponential phase and they increased during the stationary and decline phase. They differed from photoprotective pigments notably during the decline phase in *T. pseudonana*, where the ratio of photoprotective pigments to chl-*a* decreased while the ratio of photosynthetic pigments to chl-*a* increased (Fig. 4b). The PSC/chl-*a* and PPC/chl-*a* ratios for *Nannochloropsis* sp. cells were, respectively, 1.6 to 3.5 folds lower and higher than those for *T. pseudonana*, *I. rotunda* and *A. tamarense* cells.

Figure 4 : Variations in the ratios of photoprotective carotenoids to chl-*a* (PPC/chl-*a*, $g \cdot g^{-1}$, filled circles) and photosynthetic carotenoids to chl-*a* (PSC/chl-*a*, $g \cdot g^{-1}$, open circles) for (a) *Nannochloropsis* sp., (b) *I. rotunda*, (c) *T. pseudonana* and (d) *A. tamarense* cultures.

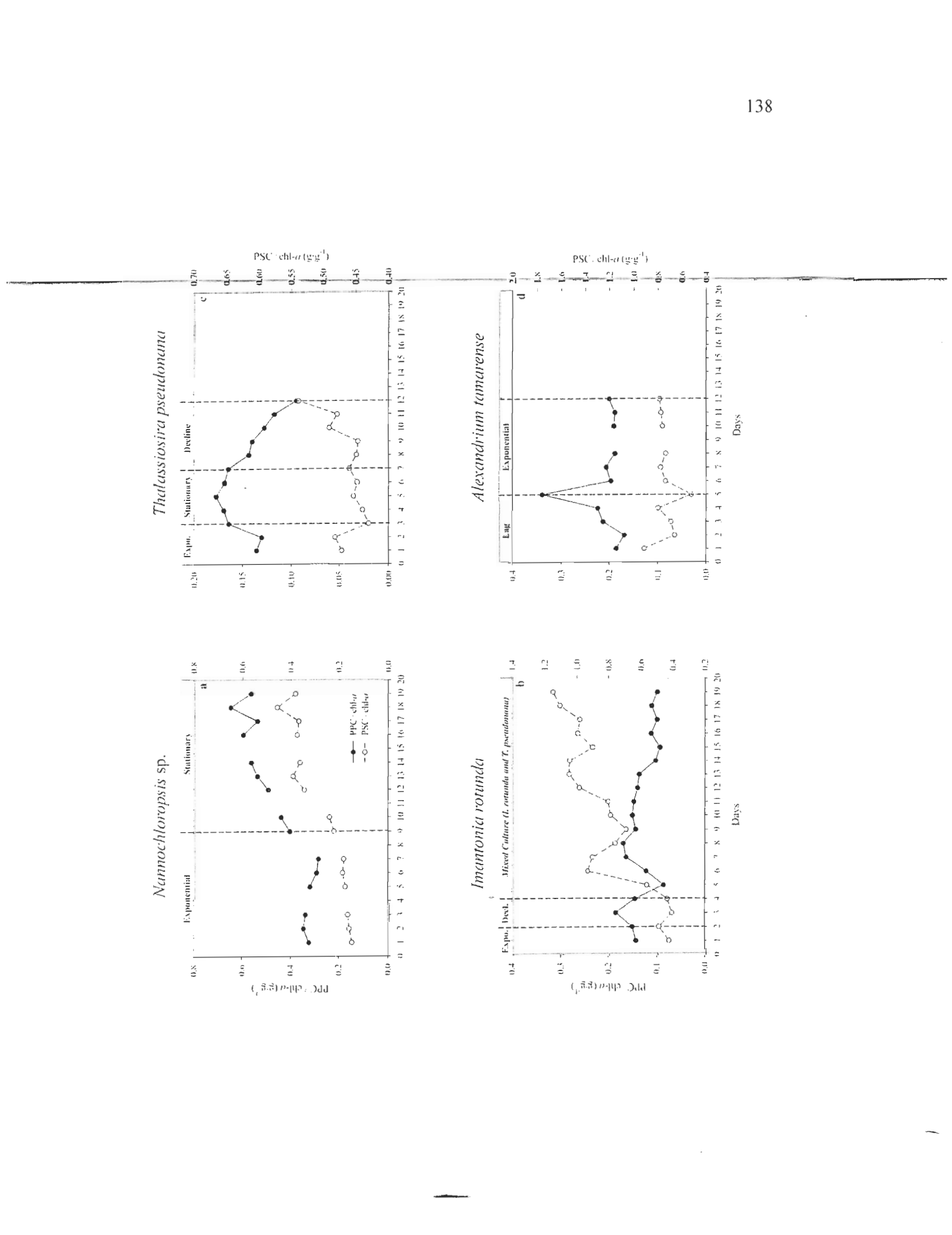
Nannochloropsis sp.
Thalassiosira pseudonana
Amantonia rotunda
Alexandrium tamarense
Mixed Culture (A. rotunda and T. pseudonana)
Expon.
Stationary
Decline
Exponential
Lag
Decl.
PPC : chl-a (pg.cell-1)
PSC : chl-a (pg.cell-1)
PPC : chl-a (g.g-1)
PSC : chl-a (g.g-1)
Days

Bulk absorption properties – The absorption coefficients of the four algal cultures, obtained from *in situ* measurements with the ac-9 profiler (a_{tot}), were compared with spectrophotometric measurements (a_p) using discrete water samples, so as to determine the contribution to absorption of non-particulate matter and particulate matter passing through the filter (i.e. bacteria). There was excellent agreement between these methods (r^2=0.97, n = 480). Although the slope was less than 1 (i.e., 0.92), the relative differences between the ac-9 and spectrophotometric absorption coefficients averaged 8% for all wavelengths, within the examined range of absorption values. While bacteria concentrations increased in the four cultures during the experiment, the contribution of bacteria to $a_{tot}(\lambda)$ was generally small and constant, as well as that of CDOM, and the relative difference between a_p and a_{tot} was small during the experiments.

In the case of *Nannochloropsis* sp., the ac-9 scattering signal was saturated from about day 5 of the experiment (depending on wavelength) because of the high cell concentration, thus these data were removed.

The contribution of phytoplankton ($a_{ph}(488)$) to particulate absorption $a_p(488)$ was high under exponential and stationary phases for all mono-specific cultures, ranging from 80 to 95%, whereas it decreased during the decline phase (*T. pseudonana*) or for the Mixed culture (not shown). In these cases, the phytoplankton contribution to $a_p(488)$ was as low as 60%, while the contribution of detrital particles ($a_d(488)$) accounted for 20 to 40% of $a_p(488)$ (not shown).

The relationships between chl-*a* and $a_{ph}(440)$ were significantly ($p<0.05$) different according to the species (Fig. 5a). The highest absorption coefficient for a given chl-*a*

concentration was found in *Nannochloropsis* sp.; specific absorption decreased as cell size increased. For the Mixed culture, the $a^*_{ph}(440)$ values were generally between those of the mono-specific *I. rotunda* and *T. pseudonana* cultures. For all species, growth phase affected a^*_{ph} spectra at some wavelengths (Fig. 5b, c, d and e), the mean a^*_{ph} values for cells in decline phase (*I. rotunda* and *T. pseudonana*), in lag phase (*A. tamarense*) or in stationary phase (*Nannochloropsis* sp. and *T. pseudonana*) were significantly different from the mean a^*_{ph} values of cells in exponential phase. Cells of *Nannochloropsis* sp. had the largest increase, with 1.6 to 3.3 fold higher a^*_{ph} value for all wavelengths during the stationary phase compared to the exponential phase. For *T. pseudonana,* a^*_{ph} was lower in the stationary phase than in the exponential phase for all wavelengths except those between 655 and 670 nm. In contrast, a^*_{ph} values were higher in the decline than in the exponential phase at wavelengths from 450 to 680 nm, likely related to the large decrease in the abundance of algal cells during decline (Fig. 1). For *I. rotunda*, a^*_{ph} values were higher in the decline phase from 450 to 500 nm and from 660 to 690 nm, while they were lower between 520 and 620 nm. For *A. tamarense*, a^*_{ph} values in the blue part of the spectrum were significantly ($p<0.05$) higher during the lag phase than during the exponential phase. For the rest of the spectra, no significant differences in a^*_{ph} values were observed between the lag and exponential phases ($p>0.05$), except between 545 and 560 nm, where photosynthetic carotenoids absorb.

Figure 5: (a) Relationships between $a_{ph}(440)$ and chl-*a* for *Nannochloropsis* sp., *T. pseudonana, I. rotunda, A. tamarense* and the Mixed culture. The black solid, red medium dashed, blue short dashed and green dotted lines refer to a linear or power regression between $a_{ph}(440)$ and chl-*a* for *Nannochloropsis* sp. (only under exponential phase), *I. rotunda, T. pseudonana* and *A. tamarense*, respectively; (b) chl-*a*-specific absorption spectra (a^*_{ph}, $m^2 \cdot [mg\ chl\text{-}a]^{-1}$) for *Nannochloropsis* sp., (c) *I. rotunda,* (d) *T. pseudonana* and (e) *A. tamarense* shown for the various growth phases. Average values and standard deviations are shown for a^*_{ph} spectra.

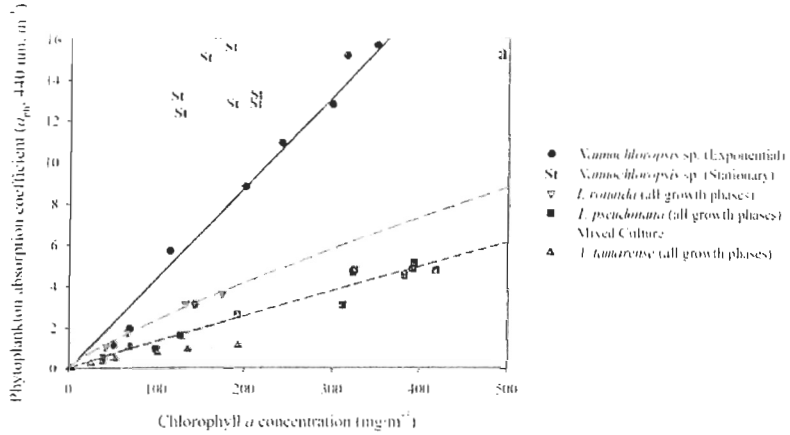

Nannochloropsis sp.

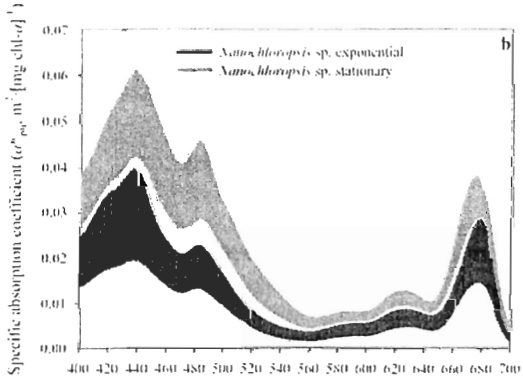

Thalassiosira pseudonana

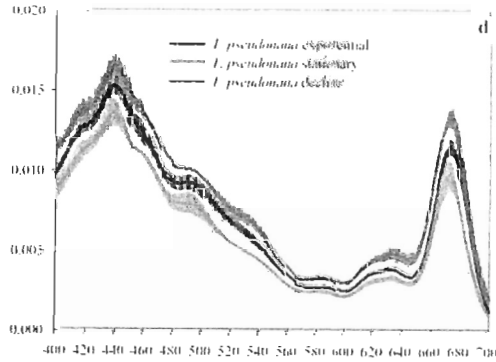

Imantonia rotunda

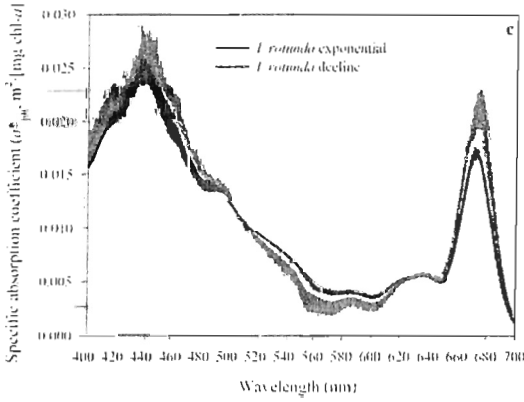

Alexandrium tamarense

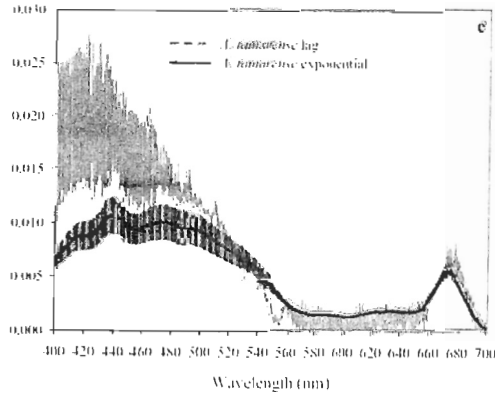

Both algal species and growth phase affected the relationships between these phytoplankton absorption ratios ($a_{ph}(440)/a_{ph}(488)$ and $a_{ph}(440)/a_{ph}(555)$) and pigment composition (PPC/chl-*a* and PSC/chl-*a* ratio). For *A. tamarense*, *Nannochloropsis* sp. and *T. pseudonana*, significant relationships were found only for cells in exponential and stationary growth phases, whereas under lag and decline phases, there was no relationship (Table 3). For *I. rotunda* cells in exponential phase, there were too few data (n=2) to assess these relationships. The $a_{ph}(440)/a_{ph}(488)$ and $a_{ph}(440)/a_{ph}(555)$ ratios were inversely related to PPC/chl-*a* and PSC/chl-*a* ratios, respectively. However, the slope of these relationships differed according to species (Table 3). The Mixed culture exhibited a significant relationship between the $a_{ph}(440)/a_{ph}(488)$ and PPC/chl-*a* ratios, only between days 5 and 13 when *T. pseudonana* was exponentially growing. The slope of this relationship was close to that of *T. pseudonana* mono-specific culture (Table 3).

Bulk scattering properties – For each culture, the phytoplankton scattering coefficient at 488 nm (b_{ph} (488)) was strongly related to chl-*a*, but this relationship varied with species (Fig. 6a). The highest phytoplankton scattering coefficient per unit chl-*a* was observed for the smallest species, *Nannochloropsis* sp. As expected from their large size, *A. tamarense* cells scattered less than the other species for a given chl-*a* concentration (Fig. 6c). Growth phases affected the results in some cases. Scattering at 488 nm was significantly higher during the stationary phase, compared to the exponential phase, for *Nannochloropsis* sp. In contrast, there was no significant difference between these two growth phases for *I. rotunda* and *T. pseudonana*, although scattering was slightly lower in the decline phase.

The presence of bacteria increased scattering for a given chl-*a* concentration. This was particularly evident for *Nannochloropsis* sp., where the highest bacterial abundance was observed (Fig. 6b). Bacteria increased the scattering by 36% in *Nannochloropsis* sp., whereas this increase was minor in the other cultures except *T. pseudonana* in decline phase (about 62%).

Table 3: Relationships between absorption ratios ($a_{ph}(440)/a_{ph}(488)$ and $a_{ph}(440)/a_{ph}(555)$) and pigment ratios (PPC/chl-*a* and PSC/chl-*a*) for the various phytoplankton cultures only under exponential (Exp) and stationary (St) phases.

	Growth phase	$a_{ph}(440)/a_{ph}(488)$ *vs.* PPC/chl-*a*	$a_{ph}(440)/a_{ph}(555)$ *vs.* PSC/chl-*a*
Nannochloropsis sp.	Exp+St	PPC/chl-*a* =8.08 exp [-1.85 $(a_{ph}(440)/a_{ph}(488))$] $r^2 = 0.88$	PSC/chl-*a* = 0.96 – 0.07 $(a_{ph}(440)/a_{ph}(555))$ $r^2 = 0.86$
Mixed culture	Exp	PPC/chl-*a* = 0.45 – 0.22 $(a_{ph}(440)/a_{ph}(488))$ $r^2 = 0.78$	no relationship
Thalassiosira pseudonana	Exp+St	PPC/chl-*a* = 0.58 – 0.26 $(a_{ph}(440)/a_{ph}(488))$ $r^2 = 0.89$	PSC/chl-*a* = 0.71 – 0.06 $(a_{ph}(440)/a_{ph}(555))$ $r^2 = 0.82$
Alexandrium tamarense	Exp	PPC/chl-*a* = 0.57 – 0.34 $(a_{ph}(440)/a_{ph}(488))$ $r^2 = 0.84$	PSC/chl-*a* = 1.09 – 0.11 $(a_{ph}(440)/a_{ph}(555))$ $r^2 = 0.85$

Relationships between the ac-9 measured total particle scattering coefficients, $b_p(488)$, and chl-*a* showed generally higher scattering values than when scattering was measured with the flow-cytometer (compare Fig. 6c with Fig. 6b). This was particularly evident for the Mixed culture, where scattering was higher compared to the individual mono-specific cultures (*I. rotunda* and *T. pseudonana*). Microscopic observations indicated that particulate matter from detritus and aggregates was present in the Mixed culture from day 5. The presence of this particulate detrital matter was also detected in the *T. pseudonana* culture on the last 3 days of the decline phase. The contribution of detritus to scattering was minor (below 4%) in the exponential and stationary phases of *Nannochloropsis* sp., *I. rotunda* and *T. pseudonana* (Fig. 7). Moreover, more than 90% of detritus scattering was due to <20 µm detrital particles. For *T. pseudonana* in the decline phase, detritus accounted for about 22% of particulate scattering (days 10 to 12), of which about 80% were due to <20 µm detrital particles (Fig. 7a). In the Mixed culture, the detritus contribution to scattering increased during the experiment and reached 47%. In this case, small <20 µm detrital particles decreased with time from about 90% to 15% of total detrital scattering, while the contribution of large (>20 µm) detritus increased (Fig. 7b).

Figure 6: Relationships between chl-*a* and scattering coefficient at 488 nm, (a) for phytoplankton (b_{ph} (488), m^{-1}), (b) for phytoplankton + bacteria ($b_{ph+bact}$ (488), m^{-1}) and (c) for total particulate matter (b_p (488), m^{-1}) for the various cultures. In (a) and (b), the lines designate a linear or power regression between b_{ph} (or $b_{ph+bact}$) and chl-*a* for the exponential phase of *Nannochloropsis* sp. (black solid lines), for combined data from exponential and stationary phases of *I. rotunda* and *T. pseudonana* and data from day 5 to day 13 of the Mixed culture (black medium dashed lines), and for combined data from the decline phase of *I. rotunda* and *T. pseudonana* and data from day 13 to day 19 of Mixed culture (black dotted lines). In (c), the lines designate a linear or power regression between b_p and chl-*a* for the exponential phase of *Nannochloropsis* sp. (black solid line), for the exponential and stationary phases of *I. rotunda* and *T. pseudonana* (black medium dashed line), for data from day 5 to day 13 of the Mixed culture (orange short dashed line), for the decline phase of *I. rotunda* and *T. pseudonana* (black dotted line), and for the lag and exponential phases of *A. tamarense* (green dot-dashed line).

Phytoplankton scattering

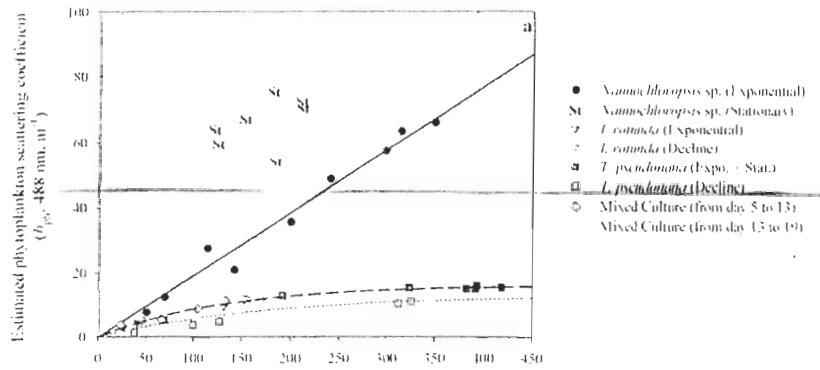

Phytoplankton + bacteria scattering

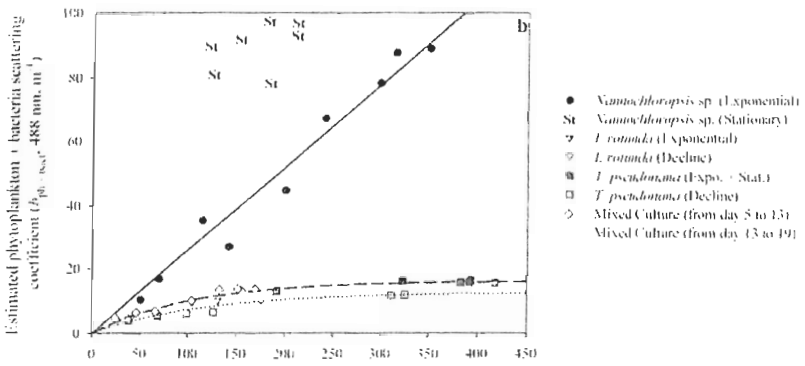

Total particulate matter scattering

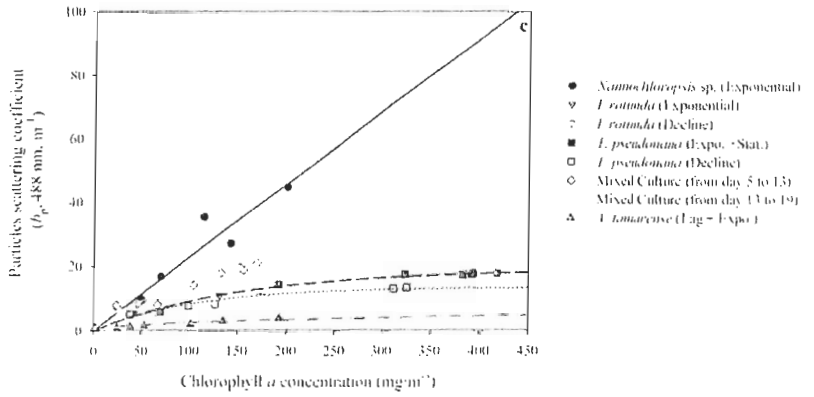

Figure 7: Contribution of phytoplankton, bacteria and detrital particles (>20 µm and <20 µm) to the scattering coefficient at 488 nm, of total particulate matter (b_p(488)) for *T. pseudonana* and *I. rotunda* cultures.

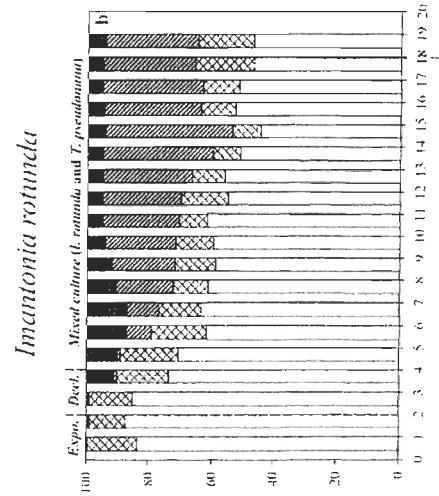
Imantonia rotunda
Expo.
Decl.
Mixed culture (I. rotunda and T. pseudonana)
b
Days

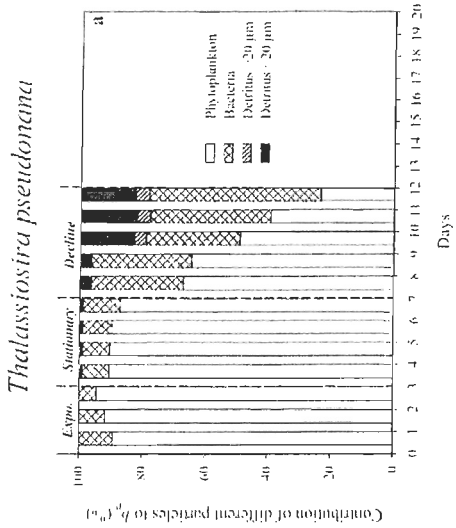
Thalassiosira pseudonana
Expo.
Stationary
Decline
a
Phytoplankton
Bacteria
Detritus · 20 µm
Detritus · 20 µm
Days
Contribution of different particles to b_p (m^2)

The shape of normalized scattering spectra differed between bacteria and phytoplankton and for the latter it varied considerably both with the species and growth phases (Fig. 8). The only particles present in the culture medium before phytoplankton inoculation were bacteria, based on the FCM measurements and microscopic observations (Fig. 8a). At that time, the normalized ac-9 scattering spectra could be described reasonably well as λ^{α}, where the best-fit value for α was -1.75 ± 0.08, close to that estimated for bacteria by Stramski and Kiefer (1998) and Stramski and Mobley (1997). Bacterial contribution to scattering is thus more important at shorter wavelengths, as shown by Morel and Ahn (1990). In contrast, phytoplankton scattering spectra showed a spectral slope less steep than that of bacteria, and flatness increased with increasing chl-*a* concentration. Troughs were generally observed at wavelengths corresponding to blue and red absorption of chl-*a*. For all mono-specific cultures, growth phases distorted the scattering spectral shape, and differences were more pronounced at <555 nm wavelengths. Normalized scattering coefficients had higher values in lag or decline phases, represented by higher bacteria to chl-*a* ratios, than in exponential or stationary phases with lower bacteria to chl-*a* ratios. In the Mixed culture, normalized scattering coefficients values were lower at <555 nm wavelengths when the contribution of detritus was higher than 25%.

Figure 8: Mean normalized scattering coefficient spectra ($b_p(\lambda)/b_p(555)$, dimensionless) for (a) bacteria, (b) *Nannochloropsis* sp., (c) *I. rotunda*, (d) *T. pseudonana* and (e) *A. tamarense* for the various growth phases. Also shown in (f) is the influence of different contributions of detrital particles to particulate matter scattering coefficient in the Mixed culture. Average values and standard deviations are shown for $b_p(\lambda)/b_p(555)$. The brown dotted curve represents a $\lambda^{-1.75}$ relationship, characteristic of bacteria. The numbers in brackets correspond to mean bacteria to chl-*a* ratios (x10^{10} bacteria cells·[mg chl-*a*]$^{-1}$) for different spectra.

Bacteria

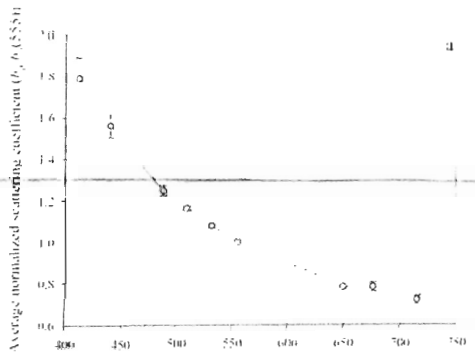

Thalassiosira pseudonana

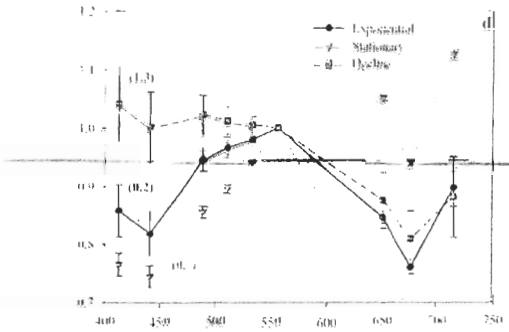

Nannochloropsis sp.

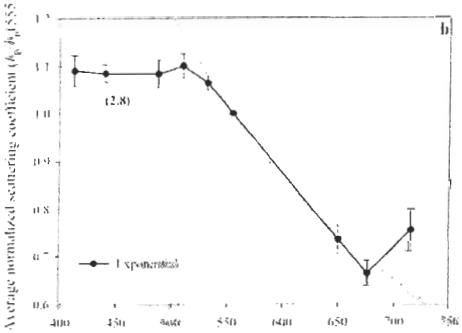

Alexandrium tamarense

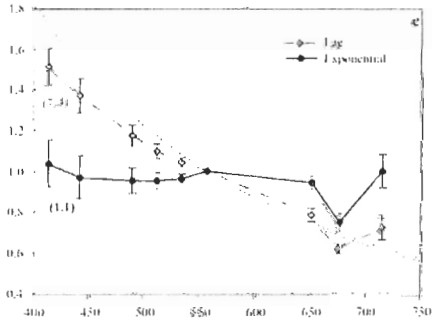

Imantonia rotunda

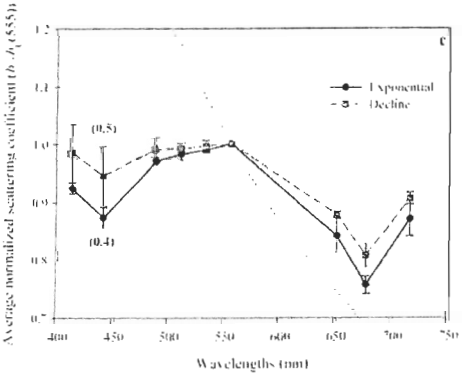

Mixed Culture

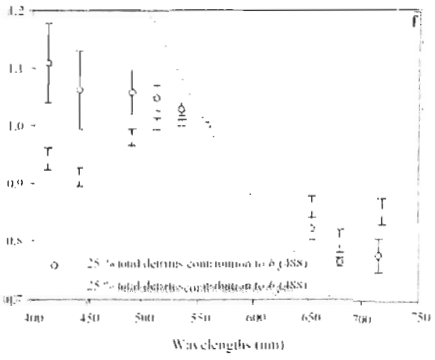

DISCUSSION

Influence of phytoplankton species composition and growth phase - Both cell-specific FSC and SSC vary with particle size, shape, cell water content, refractive index (Spinrad and Brown 1986, Spinrad and Yentsch 1987, Ackleson and Spinrad 1988), as well as cell organic compounds composition (Aas 1996). Consequently, during stationary and/or decline phase, the increase in FSC_{phy} and SSC_{phy} illustrated probably a concomitant increase in cell size and cell carbon (Robert and His 1987), cell density and refraction index due to reserve carbohydrates accumulation as phytoplankton growth declined (Myklestad 1977, Hama et al. 1988, Alderkamp et al. 2006). Cells in exponential phase likely use more energy in cell division instead of accumulating photosynthetic products.

The absorption cross section at 488 nm exhibited generally smaller variations than FSC_{phy}. For *Nannochloropsis* sp., *T. pseudonana* and *I. rotunda*, the ranges of $\sigma_a(488)$ encompassed the corresponding values reported for the same species or for cells of similar size and pigmentation (Stramski et al. 2001, DuRand et al. 2002, Mas et al. 2008). Variations in $\sigma_a(488)$ resulted from changes in cellular pigment composition and package effect, and followed the growth phase with a lag. Cells maintaining their pigment content while slowing down growth could be responsible for the lag observed between cell numbers and $\sigma_a(488)$. The optical cross-sections thus varied with growth phase as a result

of the physiological changes inducing variations in pigment concentration and composition, cell size and refraction index.

The pigment composition varied according to species and growth phases. However, for the same growth phase, the different trends in cellular pigment content and pigment ratio variations resulted from different physiological strategies (Goericke and Montoya 1998, Henriksen et al. 2002). The magnitude of pigment ratio changes due to the growth phase is thus more likely species-specific. Consistent with Henriksen et al. (2002), this precludes generalizations about pigment ratio changes as a result of growth phase succession.

The relationships between chl-*a* and $a_{ph}(440)$ were different for the four mono-specific cultures (Fig. 5). This seemed to be particularly related to the cell size of species, since for the same chl-*a* concentration, $a_{ph}(440)$ is higher for smaller species as shown by Ciotti et al. (2002). Consequently, average $a^*_{ph}(676)$ values were also higher for smaller species, particularly *Nannochloropsis* sp. (Fig. 5b). In exponential phase, the average $a^*_{ph}(676)$ value of *Nannochloropsis* sp. (0.021 $m^2 \cdot [mg\ chl\text{-}a]^{-1}$) fell in the range of species of similar size (Stramski et al. 1995, Durand et al. 2002). This value suggests only a weak packaging effect in *Nannochloropsis* sp. (Morel and Bricaud 1981, Sathyendranath et al. 1987, Stramski et al. 2002). The increase of $a^*_{ph}(676)$ value in stationary phase (*Nannochloropsis* sp., 0.032 $m^2 \cdot [mg\ chl\text{-}a]^{-1}$) and in decline phase (*T. pseudonana* and *I. rotunda*) likely suggests a decrease in package effect due to a decrease

in intracellular pigment concentration (not shown), reflecting probably nitrogen-limited conditions, consistent with previous observation on *T. pseudonana* (Reynolds et al. 1997) and the chlorophyte *Dunaliella tertiolecta* (Sosik and Mitchell 1991). For all monospecific cultures, the mean a^*_{ph} values changed with growth phase, the specific absorption coefficient was generally lowest during the exponential phase and increased in stationary (*Nannochloropsis* sp.) or decline phase (*I. rotunda* and *T. pseudonana*) in some regions of the spectrum, probably as a result of changes in pigment concentration and composition associated to the physiological state of the cells (Kiefer et al. 1979). These changes in a^*_{ph} spectra can strongly affect the absorption ratios between wavebands (such as 440, 488, and 555 nm), typically used to estimate chl-*a* concentrations with standard ocean color algorithms (Arrigo et al. 1998, O'Reilly et al. 1998, Dierssen and Smith 2000).

These absorption ratios are known to be influenced by the relative proportion of photosynthetic and photoprotective carotenoids (Bricaud et al. 1995, Culver and Perry 1999). Indeed, our relationships between $a_{ph}(440)/a_{ph}(488)$ and $a_{ph}(440)/a_{ph}(555)$ ratios varied inversely with PPC/chl-*a* and PSC/chl-*a* ratio, as observed by Stuart et al. (2000) and Eisner et al. (2003). These relationships differ between growth phases and also species according to the pigment composition of each species. Only the cells in exponential and stationary growth phases exhibited significant relationships (Table 3). The steeper slope of $a_{ph}(440)/a_{ph}(488)$ *vs.* PPC/chl-*a* and $a_{ph}(440)/a_{ph}(555)$ *vs.* PSC/chl-*a* relationships, respectively observed for *Nannochloropsis* sp. and *A. tamarense* cells (Table 3), might be due to a high concentration of violaxanthin and zeaxanthin as well as

a 1.5 to 3 fold higher concentration of PPC relative to chl-*a* (*Nannochloropsis* sp.) and to a high concentration of peridinin (*A. tamarense*). The lack of relationship in decline phase (*T. pseudonana*) was probably due to modifications of the spectra more important in some regions than others, likely associated with physiological processes occurring in senescent cells (Kiefer et al. 1979). The absence of relationship in lag phase (*A. tamarense*) resulted probably from a high variability of a^*_{ph} spectra (Fig. 5e), related to low pigment concentration in the cells. Hence, our results suggest that variation in the shape and magnitude of phytoplankton absorption spectra and in the relationships between pigments and absorption properties can be affected not only by species composition but also by the growth state. As already recognized by Kiefer et al. (1979), this can have important implications for optical studies at sea and consequently for the retrieval of chl-*a* from spectral absorption measurements.

The relationships between phytoplankton scattering coefficient at 488 nm ($b_{ph}(488)$) and chl-*a* concentration also changed according to the phytoplankton species and the growth phase. The mean chlorophyll-specific scattering at 488 nm for *Nannochloropsis* sp. was about 6 fold higher than that of *T. pseudonana*. Such differences can be explained by a size effect (Claustre et al. 2002). The relationships between cell scattering and chl-*a* were not significantly different for *I. rotunda*, *T. pseudonana* and the Mixed culture probably as a result of the weak difference between the range of variation in cell chl-*a* content, FSC and size. This confirms that it is difficult to optically discriminate phytoplankton cells of similar size (McLeroy-Etheridge and Roesler 1998). For *Nannochloropsis* sp., cells in stationary phase showed higher

scattering coefficient ($b_{ph}(488)$) for a given chl-*a* concentration, compared to cells in exponential phase. Moreover, for *T. pseudonana*, *I. rotunda* and the Mixed culture, the cells in decline phase showed a different $b_{ph}(488)$ *vs.* chl-*a* relationship than cells in exponential and stationary phase. A decrease in $b_{ph}(488)$ was observed for a given chl-*a* concentration when cells were in decline phase. These changes seem to be due to concomitant variations of cell concentration, FSC_{phy} and cell chl-*a* content. Therefore, the relationship between phytoplankton scattering characteristics and pigments may provide information about the growth stage and algal physiology throughout the development of a bloom.

Influence of bacteria - Except for *Nannochloropsis* sp. cultures, the concentration of heterotrophic bacteria followed phytoplankton abundance, consistent with Stabili et al. (2006). The highest growth rate of bacteria was found for *Nannochloropsis* sp., but it decreased to near zero from day 9, probably due to a carbon limitation, as often observed in marine ecosystems (Bratbak and Thingstad 1985, Brussaard et al. 1995). The presence of bacteria may have changed the duration of the stationary phase of phytoplankton. For *Nannochloropsis* sp. and *T. pseudonana* mono-specific cultures and the Mixed culture, a long stationary phase (10, 4 and 6 days, respectively) suggested an efficient bacterial remineralization which could have prolonged survival of nutrient-starved phytoplankton populations (Biddanda 1988, Goldman and Dennett 1991, Brussaard and Riegman 1998). During the decline of the *T. pseudonana* culture (day 7 to 13), the presence of bacteria had no pronounced effect on the phytoplankton death rates probably due to silicia deficiency.

The FSC_{bact} and SSC_{bact} increased proportionally to the bacterial growth rate (not shown), whereas the values of cell light scatter decreased when bacteria remained in stationary phase and became starved, as in the culture of *Nannochloropsis* sp. from day 9. These results suggest a decreasing size from fast growing to starved bacteria, as reported in several studies (Amy and Morita 1983, Morel and Ahn 1990, Stramski et al. 1992). This is important for ocean optics as starved bacteria may exhibit a significant decrease in cell size and thus in cell scatter compared to actively growing bacteria.

Even though the estimates of the bacterial contribution to a_{tot} are subject to uncertainties associated with difficulties to measure the true absorption by bacteria, it is clear that this contribution is small. From data on starved bacteria, Stramski et al. (2001) estimated a maximum bacterial contribution of 6% at 400 nm for oligotrophic waters. In general, the starved bacteria exhibited lower absorption cross-sections (up to 2-fold lower, Stramski and Kiefer 1998) compared to actively growing bacteria. This was attributed to changes in cell properties, such as a decrease in cell size, due to slower growth rates (Stramski et al. 1992, Stramski and Kiefer 1998), which could lead to a decrease in FSC_{bact}, as observed in this study. Consequently, the bacterial contributions to total absorption coefficient estimated by Stramski et al (2001), were underestimated and could exceed 10% at short wavelengths for oligotrophic waters.

Heterotrophic bacteria are more efficient at scattering than absorbing light, suggesting that bacteria could contribute significantly to light scattering (Morel and Ahn

1990, Stramski and Kiefer 1990, Stramski and Morel 1990, Ulloa et al. 1992). In the present study, the contribution of bacteria to bulk light scattering tended to increase with decreasing pigment concentration (Fig. 7) and led to an increase in scattering for a given chl-*a* concentration (Fig. 6b). This increase ranged from 3 to 200%, the highest increase occurring during the decline phase of the cultures when chl-*a* concentrations were low and the proportion of bacteria relative to phytoplankton were highest. The magnitude of these scattering changes will vary according to the size of bacteria, which is related to bacterial growth rate. Bacterial scattering can double if the size increases to 0.65 µm, instead of 0.55 µm (Morel and Ahn 1990). Increases in FSC_{bact} during the decline phases suggest that the size of bacterial cell increased during phytoplankton decline. This surely contributed to the increase of scattering for a given chl-*a* concentration at that time.

The total normalized scattering spectra ($b_p(\lambda)/b_p(555)$) and their shape variations could be due to particles composition (Babin et al. 2003). The changes in particles composition of the cultures, leading to variations of refractive index and size distributions (Lohrenz et al. 1997, Twardowski et al. 2001, Babin et al. 2003), were attributed to varying proportions of heterotrophic bacteria relative to phytoplankton and were indirectly related to growth phase only in the mono-specific cultures. Indeed, when the phytoplankton cells were in lag and decline phases, the proportion of heterotrophic bacteria was highest. Moreover, when the bacterial contribution increased relative to that of the algae in culture, the total normalized scattering spectra ($b_p(\lambda)/b_p(555)$) was distorted and resembled that of bacteria more closely, the depression at 675 nm was always present but less pronounced, whereas the depression at 440 nm was reduced or

disappeared. The normalized scattering spectra ($b_p(\lambda)/b_p(555)$) for *A. tamarense* during the first 5 days, was close to a $\lambda^{-1.75}$ relationship, in agreement with the high bacterial contribution during the lag phase of this culture (Fig. 8e). In waters where phytoplankton cells and/or heterotrophic bacteria dominate strongly the scattering coefficients, the bacteria to chl-*a* ratio could strongly affect the shape and magnitude of $b_p(\lambda)/b_p(555)$.

Influence of detritus – Non-phytoplanktonic particles, such as detritus, can lead to variations in the chl-*a*-specific b_p and to uncertainties in the relationship between b_p and chl-*a* (Kitchen and Zaneveld 1990, Loisel and Morel 1998, Claustre et al. 2000). The presence of particulate detritus was only detected in the Mixed culture and at the end of the decline phase of the *T. pseudonana* mono-specific culture, and was likely responsible for the large increase in scattering for a given chl-*a* concentration (Fig. 6c). The increasing relative contribution of detritus in *T. pseudonana* and the Mixed culture also affected the $b_p(\lambda)/b_p(555)$ spectra through changes in the refractive index and size distributions of the particle assemblage. The presence of detritus (mostly <2 µm from microscopic observations) in the decline phase of the *T. pseudonana* culture, increased the contribution of small particles to the particle pool. This led to an increase in $b_p(\lambda)/b_p(555)$ between 400 and 500 nm compared to cells in exponential and stationary phases. Babin et al. (2003) also reported that an increase in the contribution of small particles increased the $b_p(\lambda)/b_p(555)$ values between 400 and 500 nm. In the Mixed culture, when the detritus contribution was <25% of b_p, the <20 µm detritus constituted between 60 and 90% of all detritus, whereas when the contribution was >25%, the <20 µm detritus represented only between 15 and 30% of total organic detritus. This shift in

the detritus size structure was likely related to the formation of large size aggregates during the experiment, as observed by microscopy. These aggregates increased the contribution of large particles in the particle pool and thus decreased $b_p(\lambda)/b_p(555)$ between 400 and 500 nm.

Changes in planktonic assemblages (size, autotrophs *vs.* heterotrophs, presence of detritus), as well as growth phases, thus led to the variations in chl-*a*-specific scattering at 488 nm and in $b_p(\lambda)/b_p(555)$ spectra.

CONCLUSIONS

Cellular and bulk optical properties of phytoplankton were observed to vary in large batch cultures, according to the physiological changes due to growth state of the cultures and to the particular species. Optical variations due to growth phase can clearly contribute to the changes in ocean color particularly during bloom events and should be considered in bio-optical field studies. These growth-state related optical variations may lead to errors in the retrieval of chl-*a* from remotely-sensed data using the standard algorithms.

Bacteria also affect the bulk IOPs variability, either directly by changing particle size distribution, which results in variations in the bulk scattering or indirectly by extending the duration of phytoplankton blooms. Detrital particles can also influence

strongly the variability of bulk IOPs, through changes in the particle size distribution, which can lead to even larger variations in bulk scattering than bacteria.

The combination of FCM and ac-9 measurements was relevant in determining changes in plankton assemblages (size distribution, autotrophs *vs.* heterotrophs, presence of detritus) and/or growth phases, which generally occur during phytoplankton blooms. When bacteria and other particles were considered in the relationships between scattering coefficients ($b_{ph+bact}$ or b_p) and chl-*a*, changes due to the growth phase of the algal cultures were still detectable, particularly at high chl-*a* concentration. Therefore, for the different species and also the Mixed culture, the relationship between total scattering characteristics and pigments may provide information about the growth stage and algal physiology throughout the development of a nanophytoplankton bloom. Moreover, changes in plankton assemblages and/or growth phases affected variations of scattering properties, particularly the chl-*a*-specific scattering at 488 nm and the shape and magnitude of ($b_p(\lambda)/b_p(555)$) spectra.

This study also highlighted the discrepancy between IOPs from bulk measurements and IOPs derived from cellular measurements, particularly for scattering, since bacteria and detrital particles contribute strongly to scattering in the ocean. So, quantifying the influence of these particles is of critical importance to study IOPs variability in the ocean, especially during phytoplankton blooms.

CHAPITRE 3:

SPRINGTIME DISTRIBUTION AND BIO-OPTICAL PROPERTIES OF <20 µm PHYTOPLANKTON IN SURFACE WATERS OF THE ESTUARY AND GULF OF ST. LAWRENCE.

RÉSUMÉ

La distribution de l'abondance et des propriétés optiques du pico-, ultra- et nanophytoplancton (<2, 2-5 et 5-20 µm, respectivement) dans les eaux de surface de l'Estuaire et du Golfe du Saint-Laurent (Canada) a été étudiée au cours de deux campagnes océanographiques en mai-juin 2000 et avril-mai 2001. La variabilité spatiale et temporelle des conditions physico-chimiques du Saint-Laurent se reflétait dans la distribution des propriétés optiques et cellulaires du phytoplancton. La floraison printanière était dominée par des diatomées pour les deux années, mais les espèces dominantes étaient différentes. Les abondances de phytoplancton <20 µm étaient généralement plus fortes dans le Golfe, et largement dominées par le picophytoplancton. En dehors des périodes de floraison, la contribution du phytoplancton <20 µm à l'absorption du phytoplancton était plus importante, majoritairement due au nanophytoplancton. De plus, la variabilité spatio-temporelle des ratios d'absorption résultait de la composition taxonomique. Les différences régionales étaient aussi évidentes pour les propriétés de diffusion, la contribution du phytoplancton <20 µm à la diffusion totale était plus élevée dans le Golfe que dans l'Estuaire, dû aux plus fortes abondances de phytoplancton <20µm présentes dans le Golfe. Cependant, la contribution du phytoplancton <20 µm à la diffusion totale était généralement faible (<35%). En plus de la variabilité spatiale, les propriétés optiques cellulaires, mesurées par cytométrie en flux, présentaient des variations journalières. Les variations journalières étaient particulièrement prononcées pour le picophytoplancton, dont la périodicité était reliée à la synchronisation de la division cellulaire ; alors que les variations journalières de l'ultra-

et du nanophytoplancton reflétaient des processus de photoacclimatation. Contrairement aux propriétés optiques cellulaires, les IOPs ou les relations entre IOPs et composition pigmentaire n'étaient pas affectées par les variations journalières. La plupart des différences de propriétés bio-optiques, particulièrement l'absorption, entre les périodes de floraison et hors de ces périodes, étaient attribuables à la contribution du phytoplancton <20 µm. Le « package effect » semble être le principal facteur de variation des propriétés d'absorption du phytoplancton. Cette étude confirme donc que la structure de taille des communautés phytoplanctoniques, et plus particulièrement le changement de dominance du micro- et nanophytoplancton vers le picophytoplancton, doit être prise en compte dans les modèles bio-optiques appliqués au Saint-Laurent.

ABSTRACT

The abundance and optical properties of pico-, ultra- and nanophytoplankton (<2, 2-5 and 5-20 µm, respectively) and their relation to physical and chemical variables in surface waters were investigated during two cruises in May-June 2000 and April-May 2001 in the Estuary and the Gulf of St. Lawrence (Canada). Variability in the physico-chemical characteristics of the St. Lawrence was reflected in the phytoplankton properties. The spring bloom was dominated by diatoms for both years, but the dominant species were different. Phytoplankton <20 µm were generally the most abundant and were largely dominated by picophytoplankton. Outside bloom periods, the <20 µm phytoplankton contribution to phytoplankton absorption was larger, mostly due to nanophytoplankton. Moreover, the spatio-temporal variability in the absorption ratios resulted from taxonomic diversity. Regional differences also showed up for scattering properties, the contribution of <20 µm phytoplankton to total scattering was higher in the Gulf than in the Estuary, due to a higher abundance of <20µm phytoplankton located in the Gulf. However, the contribution of <20 µm phytoplankton to total scattering was generally small (<35%). Cellular optical properties determined by flow cytometry also showed diel variations. This was particularly evident for picophytoplankton, where diel periodicity was linked to the synchronized cell division. For ultra- and nanophytoplankton, cellular optical properties rather reflected photoacclimation processes. Contrary to the cellular optical properties, diel changes did not affect IOPs, or the relationships between IOPs and pigment composition. Most of the variability of bio-optical properties, particularly absorption, during and outside bloom periods, were

attributable to the contribution of <20 µm phytoplankton. Packaging effect seems to be the key factor in phytoplankton absorption properties variations in the St. Lawrence, this study confirms thus that the size structure of phytoplankton community, and particularly the shift from micro- and nanophytoplankton to picophytoplankton, has to be taken into account in bio-optical models applied to the St. Lawrence.

INTRODUCTION

Most of the algorithms, used to transform remote sensing reflectance (i.e. ocean color) into chlorophyll concentration or particulate carbon (Loisel and Morel 1998, Claustre et al. 2000, Balch et al. 2001) and primary production (Platt and Sathyendranath 1988, Pérez et al. 2005) were developed for waters which are poor in suspended and dissolved matter (Case 1), and generally do not perform well for waters which are rich in suspended and dissolved matter (Case 2) (Morel and Prieur 1977, O'Reilly et al. 1998). Ocean color depends on inherent optical properties (IOPs) of the oceans, such as the coefficients of absorption *(a)*, scattering *(b)* and backscattering (b_b) (Gordon et al. 1975, Morel and Prieur 1977). These IOPs are strongly influenced by particulate matter (e.g. viruses, bacterioplankton, detritus (Morel 1990, Ulloa et al. 1992) and phytoplankton (Morel 1988)), which vary in concentration and cellular optical characteristics (Morel 1990, Sosik et al. 2001, Green et al. 2003). The information on different cellular characteristics of each constituent present in the water is interesting in the context of biogeochemical cycles and carbon dynamics in the oceans. Flow cytometry (FCM) is one of the few tools available to analyze the optical properties of large numbers of individual particles and to distinguish specific groups of particles in the ocean (Green et al. 2003). The combination of *in situ* measurements (such as with an absorption and attenuation meter) and FCM measurements can provide an assessment of the contribution of phytoplankton size classes present in the water, such as pico- (0.2-2 µm), ultra (2-5 µm) and nanophytoplankton (here operationally defined as 5-20 µm), to the bulk optical properties (Ciotti et al. 2002). Micro-organisms of small size, such as pico-, ultra- and

nanophytoplankton, often dominate numerically in planktonic communities of the marine euphotic zone (Joint and Pomroy 1983). They are also a dominant source of IOP variations in the oceans (Stramski and Kiefer 1991). In surface waters, the abundance, biomass, production, cell physiological and optical characteristics of pico-, ultra and nanophytoplankton cells can respond rapidly to environmental fluctuations, such as variations in irradiance due to cloud cover (Jacquet et al. 1998), vertical mixing and turbulence (Vaulot and Marie 1999), nutrient pulses (Vaulot et al. 1996), temperature or salinity (Legendre et al. 1992, Agawin et al. 2000, Bouman et al. 2003) and they are characterized by a large variability in time and space (Margalef 1967, Rhee 1980). Knowledge of the coupling between the distribution of these organisms and their physico-chemical environment constitutes a pre-requisite to understand their eco-physiological requirements (Mostajir et al. 2001). Moreover, phytoplankton dynamics can vary at short time-scales, particularly the diurnal scale, and these short-term variations are probably relevant to understand the ecology, physiology and optical characteristics of these microbial communities (Jacquet et al. 1998, 2002). This is of particular interest since small changes in short-term processes are likely to drive long-term changes in cell populations (Vaulot and Marie 1999). Considering the importance of pico-, ultra- and nanophytoplankton in the variability of optical properties, it is then necessary to understand the processes controlling their spatial and temporal distribution as well as the variations of their cell optical properties (Sosik et al. 2001) for a better interpretation of remote sensing measurements and estimates of biomass and primary production on a large scale (Durand and Olson 1996).

The Estuary and Gulf of the St. Lawrence system (Canada) is a very convenient natural laboratory to validate remote sensing data, since it provides, over a relatively small spatial scale, optically-diverse conditions (Case 1 and 2 waters) and a wide range of hydrographic conditions, with local structures such as runoff plumes, upwelling areas, gyres, fronts, etc. (Demers and Legendre 1981, Levasseur et al. 1992, Zakardjian et al. 2000). The St. Lawrence system is a highly stratified, semi-closed water body, with connections to the Atlantic Ocean. Compared to many areas with mixed Case 1 and 2 waters, the St. Lawrence has been relatively poorly described in terms of IOPs (Babin et al. 1993, 1995, Nieke et al. 1997) as well as for the species composition, size structure, abundance and cellular optical properties of phytoplankton, in particular for the <20 μm phytoplankton (Sévigny et al. 1979, Lovejoy et al. 1993, Rivkin et al. 1996).

Consequently, the goals of the present study, which was conducted during SeaWiFs validation cruises in 2000 and 2001, were to (1) describe the surface water distribution of abundance and cell optical properties of pico-, ultra and nanophytoplankton, by flow cytometry (FCM), (2) evaluate the contribution of these different size classes to IOPs in surface waters of the Estuary and the Gulf of St. Lawrence, by coupling FCM with bulk optical measurements, (3) address the influence of environmental variables on abundance and cellular parameters of pico-, ultra- and nanophytoplankton on a variety of temporal and spatial scales, and (4) examine the diel pattern of cellular optical properties of pico-, ultra- and nanophytoplankton.

MATERIALS AND METHODS

Study Area - The St. Lawrence system can be divided into two main regions: the Estuary (stations 11 to 45), with generally important spatial variability of temperature and salinity and the Gulf (stations 51 to 114 as well as stations 1 and 2, Brunel 1970, El-Sabh et al. 1979) (Fig. 1). Based on salinity and temperature patterns, the St. Lawrence Estuary can be divided into the Upper and Lower Estuary (Brunel 1970 El-Sabh et al. 1979). The Upper Estuary is west of the Saguenay Fjord (Stations 11 to 14), whereas the Lower Estuary (Stations 21 to 45) extends from the Saguenay Fjord to Pointe-des-Monts. The Lower Estuary is characterized by an upwelling zone near the mouth of the Saguenay Fjord (Forrester 1974, Therriault and Lacroix 1976), a large freshwater plume originating from the Manicouagan and Aux-Outardes rivers (Therriault and Levasseur 1985, 1986, Therriault et al. 1985), and the Gaspé coastal jet current flowing along the Gaspé peninsula (El-Sabh 1979, Tang 1980), which results from the combination of low salinity surface outflows from the Estuary, the Saguenay Fjord and the Manicouagan/Aux-Outardes plumes.

The St. Lawrence Gulf can be also divided into two main regions: the western and the eastern, more oceanic zone. The western zone of the Gulf (stations 51 to 67 and stations 1 and 2) is located from Pointe-des-Monts to the tip of the Gaspé Peninsula and can be considered as a buffer zone between the Lower Estuary and the oceanic zone of the Gulf. Its surface waters are influenced by two major hydrographic features: a quasi-permanent cyclonic gyre, the Anticosti gyre and the Gaspé current system (El-Sabh

1976), which strongly influences the shallow, southwestern part of the Gulf (Stations 101 to 104).

Sampling - This study was conducted between 17 and 31 May 2000 and 20 April to 4 May 2001, on board the icebreaker CCGS Martha Black in the St. Lawrence. Surface water (0-2 m) sampling was carried out at 44 stations in 2000 and at 34 stations in 2001 (Fig. 1). Samples were collected with a rosette sampler, equipped with 30 L Niskin bottles a CTD (SeaBird 911), which simultaneously measured salinity, temperature, depth and a SeaTech submersible fluorometer for *in situ* fluorescence. *In situ* bio-optical parameters and optically significant biogeochemical variables of the St. Lawrence are detailed below.

Figure 1: Maps showing the different geographic areas (a) (M.I.: Magdalen Islands and P.E.I.: Prince Edward Island) and the location of the stations sampled in the Estuary and Gulf of St. Lawrence (b). In (a), the I, II, III, IV and V correspond to the Upper Estuary (stations 11 to 14), the Lower Estuary (stations 21 to 45), the Gaspé current system (stations 51, 52, 53, 66, 67, 1 and 2), the Anticosti gyre (stations 61, 62, 64 and 65) and the eastern zone of the Gulf (stations 72 to 114), respectively.

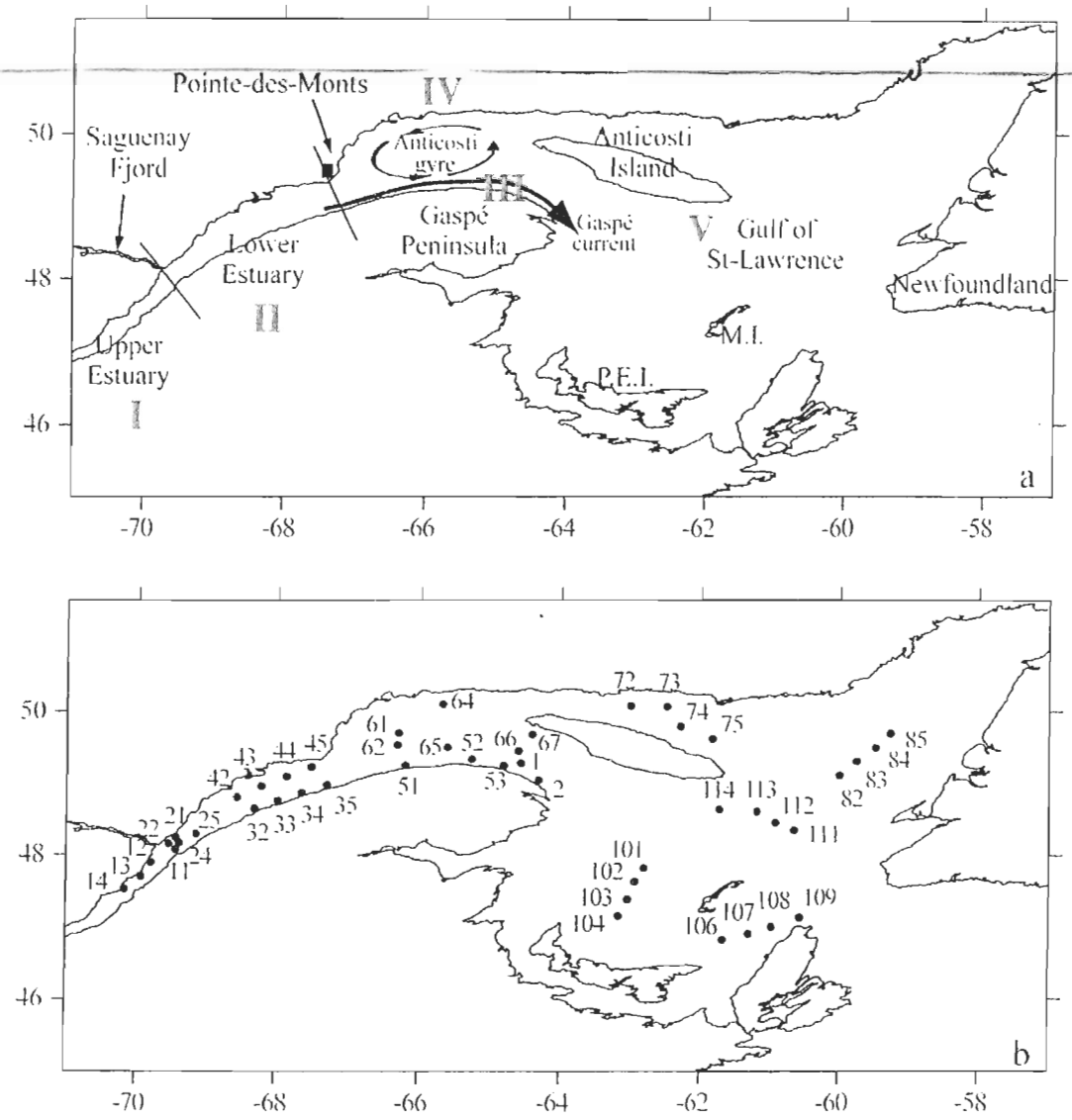
Pointe-des-Monts
IV
Saguenay
Fjord
Anticosti
gyre
Anticosti
Island
III
Gaspé
Peninsula
Gaspé
current
V
Gulf of
St-Lawrence
Newfoundland
Lower
Estuary
II
M.I.
Upper
Estuary
P.E.I.
I
a
50
48
46
-70
-68
-66
-64
-62
-60
-58
b

Light measurements - For each station, a vertical profile of downwelling irradiance E_d for photosynthetically available radiation (PAR = 400-700 nm) was acquired with an underwater PAR sensor (Satlantic SPMR with 13 visible-light channels). Values for downwelling irradiance just below the water surface, E_d (0), were determined from linear regressions of natural log of E_d against depth using only data points within the log-linear portion of the curve. The vertical attenuation coefficient for downwelling PAR (K_d, m^{-1}) in the water column was calculated using the following relationship (Kirk 1994):

$$K_d = \ln (E_d(0)/E_d(z)) / \Delta z,$$

where $E_d(0)$ and $E_d(z)$ are the downwelling irradiance just below the water surface and at depth z for PAR ($\mu E \cdot m^{-2} \cdot s^{-1}$).

Bulk inherent optical properties - *In situ* measurements of inherent optical properties (IOPs) were carried out during each cruise, along with discrete water sampling for more detailed analysis of water constituents. During both cruises, the total absorption, *a*, and total attenuation, *c*, coefficients were measured in 9 spectral bands of 10 nm width in the visible and near infrared (412, 440, 488, 510, 532, 555, 630, 650, 676, and 715 nm) by a flow-through absorption and attenuation meter (ac-9, WET Labs) with a 25-cm path length. Total attenuation and absorption coefficients of all non-water constituents were corrected for daily drift using pure water calibrations (Twardowski et al. 1999), for

changes in pure water absorption and attenuation due to temperature and salinity (Pegau et al. 1997) and for scattering artefacts (Zaneveld et al. 1994). The total scattering coefficient (b_{tot}) was obtained from the difference between the ac-9 corrected total coefficients of attenuation and absorption. The total scattering coefficient was normalized by the suspended particulate matter (SPM) concentrations to obtain the mass-specific scattering coefficient of particles (b_p^m). Additionally, measurements with the ac-9 equipped with a 0.2 µm filter (Gelman Suporcap), determined the absorption coefficient of colored dissolved organic matter (a_{CDOM}), as well as the particle absorption coefficient ($a_p = a_{tot} - a_{CDOM}$) (Twardowski et al. 1999). In 2000, the ac-9 was only available for measurements made in the Estuary.

Nutrient concentrations - For the determination of dissolved inorganic nitrogen ($NO_2^- + NO_3^-$), dissolved inorganic phosphorus (PO_4^{3-}) and ortho-silicic acid (SiO_4), 10 mL of surface water were filtered on Acrodisc filters (0.22 µm pore size, Nitrocellulose, GSWP) collected in two acid (HCl 10%) pre-washed 5 mL cryovials and stored at -80°C. Nutrient concentrations were later determined on triplicate subsamples using a Technicon autoanalyser system following the methods of Strickland and Parsons (1972). The ($NO_2^- + NO_3^-$) and (PO_4^{3-}) concentrations were used to calculate the Redfield ratio (N/P), which is 16 at equilibrium (Redfield et al. 1963).

Suspended particulate matter - Suspended particulate matter (SPM) concentrations were determined from water samples filtered through pre-burned and pre-

weighted glass fibre filters (Whatman GF/F, 0.7 µm) according to JGOFS standard protocols (JGOFS 1991). The filters were stored at -80°C until analysis. The inorganic fraction of SPM, particulate inorganic matter (PIM), was determined after burning off the organic fraction at 450°C during 5h and the percent organic matter (% OM) was calculated as the weight loss after combustion (Byers et al. 1978).

Phytoplankton absorption coefficients - To determine phytoplankton absorption coefficients, $a_{ph}(\lambda)$, aliquots of 250 to 1000 mL of surface water were filtered through 25 mm GF/F glass fibre filters (nominal pore size of 0.7 µm, Whatman GF/F) stored at -80°C in Histo-Prep tissue capsules (Fisher Scientific). The absorption coefficients for particulate material $a_p(\lambda)$ and for detritus $a_d(\lambda)$ were measured by the method of Mitchell et al. (2002) using a Perkin Elmer Lambda 2 spectrophotometer equipped with an integrating sphere (Labsphere RSA-PE-20). Air was used as a reference and corrections were done for scattering (Mitchell and Kiefer 1988, Bricaud and Stramski 1990). A quadratic fit equation determined in our laboratory from phytoplankton cultures was used to estimate the optical path-length amplification factor due to the filters (Laurion et al. 2003). Optical density values from filters (OD_f) were transformed into equivalent OD values in suspension (OD_s) with the following equation: $OD_s(\lambda) = 0.339[OD_f(\lambda)] + 0.583[OD_f(\lambda)^2]$. The values were then transformed into absorption coefficients (a_p (λ), m^{-1}) by multiplying by 2.303 (transforming base-10 to base-e logarithm), and dividing by the pathlength of light passing through the sample (= volume filtered divided by the area of filtration). Detrital absorption, $a_d(\lambda)$, was obtained using the method developed by Kishino et al. (1985), after extracting pigments from the filters, using absolute methanol

followed by filtered seawater and re-scanning the bleached filters. The absorption coefficient of phytoplankton, $a_{ph}(\lambda)$, was determined as $a_{ph}(\lambda) = a_p(\lambda) - a_d(\lambda)$. To obtain chlorophyll-specific absorption coefficients ($a^*_{ph}(\lambda)$), $a_{ph}(\lambda)$ was normalized by HPLC-determined total chlorophyll *a* (TChl *a* = chlorophyll *a* + epimers and allomers of chlorophyll *a* + chlorophyllide *a*). As the relationship between the spectrophotometric measurements of $a_p(\lambda)$ and those from the ac-9 ($a_{p,spectro}(\lambda) = 0.92\ (a_{p,ac\text{-}9}(\lambda))$, $r^2 = 0.97$, $n = 395$) for field was strong, the phytoplankton contribution on total and particle absorption could be estimated with confidence.

Cell properties of <20 µm phytoplankton - The cell properties of <20 µm phytoplankton groups, pico- (0.2-2 µm), ultra- (2-5 µm) and nanophytoplankton (5-20 µm) were estimated by using a FACSort Analyzer flow cytometer, (FCM, Becton-Dickinson) fitted with a 15 mW air-cooled laser emitting at 488 nm. The FCM provided (1) cell concentration, (2) the forward-angle light scatter (FSC, $\theta = 1\text{-}10°$) and (3) two fluorescence signals referred to as "orange" (FL2, 585 ± 21 nm), and "red" (FL3, >650 nm) fluorescence related, respectively, to phycoerythrin, and chlorophyll contents of the cells (Jacquet et al. 2001). For the determination of pico-, ultra and nanophytoplankton distributions, 2 mL triplicate samples of fresh surface water were collected at all stations and immediately analysed on board, after addition of 2, 6, 10 and 20 µm monodisperse latex-polystyrene beads (YG, Fluoresbrites, Polyscience, Inc.) used as internal standards to identify the size range of the phytoplankton populations and to control the instrument performance. Phytoplankton cells were detected using the red fluorescence FL3 corresponding to chlorophyll. FL2 fluorescence signals, characteristic of phycoerythrin

pigment, were used to verify the presence of cyanobacteria and some cryptophytes; however, no cyanobacteria were detected during both cruises. For each size classe, different populations were discriminated from measured cell parameters. The data were logged and analyzed using Cell Quest and Attractors software (Becton-Dickinson). Average values of the measured cell parameters were normalized with reference to the fluorescent beads of 2 µm.

Computations of IOPs at 488 nm for the <20 µm phytoplanktonic groups - To estimate the bulk absorption and scattering of each FCM-determined phytoplankton group, we need information on the abundance and optical cross section of each group. Previous studies (Mas et al. 2008 and in prep.) have shown a strong relationship ($\sigma_a(488) = 0.0092 \times (FL3)^{6.5}$, $r^2 = 0.95$, n = 194) between FCM chlorophyll fluorescence (FL3) and estimates of spectrophotometric absorption cross-section $\sigma_a(488)$. This has also been observed in the works of Perry and Porter (1989) and Green et al. (2003), suggesting that $\sigma_a(488)$ for the various groups of phytoplankton can be estimated with reasonable accuracy from FCM measurements of FL3. The absorption coefficients of pico-, ultra and nanophytoplankton, at 488 nm, ($a_{pico}(488)$, $a_{ultra}(488)$ and $a_{nano}(488)$), were obtained from the product of the number of cells·m^{-3} (N) and $\sigma_a(488)$ (µm^2·$cell^{-1}$) of the different phytoplankton size classes.

The measurements of FSC constitute a proxy of scattering cross section at 488 nm, $\sigma_b(488)$, since FSC values for the angles measured by FCM contribute more than 90% to

total scattering (DuRand et al. 2002). From previous experiments on large volume cultures of various phytoplankton species (mono-specific or mixed cultures) under different growth phases, we compared the bulk scattering coefficient proxy (FSC × N = b_{FCM}) of particles (phytoplankton + bacteria) to bulk ac-9 measurements of particulate matter scattering coefficient (b_p), at 488 nm; the b_p obtained from bulk methods was strongly related to the bulk scattering coefficient proxy of particles from FCM ($b_{ph+bact-FCM}(488) = (0.25 \cdot 10^{12})\ b_p(488)$, $r^2 = 0.98$, n = 23). An approximate value of scattering cross-section (σ_b) for each phytoplanktonic group (<20 µm) could thus be determined from FSC values measured by FCM. The scattering coefficients of pico- ultra and nanophytoplankton, at 488 nm, ($b_{pico}(488)$, $b_{ultra}(488)$ and $b_{nano}(488)$), were obtained from the product of the number of cells m^{-3} (N) and $\sigma_b(488)$ (µm² $cell^{-1}$) of the different phytoplankton size classes, $b_{ph<20}(488)$ is the sum of $b_{pico}(488)$, $b_{ultra}(488)$ and $b_{nano}(488)$. Although these approximate values differ from the real values, this approach provides information about the magnitude and type of σ_b variations for each <20 µm phytoplankton group as well as their contribution to total scattering coefficient measured by the ac-9.

Pigment analysis - Triplicate volumes of 250 to 1000 mL of surface water were filtered through Whatman GF/F glass fibre filters (25 mm diameter, pore size of 0.7 µm) for both cruises. For the 2001 cruise, samples were also filtered through Osmonics polycarbonate filters (25 mm diameter and pore sizes of 20 µm and 5 µm). All filters were immediately frozen in liquid nitrogen and stored at -80°C until pigment extraction.

HPLC *(high-performance liquid chromatography)* pigment analysis was based on the method by Zapata et al. (2000) using a RP-C8 Symmetry column. The compounds found in solvent-extracted filters were detected using a Spectraflow fluorometer and a SpectraPhysics fast scanning absorbance detector. The chromatogram values were transformed into volumetric concentrations of total chlorophyll *a* (TChl *a*; including chlorophyll *a*, divinyl chlorophyll *a*, chlorophyllide *a*, and chlorophyll *a* allomers and epimers), pheopigments, total accessory chlorophylls (chlorophyll *b* and chlorophylls *c*), photoprotective (PPC: alloxanthin, antheraxanthin, diadinoxanthin, diatoxanthin, lutein, zeaxanthin, violaxanthin, β,ß- and β,ε-carotene) and photosynthetic carotenoid pigments (PSC = the difference between total carotenoids and PPC, i.e. fucoxanthin, 19'-butanoyloxyfucoxanthin, 19'-hexanoyloxyfucoxanthin, peridinin, prasinoxanthin). The pigment pool (Tpig) was the sum of carotenoids (PSC and PPC), total accessory chlorophylls, pheopigments and TChl *a*. The concentrations of TChl *a* in each size fraction were determined as follows: "total" refers to all particles >0.7 µm; "microplankton" (cells >20 µm) refers to particles retained on the 20 µm filters, "nanoplankton" (cells between 5 and 20 µm) results from the difference between the >20 µm concentrations and the >5 µm concentrations, and "ultraphytoplankton + picophytoplankton" (cells <5 µm) is obtained from the difference between >5 µm concentrations and the total concentrations.

Enumeration and identification of phytoplankton communities - 200 mL samples of surface water were preserved using acid Lugol's solution (1% final concentration), for phytoplankton species identification and enumeration. Phytoplankton

species were identified and enumerated using the Utermöhl (1931) technique with a Zeiss Axiovert 10 inverted microscope.

Statistical analyses - The association between pairs of variables was measured with Spearman rank correlations, because the data were not normally distributed and did not respect homoscedasticity (Zar 1999). These statistical tests were carried out with the SPSS 9.0 program.

Multivariate approaches were applied to the community analysis. Phytoplankton cell concentrations were ordinated by non-metric multi-dimensional scaling (MDS) (Clarke 1993). The input was a similarity matrix based on Bray-Curtis similarity of fourth root transformed cell abundances, to put more weight on the species composition in the samples (Field et al. 1982). These multivariate analyses were performed with the program Primer version 5.0 (Plymouth Marine Laboratory).

RESULTS

Physical, chemical and biogeochemical parameters in the St. Lawrence system - The St. Lawrence Estuary was characterized by a strong surface salinity gradient (from 12 to 30 for both years) and an inverse surface temperature gradient (from 9 to 4°C for 2000 and from 4 to 0.7°C for 2001) from the west near the Saguenay Fjord (stations 13 and 14) to the east near Pointe-des-Monts (stations 35 and 45). The western, more estuarine zone of the Gulf presented intermediate temperature (≈ 4°C for 2000 and ≈ 1.5°C for 2001) and salinity (≈ 28 for 2000 and ≈ 30 for 2001) compared to the more oceanic waters of the Gulf (stations 72 to 114), which were characterized by cold and less variable temperatures (≈ 3°C for 2000 and ≈ 0.7°C for 2001) and high salinity (≈ 31 for 2000 and ≈ 31.5 for 2001), characteristic of Atlantic Ocean Waters (Fig. 2, Table 1).

For the two cruises, the surface waters of the Upper Estuary were characterized by the lowest TChl *a* concentrations (<0.7 $mg \cdot m^{-3}$) and sunlight penetration as well as highest concentrations of SPM and nutrients, and high N/P ratios (>16) (Fig. 2, Table 1).

Figure 2: Distribution of temperature (T, °C) and salinity (a and d); dissolved inorganic nitrogen, (NO_2^- + NO_3^-), dissolved inorganic phosphorus, PO_4^{3-}, and ortho-silicic acid, SiO_4 (b and e); diffuse attenuation coefficient (K_d, m^{-1}) and suspended particulate matter concentrations (SPM, $g \cdot m^{-3}$) (c and f) for May 2000 (left panels) and April 2001 (right panels). The I, II, III, IV and V correspond to the Upper Estuary, the Lower Estuary, the Gaspé current system, the Anticosti gyre and the eastern zone of the Gulf, respectively.

May 2000

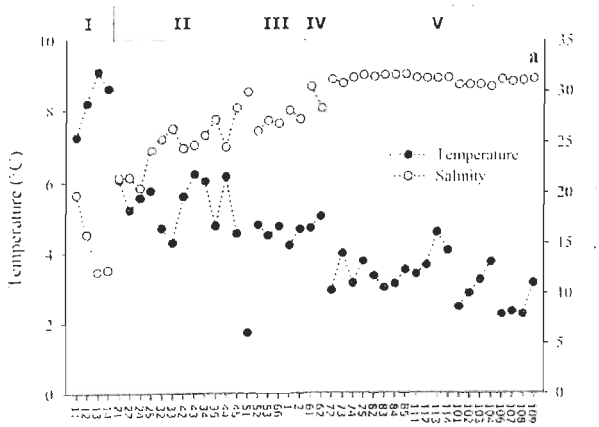

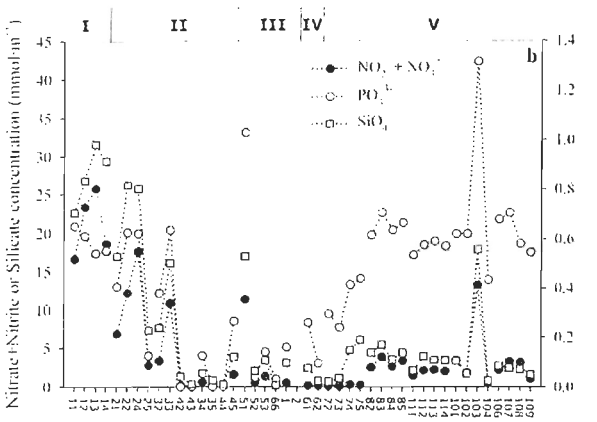

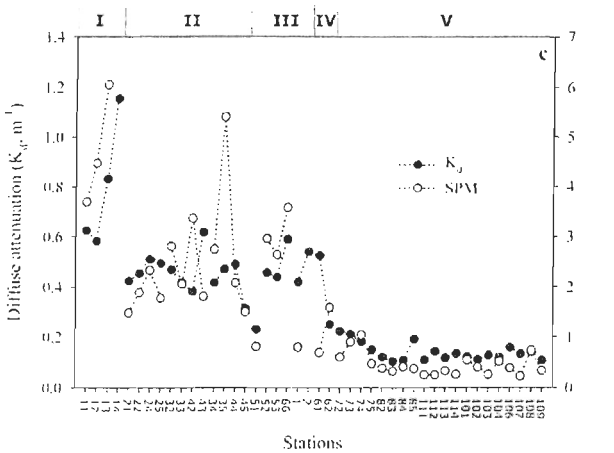

Avril 2001

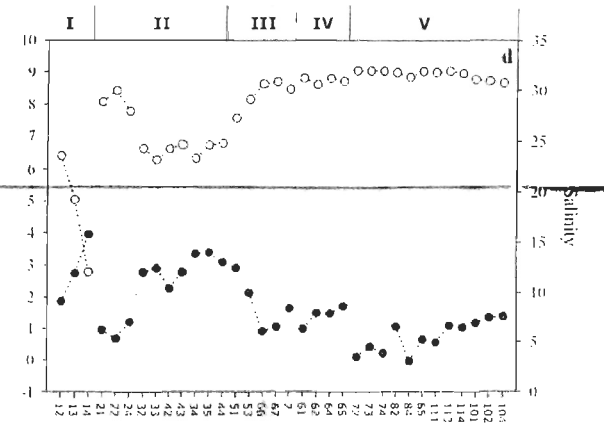

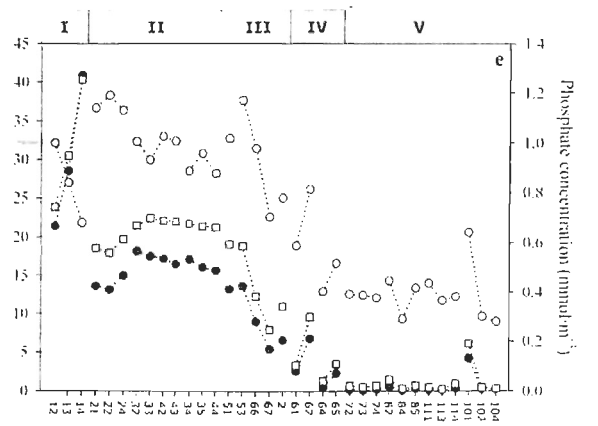

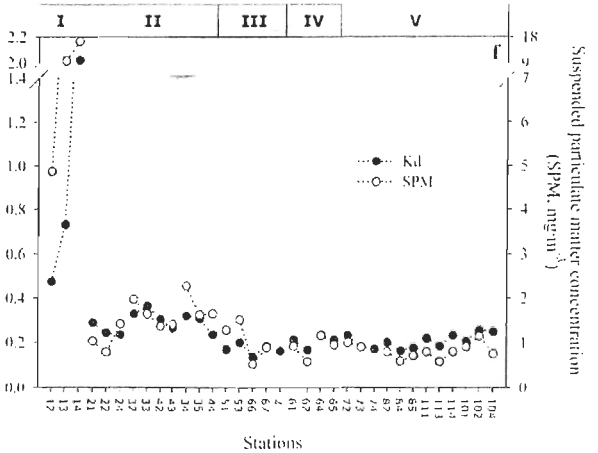

Table 1: Mean values of the different physico-chemical and biological variables, and FCM cell parameters in 2000 and 2001, in the Upper Estuary and under pre-bloom, bloom and post-bloom situations. The numbers in brackets correspond to standard deviations. The II, III, IV and V represent the Lower Estuary, the Gaspé current system, the Anticosti gyre and the eastern zone of the Gulf, respectively. bu = bead unit.

	2000			2001		
	Upper Estuary	II + III (bloom)	IV + V (post-bloom)	Upper Estuary	II +III (pre-bloom)	IV + V (bloom)
Physico-chemical variables						
Temperature (°C)	8.3 (0.8)	5.0 (1.1)	3.4 (0.8)	2.9 (1.0)	2.1 (1.0)	0.9 (0.5)
Salinity	15.0 (3.6)	25.5 (2.5)	30.9 (0.7)	18.3 (5.8)	26.9 (2.9)	31.4 (0.5)
$N0_3$+$N0_2$ (µM)	21.1 (4.2)	4.1 (5.5)	2.3 (2.8)	30.3 (9.8)	13.8 (3.9)	1.2 (1.9)
PO_4 (µM)	0.6 (0.1)	0.3 (0.3)	0.6 (0.2)	0.9 (0.2)	1.0 (0.1)	0.4 (0.1)
N/P ($M \cdot M^{-1}$)	36.4 (9.2)	12.9 (7.6)	3.3 (2.4)	38.5 (19.7)	14.0 (3.9)	2.0 (2.5)
$Si0_4$ (µM)	27.6 (2.8)	7.9 (9.0)	3.6 (3.5)	31.5 (8.3)	18.5 (4.5)	1.9 (2.6)
K_d (m^{-1})	0.8 (0.3)	0.5 (0.1)	0.2 (0.1)	1.1 (0.8)	0.3 (0.1)	0.2 (0.03)
SPM ($g \cdot m^{-3}$)	4.7 (1.2)	2.4 (1.1)	0.5 (0.3)	10.3 (5.8)	1.4 (0.5)	0.8 (0.2)
OM contribution to SPM (%)	*24 (2)*	*43 (8)*	*42 (5)*	*21 (4)*	*33 (11)*	*45 (6)*
Biological variables						
TChl*a* ($mg \cdot m^{-3}$)	0.7 (0.3)	8.7 (5.6)	0.7 (0.9)	0.3 (0.2)	1.0 (0.8)	5.9 (2.3)
TChla in <5 µm fraction (%)	*/*	*/*	*/*	*18 (8)*	*38 (20)*	*27 (11)*
TChla in (5-20 µm) fraction (%)	*/*	*/*	*/*	*64 (4)*	*32 (13)*	*40 (28)*
TChla in >20 µm fraction (%)	*/*	*/*	*/*	*18 (5)*	*30 (19)*	*33 (34)*
<20 µm abundance ($cells.mL^{-1}$)	300 (112)	1331 (877)	4627 (3674)	1019 (479)	6676 (5115)	8969 (6780)
Picophytoplankton (%)	*65 (7)*	*51 (12)*	*67 (19)*	*73 (4)*	*71 (13)*	*61 (19)*
Ultraphytoplankton (%)	*22 (21)*	*19 (9)*	*14 (12)*	*21 (3)*	*19 (10)*	*28 (11)*
Nanophytoplankton (%)	*13 (16)*	*30 (9)*	*18 (24)*	*6 (1)*	*10 (8)*	*11 (11)*
FCM cell parameters						
FSC_{pico} (bu)	0.76 (0.09)	0.73 (0.14)	0.68 (0.07)	0.85 (0.08)	0.79 (0.08)	0.56 (0.08)
$FL3_{pico}$ (bu)	1.94 (0.09)	1.90 (0.16)	1.52 (0.31)	1.60 (0.08)	1.54 (0.18)	1.42 (0.15)
FSC_{ultra} (bu)	2.80 (0.03)	2.80 (0.11)	2.68 (0.18)	1.86 (0.07)	2.23 (0.07)	1.84 (0.10)
$FL3_{ultra}$ (bu)	3.03 (0.08)	2.79 (0.17)	2.46 (0.21)	2.27 (0.10)	2.36 (0.11)	2.31 (0.16)
FSC_{nano} (bu)	4.04 (0.10)	4.34 (0.26)	4.33 (0.36)	3.27 (0.11)	3.79 (0.28)	3.79 (0.18)
$FL3_{nano}$ (bu)	3.10 (0.01)	3.50 (0.16)	3.19 (0.12)	3.11 (0.06)	2.98 (0.12)	3.26 (0.23)

During May 2000, the sampling area showed evidence of regions undergoing the spring algal bloom, and others that were characteristic of post-bloom conditions. The bloom was located in the Lower Estuary (stations 32, 34, 35, 42 and 44) and in the western zone of the Gulf, more specifically in the Gaspé current region (stations 52, 53, 1, 2 and 66). Bloom stations were characterized by high concentrations of TChl *a* (8.7 $mg \cdot m^{-3}$), SPM, high K_d, and by a N/P mean ratio slightly below 16 (Fig. 2, Table 1), which suggests a possible deficiency in dissolved nitrogen relative to phosphorus. The dissolved inorganic nitrogen, phosphorus and silicate concentrations varied strongly (Fig. 2, Table 1) and were generally low with peaks in the plume region of the Manicouagan and Aux-Outardes rivers (St. 51, 33 and 2). Conversely, the surface waters of the eastern zone of the Gulf were characterized by low values of TChl *a* (<1 $mg \cdot m^{-3}$), SPM, K_d and very low N/P ratios (suggesting nitrate limitation) (Table 1). These conditions are typical of the post-bloom period, since the spring algal bloom normally occurs in April in the Gulf region (see below).

In April 2001, the bloom was located in the Gulf, characterized by high TChl *a* concentrations (5.9 $mg \cdot m^{-3}$) and low N/P ratios. Surface dissolved inorganic nitrogen and silicate concentrations were more depleted in the surface layer of the eastern Gulf compared to its western region and the Estuary. At that time, the Lower Estuary showed pre-bloom conditions with low TChl *a* (1.0 $mg \cdot m^{-3}$) and SPM concentrations, low K_d values, high concentrations of nutrients, and N/P ratios around 16 (Fig. 2, Table 1).

For both years, the spatial distribution of SPM exhibited the same west-to-east decrease as did salinity (Fig. 2, Table 1) and CDOM (see Çizmeli 2008). In the Upper

Estuary, the organic matter contributed up to 20% of the SPM on average for both years. This fraction was less than 50% for the Gulf and the Lower Estuary in May 2000; whereas in April 2001 the composition varied regionally and was higher in the regions undergoing the spring algal bloom: 40-60% of OM in the Gulf, around 28% in the Lower Estuary and 47% in the Gaspé current.

Spatial and temporal variability of phytoplankton community – Multidimensional scaling analyses performed on species abundances discriminated between the bloom and pre- or post-bloom conditions for both years, and highlighted the different character of the stations from the Upper Estuary (Fig. 3). Taxonomic and pigment composition confirmed these trends (Tables 2 and 3, respectively). For both years, the accessory pigment pool under bloom conditions was clearly dominated by fucoxanthin and Chl c_{1+2}, associated with high diatom abundance (>70% of total phytoplankton abundance), mostly *Skeletonema costatum* (Greville) Cleve (3-16 µm diameter, 52%) in May 2000 and *Neodenticula seminae* (Simonsen and Kanaya) Akiba and Yanagisawa (8 µm wide x 20 µm long, 40%) in April 2001 (Tables 2 and 3). Pigment composition was more variable in the Upper Estuary and under pre- and post-bloom conditions, reflecting high flagellates abundance (>50%) and a higher taxonomic diversity (Table 2).

Table 2: Average percent contribution of the major phytoplankton groups and dominant diatom species to phytoplankton abundance in 2000 and 2001, in the Upper Estuary and under pre-bloom, bloom and post-bloom situations. The numbers in brackets correspond to standard deviations. The II, III, IV and V represent the Lower Estuary, the Gaspé current system, the Anticosti gyre and the eastern zone of the Gulf, respectively.

	2000			2001		
	Upper Estuary	II + III (bloom)	IV + V (post-bloom)	Upper Estuary	II + III (pre-bloom)	IV + V (bloom)
Total number of cells per mL	633	4957 (3973)	1846 (1276)	58	886 (602)	2102 (617)
Taxonomic composition (%)						
Diatoms	**24.6**	**74.4 (15.2)**	**45.3 (28.8)**	**33.1**	**42.7 (20.1)**	**73.8 (9.9)**
Chaetoceros debilis (10-40 µm)	0	0.3 (0.1)	1.0 (1.8)	0	0.02 (0.03)	2.6 (4.8)
Chaetoceros furcellatus (5-19 µm)	0	2.2 (3.4)	2.8 (4.1)	0	0.05 (0.07)	0.2 (0.5)
Chaetoceros socialis (5-14 µm)	0	0.2 (0.2)	16.3 (26.7)	0	0	10.2 (13.4)
Fragilariopsis pseudonana (8 x 10 µm)	0	0	0	0	0.4 (0.8)	1.0 (1.5)
Neodenticula seminae (8 x 20 µm)	0	0	0	4.1	1.9 (3.1)	39.4 (19.2)
Skeletonema costatum (3-16 µm)	15.1	52.2 (18.7)	4.8 (12.8)	18.0	29.2 (23.7)	0.9 (1.9)
Thalassiosira nordenskioeldii (11-41 µm)	0.7	17.1 (5.4)	1.7 (3.0)	0.5	1 (0.5)	4.5 (9.8)
Thalassiosira pacifica (9-48 µm)	8.6	0.6 (0.4)	0.1 (0.1)	3.7	8.8 (5.9)	0
Unidentified pennate diatoms (2-5 µm)	0	0	0.1 (0.3)	3.8	0.7 (0.6)	10.1 (8.8)
Unidentified pennate diatoms (5-10 µm)	0	1.1 (2.4)	16.3 (22.0)	0	0	0.1 (0.3)
Flagellates	**75.4**	**25.6 (15.2)**	**54.7 (28.8)**	**66.9**	**57.3 (20.1)**	**26.2 (9.9)**
Dinoflagellates	2.2	5.0 (5.2)	11.3 (7.8)	6.2	7.9 (3.9)	4.7 (5.6)
Chlorophytes	0.1	0	0	0.1	0	0
Chrysophytes	0	0.6 (0.5)	0.9 (1.2)	0.2	0.5 (0.6)	0.2 (0.2)
Cryptophytes	0.4	4.8 (4.2)	6.0 (3.8)	3.4	12.5 (9.4)	5.4 (2.7)
Dictyochophytes	0	0.5 (0.8)	1.2 (1.6)	0	2.8 (2.0)	0.3 (0.5)
Euglenopytes	0.1	0.3 (0.6)	0.9 (1.2)	0.3	0.2 (0.2)	0.1 (0.1)
Prasinophytes	0	1.0 (1.0)	3.9 (4.6)	0.1	3.2 (3.3)	0.9 (0.9)
Prymnesiophytes	0	2.4 (2.0)	7.0 (4.6)	21.4	15.1 (8.8)	5.8 (4.1)
Raphidophytes	0	0.1 (0.1)	0.1 (0.2)	1.5	0.1 (0.2)	0.1 (0.1)
Unidentified flagellates (2-5 µm)	72.6	10.9 (6.1)	23.4 (27.1)	33.7	15.0 (11.2)	8.7 (3.9)

Highest abundances of <20 μm phytoplankton were observed in the eastern Gulf under post-bloom conditions in May 2000 and in the western Gulf in April 2001 during the bloom; the maximum was two-fold higher in April 2001 than May 2000 (Fig. 4). In May 2000, cell concentrations of picophytoplankton and ultraphytoplankton were 4-5 fold lower under bloom conditions compared to their concentrations in post-bloom (Table 1). During the April 2001 bloom, the highest concentrations of the three size classes were recorded in the western Gulf (Table 1). For both years and in all regions, picophytoplankton dominated numerically the small-sized phytoplankton (generally >50%). For both years, the mean cell concentration of picophytoplankton was 2.5 to 8 fold higher than that of ultra- and nanophytoplankton.

Figure 3: MDS ordination plot of phytoplankton species abundances in 2000 (Δ: Upper Estuary, ● : bloom, ◆ : post-bloom) and 2001 (Δ: Upper Estuary, ● : pre-bloom, ◆ : bloom).

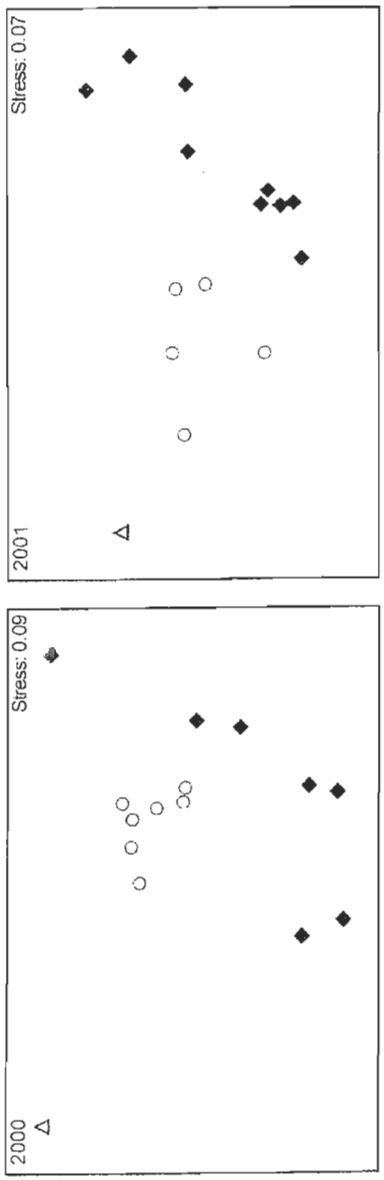
Stress: 0.09
2000
Stress: 0.07
2001

Figure 4: Distribution of total chlorophyll *a* concentration (TChl *a*, $mg \cdot m^{-3}$) (a and c) and <20 µm phytoplankton abundances ($cells \cdot mL^{-1}$) (b and d) for May 2000 (left panels) and April 2001 (right panels). The I, II, III, IV and V correspond to the Upper Estuary, the Lower Estuary, the Gaspé current, the Anticosti gyre system and the eastern zone of the Gulf, respectively.

May 2000

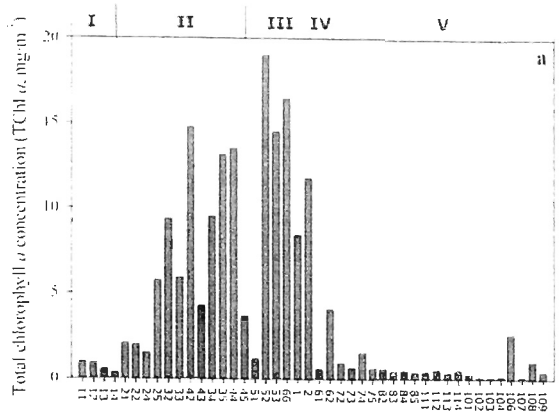

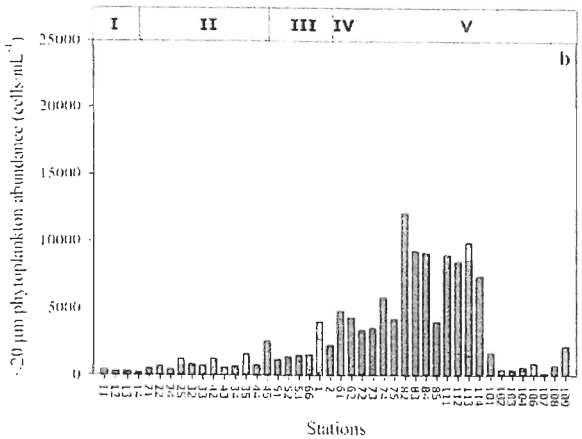

Avril 2001

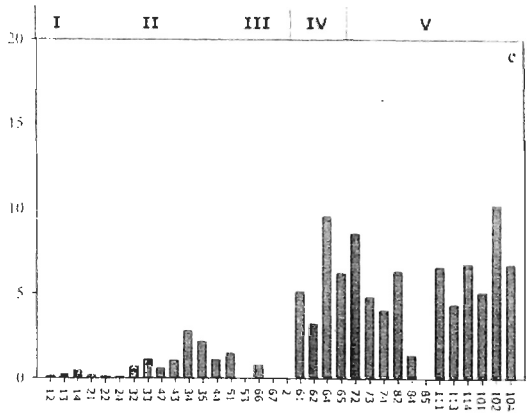

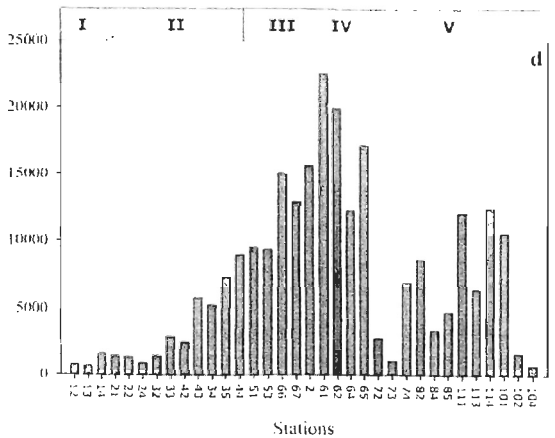

Table 3: Mean pigment ratios in 2000 and 2001, in the Upper Estuary and under pre-bloom, bloom and post-bloom situations. The numbers in brackets correspond to standard deviations. The II, III, IV and V represent the Lower Estuary, the Gaspé current system, the Anticosti gyre and the eastern zone of the Gulf, respectively.

	2000			2001		
	Upper Estuary	II + III (bloom)	IV + V (post-bloom)	Upper Estuary	II + III (pre-bloom)	IV + V (bloom)
Pigment composition ($x10^{-2}$, $g \cdot g^{-1}$)						
TChl *a*/Tpig	49.6 (3.6)	52.0 (2.3)	41.5 (4.9)	57.6 (9.8)	57.6 (5.4)	52 (3.1)
TChl *b*/Tpig	0	0.9 (1.3)	5.4 (3.5)	0	3.1 (4.1)	0.6 (0.5)
TChl c/Tpig	11.2 (7.6)	13.2 (0.9)	14.2 (3.5)	0	7.5 (2.9)	10.1 (1.0)
TChl c_{1+2}/Tpig	*11.2 (7.6)*	*13.2 (1.0)*	*11.7 (3.3)*	*0*	*6.8 (2.7)*	*9.6 (0.9)*
TChl c_3/Tpig	*0*	*0.1 (0.2)*	*2.5 (1.6)*	*0*	*0.7 (0.7)*	*0.5 (0.2)*
Pheo./Tpig	10.5 (5.9)	6.7 (2.5)	7.1 (4.6)	14.5 (9.7)	2.3 (1.9)	1.9 (0.7)
PSC/Tpig	18.2 (4.2)	22.6 (1.8)	16.8 (3.7)	18.7 (5.9)	21.6 (3.2)	28.6 (2.0)
BFU/Tpig	*0*	*0.1 (0.1)*	*1.0 (1.1)*	*0*	*0.3 (0.7)*	*0.03 (0.11)*
HFU/Tpig	*0*	*0*	*0.2 (0.4)*	*0*	*0.1 (0.3)*	*0.1 (0.3)*
Fuco/Tpig	*16.8 (3.6)*	*22.4 (2.2)*	*12.3 (5.0)*	*18.7 (5.9)*	*19.5 (4.9)*	*28.1 (2.1)*
Peridinin/Tpig	*1.4 (2.9)*	*0.1 (0.4)*	*3.0 (2.8)*	*0*	*1.3 (1.7)*	*0.3 (0.4)*
Prasino/Tpig	*0*	*0.02 (0.10)*	*0.4 (0.4)*	*0*	*0.3 (0.8)*	*0.03 (0.09)*
PPC/Tpig	10.5 (1.5)	4.6 (1.3)	15.0 (7.6)	9.2 (8.0)	7.8 (4.5)	7.3 (2.2)
β,ε-carotene/Tpig	*0*	*0.1 (0.2)*	*0.2 (0.4)*	*0*	*0.1 (0.2)*	*0*
β,β-carotene/Tpig	*0.5 (1.0)*	*1.3 (0.3)*	*1.6 (1.0)*	*0*	*1.4 (1.0)*	*1.1 (0.3)*
Allo/Tpig	*5.3 (2.2)*	*0.3 (0.4)*	*1.8 (1.3)*	*6.3 (6.8)*	*1.8 (1.2)*	*0.5 (0.6)*
Anthe/Tpig	*0*	*0.1 (0.2)*	*1.1 (1.3)*	*0*	*0.04 (0.13)*	*0.3 (0.4)*
(Dd+Dt)/Tpig	*4.8 (0.6)*	*2.8 (0.5)*	*6.6 (3.1)*	*1.3 (2.3)*	*4.0 (2.9)*	*5.1 (1.6)*
Lut/Tpig	*0*	*0.01 (0.04)*	*0.6 (0.8)*	*0*	*0.05 (0.16)*	*0.03 (0.05)*
Viola/Tpig	*0*	*0.04 (0.15)*	*2.8 (2.1)*	*0*	*0.3 (0.6)*	*0.1 (0.2)*
Zea/Tpig	*0*	*0.01 (0.03)*	*0.4 (0.6)*	*1.6 (2.8)*	*0.03 (0.10)*	*0.1 (0.1)*

In April 2001, nanophytoplankton dominated (64%) the TChl *a* concentration (>0.7 µm) in the Upper Estuary, while the <5 µm phytoplankton and microphytoplankton accounted for the remainder in similar proportions (18% each, Table 1). For the pre-bloom stations, the TChl *a* concentrations in the <5 µm and 5-20 µm fractions were almost of equal importance, i.e., about 35% each. Finally, under bloom conditions, the <5 µm phytoplankton, nano- and microphytoplankton contributed on average to 27%, 40% and 33% of TChl *a*, respectively (Table 1).

TChl *a*/Tpig proportions showed little spatial differences and ranged from 42 to 58% (Table 3). The PSC/Tpig ratio was higher under bloom conditions (23–29%) than in other conditions (17–22%, Table 3). In contrast, the PPC/Tpig ratio was very low under bloom conditions (5%-7%) and substantially greater in other conditions (8%-15%). However, the total carotenoid pool was not different (ranging from 28 to 36%) between the different conditions.

Optical properties – In the Upper Estuary, particulate absorption represented generally only a small proportion of the bulk absorption coefficient (15% in 2000, and 33% in 2001, Table 4) compared to the other regions. CDOM dominated the total absorption everywhere except in the Gulf in April 2001. Detritus dominated the particulate absorption in the Upper (both years) and Lower Estuary (in April 2001), although at other locations phytoplankton was more important.

The phytoplankton absorption coefficients at 488 nm (a_{ph}) had expectedly the highest values during the bloom for both years (Fig. 5). The <20 µm fraction dominated (>55%) the a_{ph} during post-bloom (May 2000) and pre-bloom (April 2001) conditions, while during the blooms its contribution was only about 25% (Table 4). During both years, nanophytoplankton, as well as ultraphytoplankton for some stations, were the most important contributors to phytoplankton absorption for the <20 µm fraction (Fig. 5). The absorption ratios, $a_{ph}(440)/a_{ph}(555)$, $a_{ph}(440)/a_{ph}(675)$ and $a_{ph}(488)/a_{ph}(555)$, were lower under bloom situation than under pre- or post-bloom conditions (Table 4). Relationships between $a_{ph}(488)$ and TChl *a* showed differences according to the presence or not of the spring diatom bloom, irrespective of the actual geographic region considered. Phytoplankton absorption was lowest for a given TChl *a* concentration during the blooms (Fig. 6), as also seen in the $a^*_{ph}(488)$ values (Table 4).

The total scattering coefficient (b_{tot}), at 488 and 555 nm, decreased from the Upper Estuary to the Gulf in both years (Fig. 7). Conversely, the contribution of <20 µm phytoplankton to b_{tot} (488) increased from the Upper Estuary (<0.1% for both years, Table 4) toward the Gulf (up to 35% at St. 66 in April 2001, Fig. 7). The <5 µm (pico- and ultraphytoplankton) fraction dominated generally the scattering coefficient of <20 µm phytoplankton (Table 4). Their maximum contribution was observed north of the oceanic zone of the Gulf in May 2000, while the maximum for the 5-20 µm fraction was located in the western part of the Gulf. In April 2001, maximum contributions of picophytoplankton were located in that sector, whereas the maxima for the two other classes were observed in the oceanic part of the Gulf.

Table 4: Mean values of optical variables in 2000 and 2001, in the Upper Estuary and under pre-bloom, bloom and post-bloom situations. The numbers in brackets correspond to standard deviations. The II, III, IV and V represent the Lower Estuary, the Gaspé current system, the Anticosti gyre and the eastern zone of the Gulf, respectively.

Figure 5: Distribution of phytoplankton absorption coefficient, a_{ph} (488, m^{-1}) for each size class (<2, 2-5, 5-20 and >20 µm) in the Upper Estuary (a and d), in the Lower Estuary and the Gaspé current system under bloom (b) and pre-bloom conditions (e), and in the Anticosti gyre and the eastern zone of the Gulf under post-bloom (c) and bloom conditions (f) for May 2000 (left panels) and April 2001 (right panels).

May 2000

Avril 2001

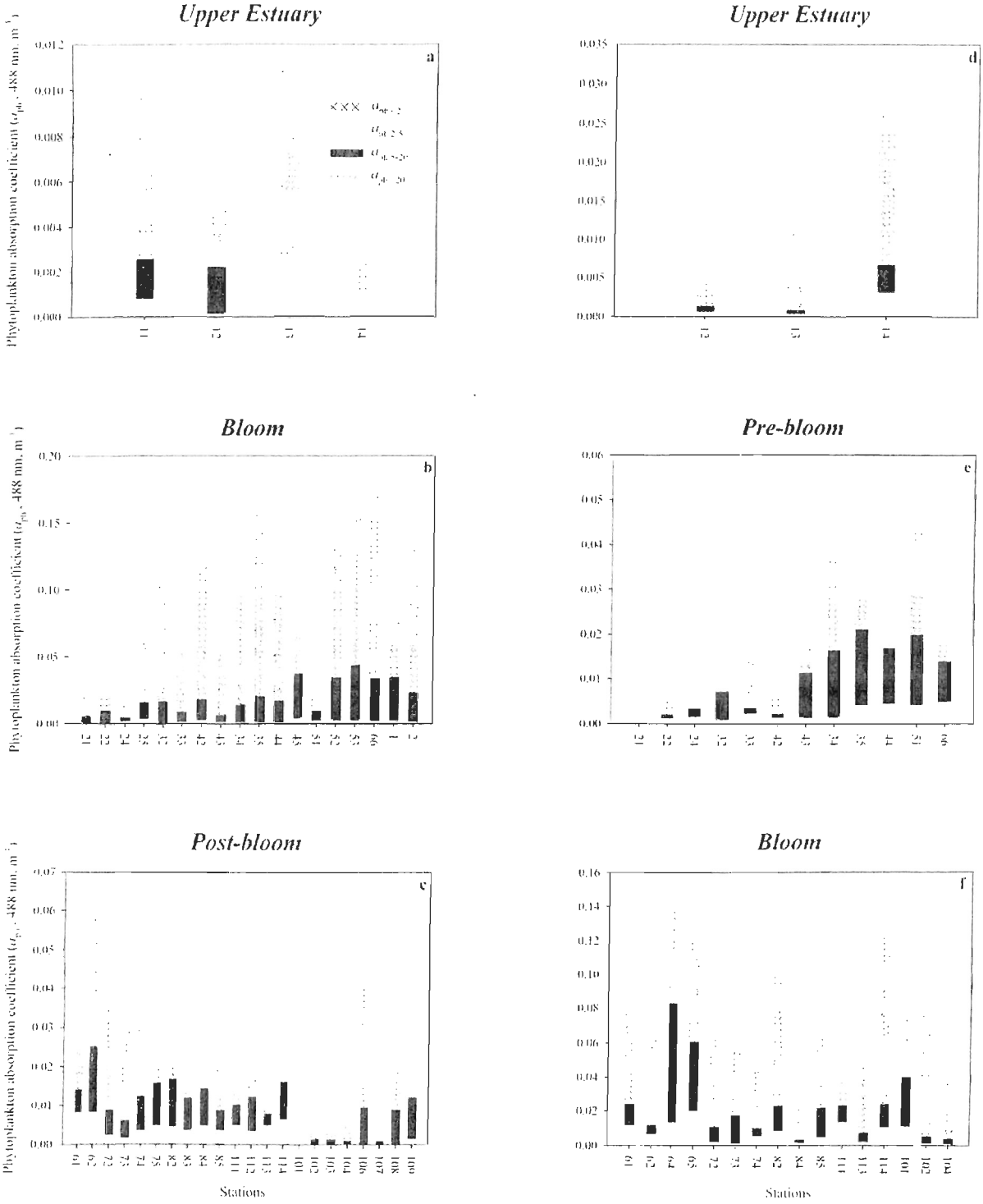

Figure 6: Relationships between total phytoplankton absorption coefficients (a_{ph}, 488 nm, m^{-1}) and total chlorophyll *a* concentrations in 2000 (circles; black symbols: Upper Estuary, red symbols: bloom, dark yellow symbols: post-bloom) and 2001 (triangles; open symbols: Upper Estuary, green symbols: pre-bloom, blue symbols: bloom) with the fitted curves (green dotted line: pre-bloom, r^2=0.96; dark yellow dot-dashed line: post-bloom, r^2=0.85; red continuous line: bloom 2000, r^2=0.94; and blue dashed line: bloom 2001, r^2=0.52).

0.25
0.20
0.15
0.10
0.05
0.00
0
5
10
15
20
2000
U. Estuary
Bloom
Post-Bloom
Pre-bloom
Bloom 2000
Bloom 2001
2001
U. Estuary
Pre-bloom
Bloom
Total phytoplankton absorption coefficient
(a_{ph}, 488 nm, m^{-1})
Total chlorophyll *a* concentration ($mg \cdot m^{-3}$)

Figure 7: Distribution of total scattering coefficient, b_{tot} (488, m^{-1}) in the whole area (a and e) and contribution to b_{tot} (488) (%) of each FCM size class (<2, 2-5 and 5-20 μm) in the Upper Estuary (b and f), in the Lower Estuary and the Gaspé current system under bloom (c) and pre-bloom conditions (g), and in the Anticosti gyre and the eastern zone of the Gulf under post-bloom (d) and bloom conditions (h) for May 2000 (left panels) and April 2001 (right panels).

May 2000

Avril 2001

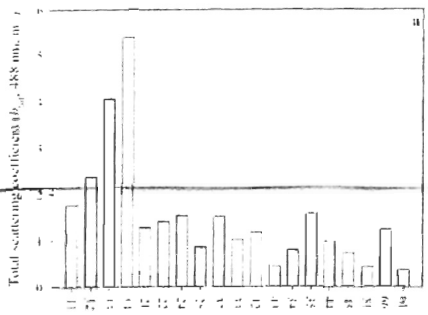

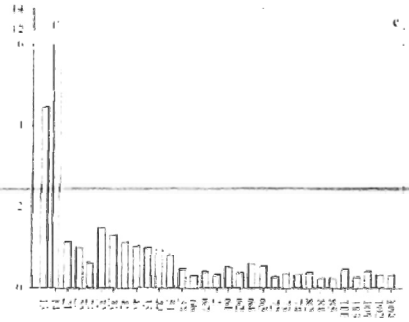

Upper Estuary

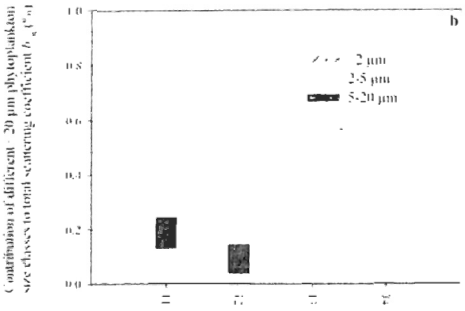

Upper Estuary

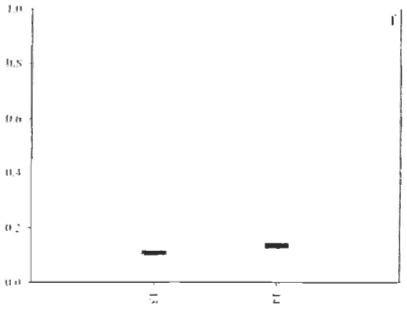

Bloom

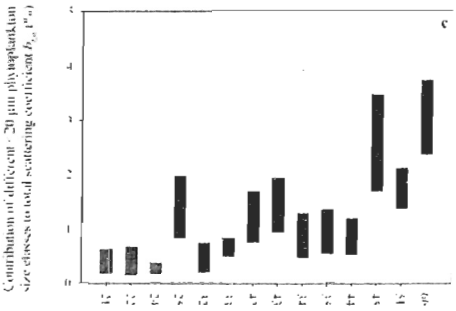

Pre-bloom

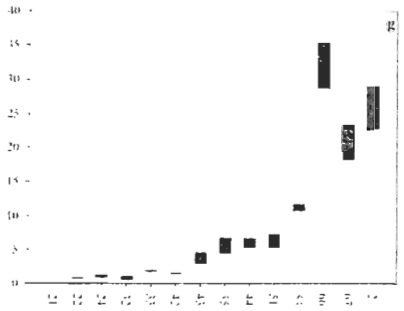

Post-bloom

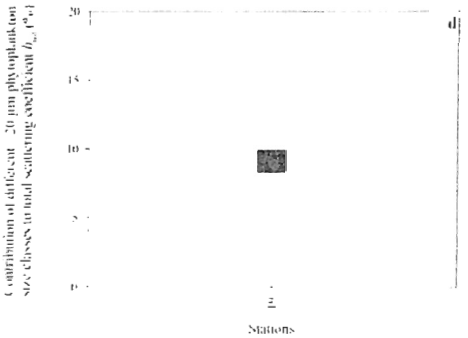

Bloom

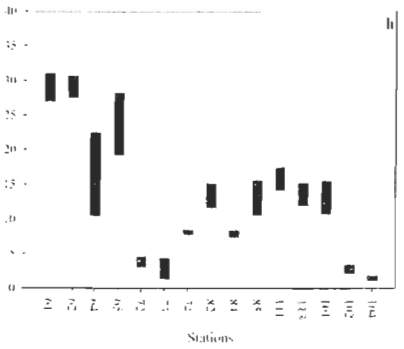

In May 2000, the mean values of chlorophyll-specific absorption coefficient ($a^*_{ph}(488)$) and mass-specific scattering coefficient of particles ($b_p^m(488)$) were lowest under bloom conditions, while the highest mean values were measured in post-bloom conditions (Table 4). In April 2001, stations of the Upper Estuary, but also those close to the Saguenay Fjord (St. 21, 22 and 24), were distinct and presented the highest $a^*_{ph}(488)$ values associated with very low TChl *a* concentrations. The $a^*_{ph}(488)$ and $b_p^m(488)$ mean values were lower under bloom conditions as in May 2000. Differences in $a^*_{ph}(488)$ and $b_p^m(488)$ mean values between bloom and post-bloom regions were larger in May 2000 than those between pre-bloom and bloom regions in April 2001, reflecting the higher TChl *a* concentration under bloom conditions in May 2000 compared to April 2001. For both years, the distribution of $b_p^m(555)$ followed generally that of $b_p^m(488)$; 555 nm is in the spectral domain where algal absorption is generally low and where scattering budgets are often performed (Morel and Ahn 1991, Stramski and Kiefer 1991). Moreover, the $b_p^m(555)$ and $b_p^m(488)$ average values were close under all situations (Table 4).

For April 2001, the relationships between specific absorption or scattering coefficient and TChl *a* of different size fractions were examined (Fig. 8). Stations from the Upper Estuary and Saguenay Fjord region (St. 12 to 24) were clear outliers; consequently they were not taken into account in the relationships. Since particles other than phytoplankton were very abundant and contributed highly to scattering, particularly in the Estuary and the Gaspé current, the relationship between $b_p^m(488)$ and TChl *a* of different size fractions was only presented for the Gulf region. Specific absorption and

scattering both increased as the fraction of chl-*a* in the <5 or 5-20 μm fractions increased. In contrast, they both decreased as microplankton increased (Fig. 8).

Figure 8: Relationships between TChl *a*-specific phytoplankton absorption coefficients (a^*_{ph}, 488 nm, $m^2 \cdot [mg\ TChl\ a]^{-1}$) and total chlorophyll *a* concentrations for <5, 5-20 and >20 µm fractions ($mg \cdot m^{-3}$) in the Saguenay region (stations 12 to 24, open circles), in the rest of Lower Estuary (stations 32 to 44) and the Gaspé current system under pre-bloom conditions (green squares), and in the Anticosti gyre and the eastern zone of the Gulf under bloom conditions (blue inverted triangles) for April 2001 (left panels); and relationships between mass-specific phytoplankton scattering coefficient (b^m_p, 488 nm, $m^2 \cdot mg^{-1}$) and total chlorophyll *a* concentration for <5, 5-20 and >20 µm fractions ($mg \cdot m^{-3}$) only in the Anticosti gyre and the eastern zone of the Gulf under bloom conditions (blue inverted triangles) for April 2001 (right panels).

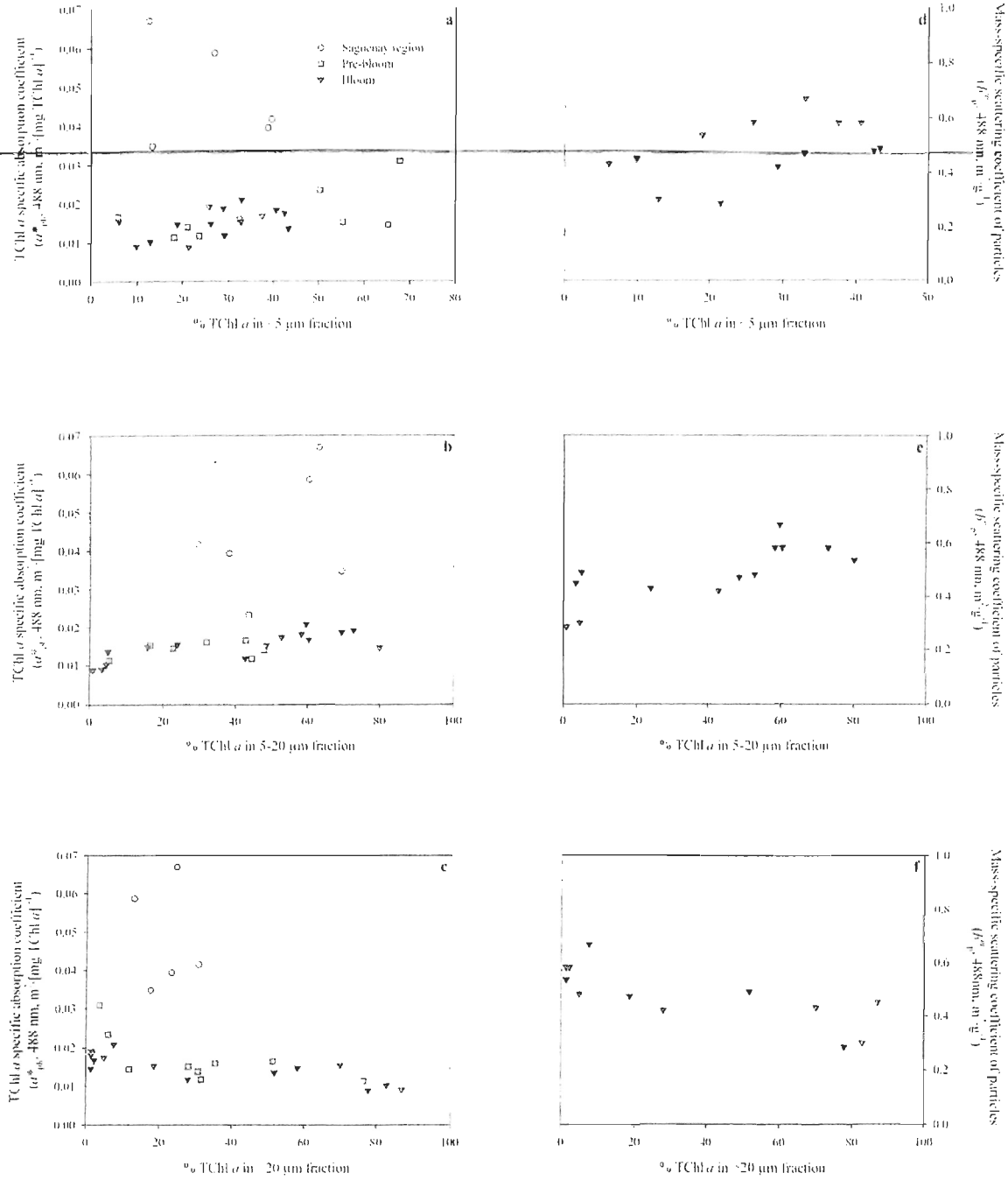
a
b
c
d
e
f
Saguenay region
Pre-bloom
Bloom
TChl a specific absorption coefficient
(a*ph 488 nm, m2 (mg TChl a)-1)
Mass-specific scattering coefficient of particles
(b*p 488 nm, m2 g-1)
% TChl a in < 5 µm fraction
% TChl a in 5-20 µm fraction
% TChl a in > 20 µm fraction

Diel variation of cell optical properties - On a number of occasions during these cruises, three to four nearby stations were sampled on the same day at different times of the day. Since temperature, salinity and nutrients showed little variation between these stations, we considered that the same water mass had been sampled and we examined the diel variations in optical properties of <20 µm phytoplankton from FCM measurements. Some general trends were observed in all these cases: for picophytoplankton, the cell size index (FSC) and cell fluorescence (FL3) increased throughout the light period, while for ultra- and nanophytoplankton, cell size showed a maximum, and cell fluorescence a minimum, at mid-day when irradiance was highest (Fig. 9). However, diel variations of cell chl-*a* content and chlorophyll-specific absorption and scattering coefficients were very heterogeneous over the whole area and for all size classes (<5 µm and nanophytoplankton), thus no diel pattern could be characterized for these variables.

Diel variability of FSC for picophytoplankton was higher under bloom conditions (up to 44%) than under pre- or post-bloom conditions. The ultraphytoplankton fraction showed a higher FSC diel variability under post-bloom situation in 2000 (Table 5). Apart from the 2000 post-bloom situation, ultraphytoplankton and nanophytoplankton displayed similar FSC diel variability for both years. Irrespective of the conditions, picophytoplankton FSC diel variability was always greater (up to 7-fold) than that of ultra- and nanophytoplankton. For pico-, ultra- and nanophytoplankton, the diel variability of FL3 was roughly the same for bloom, pre- or post-bloom conditions, except under post-bloom conditions but only for picophytoplankton (Table 5). The FL3 diel

variability generally had similar amplitudes to that of FSC, and larger size phytoplankton showed less variability than picophytoplankton.

Figure 9: Diel variations of forward-angle light scatter (FSC, bead unit) (a and c) and cell chlorophyll fluorescence (FL3, bead unit) (b and d), measured by flow cytometry, for one station group (111-112-113-114) of the Gulf in May 2000 (left panels) and April 2001 (right panels).

Forward-angle light scatter for ultra- and nanophytoplankton (FSC_{ultra} and FSC_{nano}, bead unit)
Cell chlorophyll fluorescence for ultra- and nanophytoplankton ($FL3_{ultra}$ and $FL3_{nano}$, bead unit)
Forward-angle light scatter for picophytoplankton (FSC_{pico}, bead unit)
Cell chlorophyll fluorescence for picophytoplankton ($FL3_{pico}$, bead unit)
Hours
8h13
11h29
14h22
17h16
8h42
13h22
17h29
a
b
c
d

Table 5: Amplitude of diel variations of FCM cell parameters for pico-, ultra- and nanophytoplankton (calculated as follows: (%) = (|Max – Min| / Min) × 100) in 2000 and 2001, in the Upper Estuary and under pre-bloom, bloom and post-bloom situations. The numbers in brackets correspond to standard deviations. The II, III, IV and V represent the Lower Estuary, the Gaspé current system, the Anticosti gyre and the eastern zone of the Gulf, respectively.

	2000			2001		
	Upper Estuary	II + III (bloom)	IV + V (post-bloom)	Upper Estuary	II + III (pre-bloom)	IV + V (bloom)
Amplitude of diel variation						
FSC_{pico} (%)	27	48 (26)	17 (5)	15	14 (12)	21 (9)
$FL3_{pico}$ (%)	12	10 (6)	21 (10)	7	20 (9)	15 (9)
FSC_{ultra} (%)	2	4 (3)	12 (5)	7	9 (6)	8 (3)
$FL3_{ultra}$ (%)	5	8 (4)	8 (2)	9	8 (5)	10 (7)
FSC_{nano} (%)	3	6 (3)	5 (4)	7	7 (3)	7 (3)
$FL3_{nano}$ (%)	/	5 (2)	4 (3)	4	6 (3)	5 (2)

DISCUSSION

Oceanographic processes in the St. Lawrence system - Variability in phytoplankton biomass (TChl *a*) can be ascribed to the influence of specific hydrographic features in the Upper and Lower Estuary and the Gulf of St. Lawrence (Therriault and Levasseur 1986, Therriault et al. 1990, De Lafontaine et al. 1991). The low <20 µm phytoplankton abundances and TChl *a* concentrations of the Upper Estuary are well-known features of this region, resulting from high inorganic sediment and dissolved organic matter concentrations, and to the strong currents rapidly flushing particles downstream.

The Anticosti gyre and the Gaspé current harbour two distinct pelagic ecosystems explaining the different location of high TChl *a* concentrations in the western part of the Gulf, between May 2000 and April 2001. The biological and chemical properties of the Gaspé current resemble those of the Lower Estuary whereas those found in the Anticosti gyre are more typical of the conditions prevailing over the Gulf (Levasseur et al. 1992).

The phytoplankton spring bloom typically takes place earlier in the oceanic zone of the Gulf as a result of a decreased exchange between the deeper layer and the surface during the high freshwater runoff period (Levasseur et al. 1984, Therriault and Levasseur 1985, 1986, Zakardjian et al. 2000). Indeed, the spring decrease in surface nutrients

occurred earlier in the Anticosti gyre (April) than in the Gaspé current (May), consistent with the earlier bloom in the gyre.

Variability in abundance and cell parameters of <20 µm phytoplankton - The abundance of small-sized phytoplankton was generally higher in the Gulf than in the Estuary, perhaps as a result of the more stable water column conditions in the Gulf (Levasseur et al. 1984). The concentration of <20 µm phytoplankton was low during the algal blooms, compared to the pre- or post-bloom situations, and it was lower in May 2000 than in April 2001, reflecting the preferential spatial distribution of this group in the Gulf. The concentration of the three size classes of <20 µm phytoplankton appeared as a constant background in the Gulf, indicating that growth and loss processes could be balanced over a large temporal scale (Bouman et al. 2003). Nutrient regeneration, which is important in the Gulf (Rivkin et al. 1996), probably helps to maintain the abundance of small-sized phytoplankton in this region.

In 2000, high TChl *a* values were associated with nutrient poor waters, suggesting that nutrients had already been consumed and phytoplankton reached the end of the bloom at time of sampling. The overall strong correlation between <20 µm phytoplankton abundance and Chl *b* concentration ($r=0.587$, $p<0.01$) suggests that green algae were important in that size fraction (Roy et al. in press). Furthermore, under post-bloom conditions, picophytoplankton dominated the <20 µm phytoplankton abundance and was

the only size fraction correlated with Chl *b* concentration ($r=0.748$, $p<0.01$), likely resulting from the presence of small green algae species.

On a large spatial scale, the distribution of optical cell parameters derived from FCM was related to the salinity field. The salinity was negatively correlated with FL3 and FSC of pico- and ultraphytoplankton ($p<0.01$), implying that cells that scatter and absorb more were distributed in the Estuary and the western part of the Gulf, while cells with lower FL3 and FSC values were in the oceanic part of the Gulf. Part of the variation in optical cell parameters was also linked to the surface irradiance for all the <20 µm phytoplankton size classes, suggesting the influence of diel variations on phytoplankton cell optical properties (Stramski and Mobley 1997, DuRand and Olson 1998, DuRand et al. 2000, Mas et al. 2008).

Changes within the phytoplankton pigment pool in surface waters appear to be related to shifts in community structure. The TChl *c*/Tpig (mostly determined by the Chl c_{1+2}/Tpig ratio) and PSC/Tpig (mostly determined by the Fuco/Tpig ratio) ratios were higher under bloom conditions for both years (Table 3), indicating that diatoms increased the proportion of chlorophyll *c* and photosynthetic carotenoids to optimize their light-harvesting capability. Moreover, higher PPC/Tpig ratios were characteristic of regions mainly dominated by <5 µm phytoplankton, consistent with the usually high contents of photoprotective carotenoids of small-sized phytoplankton in low nitrate environments (Barlow et al. 2004). Furthermore, downwelling irradiance below the water surface was

higher in May, suggesting that photoacclimation was greater in May 2000 than in April 2001, as indicated by the higher PPC/TPig ratio in May in the Gulf region, which is consistent with Roy et al. observations (in press).

Variability in optical properties distribution - The particles contribution to a_{tot} was higher in the bloom regions for both years, following TChl *a* concentrations. Moreover, detritus contribution to a_p decreased from the Upper Estuary toward the Gulf, as the SPM concentrations. The same trend was observed for the contribution of CDOM to a_{tot}; however this contribution was greater in May 2000 than in April 2001, this is likely due to the spring run-off which usually occurs at the beginning of May (Koutitonsky and Bugden 1991).

Among the <20 µm phytoplankton, nanophytoplankton contributed more to a_{ph} than pico- and ultraphytoplankton outside bloom periods, owing to their high chlorophyll content compared to the smaller size classes. The 2000 bloom was dominated by the nanoplankton diatom *S. costatum*, although the contribution of nanophytoplankton to a_{ph} was only about 20%. However this species can form chains (Bérard-Therriault et al. 1999), so most of *S. costatum* a_{ph} contribution could have been taken into account in the microphytoplankton size fraction. Cells in chains were not measured directly by the FCM, though they could be broken and counted by the FCM.

The relationships between a_{ph} and TChl *a* showed differences between bloom and pre- or post-bloom conditions, which were more likely due to changes in the dominant taxa sizes. Absorption coefficient under bloom conditions, dominated by large cells (i.e. diatoms) with a greater packaging, was smaller than under the other conditions with a high proportion of small cells for a given TChl *a* concentration. The relationships between a^*_{ph} and the size class contribution to TChl *a* concentration (Fig. 8) highlighted the increase of a^*_{ph} when the <20 µm phytoplankton contribution increased. This trend likely result from a reduced package effect for small cells compared to large cells (Roy et al. in press), as. high packaging is well known in large diatoms (Bricaud et al. 1995, Babin et al. 1996, Stuart et al. 1998). This confirms the influence of the size structure of phytoplankton community in determining a^*_{ph} variations, which has been shown to be the main factor controlling the packaging effect (Bricaud et al. 2004). The variability of the relationship was also due to the pigment composition since a^*_{ph} was always correlated to the PPC/TChl *a* ratio ($r = 0.418$, $p<0.01$) (Claustre et al. 1994, Fujiki and Taguchi 2001). Roy et al. (in press) showed that pigment composition contributed only to 6-13% of the a^*_{ph} variation. However, as the carotenoid pigments pool was roughly constant and the contributions of the various pigments might follow inverse trends (e.g., Chl *b* and Chl *c*, photosynthetic and nonphotosynthetic carotenoids) and partially compensate one another (Bricaud et al. 2004), the actual impact on absorption was finally reduced.

The absorption ratios showed noticeable regional differences (Table 4), which could be mainly explained by the species composition. The pigment composition of

flagellates favors high absorption in the blue region relative to the red (Babin et al. 1996, Allali et al. 1997, Lohrenz et al. 2003). Flagellates dominated (>50%) in the Upper Estuary and outside of the bloom periods, and were related to high $a_{ph}(440)/a_{ph}(675)$ ratios, through their high PPC (absorption from 400 to 530 nm, with main maxima around 460-490 nm) and accessory chlorophylls (Chl *b* and Chl c_3). Compared to pre- and post-bloom conditions, the dominance of diatoms (>70%), during the blooms, resulted in high Fuco/Tpig ratios (fucoxanthin absorbs in the 450 to 560 nm domain), and thus in low $a_{ph}(440)/a_{ph}(555)$ ratios, as well as low $a_{ph}(488)/a_{ph}(555)$ ratios but only in May 2000 (Arrigo et al. 1998, Stuart et al. 1998, Cota et al. 2003). Contrary to May 2000, the values of the $a_{ph}(488)/a_{ph}$ (555) ratios were closer in April 2001 when the bloom period was compared with pre-bloom. During the 2001 spring bloom, higher $a_{ph}(488)/a_{ph}(555)$ ratios may be attributed to an increased contribution of prymnesiophytes (Arrigo et al. 1998, Stuart et al. 2000, Mas et al. 2008).

In the Saguenay fjord region, the contribution of <20 µm phytoplankton to b_{tot} was very small, because most of the scattering was due to mineral, particulate organic matter and detritus of terrestrial origin. This is consistent with the b_{tot} decrease toward the Gulf as a result of particles dilution, thus the contribution of phytoplankton to b_{tot} in the Gulf was more important. In the Estuary, under pre-bloom conditions (April 2001), the <20 µm phytoplankton contribution to b_{tot} was higher than during the bloom (May 2000). Factors responsible for this difference could include the large quantity of mineral and terrigenous particles, due to the higher freshwater runoff in May, but also the presence of detritus and bacteria associated with the large cells during the bloom, which can

significantly contribute to b_{tot}. Maximum <20 µm phytoplankton contribution to b_{tot} reached 35% in the Gaspé current under pre-bloom conditions. This is lower than the contribution of 45-69% of eukaryote phytoplankton measured over the New England continental shelf (Green and Sosik 2004), most likely as a result of higher suspended material in our system. Even during the bloom, the <20 µm phytoplankton contribution to b reached only 30% in the Anticosti gyre, which is less influenced by continental inputs than the Estuary. However, mineral particles, which represented >50% of suspended particulate matter (Table 2), were likely major contributors to b_{tot} along with bacteria and organic detritus associated with the bloom. Under post-bloom conditions in the same region, the <20 µm phytoplankton contribution to b_{tot} was only about 10%. This decrease could be the result of the presence, after the bloom, of high amount of cell detritus, which scatter more than whole cells (Aas 1996).

The relationship between b_p^m and the size class contribution to TChl *a* concentration (Fig. 8) is strongly influenced by size, refraction index and absorption (Babin et al. 2003). The size affects strongly the scattering efficiency, a 3.5 µm flagellate is 4.3 times more efficient in scattering than a 15 µm diatom (assuming that n = 1.05), although other factors such as the chlorophyll content can play a major role (Claustre et al. 2002). When large absorbing cells were abundant, as during the diatom blooms, b_p^m was lower (Babin et al. 2003), as supported by the inverse relationship between b_p^m and the contribution of >20 µm phytoplankton contribution to TChl *a* (Figure 8). The variability of the relationships between b_p^m and the size class contribution was more

likely due to the size distribution of particles and to the composition of the particle assemblage, i.e. percentage of organic to inorganic matter (Babin et al. 2003).

Diel variations - On a daily scale, phytoplankton abundances were highly variable and did not show any diel pattern, as observed in other studies on phytoplankton diel variations (Vaulot and Marie 1999, Jacquet et al. 2002). Short-time scale variability of phytoplankton abundance in the open ocean has been attributed to temporary imbalances between growth and loss processes (Vaulot and Marie 1999). For picophytoplanktonic cells, growth and division were probably the most important factors of diel variability in cell abundance (Waterbury et al. 1986, Vaulot and Marie 1999). Strong diel patterns of picophytoplankton cell parameters, measured by FCM, were observed, and were generally homogeneous across the whole area (Table 5). The picophytoplankton size class was constituted by one single population, and this could explain the strength of the diel patterns. Maxima and minima of FSC and chlorophyll fluorescence (FL3) values were recorded around dusk and dawn respectively, as previously observed in oceanic waters (Durand and Olson 1996, Vaulot and Marie 1999). The FSC increase during the light period would be consistent with the accumulation of carbon through photosynthesis (Stramski et al. 1995, Durand and Olson 1998), whereas the FL3 increase was likely a consequence of daytime chl-*a* synthesis (Stramski and Reynolds 1993, Stramski et al. 1995, Sciandra et al. 1997). The clear diel pattern of FSC and FL3 suggests that the cell division took place at night. The cell cycle of many phytoplanktonic organisms is known to be tightly phased to the day-night cycle (Chisholm 1981) and picophytoplankton makes no exception, as shown either in culture (DuRand et al. 2002) or in the ocean

(DuRand and Olson 1996, Vaulot et al. 1995). Our study confirms the strong synchronization of picophytoplankton cell division to the day-night cycle.

Picophytoplankton FSC diel patterns were more variable under bloom situations. Cell division can be affected by a variety of factors, e.g. light stress (Vaulot et al. 1995) or nutrient depletion (Vaulot et al. 1996), which slows down the cell division cycle, thereby influencing the FSC diel pattern. Under bloom situations, the highly variable nutrient concentrations and light conditions (i.e. attenuation coefficient K_d) in 2000, as well as the nutrient depletion in 2001, might be responsible for the variability in the picophytoplankton diel patterns.

Contrary to the picophytoplankton, the FSC and FL3 diel variations for the ultra- and nanophytoplankton did not reflect any cell division pattern. Several populations belonged to these size classes, so differences in cell division phasing of each population to the daily light cycle may not result in a clear 24h periodicity (Jacquet et al. 2002). The observed diel changes in ultra- and nanophytoplankton cell parameters were likely caused by photoacclimation processes in response to daily irradiance fluctuation (Vaulot and Marie 1999), such as phytoplankton swelling (Ackleson et al. 1990, Ackleson et al. 1993), chloroplast configuration (Kiefer 1973) and changes in cellular pigment content and composition (Falkowski 1980, 1984a). Phytoplankton swelling is accompanied by a change of cell size and refraction index, which affect diel patterns in cell scattering (Ackleson et al. 1990, Ackleson et al. 1993). The ultra- and nanophytoplankon cells were

larger and scattered more at midday, under high light levels, as a result of cell swelling (Ackleson et al. 1990). The clear midday FL3 decrease could be due either to non-photochemical quenching or to PSII reaction centers photo-damage due to high irradiance (Vaulot and Marie 1999). When irradiance decreased after midday, quenching was obviously reversed or repair took place. A similar influence of daily irradiance fluctuation on chlorophyll fluorescence quenching or phytoplankton photoacclimation has already been observed in the field (Stramska and Dickey 1992, Sosik et al. 1998) and in cultures (Stramski and Morel 1990). For picophytoplankton, no evidence of midday FL3 depression due to photoquenching was observed, as in previous studies (Jacquet et al. 1998, Vaulot and Marie 1999), suggesting that picophytoplankton are less sensitive to light stress in surface waters (Jacquet et al. 2002).

Furthermore, the ultra- and nanophytoplankton diel pattern was less variable than that of picophytoplankton, whatever the conditions. The smaller variability was probably due to the different photoacclimation processes of the larger cells. The diel variability was even lower for nanophytoplankton, which was mostly composed of small diatom species. Diatoms can generally tolerate higher light environments before inducing photo-protective mechanisms, compared to flagellates (Richardson et al. 1983, Demers et al. 1991). The diel variations of FSC and FL3 for ultra- and nanophytoplankton, as well as the variability between days, seemed to be mainly driven by the species composition and photoacclimation strategies.

CONCLUSIONS

The small-sized phytoplankton cells were always numerically dominated by picophytoplankton and these were most abundant in the Gulf. The contribution of <20 µm phytoplankton to phytoplankton absorption was higher outside of bloom periods and among the <20 µm phytoplankton, nanophytoplankton was the major contributor to phytoplankton absorption. In addition, the highest contributions of <20 µm phytoplankton to total scattering were observed in the Gulf. However, the contribution of <20 µm phytoplankton to total optical properties (particularly total scattering) remained generally weak, due to the important role of CDOM and non-phytoplanktonic particles (particularly detritus) on optical properties of St. Lawrence waters.

Differences in bio-optical characteristics (particularly absorption) between bloom and pre- or post-bloom conditions were related to taxonomic composition, especially changes in contribution of small cells relative to total phytoplankton abundance. Packaging, which is size-related, has been shown to be the dominant factor responsible for the variation of phytoplankton absorption in the St. Lawrence region (Roy et al. in press). Cell size may thus be responsible for some of the discrepancies in the performance of ocean-color algorithms and impact the retrieval of chl-*a* (Arrigo et al. 1998, Stuart et al. 1998). Our study confirms that the size structure of phytoplankton

communities should be taken into consideration in bio-optical models for chl-*a* retrieval in the St. Lawrence Estuary and Gulf.

Finally, diel variations of ultra- and nanophytoplankton were about 4-12% for scattering and absorption cross section proxies, whereas for picophytoplankton diel variations were up to 14-44% for the scattering cross-section proxy and 10-20% for the absorption cross-section proxy. However, diel patterns of phytoplankton populations are difficult to observe in whole water measurements, since each population and each cellular parameter displays its own behavior, partly modulated by cell growth, light availability and nutrients level. The influence of diel patterns may therefore be more relevant in the case of mono-specific blooms, or for some fraction of the phytoplankton community (as for picophytoplankton here).

CONCLUSIONS

Les recherches exposées dans cette thèse ont été réalisées dans le cadre du programme de recherche de validation des données SeaWiFS ayant pour objectif d'élaborer des algorithmes qui permettront d'estimer les concentrations de chl-*a* dans les eaux de l'estuaire et du golfe du Saint-Laurent à partir d'images satellitaires. L'estimation des variables océanographiques (concentration de chl-*a* ou la production primaire) à partir des signaux satellitaires est basée sur la connaissance des propriétés optiques inhérentes (IOPs) telles que l'absorption et la diffusion. Les variations des IOPs sont reliées aux changements de concentration et de composition des assemblages phytoplanctoniques, ainsi qu'à leurs propriétés optiques. De plus, les fluctuations environnementales (couverture nuageuse, mélange vertical, intensité lumineuse incidente,...) peuvent induire des variations rapides de l'abondance et des paramètres cellulaires, physiologiques et optiques, des cellules phytoplanctoniques, et par conséquent des variations des IOPs.

Dans ce contexte, les travaux de cette thèse ont porté sur le rôle du phytoplancton sur les variations des IOPs des eaux de surface de l'estuaire et du golfe du Saint-Laurent. Cette étude s'est attardée plus particulièrement sur les cellules phytoplanctoniques <20 µm, puisque cette classe de taille contribue significativement à l'absorption du phytoplancton et de manière importante à la diffusion. Par conséquent, différentes voies ont été explorées telles (1) la variabilité journalière des IOPs du phytoplancton associée à l'augmentation de lumière en milieu contrôlé, (2) les variations des IOPs dues aux phases de croissance du phytoplancton ainsi que l'interférence liée à la présence de bactéries et

de détritus en milieu contrôlé et (3) la distribution spatio-temporelle de l'abondance et des propriétés cellulaires des cellules phytoplanctoniques <20 µm, ainsi que leur contribution aux IOPs des eaux de surface de l'estuaire et du golfe du Saint-Laurent.

Dans le Chapitre I, les variations journalières des propriétés optiques cellulaires ont été examinées pour deux espèces nanophytoplanctoniques, une haptophyte (*Imantonia rotunda*) et une diatomée (*Thalassiosira pseudonana*) cultivées sous un cycle jour-nuit, puis transférées à de plus fortes intensités lumineuses avec maintien du cycle jour-nuit. Ces deux espèces du nanophytoplancton sont cosmopolites et fréquemment présentes dans les eaux de l'estuaire et du golfe du Saint-Laurent. Les différents patrons journaliers observés entre les deux espèces pour les caractéristiques cellulaires et optiques, sont reliés à une meilleure synchronisation de la division cellulaire de l'haptophyte, comparativement à la diatomée. Les variations journalières des propriétés cellulaires et optiques rapportées dans ce travail peuvent avoir des implications notables pour les observations de terrain. Au cours d'une journée, l'amplitude des variations journalières est supérieure à 100% pour les pigments photoprotecteurs, le volume cellulaire moyen (haptophyte) et la concentration de pigments photosynthétiques (diatomée). De plus, l'amplitude de ces variations est plus importante lorsque les variations journalières sont combinées à une augmentation d'intensité lumineuse, tel qu'il peut se produire dans le milieu naturel lors d'épisodes de mélange vertical. L'augmentation de l'amplitude des variations est également plus élevée pour les pigments que pour les propriétés optiques. *I. rotunda* et *T. pseudonana* présentent différents mécanismes de photoacclimatation en réponse à l'augmentation de lumière : (1) changement de la concentration et de la

composition pigmentaire (pigments photosynthétiques et photoprotecteurs), ce processus est commun aux deux espèces, et (2) augmentation du contenu cellulaire en eau, ce qui se produit principalement pour les diatomées, donc ici seulement pour *T. pseudonana*. Par conséquent, l'augmentation de lumière induit des variations de volume cellulaire moyen pour la diatomée, alors que l'haptophyte conserve les variations de volume cellulaire moyen associées au cycle de division cellulaire. Les propriétés optiques reliées à la taille cellulaire sont donc plus affectées pour la diatomée lorsque les changements d'intensité lumineuse sont combinés au cycle journalier. Le cycle jour-nuit associé à une augmentation d'intensité lumineuse entraîne des variations journalières d'amplitude variant de 27 à 53% pour l'absorption spécifique à la chl-*a*, jusqu'à 176% pour la diffusion spécifique à la chl-*a* et de plus de 200% pour la pigmentation (i.e. contenu cellulaire en pigments accessoires photoprotecteurs et photosynthétiques pour l'haptophyte et pour la diatomée, respectivement). De plus, les relations entre ratios d'absorption et ratios pigmentaires sont nettement affectées par les réponses à l'augmentation de lumière, et ce particulièrement pour la diatomée. Ce type de variation à court terme affecte également le spectre d'absorption et pourrait contribuer à l'erreur d'estimation de la concentration de chl-*a*. D'autre part, l'amplitude des variations journalières intraspécifiques de la diffusion spécifique à la chl-*a* (>70%) est beaucoup plus faible qu'entre espèces (jusqu'à 550%). Les variations de la diffusion spécifique à la chl-*a*, en milieu naturel, seront donc principalement déterminées par les changements de la composition des communautés phytoplanctoniques. Néanmoins, les variations journalières de la diffusion spécifique à la chl-*a* auront une influence significative lors de floraisons dominées par une seule espèce. Cette étude souligne l'importance des

variations morphologiques et physiologiques sur la variabilité des IOPs, la nécessité d'étudier la structure des communautés lors des campagnes bio-optiques, l'influence du choix de l'heure d'échantillonnage, ainsi que le besoin d'informations sur le mélange vertical et l'état de photoacclimatation du phytoplancton, afin d'interpréter la variabilité naturelle des propriétés d'absorption et de diffusion.

Dans le Chapitre II, l'effet des phases de croissance sur les propriétés optiques cellulaires et totales a été étudié pour quatre espèces (*Thalassiossira pseudonana*, *Alexandrium tamarense*, *Imantonia rotunda* et *Nannochloropsis* sp.). Le type de culture utilisé permet de simuler des conditions pouvant représenter des floraisons phytoplanctoniques, mais aussi d'évaluer l'effet de la présence de bactéries et de détritus sur les propriétés optiques totales. Les variations de concentration pigmentaire induites par la succession des stades de croissance sont différentes pour chaque espèce. Ces réponses taxospécifiques préviennent donc toute généralisation sur les changements pigmentaires dus aux phases de croissance. D'une manière générale, la phase de croissance ne semble pas avoir d'effet sur les relations entre la concentration de chl-*a* et l'absorption du phytoplancton à 440 nm. La différence entre les relations pour chaque espèce est affectée principalement à la taille des cellules. Par contre, la forme du spectre de l'absorption spécifique à la chl-*a* est affectée par les phases de croissance. Ces distorsions du spectre modifient les ratios d'absorption typiquement utilisés pour estimer les concentrations de chl-*a* à partir de données satellitaires. En outre, les relations entre ratios d'absorption et ratios pigmentaires sont significatives, pour toutes les espèces, exceptées en phase de déclin. La phase de croissance influence également la diffusion du

phytoplancton <20 µm, et par conséquent la relation entre diffusion du phytoplancton <20 µm et concentration de chl-*a*, ainsi que la forme du spectre normalisé de diffusion. En effet, aux courtes longueurs d'ondes, le coefficient de diffusion est plus fort pour les cellules en phase de latence ou de déclin. De plus, la présence de bactéries ou de détritus déforme le spectre de diffusion normalisé, à travers la distribution de taille et l'indice de réfraction. Les bactéries et les détritus de petite taille augmentent la diffusion aux courtes longueurs d'ondes, et augmentent l'erreur de la relation entre la diffusion de la matière particulaire et la concentration de chl-*a*, particulièrement en phase de déclin. En outre, la présence de détritus de grande taille, liés à l'agrégation, contribue à la diminution de la diffusion aux courtes longueurs d'ondes.

Les propriétés optiques totales et cellulaires du phytoplancton varient donc en fonction de l'âge des cultures et de l'espèce, à travers des changements physiologiques. Ces variations des propriétés optiques dues aux phases de croissance modifient la couleur des océans, particulièrement pendant le développement de floraisons, et contribuent à l'erreur d'estimation de la concentration de chl-*a* à partir de données satellitaires. De plus, la présence de bactéries affecte les IOPs totales soit par effet direct sur la diffusion, en changeant la distribution de taille des particules, soit indirectement, en prolongeant la période de floraison en facilitant l'accès aux nutriments par reminéralisation de la matière organique. Les détritus modifient également la distribution de taille des particules et peuvent induire des variations des IOPs totales plus importantes que les bactéries. L'association des mesures de la cytométrie en flux et de la sonde ac-9 est donc intéressante et appropriée pour déterminer les changements d'assemblages planctoniques

et de phases de croissance, qui se succèdent généralement lors des périodes de floraison phytoplanctonique. Finalement, cette étude illustre aussi la divergence entre les mesures des IOPs totales et des IOPs dérivées des mesures cellulaires, principalement pour la diffusion, puisque les bactéries et les détritus sont des contributeurs majeurs dans les océans. L'évaluation du rôle de ces particules est donc cruciale afin d'étudier la variabilité des IOPs, et plus particulièrement pendant les floraisons phytoplanctoniques.

Des campagnes d'échantillonnage dans l'estuaire et le golfe du Saint-Laurent en mai 2000 et en avril 2001 ont permis d'étudier les IOPs du phytoplancton en milieu naturel dans le chapitre III. Au printemps, la période de floraison est précoce dans le golfe (avril) et plus tardive dans la zone de l'estuaire (mai). Pour les deux années, la floraison printanière était dominée par des diatomées, mais les espèces dominantes différaient. Dans le golfe, les cellules <20 µm sont généralement les plus abondantes. De plus, l'abondance des cellules <20 µm est typiquement dominée par le picophytoplancton (<2 µm). Les cellules <20 µm contribuent de manière plus importante à l'absorption du phytoplancton hors des périodes de floraison. Cependant, ce sont les cellules du nanophytoplancton (5-20 µm) qui sont les plus responsables de l'absorption du phytoplancton, en raison de leur contenu cellulaire en pigment plus important. Les variations des ratios d'absorption sont le reflet de l'influence de la composition spécifique sur les ratios pigmentaires. De plus, la contribution des pigments photoprotecteurs varie aussi selon les saisons et augmente en réponse à l'augmentation de lumière. Comme pour l'absorption totale, la contribution des cellules <20 µm à la diffusion totale est faible, bien que plus importante dans le golfe que dans l'estuaire. Les

relations entre l'absorption spécifique à la chl-*a* et la contribution des classes de taille à la chl-*a* ont permis de mettre en évidence une augmentation de l'absorption spécifique à la chl-*a* lorsque la contribution du phytoplancton <20 µm augmente. Cette augmentation est attribuable à une réduction du « package effect » pour les cellules <20 µm comparativement aux cellules microphytoplanctoniques. Cette étude a également permis d'étudier les variations journalières des propriétés optiques des cellules phytoplanctoniques. Les variations des paramètres optiques cellulaires du picophytoplancton, déterminés par FCM, mettent en évidence une périodicité reliée à la synchronisation de la division cellulaire. Ce type de périodicité est absent pour l'ultra- et le nanophytoplancton en raison de la présence de plusieurs populations, chacune avec son propre cycle cellulaire. Par contre, les variations journalières des paramètres optiques cellulaires reflètent les mécanismes de photoacclimatation.

Les variations journalières des paramètres optiques cellulaires sont importantes, seulement pour le picophytoplancton. Pourtant, les variations journalières n'affectent pas les relations entre les IOPs et les pigments. A grande échelle, les patrons journaliers sont complexes en raison des réponses différentes de chaque population phytoplanctonique. D'autre part, les différences des propriétés bio-optiques, particulièrement d'absorption, entre les conditions de floraison ou de « pre-bloom » et « post-bloom », sont dues principalement aux variations de la contribution des cellules <20 µm au phytoplancton. Le « package effect » serait le facteur impliquant le plus de variations des propriétés d'absorption du phytoplancton dans le Saint-Laurent, et cet effet de la distribution de taille serait, avec la présence de CDOM et de la matière particulaire en suspension non-

algale, une des sources d'erreur d'estimation des concentrations de chl-*a* à partir de données satellitaires. Cette étude confirme que la structure de taille des communautés phytoplanctoniques est un point crucial à prendre en compte dans les modèles bio-optiques appliqués au Saint-Laurent ; et que l'effet du « package effect » devrait être quantifié relativement à l'effet des autres composantes bio-optiques (CDOM et matière particulaire en suspension non-algale).

L'ensemble des travaux de cette thèse nous amène à plusieurs constats sur le plan expérimental ainsi qu'en milieu naturel. A partir des expériences en laboratoire, nous avons mis en évidence l'importance des mécanismes de photoacclimatation et de la synchronisation du cycle cellulaire du phytoplancton sur les variations journalières à court terme des propriétés optiques cellulaires, ainsi que de l'état physiologique relié au stade de croissance sur ces variations à long terme. De plus, la taxonomie et la taille des cellules phytoplanctoniques influencent non seulement les propriétés optiques cellulaires, mais aussi les IOPs. En milieu naturel, les variations journalières des IOPs n'ont pu être caractérisées, étant donné que les variations interspécifiques sont nettement plus élevées que les variations journalières pour chaque espèce. De plus, de nombreux facteurs induisent des réponses physiologiques différentes pour chaque population phytoplanctonique, et modifient subséquemment les IOPs (mélange vertical, couverture nuageuse, disponibilité en nutriments...) ; les particules non-phytoplanctoniques et le CDOM contribuent aussi de manière importante aux IOPs. De ce fait, de nombreuses sources de variabilités des IOPs, comme les variations journalières, ne sont pas détectées

dans les régions fortement dynamiques et influencées par les apports continentaux, comme l'estuaire et le golfe du Saint-Laurent.

A la lumière de ces travaux de thèse, il apparaît difficile d'extraire les variations des IOPs de type journalier ou liées à la physiologie du phytoplancton dans des milieux très dynamiques. Il conviendrait donc de s'intéresser dans un premier temps à des zones plus océaniques caractérisées par des régimes hydrologiques plus stables et des eaux plus pauvre en matière particulaire en suspension, comme la zone océanique du golfe du Saint-Laurent. De plus, des échantillonnages en période estivale et automnale permettraient de déterminer l'évolution au cours des saisons de la contribution des petites cellules phytoplanctoniques sur les propriétés optiques des eaux du Saint-Laurent.

La synchronisation de certaines populations naturelles s'étend en profondeur dans la colonne d'eau mais avec un décalage dans le temps (Vaulot et al. 1995) et les processus de photoacclimatation sont également présents en profondeur. Dans un second temps, il serait donc intéressant d'évaluer le maintien des variations journalières des propriétés optiques cellulaires et des IOPs en profondeur dans la zone euphotique, et de confronter les temps de réponse du phytoplancton à l'intensité du mélange vertical.

Afin d'évaluer les variations journalières des propriétés optiques cellulaires du phytoplancton et des IOPs, il conviendrait d'optimiser les plans d'échantillonnage. Une fréquence d'échantillonnage élevée, par exemple toutes les deux heures, comme pour les

expériences du premier chapitre, est primordiale ainsi que le suivi de la même masse d'eau. Pour le suivi d'une période de floraison, un suivi lagrangien, utilisant une bouée dérivant au sein d'une même masse d'eau, serait pertinent.

Tout l'éventail des mesures bio-optiques n'a pu être pris en compte lors de cette thèse. La mesure du carbone, de l'indice de réfraction et de la distribution de taille est très importante pour les études bio-optiques, et notamment pour l'étude des particules non-algales, dont les propriétés optiques sont peu connues. Ces mesures complémentaires permettent de décomposer l'influence du phytoplancton, des bactéries et des détritus sur les IOPs. Il existe très peu d'études traitant de l'indice de réfraction des détritus alors que de nombreux travaux ont été menés pour évaluer l'indice de réfraction du matériel vivant, qu'il soit autotrophe ou hétérotrophe. Les assemblages particulaires en océan ouvert sont composés de cellules vivantes et de leurs produits de dégradation. La possibilité de discriminer *in situ* les proportions de matériel vivant et détritique de tels assemblages met en exergue la nécessité de conduire des recherches plus approfondies sur l'indice de réfraction du matériel détritique par l'expérimentation en laboratoire.

La cytométrie en flux, utilisée seule, montre clairement ses limites pour l'identification des populations procaryotes et eucaryotes. Pour accéder à la diversité des communautés phytoplanctoniques (<20 µm), le recours aux techniques de biologie moléculaire apporterait une solution, avec l'utilisation de sondes nucléotidiques fluorescentes permettant la reconnaissance de groupes voire de taxons

phytoplanctoniques (par exemple avec la méthode FISH). Le couplage de ce type de techniques avec la cytométrie en flux serait particulièrement intéressant pour i) étudier la distribution et l'importance relative des différents groupes phytoplanctoniques, et ii) obtenir les caractéristiques cellulaires et optiques de chacun de ces groupes. Les techniques d'immunocytochimie, utilisant des anticorps ciblant des protéines spécifiques à la surface des cellules phytoplanctoniques, pourrait constituer un autre moyen de discriminer les différents groupes (Campbell et Iturriaga 1988, Campbell et al. 1994). Couplée avec la cytométrie en flux, l'immunofluorescence faciliterait la détection de certains organismes. L'identification des populations déjà détectées par cytométrie en flux avec des protocoles d'étude des propriétés optiques, ainsi que l'appartenance de ces populations à différents groupes phytoplanctoniques, permettrait de suivre les variations des propriétés optiques (dues au cycle journalier, à la photoacclimation ou encore aux états physiologiques successifs (floraison)) pour chaque population et pas seulement pour des classes de taille, et de relier ces variations à des groupes spécifiques.

Le bilan de la contribution des divers composants à l'atténuation, l'absorption et la diffusion des eaux du Saint-Laurent met en évidence le rôle prédominant du CDOM et des particules non-algales. La contribution élevée de l'absorption par le CDOM et de la diffusion par les détritus est particulièrement critique pour les estimations de concentration en chl-*a* à partir des capteurs de couleur de l'océan. Cependant, le compartiment phytoplanctonique est nettement plus "réactif" que le compartiment "non vivant" (détritique et dissous). Si, au cours de cette étude, et particulièrement sur les cultures, nous avons pu extraire l'effet des variations journalières et des phases de

croissance sur les IOPs et les relations bio-optiques, il reste toutefois à établir une quantification de cet effet sur les variations des IOPs en milieu naturel. Les conditions nécessaires à ce type d'estimation ont été difficiles à réunir sur le terrain. Aussi, il semble nécessaire de poursuivre cette étude afin de valider ou non l'hypothèse de l'effet des variations journalières et des phases de croissance sur les IOPs et les relations bio-optiques dans les eaux du Saint-Laurent. L'erreur systématique d'estimation des concentrations en chl-*a*, par les capteurs de couleur de l'océan, a été imputée à la présence dans la couche de surface de substances (CDOM et matériel non-algal) qui rendent les algorithmes bio-optiques standards inadaptés aux estimations de faibles concentrations en chlorophylle. Bien que l'algorithme appliqué au Saint-Laurent puisse corriger ce biais, d'autres facteurs de variation des IOPs, tels que les variations journalières et liées à la phase de croissance, pourraient avoir des conséquences sur les estimations de la biomasse phytoplanctonique à l'échelle du Saint-Laurent. Ce biais n'est probablement pas limité à la région du Saint-Laurent et pourrait affecter les estimations de la biomasse phytoplanctonique à l'échelle mondiale, particulièrement dans les zones côtières.

RÉFÉRENCES

Aas E (1996) Refractive index of phytoplankton derived from its metabolite composition. J Plankton Res 18:2223-2249

Ackleson SG, Spinrad RW (1988) Size and refractive index of individual marine particulates: a flow cytometric approach. Appl Opt 27:1270-1277

Ackleson SG, Cullen JJ (1991) Variability in phytoplankton light scatter: Effects of high light intensity. Signal & Noise Flow cytometry and cell sorting 4:1-2

Ackleson SG, Cullen JJ, Brown J, Lesser MP (1990) Some changes in the optical properties of marine plankton in response to high light intensity. Proc SPIE, Ocean Opt X, 1302:238-249

Ackleson SG, Cullen JJ, Brown J, Lesser MP (1993) Irradiance-induced variability in light scatter from marine phytoplankton in culture. J Plankton Res 15(7):737-759

Agawin NSR, Duarte CM, Agusti S (2000) Nutrient and temperature control of contribution of picoplankton to picoplankton biomass and production. Limnol Oceanogr 45(3):591-600

Agustí S (1991) Allometric scaling of light absorption and scattering by phytoplankton cells. Can J Fish Aquat Sci 48:763–767

Ahn Y-H (1990) Propriétés optiques des particules biologiques et minérales présentes dans l'océan; Application: inversion de la réflectance. Thèse de doctorat de l'Université Pierre et Marie Curie (France), 208 pp

Ahn Y-H, Bricaud A, Morel A (1992) Light backscattering efficiency and related properties of some phytoplankters. Deep-Sea Res 39(11/12):1835-1855

Alderkamp A-C, Nejstgaard JC, Verity PG, Zirbel MJ, Sazhin AF, van Rijssel M (2006) Dynamics in carbohydrate composition of *Phaeocystis pouchetii* colonies during spring blooms in mesocosms. J Sea Res 55:169-181

Allali KA, Bricaud A, Claustre H (1997) Spatial variations in the chlorophyll-specific absorption coefficients of phytoplankton and photosynthetically active pigments in the equatorial Pacific. J Geophys Res 102:12413-12423

Aluwihare LI, Repeta DJ, Chen RF (1997) A major biopolymeric component to dissolved organic carbon in surface sea water. Nature 387:166-169

Aluwihare LI, Repeta DJ (1999) A comparison of the chemical characteristics of oceanic DOM and extracellular DOM produced by marine algae. Mar Ecol Prog Ser 186:105-117

Amy PS, Morita RY (1983) Starvation-survival patterns of sixteen freshly isolated open-ocean bacteria. Appl Environ Microbiol 45:1109-1115

Andrews SS, Caron S, Zafiriou OC (2000) Photochemical oxygen consumption in marine waters: A major sink for colored dissolved organic matter? Limnol Oceanogr 45(2):267-277

Armbrust EV, Berges JA, Bowler C, Green BR, Martinez D, Putnam NH, Zhou S, Allen AE, Apt KE, Bechner M, Brzezinski MA, Chaal BK, Chiovitti A, Davis AK, Demarest MS, Detter JC, Glavina T, Goodstein D, Hadi MZ, Hellsten U, Hildebrand M, Jenkins BD, Jurka J, Kapitonov VV, Kröger N, Lau WWY, Lane TW, Larimer FW, Lippmeier JC, Lucas S, Medina M, Montsant A, Obornik M, Schnitzler Parker M, Palenik B, Pazour GJ, Richardson PM, Rynearson TA, Saito MA, Schwartz DZ, Thamatrakoln K, Valentin K, Vardi A, Wilkerson FP, Rokhsar

DS (2004) The Genome of Diatom *Thalassiosira pseudonana*: ecology, evolution, and metabolism. Science 306:79-86

Arrigo KR, Robinson DH, Worthen DL, Schieber B, Lizotte MP (1998) Bio-optical properties of the southwestern Ross Sea. J Geophys Res 103:21683–21695

Babin M, Morel A, Claustre H, Bricaud A, Kolber Z, Falkowski PG (1996) Nitrogen- and irradiance-dependent variations of the maximum quantum yield of carbon fixation in eutrophic, mesotrophic and oligotrophic marine systems. Deep-Sea Res I 43:1241-1272

Babin M, Morel A, Fournier-Sicre V, Fell F, Stramski D (2003) Light scattering properties of marine particles in coastal and open ocean waters as related to the particle mass concentration. Limnol Oceanogr 48(2):843-859

Babin M, Morel M, Gentili B (1996) Remote sensing of sea-surface sun-induced chlorophyll fluorescence: consequences of natural variations in the optical characteristics of phytoplankton and the quantum yield of chlorophyll-*a* fluorescence. Int J Remote Sens 17:2417-2448

Babin M, Sadoudi N, Lazzara L, Gostan J, Partensky F, Bricaud A, Veldhuis M, Morel A, Falkowski PG (1997) Photoacclimation strategy of *Prochlorococcus* sp. and consequences on large scale variations of photosynthetic parameters. Proc SPIE, Ocean Optics X, 2963:314-319

Babin M, Therriault J-C, Legendre L, Condal A (1993) Variations in the specific absorption coefficient for natural phytoplankton assemblages: Impact on estimates of primary production. Limnol Oceanogr 38(1):154-177

Babin M, Therriault J-C, Legendre L, Nieke B, Reuter R, Condal A (1995) Relationship between the maximum quantum yield of carbon fixation and the minimum quantum yield of chlorophyll *a* in vivo fluorescence in the Gulf of St. Lawrence. Limnol Oceanogr 40(5):956-968

Bader H (1970) The hyperbolic distribution of particle sizes. J Geophys Res 75:2822-2830

Baker ET, Lavelle JW (1984). The effect of particle size on the light attenuation coefficient of natural suspensions. J Geophys Res 89(C5):8197-8203

Balch WM (2000) Light scattering by viral suspensions. Limnol Oceanogr 45(2):492-498

Balch WM, Drapeau DT, Cucci TL, Vaillancourt RD, Kilpatrick KA, Fritz JJ (1999) Optical backscattering by calcifying algae: Separating the contribution of particulate inorganic and organic carbon fractions. J Geophys Res 140:1541-1558

Balch WM, Drapeau DT, Fritz JJ, Bowler BC, Nolan J (2001) Optical backscattering in the Arabian Sea - Continuous underway measurements of particulate inorganic and organic carbon. Deep-Sea Res I 48:2423–2452

Balch WM, Holligan PM, Ackleson SG, Voss KJ (1991) Biological and optical properties of mesoscale coccolithophore blooms in the Gulf of Maine. Limnol Oceanogr 36(4):629-643

Barlow RG, Aiken J, Moore GF, Holigan PM, Lavender S (2004) Pigment adaptations in surface phytoplankton along the eastern boundary of the Atlantic Ocean. Mar Ecol Prog Ser 281:13-26

Bérard-Therriault L, Poulin M, Bossé L (1999) Guide d'identification du phytoplancton marin de l'estuaire et du golfe du Saint-Laurent incluant également certains protozoaires. Presses scientifiques du CNRC, Ottawa, 387 pp

Berner T, Dubinsky A, Wyman K, Falkowski PG (1989) Photoadaptation and the "package" effect in *Dunaliella tertiolecta* (Chlorophyceae). J Phycol 25:70-78

Biddanda BA (1988) Microbial aggregation and degradation of phytoplankton-derived detritus in seawater. 2. Microbial metabolism. Mar Ecol Prog Ser 42:89-95

Bidigare RR, Morrow JH, Kiefer DA (1988) Derivative analysis of spectral absorption by phytoplankton pigments. Proc SPIE Ocean Optics IX, 925:101-108

Bidigare RR, Ondrusek ME, Morrow JH, Kiefer DA (1990) *In vivo* absorption properties of algal pigments. Proc SPIE, Ocean Optics X, 1302:290-302

Blanchot J, André J-M, Navarette C, Neveux J (1997) Picophytoplankton dynamics in the equatorial Pacific: diel cycling from flow-cytometer observations. C.R. Acas Sci 320:925-931

Bouman HA, Platt T, Satheyndranath S, Li WKW, Stuart V, Fuentes Yaco C, Maass H, Horne EPW, Ulloa O, Lutz V, Kyewalyanga M (2003) Temperature as indicator of optical properties and community structure of marine phytoplankton: implications for remote sensing. Mar Ecol Prog Ser 258:19-30

Bratbak G, Thingstad TF (1985) Phytoplankton-bacteria interactions: An apparent paradox? Analysis of a model system with both competition and commensalism. Mar Ecol Prog Ser 25:23–30

Bricaud A, Allali K, Morel A, Marie D, Veldhuis MJW, Partensky F, Vaulot D (1999) Divinyl chlorophyll *a*-specific absorption coefficients and absorption efficiency

factors for *Prochlorococcus marinus*: Kinetics of photoacclimation. Mar Ecol Prog Ser 188:21–32

Bricaud A, Babin M, Morel A, Claustre H (1995) Variability in the chlorophyll-specific absorption coefficients of natural phytoplankton: Analysis and parameterizations. J Geophys Res 100:13321-13332

Bricaud A, Bédhomme AL, Morel A (1988) Optical properties of diverse phytoplanktonic species: experimental results and theoretical interpretation. J Plankton Res 10:851-873

Bricaud A, Claustre H, Ras J, Oubelkheir K (2004) Natural variability of phytoplanktonic absorption in oceanic waters: Influence of the size structure of algal populations. J Geophys Res 109:C11010, doi:10.1029/2004JC002419

Bricaud A, Morel A (1986) Light attenuation and scattering by phytoplanktonic cells: A theoretical modeling. Appl Opt 25:571-580

Bricaud A, Morel A, Babin M, Allali K, Claustre H (1998) Variations of light absorption by suspended particles with chlorophyll *a* concentration in oceanic (Case 1) waters: Analysis and implications for bio-optical models. J Geophys Res 103:31033-31044

Bricaud A, Morel A, Prieur L (1981) Absorption by dissolved organic matter of the sea (yellow substance) in the UV and visible domains. Limnol Oceanogr 26(1):43-53

Bricaud A, Morel A, Prieur L (1983) Optical efficiency factors of some phytoplanktoners. Limnol Oceanogr 28(5):816-832

Bricaud A, Roesler CS, Zaneveld JRV (1995) In situ methods for measuring the inherent optical properties of ocean waters. Limnol Oceanogr 40(2):393-410

Bricaud A, Stramski D (1990) Spectral absorption coefficients of living phytoplankton and nonalgal biogenous matter: A comparison between the Peru upwelling area and the Sargasso Sea. Limnol Oceanogr 35(3):562-582

Brown OB, Evans RH, Brown JW, Gordon HR, Smith RC, Baker KS (1985) Phytoplankton blooming off the US East Coast: A satellite description. Science 229:163–167

Brunel P (1970) The Gaspe cod ecosystem in the Gulf of St. Lawrence. 1. Seasonal and annual trends of physical oceanographic and climatic factors from 1952 to 1962. Natur Can 97(6):749-781

Brussaard CPD, Riegman R (1998) Influence of bacteria on phytoplankton cell mortality with phosphorus or nitrogen as the algal-growth-limiting nutrient. Aquat Microb Ecol 14(3):271-280

Brussaard CPD, Riegman R, Noordeloos AAM, Cadée GC, Witte H, Kop AJ, Nieuwland G, Van Duyl FC, Bak RPM (1995) Effects of grazing, sedimentation and phytoplankton cell lysis on the structure of a coastal pelagic food web. Mar Ecol Prog Ser 123:259–271

Brussaard CPD, Thyrhaug R, Marie D, Bratbak G (1999) Flow cytometric analyses of viral infection in two marine phytoplankton species: *Micromonas pusilla* (Prasinophyceae) and *Phaeocystis pouchetii* (Prymnesiophyceae). J Phycol 35:941-948

Bruyant F, Babin M, Genty F, Prasil O, Behrenfeld MJ, Claustre H, Bricaud A, Holtzendorff J, Koblizek M, Garczareck L, Partensky F (2005) Diel variations in

the photosynthetic parameters of *Prochlorococcus* strain PCC 9511: combined effects of light and cell cycle. Limnol Oceanogr 50(3):850-863

Buiteveld H, Hakvoort JHM, Donze M (1994) The optical properties of pure water. Proc SPIE, Ocean Optics XII, 2258:174-183

Bukata RP, Jerome JH, Kondratyev KY, Pozdnyakov DV (1995) Optical properties and remote sensing of inland and coastal waters. CRC Press, Boca Raton, Fla, pp 362

Byers SC, Mills EL, Stewart PL (1978) A comparison of methods of determining organic carbon in marine sediments, with suggestions for a standard method. Hydrobiologia 58(1):43-47

Campbell L, Iturriaga R (1988) Identification of *Synechococcus* spp. in the Sargasso Sea by immunofluorescence and fluorescence excitation spectroscopy performed on individual cells. Limnol Oceanogr 33(5):1196-1201

Campbell L, Shapiro LP, Haugen E (1994) Immunocharacterization of eukaryotic ultraplankton from the Atlantic and Pacific Oceans. J Plankton Res 16(1):35-51

Carder KL, Steward RG, Harvey GR, Otner PB (1989) Marine humic and fulvic acids: Their effects on remote sensing of ocean chlorophyll. Limnol Oceanogr 34(1):68-81

Chang GC, Dickey T (1999) Partitioning in situ total spectral absorption by use of moored spectral absorption-attenuation meters. Appl Opt 38(18):3876-3887

Chisholm SW (1981) Temporal patterns of cell division in unicellular algae. Physiological basis of phytoplankton ecology. Can Bull Fish Aquat Sci 210:150-181

Chisholm SW, Costello JC (1980) Influence of environmental factors and population composition on the timing of cell division in *Thalassiosira fluviatilis* (Bacillariophyceae) grown on light/dark cycles. J Phycol 16:375–383

Chung SP, Gardner WD, Landry MR, Richardson MJ, Walsh ID (1998) Beam attenuation by microorganisms and detrital particles in the equatorial Pacific. J Geophys Res 103:12669-12681.

Ciotti AM, Cullen JJ, Lewis MR (1999) A semi-analytical model of the influence community structure on the relationship between light attenuation and ocean color. J Geophys Res 104:1559-1578

Ciotti AM, Lewis MR, Cullen JJ (2002) Assessment of the relationships between dominant cell size in natural phytoplankton communities and the spectral shape of the absorption coefficient. Limnol Oceanogr 47(2):404-417

Çizmeli SA (2008) Propriétés optiques intrinsèques et apparentes des eaux du golfe et de l'estuaire du Saint-Laurent : concordance optique, paramétrisation et variabilité spatio-temporelle. Thèse de doctorat de l'Université de Sherbrooke (Canada)

Clarke KR (1993) Non-parametric analyses of changes in community structure. Aust J Ecol 18:117–143

Claustre H, Bricaud A, Babin M, Bruyant F, Guillou L, Le Gall F, Marie D, Partensky F (2002) Diel variations in *Prochlorococcus* optical properties. Limnol Oceanogr 47(6):1637-1647

Claustre H, Fell F, Oubelkheir K, Prieur L, Sciandra A, Gentilli B, Babin M (2000) Continuous monitoring of surface optical properties across a geostrophic front: biogeochemical inferences. Limnol Oceanogr 45(2):309-321

Claustre H, Gostan J (1987) Adaptation of biochemical composition and cell size to irradiance in two microalgae: possible ecological implications. Mar Ecol Prog Ser 40:167-174

Claustre H, Morel A, Babin M, Cailliau C, Marie D, Marty JC, Tailliez D, Vaulot D (1999) Variability in particle attenuation and chlorophyll fluorescence in the tropical Pacific: Scales, patterns and biogeochemical implications. J Geophys Res 104(C2):3401-3422

Claustre H, Kerherve P, Marty JC, Prieur L (1994) Phytoplankton photoadaptation related to some frontal physical processes. J Mar Syst 5:251-265

Cleveland JS, Perry MJ (1987) Quantum yields, relative specific absorption and fluorescence in nitrogen limited *Chaetoceros gracilis*. Mar Biol 94:489-497

Cleveland JS, Weidemann AD (1993) Quantifying absorption by aquatic particles: a multiple scattering correction for glass-fiber filters. Limnol Oceanogr 38(6):1321-1327

Coble PG, Green SA, Blough NV, Gagosian RB (1990) Characterization of dissolved organic matter in the Black Sea by fluorescence spectroscopy. Nature 348:432-435

Collier JL (2000) Flow cytometry and the single cell in phycology. J Phycol 36:628-644

Cota GF, Harisson WG, Platt T, Sathyendranath S, Stuart V (2003) Bio-optical properties of the Labrador Sea. J Geophys Res 108(C7):3228, doi:10.1029/2000JC000597

Cullen JJ, Ciotti AM, Lewis MR (1994) Observing biologically induced optical variability in coastal waters. Proc SPIE, Ocean Optics XII, 2258:105-115

Cullen JJ, Yentsch CM, Cucci TL, MacIntyre HL (1988) Autofluorescence and other optical properties as tools in biological oceanography. Proc SPIE, Ocean Optics IX, 925:149-156

Culver ME, Perry MJ (1999) The response of photosynthetic absorption coefficients to irradiance in culture and in tidally mixed estuarine waters. Limnol Oceanogr 44:24-36

D'Sa EJ, Steward RG, Vodacek A, Blough NV, Phinney D (1999) Determining optical absorption of colored dissolved organic matter in seawater with a liquid capillary waveguide. Limnol Oceanogr 44(4):1142-1148

Davies-Colley RJ (1992) Yellow substance in coastal and marine waters around the South Island, New Zealand. N Z J Mar Freshwat Res 26:311-322

de Lafontaine Y, Demers S, Runge J (1991) Pelagic food web interactions and productivity in the gulf of St. Lawrence: a perspective. In: Therriault J-C (ed) The gulf of St. Lawrence: Small ocean or big estuary? Can Spec Publ Fish Aquat Sci 113:99-123

Demers S, Davis K, Cucci TL (1989) A flow cytometric approach to assessing the environmental and physiological status of phytoplankton. Cytometry 10:644-652

Demers S, Legendre L (1981) Mélange vertical et capacité photosynthétique du phytoplankton estuarien (estuaire du Saint-Laurent). Mar Biol 64:243-250

Demers S, Roy S, Gagnon R, Vignault C (1991) Rapid light-induced changes in cell fluorescence and in xanthophyll-cycle pigments of *Alexandrium excavatum* (Dinophyceae) and *Thalassiosira pseudonana* (Bacillariophyceae): A photo-protection mechanism. Mar Ecol Prog Ser 76(2):185-193

Demman KL, Powell TM (1984) Effects of physical processus on plankton ecosystems in the coastal ocean. Oceanogr Mar Biol Annu Rev 22:125-168

Dierssen HM, Smith RC (2000) Bio-optical properties and remote sensing ocean color algorithms for Antarctic Peninsula waters. J Geophys Res 105:26301-26312

Doyon P, Klein B, Ingram RG, Legendre L, Tremblay J-E, Therriault J-C (2000) Influence of wind mixing and upper-layer stratification on phytoplankton biomass in the Gulf of St. Lawrence. Deep-Sea Res II 47(3-4):415-433

Dubelaar GBJ, Visser JWM, Donze M (1987) Anomalous behaviour of forward and perpendicular light scattering of a cyanobacterium owing to intracellular gas vacuoles. Cytometry 8:405-412

Duce RA, Tindale NW (1991) Atmospheric transport of iron and its deposition in the ocean. Limnol Oceanogr 36(8):1715-1726

Dupouy C, Petit M, Dandonneau Y (1988) Satellite detected cyanobacteria bloom in the southwestern tropical Pacific: implication for oceanic nitrogen fixation. Intl J Remote Sens 9:389-396

DuRand MD, Green RE, Sosik HM, Olson RJ (2000) Diel variations in optical properties of *Micromonas pusilla*, a prasinophyte. Proc SPIE, Ocean Optics XV, 11 pp

DuRand MD, Green RE, Sosik HM, Olson RJ (2002) Diel variations in optical properties of *Micromonas pusilla* (Prasinophyceae). J Phycol 38(6):1132-1142

DuRand MD, Olson RJ (1996) Contributions of phytoplankton light scattering and cell concentration changes to diel variations in beam attenuation in the equatorial Pacific from flow cytometric measurements of pico-, ultra- and nanoplankton. Deep-Sea Res II 43(4-6):891-906

DuRand MD, Olson RJ (1998) Diel patterns in optical properties of the chlorophyte *Nannochloris* sp.: Relating individual-cell to bulk measurements. Limnol Oceanogr 43(6):1107-1118

DuRand MD, Olson RJ, Zettler ER (1994) Flow cytometric analyses of phytoplankton growth during diel studies in the Equatorial Pacific. EOS, Transactions, American Geophysical Union 75(3):28-29

Duysens LMN (1956) The flattening effect of the absorption spectra of suspensions as compared to that of solutions. Biochem Biophys Acta 19:1-12

Eisner LB, Twardowski MS, Cowles TJ, Perry, MJ (2003) Resolving phytoplankton photoprotective: photosynthetic carotenoid ratios on fine scales using in situ spectral absorption measurements. Limnol Oceanogr 48(2):632-646

El-Sabh MI (1976) Surface circulation pattern in the Gulf of St. Lawrence. J Fish Res Board Can 33:124-138

El-Sabh MI (1979) The lower St. Lawrence Estuary as a physical oceanographic system. Nat Can 106(1):55-73

Falkowski PG (1980) Light-shade adaptation in marine phytoplankton. In: Falkowski PG (ed) Primary productivity in the sea. Plenum Press, New York, p 99-119

Falkowski PG (1984a) Physiological response of phytoplankton to natural light regimes. J Plankton Res 6:62-68

Falkowski PG (1984b) Kinetics of adaptation to irradiance in *Dunaliella tertiolecta*. Photosynthetica 18:62-68

Falkowski PG (1992) Molecular ecology of phytoplankton photosynthesis. In: Falkowski PG, Woodhead AD (eds) Primary productivity and biogeochemical cycles in the sea. Plenum, New York, p 47-67

Falkowski PG, LaRoche J (1991) Acclimatation to spectral irradiance in algae. J Phycol 27:8-14

Field JG, Clarke KR, Warwick RM (1982) A practical strategy for analyzing multispecies distribution patterns. Mar Ecol Prog Ser 8:37–52

Fisher T, Minnaard J, Dubinsky Z (1996) Photoacclimatation in the marine alga *Nannochloropsis sp.* (Eustigmatophyte): a kinetic study. J Plankton Res 18:1797-1818

Forrester WD (1974) Internal tides in St. Lawrence estuary. J Mar Res 32(1):55-66

Fuentes-Yaco C (1997) Télédetection de la biomasse phytoplanctonique dans le golfe du Saint-Laurent, Canada : analyse des données du capteur Coastral Zone Color Scanner. Thèse de doctorat de l'Université du Québec à Rimouski (Canada), 176 pp

Fuentes-Yaco C, Larouche P, Vézina AF, Vigneau C, Gosselin M (1995) Catalogue of phytoplankton pigment images from the Gulf of St. Lawrence: Nimbus-7 Coastal Zone Color Scanner data from 1979 to 1981. Canadian Data Report of Hydrogrophy and Ocean Sciences 135, 91 pp

Fuentes-Yaco C, Vézina AF, Platt T, Harrison WG, Connier PG, Waite LE, Devine L (1998) Spatio-temporal distribution of phytoplankton pigments in Northumberland Strait: CZCS imagery and *in situ* data. Can Tech Rep Hydrogr Ocean Sci 195, 37 pp

Fujiki T, Taguchi S (2001) Variability in chlorophyll *a* specific absorption coefficient in marine phytoplankton as a function of cell size and irradiance. J Plankton Res 24(9):859-874

Fuller NJ, Campbell C, Allen DJ, Pitt FD, Zwirglmaier K, Le Gall F, Vaulot D, Scanlan DJ (2006) Analysis of photosynthetic picoeukaryote diversity at open ocean sites in the Arabian Sea using a PCR biased towards marine algal plastids. Aquat Microb Ecol 43:79-93

Gallegos CL, Platt T, Harrison WG, Irwin B (1983) Photosynthetic parameters of Arctic marine phytoplankton: Vertical variations and time scales of adaptation. Limnol Oceanogr 28(4):698-708

Gardner WD, Walsh ID, Richardson MJ (1993) Biophysical forcing of particle production and distribution during a spring bloom in the North Atlantic. Deep-Sea Res II 40:171-195

Garver SA, Siegel DA (1997) Inherent optical property inversion of ocean color spectra and its biogeochemical interpretation. 1. Time series from the Sargasso Sea. J Geophys Res 102:18607-18625

Geider RJ, MacIntyre HL, Kana TM (1996) A dynamic model of photoadaptation in phytoplankton. Limnol Oceanogr 41(1):1-15

Geider RJ, MacIntyre HL, Kana TM (1998) A dynamic regulatory model of phytoplanktonic acclimation to light, nutrients, and temperature. Limnol Oceanogr 43(4):679-694

Geider RJ, Osborne BA, Raven JA (1985) Light dependence of growth and photosynthesis in *Phaeodactylum tricornutum* (Bacillariophyceae). J Phycol 21:609-619

Glover HE, Smith AE, Shapiro L (1985) Diurnal variations in photosynthetic rates: Comparisons of ultraphytoplankton with a larger phytoplankton size fraction. J Plankton Res 7(4):519-535

Goericke R, Montoya JP (1998) Estimating the contribution of microalgal taxa to chlorophyll *a* in the field: variations of pigment ratios under nutrient- and light-limited growth. Mar Ecol Prog Ser 169:97-112

Goldman JC, Dennett MR (1991) Ammonium regeneration and carbon utilization by marine bacteria grown on mixed substrates. Mar Biol 109:369-378

Gons HJ, Rijkeboer M, Bagheri S, Ruddick KG (2000) Optical teledetection of chlorophyll *a* in estuarine and coastal waters. Environ Sci Technol 34(24):5189-5192

Gordon HR (1989) Can the Lambert-Beer law be applied to the diffuse attenuation coefficient of ocean water? Limnol Oceanogr 34(8):1389-1409

Gordon HR, Brown OB, Evans RH, Brown JW, Smith RC, Baker KS, Clark DK (1988) A semianalytic radiance model of ocean color. J Geophys Res 93:10909-10924

Gordon HR, Brown OB, Jacobs MM (1975) Computed relationships between the inherent and apparent optical properties of a flat homogeneous ocean. Appl Opt 14:417-427

Gordon HR, Morel AY (1983) Remote assessment of ocean color for interpretation of satellite visible imagery. A review. Lect Notes Coast Estuar Stud, vol 4, Springer-Verlag, New York (USA), 114 pp

Gordon HR, Smith RC, Zaneveld JRV (1984) Introduction to ocean optics. Proc SPIE, Ocean Optics VII, 489:2-41

Green SA, Blough NV (1994) Optical absorption and fluorescence properties of chromophoric dissolved organic matter in natural waters. Limnol Oceanogr 39(8):1903-1916

Green RE, Sosik HM (2004) Analysis of apparent optical properties and ocean color models using measurements of seawater constituents in New England continental shelf surface waters. J Geophys Res 109(C3), C03026, doi:10.1029/2003JC001977

Green RE, Sosik HM, DuRand MD, Olson RJ (2000) Comparison of refractive index estimated from single-cell and bulk optical properties. Proc SPIE, Ocean Optics XV, 9 pp

Green RE, Sosik HM, Olson RJ (2002) The contribution of phytoplankton and non-phytoplankton particles to inherent and apparent optical properties in New England continental shelf waters. Proc SPIE, Ocean Optics XVI, 11 pp

Green RE, Sosik HM, Olson RJ, DuRand MD (2003) Flow cytometric determination of size and complex refractive index for marine particles: comparison with independent and bulk estimates. Appl Opt 42:526-541

Guillard RRL, Ryther JH (1962) Studies on marine planktonic diatoms. I. *Cyclotella nana* and *Denotula confervacea* (Cleve) Gran. Can J Microbiol 8:229-239

Hama T, Handa N, Takahashi M, Whitney F, Wong CS (1988) Changes in distribution pattern of photosynthetically incorporated C during phytoplankton bloom in controlled experimental ecosystem. J Exp Mar Biol Ecol 120:39–55

Henriksen P, Riemann B, Kaas H, Sorensen HM, Sorensen HL (2002) Effects of nutrient-limitation and irradiance on marine phytoplankton pigments. J Plankton Res 24(9):835-858

Hillebrand H, Dürselen CD, Kirschyel D, Pollingher U, Zohary T (1999) Biovolume calculation for pelagic and benthic macroalgae. J Phycol 35:403-424

Hoepffner N, Sathyendranath S (1991) Effect of pigment composition on absorption properties of phytoplankton. Mar Ecol Prog Ser 73:11-23

Hoepffner N, Sathyendranath S (1992) Bio-optical characteristics of coastal waters: absorption spectra of phytoplankton and pigment distribution in the western North Atlantic. Limnol Oceanogr 37(8):1660-1679

Hoge FE, Wright CW, Swift RN, Yungel JK, Berry RE, Mitchell R (1998) Airborne bio-optics survey of the Galapagos Islands margins. Deep-Sea Res II 45:1083-1092

Ingram RG (1975) Influence of tidal-induced vertical mixing on primary productivity in the St. Lawrence estuary. Mem Soc Roy Sci Liege 7:59-74

Ingram RG, El-Sabh MI (1990) Fronts and mesoscale features in the St. Lawrence Estuary. In: El-Sabh MI, Silverberg N (eds) Oceanography of a Large-Scale Estuarine System, The St. Lawrence. Springer-Verlag, New York, NY. Coast Estuar Studies 39:71-93

IOCCG (2000) Remote sensing of ocean colour in coastal, and other optically-complex, waters. Sathyendranath S (ed) Reports of the International Ocean-Colour coordinating Group, No. 3, IOCCG, Dartmouth, Canada, 145 pp

Iturriaga R, Siegel DA (1988) Discrimination of the absorption properties of marine particulates using a microphotometer technique. Proc SPIE, Ocean Optics IX, 925:277-287

Iturriaga R, Siegel DA (1989) Microphotometric characterization of phytoplankton and detrital absorption properties in the Saragasso Sea. Limnol Oceanogr 34(8):1706-1726.

Jacquet S, Lennon JF, Marie D, Vaulot D (1998) Picoplankton population dynamics in coastal waters of the northwestern Mediterranean Sea. Limnol Oceanogr 43(8):1916-1931

Jacquet S, Partensky F, Lennon JF, Vaulot D (2001) Diel patterns of growth and division in marine picoplankton in culture. J Phycol 37:357-369

Jacquet S, Prieur L, Avois-Jacquet C, Lennon JF, Vaulot D (2002) Short-timescale variability of picophytoplankton abundance and cellular parameters in surface waters of the Alboran Sea (western Mediterranean). J Plankton Res 24(7):635-651

Jeffrey SW, Mantoura RFC, Wright SW (1997) Phytoplankton pigments in oceanography. UNESCO. Paris.

Jerlov NG (1968) Optical oceanography. Elsevier.

JGOFS (1991) JGOFS Core measurements protocols. JGOFS Report 6, SCOR

Johnsen G, Sakshaug E (1993) Bio-optical characteristics and photoadaptive responses in the toxic and bloom-forming dinoflagellates *Gyrodinium aureolum*, *Gymnodinium galatheanum* and two strains of *Prorocentrum minimum*. J Phycol 29:627-642

Johnsen G, Samset O, Granskog L, Sakshaug E (1994) In vivo absorption characteristics in 10 classes of bloom-forming phytoplankton: Taxonomic characteristics and responses to photoadaptation by means of discriminant and HPLC analysis. Mar Ecol Prog Ser 105:149-157

Johnson KM, Sieburth JM (1979) Chroococcoid cyanobacteria in the sea: A ubiquitous and diverse phototrophic biomass. Limnol Oceanogr 24(5):928-935

Joint IR, Pomroy AJ (1983) Production of picoplankton and small nanoplankton in the Celtic Sea. Mar Biol 77(1):19-27

Jonasz M (1983) Particulate matter in the Ezcurra Inlet: Concentration and size distributions. Oceanologia 15:65-74

Kiefer DA (1973) Chlorophyll *a* fluorescence in marine centric diatoms: responses of chloroplasts to light and nutrient stress. Mar Biol 23:39-46

Kiefer DA (1984) Microplankton and optical variability in the sea: Fundamental relationships. Proc SPIE, Ocean Optics VII, 489:42-48

Kiefer DA, Olson RJ, Wilson WH (1979) Reflectance spectroscopy of marine phytoplankton. Part 1. Optical properties as related to age and growth rate. Limnol Oceanogr 24(4):664-672

Kirk JTO (1994). Light and photosynthesis in aquatic ecosystems. Cambridge University Press, New York 509 pp

Kishino M, Takahashi M, Okami N, Ichimura S (1985) Estimation of the spectral absorption coefficients of phytoplankton in the sea. Bull Mar Sci 37:634-642

Kishino M, Booth CR, Okami N (1986) Light utilization efficiency and quantum yield of phytoplankton in a thermally stratified sea. Limnol Oceanogr 31(3):557-566

Kitchen JC, Zaneveld JRV (1990) On the noncorrelation of the vertical structure of light scattering and chlorophyll a in case I waters. J Geophys Res 95(C11):20237-20246

Kitchen JC, Zaneveld JRV, Pak H (1982). Effect of particle size distribution and chlorophyll content on beam attenuation spectra. Appl Opt 21:3913-3918

Koike I, Hara S, Terauchi K, Kogure K (1990) Role of sub-micrometre particles in the ocean. Nature 345: 242-244

Koutitonsky VG, Bugden GL (1991) The physical oceanography of the Gulf of St. Lawrence: a review with emphasis on the synoptic variability of the motion. In: Therriault J-C (ed) The gulf of St. Lawrence: small ocean or big estuary? Can Spec Publ Fish Aquat Sci 113:57-90

Król T, Zielinski A, Witkowski K (1992) Light scattering in *Chlorella vulgaris* cell. Proc SPIE, Ocean Optics XI, 1750:47-53

Laurion I, Blouin F, Roy S (2003) The quantitative filter technique for measuring phytoplankton absorption: Interference by MAAs in the UV waveband. Limnol Oceanogr Methods 1:1-9

Lebaron P, Parthuisot N, Catala P (1998) Comparison of blue nucleic acid dyes for flow cytometric enumeration of bacteria in aquatic systems. Appl Environ Microbiol 64(5):1725-1730

Legendre L, Martineau M-J, Therriault J-C, Demers S (1992) Chlorophyll *a* biomass and growth of sea-ice microalgae along a salinity gradient (southeastern Hudson Bay, Canadian Arctic). Polar Biol 12:445-453

LeRoi J-M, Hallegraeff GM (2006) Scale-bearing nanoflagellates from southern Tasmanian coastal waters, Australia. II. Species of Chrysophyceae (Chrysophyta), Prymnesiophyceae (Haptophyta, excluding *Chrysochromulina*) and Prasinophyceae (Chlorophyta). Bot Mar 49(3):216-235

Levasseur M, Fortier L, Therriault J-C, Harrison PJ (1992) Phytoplankton dynamics in a coastal jet frontal region. Mar Ecol Prog Ser 86:283-295

Levasseur M, Therriault J-C, Legendre L (1984) Hierarchical control of phytoplankton succession by physical factors. Mar Ecol Prog Ser 19(3):211-222

Li WKW, Subba Rao DV, Harrison WG, Smith JC, Cullen JJ, Irwin B, Platt T (1983) Autotrophic picoplankton in the tropical ocean. Science 219(4582):292-295

Li WKW, Wood AM (1988) Vertical distribution of North Atlantic ultraphytoplankton: Analysis by flow cytometry and epifluorescence microscopy. Deep-Sea Res 35(9A):1615-1638

Lohrenz SE, Fahnenstiel GL, Kirkpatrick GJ, Carroll CL, Kelly KA (1997) Microphotometric assessment of spectral absorption and its potential application for characterization of harmful algal species. J Phycol 35:1438-1446

Lohrenz SE, Weidemann AD, Tuel M (2003) Phytoplankton spectral absorption as influenced by community size structure and pigment composition. J Plankton Res 25(1):35-61

Loisel H, Morel A (1998) Light scattering and chlorophyll concentration in case I waters: A reexamination. Limnol Oceanogr 43(5):847-858

Lovejoy C, Vincent WF, Frenette JJ, Dodson JJ (1993) Microbial gradients in a turbid estuary: Application of a new method for protozoan community analysis. Limnol Oceanogr 38(6):1295-1303

Margalef R (1967) Some concepts relative to the organization of plankton. Oceanogr Mar Biol Ann Rev 5:257-289

Marie D, Partensky F, Jacquet S, Vaulot D (1997) Enumeration and cell cycle analysis of natural populations of marine picoplankton by flow cytometry using the nucleic acid stain SYBR Green I. App Environ Microbiol 63(1):186-193

Martin-Olivier V (1997) Etude par cytométrie en flux de la distribution des populations phytoplanctoniques en Méditerranée. Mise en relation avec la production métabolique de CO_2 et comparaison avec le golfe du Saint-Laurent. Thèse de doctorat de l'Université de la Méditerranée (France), 245 pp

Mas S, Roy S, Blouin F, Mostajir B, Therriault J-C, Nozais C, Demers S (2008) Diel variations in optical properties of *Imantonia rotunda* (Haptophyceae) and *Thalassiosira pseudonana* (Bacillariophyceae) exposed to different irradiance levels. J Phycol 44(3):551–563

Maske H, Haardt H (1987) Quantitative in-vivo absorption spectra of phytoplankton: Detrital absorption and comparison with fluorescence excitation spectra. Limnol Oceanogr 32(3):620-630

Merien D (2003) Variabilité bio-optique à différentes échelles spatiales et temporelles dans l'Atlantique nord-est : interprétations biogéochimiques. Thèse de doctorat de l'Université Pierre et Marie Curie (France), 273 pp

McLeroy-Etheridge S, Roesler C (1998) Are the inherent optical properties of phytoplankton responsible for the distinct ocean colors observed during harmful algal blooms? Proc SPIE, Ocean Optics XIV, 1:109-116

Miller WL, Zepp RG (1995) Photochemical production of dissolved inorganic carbon from terrestrial organic matter: Significance to the oceanic organic carbon cycle. Geophys Res Lett 22:417-420

Mitchell BG, Kahr M, Wieland J, Stramska M (2002) Determination of spectral absorption coefficients of particles, dissolved material and phytoplankton for discrete water samples. In: Mueller JL, Fargion GS (eds). Ocean optics protocols for satellites ocean color sensor validation, Revision 3. NASA Technical memorandum, 2002-21004/Rev3, vol 2. Maryland: NASA Goddard space center, Greenbelt. p 231-257

Mitchell BG, Kiefer DA (1984) Determination of absorption and fluorescence excitation spectra for phytoplankton. In: Holm-Hansen O, Bolis L, Gilles R (eds) Marine phytoplankton and productivity. Springer-Verlag, Berlin, p 157-169

Mitchell BG, Kiefer DA (1988) Chlorophyll *a* specific absorption and fluorescence excitation spectra for light-limited phytoplankton. Deep-Sea Res 35:639-663

Mobley C (1994) Light and water: radiative transfer in natural waters. Academic Press Inc, London, 592 pp

Mobley CD, Stramski D (1997) Effects of microbial particles on oceanic optics: Methodology for radiative transfer modeling and example simulations. Limnol Oceanogr 42(3):550-560

Moisan TA, Mitchell BG (1999) Photophysiological acclimation of *Phaeocystis antarctica* Karsten under light limitation. Limnol Oceanogr 44(2):247-258

Moran MA, Sheldon WM, Zepp RG (2000) Carbon loss and optical property changes during long-term photochemical and biological degradation of estuarine dissolved organic matter. Limnol Oceanogr 45(6):1254-1264

Moreira-Turcq PF, Martin JM (1998) Characterization of fine particles by flow cytometry in estuarine and coastal Arctic waters. J Sea Res 39(3-4):217-226

Morel A (1973) Diffusion de la lumière par les eaux de mer; résultats expérimentaux et approche théorique. AGARD Lect Ser 63:3.1.1.-3.1.76.

Morel A (1974) Optical properties of pure water and pure sea water. In: Jerlov, Steeman-Nielsen (eds) Optical aspects of oceanography. Academic Press

Morel A (1987) Chlorophyll-specific scattering coefficient of phytoplankton: A simplified theoretical approach. Deep-Sea Res 34:1093-1105

Morel A (1988) Optical modeling of the upper ocean in relation to its biogenous matter content (case I water). J Geophys Res 93:10749-10768

Morel A (1990) Optics of marine particles and marine optics. In: Demers S (ed) Particle analysis in oceanography, NATO ASI Series, Springer-Verlag, Heidelberg, Serie G, Ecological Sciences 27:141-188

Morel A (1991) Light and marine photosynthesis: a spectral model with geochemical and climatological implications. Prog Oceanog 26:263-306

Morel A, Ahn Y, Partensky F, Vaulot D, Claustre H (1993) *Prochlorococcus* and *Synechococcus*: a comparative study of their optical properties in relation to their size and pigmentation. J Mar Res 51:617-649

Morel A, Ahn Y-H (1990) Optical efficiency factors of free-living marine bacteria: Influence of bacterioplankton upon the optical properties and particulate organic carbon in oceanic waters. J Mar Res 48:145-175

Morel A, Ahn Y-H (1991) Optics of heterotrophic nanoflagellates and ciliates: A tentative assessment of their scattering role in oceanic waters compared to those of bacterial and algal cells. J Mar Res 49:177-202

Morel A, André JM (1991) Pigment distribution and primary production in the western Mediterranean as derived and modeled from coastal zone color scanner observations. J Geophys Res 96:12685-12698

Morel A, Berthon JF (1989) Surface pigments, algal biomass profiles, and potential production of the euphotic layer: Relationships reinvestigated in view of remote-sensing applications. Limnol Oceanogr 34(8):1545-1562

Morel A, Bricaud A (1981) Theoretical results concerning light absorption in a discrete medium, and application to specific absorption of phytoplankton. Deep-Sea Res 28:1375-1393

Morel A, Bricaud A (1986) Inherent optical properties of algal cells including picoplankton: Theoretical and experimental results. In: Platt T, Li WKW (eds) Photosynthetic picoplankton. Can Bull Fish Aquat Sci 214:521-559

Morel A, Gentili B (1991) Diffuse reflectance of oceanic waters: its dependence on sun angle as influence by molecular scattering contribution. Appl Opt 30:4427-4438

Morel A, Lazzara L, Gostan J (1987) Growth rate and quantum yield time response for a diatom to changing irradiances (energy and color). Limnol Oceanogr 32(5):1066-1084

Morel A, Maritorena S (2001) Bio-optical properties of oceanic waters: a reappraisal. J Geophys Res 106:7163-7180

Morel A, Prieur L (1977) Analysis of variations in ocean color. Limnol Oceanogr 22(4):709-722

Morrison JR, Sosik HM (2002) Inherent optical properties in New England coastal waters: Decomposition into contributions from optically important constituents. Proc SPIE, Ocean Optics XVI, 10 pp

Mostajir B, Gosselin M, Gratton Y, Booth B, Vasseur C, Garneau M-E, Fouilland E, Vidussi F, Demers S (2001) Surface water distribution of pico- and nanophytoplankton in relation to two distinctive water masses in the North Water, Canadian Arctic, during fall. Aquat Microb Ecol 23:205-212

Myklestad S (1977) Production of carbohydrates by marine planktonic diatoms. II. Influence of the N/P ratio in the growth medium on the assimilation ratio, growth rate, and production of cellular and extracellular carbohydrates by *Chaetoceros affinis* var. *willei* (Gran) Hustedt and *Skeletonema costatum* (Grev.) Cleve. J Exp Mar Biol Ecol 29:161–179

Neori A, Holm-Hansen O, Mitchell BG, Kiefer DA (1984) Photoadaptation in marine phytoplankton. Plant Physiol 76:518-524

Neu HJA (1970) A study on mixing and circulation in the St. Laurence estuary up to 1964. Atlant. Oceanogr Lab Bedford Inst Oceanogr, Rep Ser 1970-9. Dartmouth, Canada, 31 pp

Nieke B, Reuter R, Heuermann R, Wang H, Babin M, Therriault JC (1997) Light absorption and fluorescence properties of chromophoric dissolved organic matter (CDOM), in the St. Lawrence Estuary (Case 2 waters). Cont Shelf Res 17(3):235-252

Nielsen MV, Sakshaug E (1993) Photobiological studies of *Skeletonema costatum* adapted to spectrally different light regimes. Limnol Oceanogr 38(7):1576-1581

O'Reilly JE, Maritorena S, Mitchell BG, Siegel DA, Carder KL, Garver SA, McClain CR (1998) Ocean color chlorophyll algorithms for SeaWiFS. J Geophys Res 103:24937-24953

Ohi N, Ishiwata Y, Taguchi S (2002) Diel patterns in light absorption and absorption efficiency factors of *Isochrysis galbana* (Prymnesiophyceae). J Phycol 8(4):730-737

Olson RJ, Chisholm SW, Zettler ER, Armbrust EV (1990) Pigments, size, and distribution of *Synechococcus* in the North Atlantic and Pacific oceans. Limnol Oceanogr 35(1):45-58

Olson RJ, Vaulot D, Chisholm SW (1985) Marine phytoplankton distributions measured using shipboard flow cytometry. Deep-Sea Res 32:1273-1280

Owens TG, Falkowski PG, Whitledge TE (1980) Diel periodicity in cellular chlorophyll content in marine diatoms. Mar Biol 59:71-77

Pegau WS, Gray D, Zaneveld JRV (1997) Absorption and attenuation of visible and near-infrared light in water: dependence on temperature and salinity. Appl Opt 36:6035-6046

Pérez V, Fernández E, Marañón E, Serret P, García-Soto C (2005) Seasonal and interannual variability of chlorophyll *a* and primary production in the Equatorial Atlantic: in situ and remote sensing observations. J Plankton Res 27:189-197

Perry MJ, Porter SM (1989) Determination of the cross-section absorption coefficient of individual phytoplankton cells by analytical flow cytometry. Limnol Oceanogr 34(8):1727-1738

Perry MJ, Talbot MC, Alberte RS (1981) Photoadaption in marine phytoplankton: Response of the photosynthetic unit. Mar Biol 62:92-101

Platt T, Harrison WG, Lewis MR, Li WKW, Sathyendranath S, Smith RE, Vézina AF (1989) Biological production of the oceans: the case for a consensus. Mar Ecol Prog Ser 52:77-88

Platt T, Rao DVS, Irwin B (1983) Photosynthesis of picoplankton in the oligotrophic ocean. Nature 301:702-704

Platt T, Sathyendranath S (1988) Oceanic primary production: Estimation by remote sensing at local and regional scales. Science 241(4873):1613-1620

Pope RM, Fry ES (1997) Absorption spectrum (380-700 nm) of pure water. II. Integrating cavity measurements. Appl Opt 36:8710-8723

Post AF, Dubinsky Z, Wyman K, Falkowski PG (1984) Kinetics of light-intensity adaptation in a marine planktonic diatom. Mar Biol 83(3):231-238

Prakash A (1975) Dinoflagellate blooms - an overview. Proceedings of the First International Conference on Toxic Dinoflagellate B, 532 pp

Preisendorfer RW (1961) Application of radiative transfer theory to light measurements in the sea. Union Geod Geophys Inst Monogr 10, Paris

Prézelin BB, Matlick HA (1980) Time-course of photoadaptation in the photosynthesis-irradiance relationship of a dinoflagellate exhibiting photosynthetic periodicity. Mar Biol 58:85-96

Prieur L, Morel A (1975) Relations théoriques entre le facteur de réflexion diffuse de l'eau de mer, à diverses profondeurs, et les caractéristiques optiques. UGGI XVI Assemblée Générale, août 1975, Grenoble, IS 30(13):250-251

Redfield AC, Ketchum BH, Richards FA (1963) The influence of organisms on the composition of sea-water. In: Hill MN (ed) The sea, Vol 2. Interscience, New-York, p 26-77

Reynolds RA, Stramski D, Kiefer DA (1997) The effect of nitrogen limitation on the absorption and scattering properties of marine diatom *Thalassiosira pseudonana*. Limnol Oceanogr 42(5):881-892

Reynolds RA, Stramski D, Mitchell BG (2001) A chlorophyll-dependent semianalytical reflectance model derived from field measurements of absorption and backscattering coefficients within the Southern Ocean. J Geophys Res 106(C4):7125-7138

Rhee G-Y (1980) Continuous culture in phytoplankton ecology. In: MR Droop, HW Jannasch, (eds) Advances in Aquatic Microbiology, vol. 2. Academic Press, London/N.Y., p 151–203

Richardson K, Beardall J, Raven JA (1983) Adaptation of unicellular algae to irradiance: an analysis of strategies. New Phytol 93:157-191

Rivkin RB, Phinney DA, Yentsch CM (1996) Effects of flow cytometric analysis and cell sorting on photosynthetic carbon uptake by phytoplankton in cultures and from natural populations. Appl Environ Microbiol 52(4):935-938

Robert R, His E (1987) Growth and size frequency distribution of six marine unicellular algae in batch cultures used as food for larvae of bivalve molluscs. Rev Trav Inst Pêches marit 49(3-4):165-173

Roesler CS, Perry MJ (1995). In situ phytoplankton absorption, fluorescence emission, and particulate backscattering spectra determined from reflectance. J Geophys Res 100(C7):13279-13294

Romero OE, Lange CB, Swap R, Wefer G (1999) Eolian-transported freshwater diatoms and phytoliths across the equatorial Atlantic record: Temporal changes in Saharan dust transport patterns. J Geophys Res 104(C2):3211-3222

Roy, S, Chanut JP, Gosselin M et Sime-Ngando T (1996) Characterization of phytoplankton communities in the Lower St. Lawrence Estuary using HPLC-detected pigments and cell microscopy. Mar Ecol Prog Ser 142 : 55-73

Roy S, Blouin F, Jacques A, Therriault J-C (In press) Absorption properties of phytoplankton in the Lower Estuary and Gulf of St. Lawrence (Canada). Can J Fish Aquat Sci

Sakshaug E, Demers S, Yentsch CM (1987) *Thalassiosira oceanica* and *T. pseudonana*: two different photoadaptational responses. Mar Ecol Prog Ser 41:275-282

Sathyendranath S, Lazzara L, Prieur L (1987) Variations in the spectral values of specific absorption of phytoplankton. Limnol Oceanogr 32(2):403-415

Sathyendranath S, Longhurst A, Caverhill CM, Platt T (1995) Regionally and seasonally differentiated primary production in the North Atlantic. Deep-Sea Res 42(10):1773-1802

Sciandra A, Gostan J, Collos Y, Descolas-Gors C, Leboulanger C, Martin-Jézéquel V, Denis M, Lefèvre D, Copin-Montégut C, Avril B (1997) Growth compensating phenomena in continuous cultures of *Dunialiella tertiolecta* limited simultaneously by light and nitrate. Limnol Oceanogr 42(6):1325-1339

Sciandra A, Lazzara L, Claustre H, Babin M (2000) Responses of the growth rate, pigment composition and optical properties of *Cryptomonas* sp. to light and nitrogen stresses. Mar Ecol Prog Ser 201:107-120

Sévigny JM, Sinclair M, El-Sabh MI, Poulet S, Coote A (1979) Summer plankton distributions associated with the physical and nutrient properties of the northwestern Gulf of St. Lawrence. J Fish Res Board Can 36:187-203

Shapiro HM (1988) Practical Flow Cytometry. 2nd ed, Wiley-Liss, New York, 353 pp

Sherr BF, Sherr EB (2000) Marine microbes: an overview. In: Kirchman D (ed) Microbial ecology of the oceans, Wiley-Liss, New York, p 13-46

Siegel DA, Dickey TD, Washburn L, Hamilton MK, Mitchell BG (1989) Optical determination of particle abundance and production variations in the oligotrophic ocean. Deep-Sea Res 36(2):211-222

Smith RC, Baker KS (1978a) The bio-optical state of ocean waters and remote sensing. Limnol Oceanogr 23(2):247-259

Smith RC, Baker KS (1978b) Optical classification of natural waters. Limnol Oceanogr 23(2):260-267

Smith RC, Baker KS (1981) Optical properties of the clearest natural waters (200-800 nm). Appl Opt 20:177-184

Sogandares FM, Fry ES (1997) Absorption spectrum (340-640 nm) of pure water. I. Photothermal measurements. Appl Opt 36(33):8699-8709

Sosik HM, Green RE, Olson RJ (1998) Optical variability in coastal waters of the northwest Atlantic. Proc SPIE, Ocean Optics XIV, 14 pp

Sosik HM, Green RE, Pegau WS, Roesler CS (2001) Temporal and vertical variability in optical properties of New England shelf waters during late summer and spring. J Geophys Res 106(C5):9455-9472

Sosik HM, Mitchell BG (1991) Absorption, fluorescence and quantum yield in nitrogen-limited *Duniella tertiolecta*. Limnol Oceanogr 36(5):910-921

Spinrad RW (1984) Flow cytometric analysis of the optical characteristics of marine particulates. Proc SPIE, Ocean Optics VII, 489:335-342

Spinrad RW, Brown JF (1986) Relative real refractive index of marine microorganisms: a technique for flow cytometric estimation. Appl Opt 25:1930-1934

Spinrad RW, Yentsch CM (1987) Observations on the intra- and interspecific single cell optical variability of marine phytoplankton. Appl Opt 26:357-362

Spinrad RW, Yentsch CM, Brown J, Dortch Q, Haugen E, Revelante N, Shapiro L (1989) The response of beam attenuation to heterotrophic growth in a natural population of plankton. Limnol Oceanogr 34(8):1601-1605

Spinrad RW, Zaneveld JRV, Kitchen JC (1983) A study of the optical characteristics of the suspended particles in the benthic nepheloid layer of the Scotian Rise. J Geophys Res 88:7641-7645

Stabili L, Caroppo C, Cavallo RA (2006) Monitoring of a coastal Mediterranean area: culturable bacteria, phytoplankton, environmental factors and their relationships in the southern Adriatic sea. Environ Monit and Assess 121:303-325

Stoermer EF, Sicko-Goad L (1985) A comparative ultrastructural and morphometric study of six species of the diatom genus *Stephanodiscus*. J Plankton Res 7:125-135

Stramska M, Dickey TD (1992) Variability of bio-optical properties of the upper ocean associated with diel cycles in phytoplankton population. J Geophys Res 97(C11):17873-17887

Stramski D (1999) Refractive index of planktonic cells as a measure of cellular carbon and chlorophyll a content. Deep-Sea Res. 46: 335-351

Stramski D, Bricaud A, Morel A (2001) Modeling the inherent optical properties of the ocean based on the detailed composition of the planktonic community. Appl Opt 40(18):2929-2945

Stramski D, Kiefer DA (1990) Optical properties of marine bacteria. Proc SPIE, Ocean Opt X, 1302:250-268

Stramski D, Kiefer DA (1991) Light scattering by micro-organisms in the open ocean. Prog Oceanogr 28:343-383

Stramski D, Kiefer DA (1998) Can heterotrophic bacteria be important to marine light absorption? J Plankton Res 20:1489-1500

Stramski D, Mobley CD (1997) Effects of microbial particles on oceanic optics: A database of single-particle optical properties. Limnol Oceanogr 42(3):538-549

Stramski D, Morel A (1990) Optical properties of photosynthetic in different physiological states as affected by growth irradiance. Deep-Sea Res 37:245-266

Stramski D, Rassoulzadegan F, Kiefer DA (1992) Changes in the optical properties of a particle suspension caused by protist grazing. J Plankton Res 14(7):961-977

Stramski D, Reynolds RA (1993) Diel variations in the optical properties of a marine diatom. Limnol Oceanogr 38(7):1347-1364

Stramski D, Rosenberg G, Legendre L (1993) Photosynthetic and optical properties of the marine chlorophyte *Dunaliella tertiolecta* grown under fluctuating light caused by surface-wave focusing. Biol Morya 115:363-372

Stramski D, Sciandra A, Claustre H (2002) Effects of temperature, nitrogen and light limitation on the optical properties of the marine diatom *Thalassiosira pseudonana*. Limnol Oceanogr 47(2):392-403

Stramski D, Shalapyonok A, Reynolds RA (1995) Optical characterization of the oceanic unicellular cyanobacterium *Synechococcus* grown under a day-night cycle in natural irradiance. J Geophys Res 100:13295-13307

Stramski D, Boss E, Bogucki D, Voss KJ (2004) The role of seawater constituents in light backscattering in the ocean. Prog Oceanogr 61:27–56

Strickland JDH, Parsons TR (1972) A practical handbook of seawater analysis. Fisheries Research Board of Canada Bulletin 167:1-310

Stuart V, Sathyendranath S, Head EJH, Platt T, Irwin B, Maass H (2000) Bio-optical characteristics of diatom and prymnesiophyte populations in the Labrador Sea. Mar Ecol Prog Ser 201:91-106

Stuart V, Sathyendranath S, Platt T, Maass H, Irwin BD (1998) Pigments and species composition of natural phytoplankton populations: effect on the absorption spectra. J Plankton Res 20:187-217

Takahashi M, Bienfang PK (1983) Size structure of phytoplankton biomass and photosynthesis in subtropical Hawaiian waters. Mar Biol 76(2):203-211

Tang CL (1980) Mixing and circulation in the northwestern Gulf of St. Lawrence: a study of a buoyancy-driven current system. J Geophys Res 85(C5):2787-2796

Therriault J-C, Booth D, Legendre L, Demers S (1990) Phytoplankton photoadaptation to vertical excursion as estimated by an in vivo fluorescence ratio. Mar Ecol Prog Ser 60(1-2):97-111

Therriault J-C, Lacroix G (1976) Nutrients, chlorophyll, and internal tides in the St. Lawrence estuary. J Fish Res Bd Can 33(12):2747-2757

Therriault J-C, Levasseur M (1985) Control of phytoplankton production in the lower St. Lawrence Estuary: Light and freshwater runoff. Nat Can 112(1):177-96

Therriault J-C, Levasseur M (1986) Freshwater runoff control of the spatio-temporal distribution of phytoplankton in the lower St. Lawrence Estuary (Canada). Ecol Sci 7:251-260

Therriault JC, Painchaud J, Levasseur M (1985) Factors controlling the occurrence of *Protogonyaulax tamarensis* and shellfish toxicity in the St. Lawrence Estuary:

Freshwater runoff and the stability of the water column. In: Anderson DM, White AW, Baden DC (eds) Toxic Dinoflagellate, Elsevier, New York, p 141-146

Thompson PA, Harrison PJ, Parslow JS (1991) Influence of irradiance on cell volume and carbon quota for ten species of marine phytoplankton. J Phycol 27:351-360

Twardowski MS, Boss E, Macdonald JB, Pegau WS, Barnard AH, Zaneveld JRV (2001) A model for estimating bulk refractive index from the optical backscattering ratio and the implications for understanding particle composition in case I and case II waters. J Geophys Res 106(C7):14129-14142

Twardowski MS, Sullivan JM, Donaghay PL, Zaneveld JRV (1999) Microscale quantification of the absorption by dissolved and particulate material in coastal waters with an AC-9. J Atmos Ocean Technol 16:691-707

Ulloa O, Sathyendranath S, Platt T, Quinones RA (1992) Light scattering by marine heterotrophic bacteria. J Geophys Res 97(C6):9619-9629

Utermöhl, H. (1931) Neue Wege in der quantitativen Erfassung des Planktons. Verhanlungen der internationalen Vereinigung für theoretische und angewandte. Limnologie 5:567-596

Vaillancourt RD, Brown CW, Guillard RRL, Balch WM (2004) Light backscattering properties of marine phytoplankton: Relationships to cell size, chemical composition and taxonomy. J Plankton Res 26:191–212

Van Bleijswijh JDL, Kempers RS, Veldhuis MJ, Westbroek P (1994) Cell and growth characteristics of types A and B of *Emiliania huxleyi* (Prymnesiophyceae) as determined by flow cytometry and chemical analyses. J Phycol 30:230-241

Van de Hulst HC (1957) Light scattering by small particles. Wiley, New-York, 176 pp

Vaulot D, Le Bot N., Marie D, Fulkai E (1996) Effect of phosphorus on the *Synechococcus* cell cycle in surface mediterranean waters during summer. Appl Env Microl 62:2527-2533

Vaulot D, Marie D (1999) Diel variability of photosynthetic picoplankton in the equatorial Pacific. J Geophys Res 104(C2):3297-3310

Vaulot D, Marie D, Olson RJ, Chisholm SW (1995) Growth of *Prochlorococcus*, a photosynthetic prokaryote, in the equatorial Pacific Ocean. Science 268:1480-1482

Vidussi F (1998) Variabilié spatiale et temporelle des marqueurs pigmentaires des communautés autotrophes en Méditerranée: implications biogéochimiques. Thèse de doctorat de l'Université Pierre et Marie Curie (France), 181 pp

Vodacek A (1992) An explanation of the spectral variation in freshwater CDOM fluorescence. Limnol Oceanogr 37(8):1808-1813

Vodacek A, Blough NV, DeGrandpre MD, Peltzer ET, Nelson RK (1997) Seasonal variation of CDOM and DOC in the Middle Atlantic Bight: Terrestrial inputs and photooxidation. Limnol Oceanogr 42(4):674-686

Vodacek A, Hoge FE, Swift RN, Yungel JK, Peltzer ET, Blough NV (1995) The use of in situ and airborne fluorescence measurements to determine UV absorption coefficients and DOC concentrations in surface waters. Limnol Oceanogr 40(2):411-415

Volten H, de Haan JF, Hovenier JW, Schreurs R, Vassen W, Dekker AG, Hoogenboom HJ, Charlton F, Wouts R (1998) Laboratory measurements of angular

distributions of light scattered by phytoplankton and silt. Limnol Oceanogr 43(6):1180-1197

Voss KJ, Balch WM, Kilpatrick KA (1998) Scattering and attenuation properties of *Emiliania huxleyi* cells and their detached coccoliths. Limnol Oceanogr 43(5):870-876

Waterbury JB, Watson SW, Valois FW, Franks DG (1986) Biological and ecological characterization of the marine unicellular cyanobacterium *Synechococcus*. In: Platt T, Li WKW (eds) Photosynthetic picoplankton. Can Bull Fish Aquat Sci 214:71-120

Whitehead RF, de Mora S, Demers S, Gosselin M, Monfort P, Mostajir B (2000) Interactions of ultraviolet-B radiation, mixing, and biological activity on photobleaching of natural chromophoric dissolved organic matter: A mesocosm study. Limnol Oceanogr 45(2):278-291

Yentsch CM, Horan PK, Muihread K, Dortch Q, Haugen E, Legendre L, Murphy LS, Perry MJ, Phinney DA, Pomponi SA, Spinrad RW, Wood M, Yentsch CS, Zahuranec BJ (1983) Flow cytometry and cell sorting: a technique for analysis and sorting of aquatic particles. Limnol Oceanogr 28(6):1275-1280

Yentsch CS (1962) Measurements of visible light absorption by particulate matter in the ocean. Limnol Oceanogr 7(2):207-217

Zafiriou OC, Andrews SS, Wang W (2003) Concordant estimates of oceanic carbon monoxide source and sink processes in the Pacific yield a balance global "blue-water" CO budget. Global Biogeochemical Cycles 17(1):1015

Zakardjian B, Gratton Y, Vézina A F (2000) Late spring phytoplankton bloom in the Lower St. Lawrence Estuary: the flushing hypothesis revisited. Mar Ecol Prog Ser 192:31-48

Zaneveld JRV, Kitchen JC (1995) The variation in the inherent optical properties of phytoplankton near an absorption peak as determined by various models of cell structure. J Geophys Res 100(C7):13309-13320

Zaneveld JRV, Kitchen JC, Moore CM (1994) The scattering error correction of reflecting-tube absorption meters. Proc SPIE, Ocean Optics XII, 2258:44-55

Zapata M, Rodriguez F, Garrido J L (2000) Separation of chlorophylls and carotenoids from marine phytoplankton: a new HPLC method using a reversed phase C8 column and pyridine-containing mobile phase. Mar Ecol Prog Ser 195:29-45

Zar JH (1999) Biostatistical analysis. 4th ed, Prentice-Hall, Upper Saddle River, 663 pp

Zhang X, Lewis M, Lee M, Johnson B, Korotaev G (2002) The volume scattering function of natural bubble populations. Limnol Oceanogr 47(5):1273-1282